Exploring Nuclear Structure at the Ultra-Relativistic Heavy-Ion Collisions

You Zhou (周铀)

Niels Bohr Institute

UNIVERSITY OF COPENHAGEN

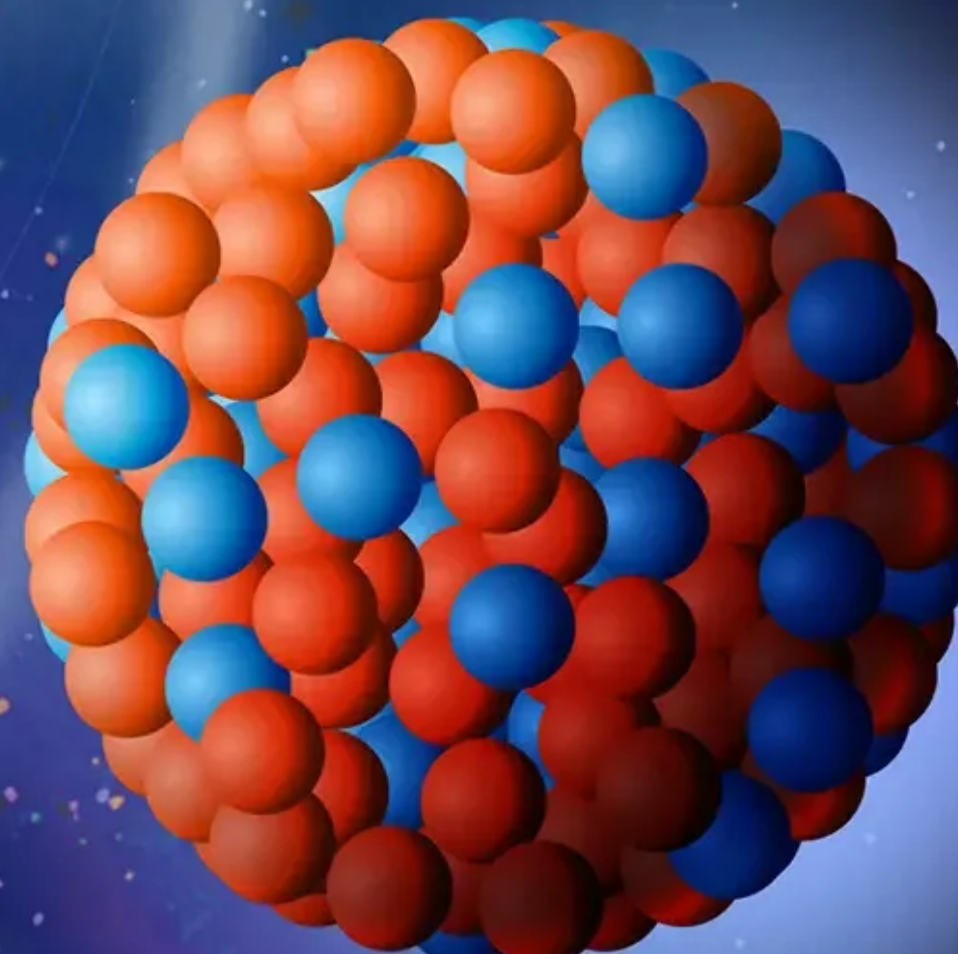

Funded by the European Union

erc European Research Council Established by the European Commission

VILLUM FONDEN

INDEPENDENT RESEARCH FUND DENMARK

见微学术沙龙

Study of Quark-Gluon Plasma in the *Little Bang*

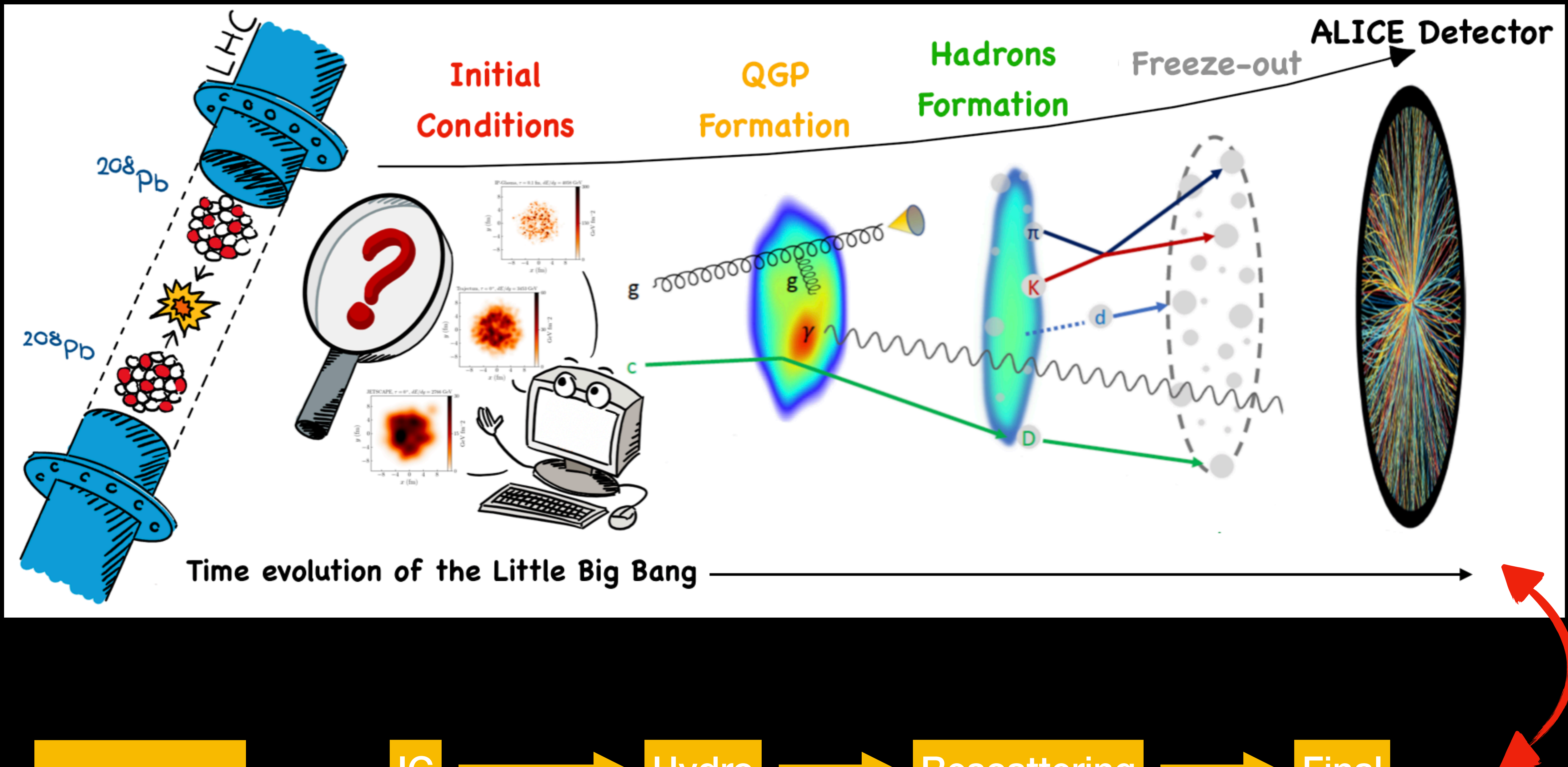

TH

IC → Hydro → Rescattering → Final

IC → Partonic/hadronic transport → Final

State-of-the-art: Viscosities of QGP

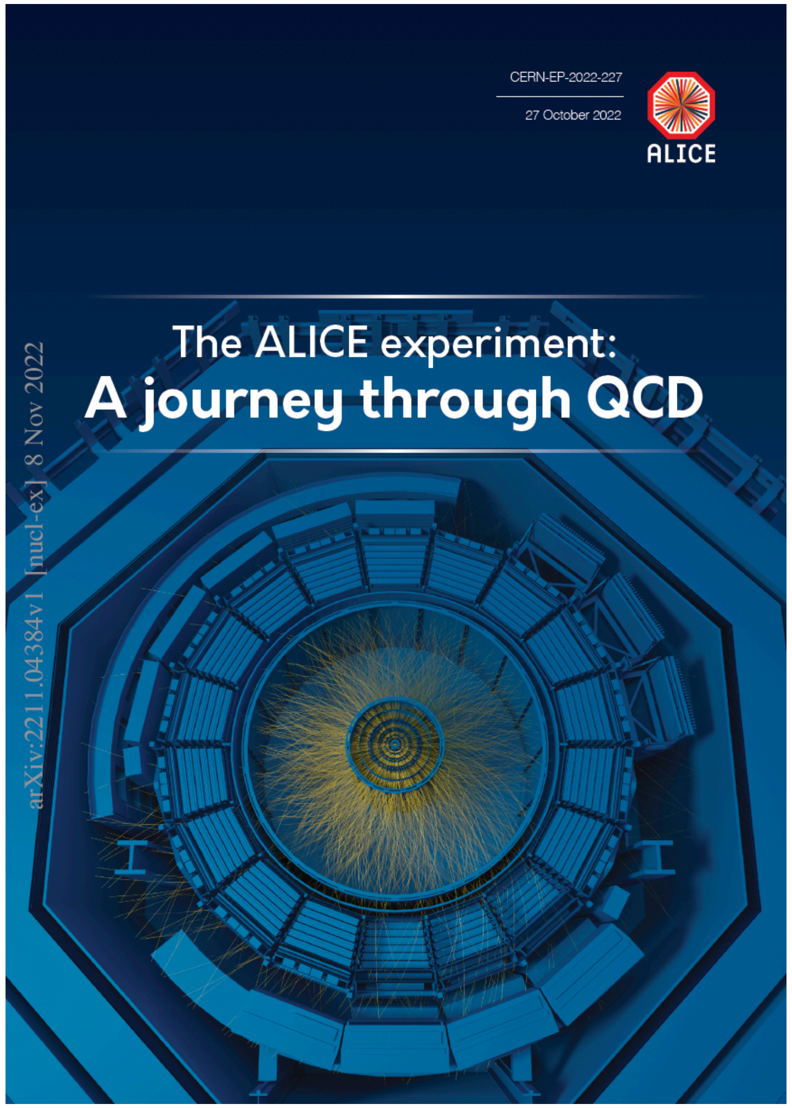

State-of-the-art: Viscosities of QGP

Extracted viscosities of QGP

- shear viscosity η/s
- bulk viscosity ζ/s

Duke: *Nature Phys.* 15 (2019) 11, 1113
Jyväskylä: *Phys. Rev. C* 104, 054904 (2021)
Trajectum: *Phys. Rev. Lett.* 126, 202301 (2021)
JETSCAPE: *Phys. Rev. Lett.* 126, 242301 (2021)
IP-Glasma: *Phys. Rev. Lett.* 128, 042301 (2022)

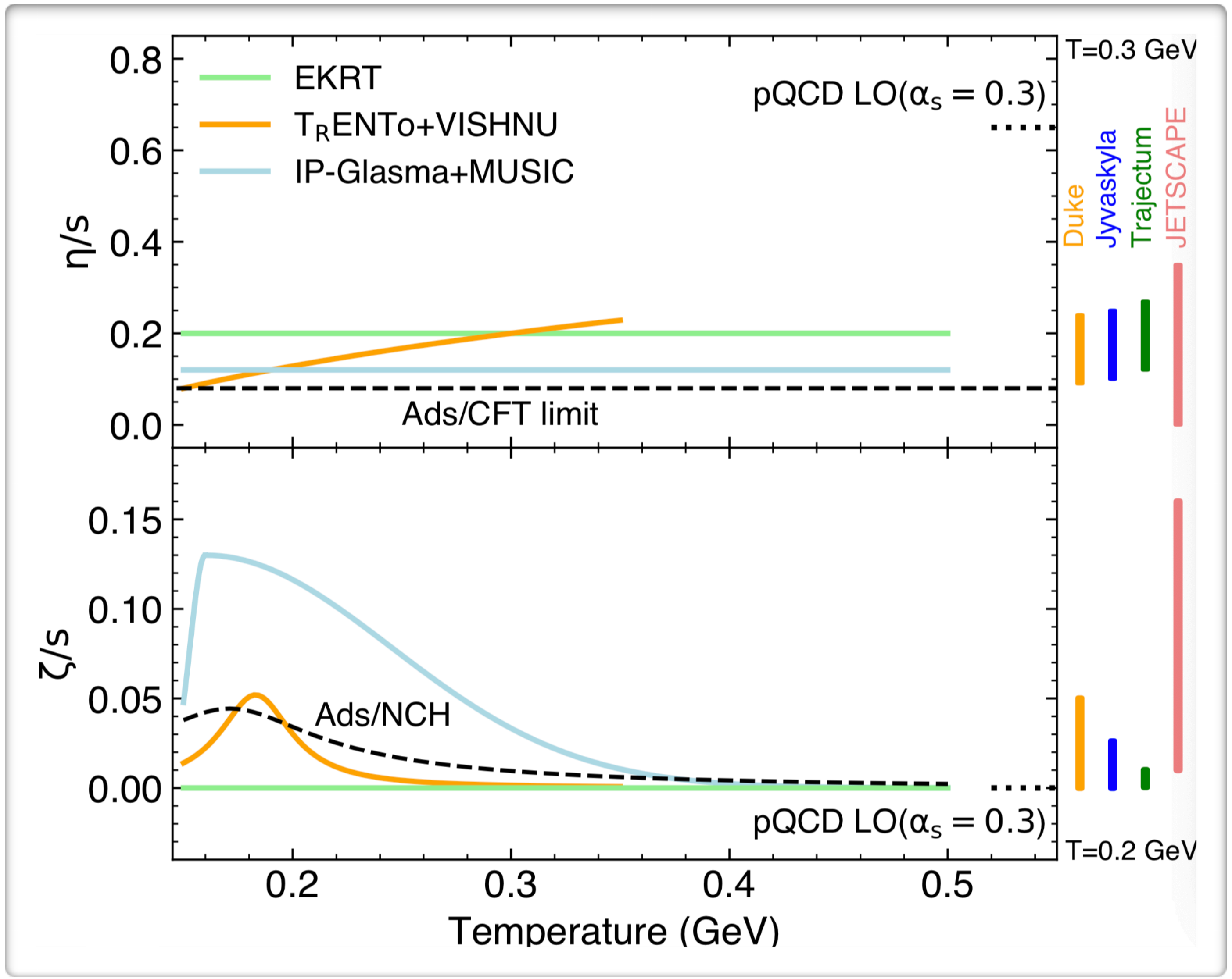

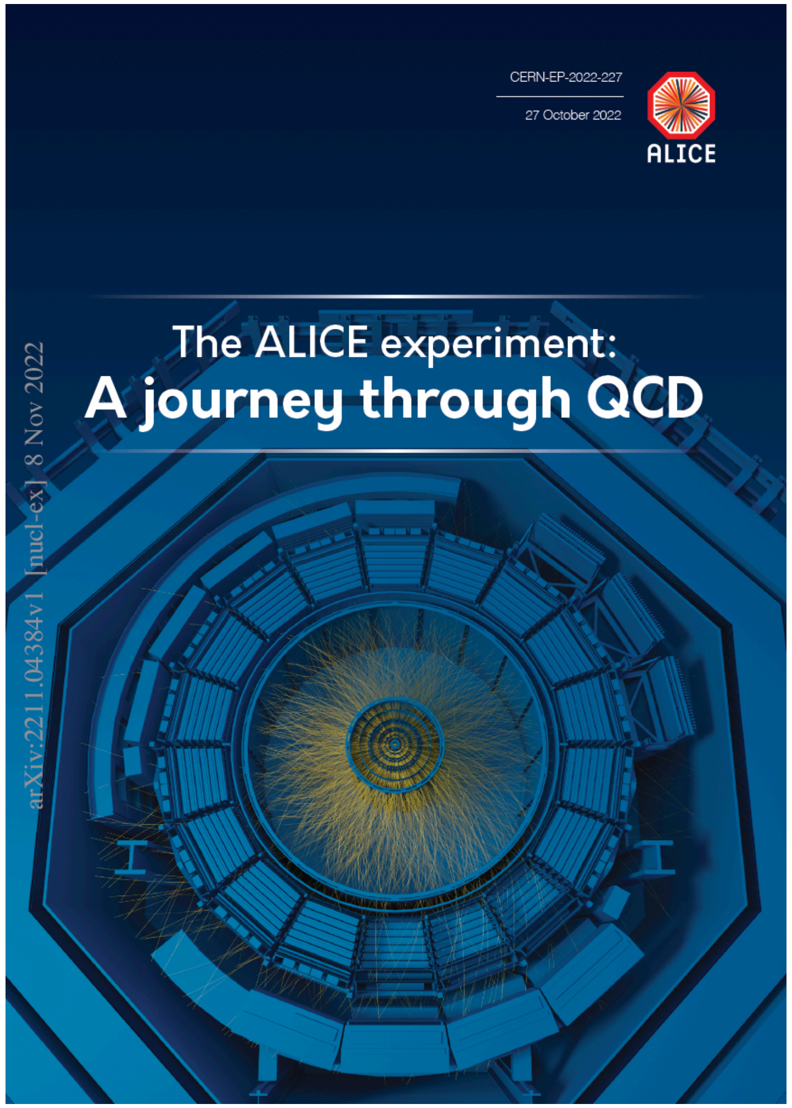

State-of-the-art: Viscosities of QGP

Extracted viscosities of QGP

- shear viscosity η/s
- bulk viscosity ζ/s

Duke: *Nature Phys.* 15 (2019) 11, 1113
Jyväskylä: *Phys. Rev. C 104, 054904 (2021)*
Trajectum: *Phys. Rev. Lett. 126, 202301 (2021)*
JETSCAPE: *Phys. Rev. Lett. 126, 242301 (2021)*
IP-Glasma: *Phys. Rev. Lett. 128, 042301 (2022)*

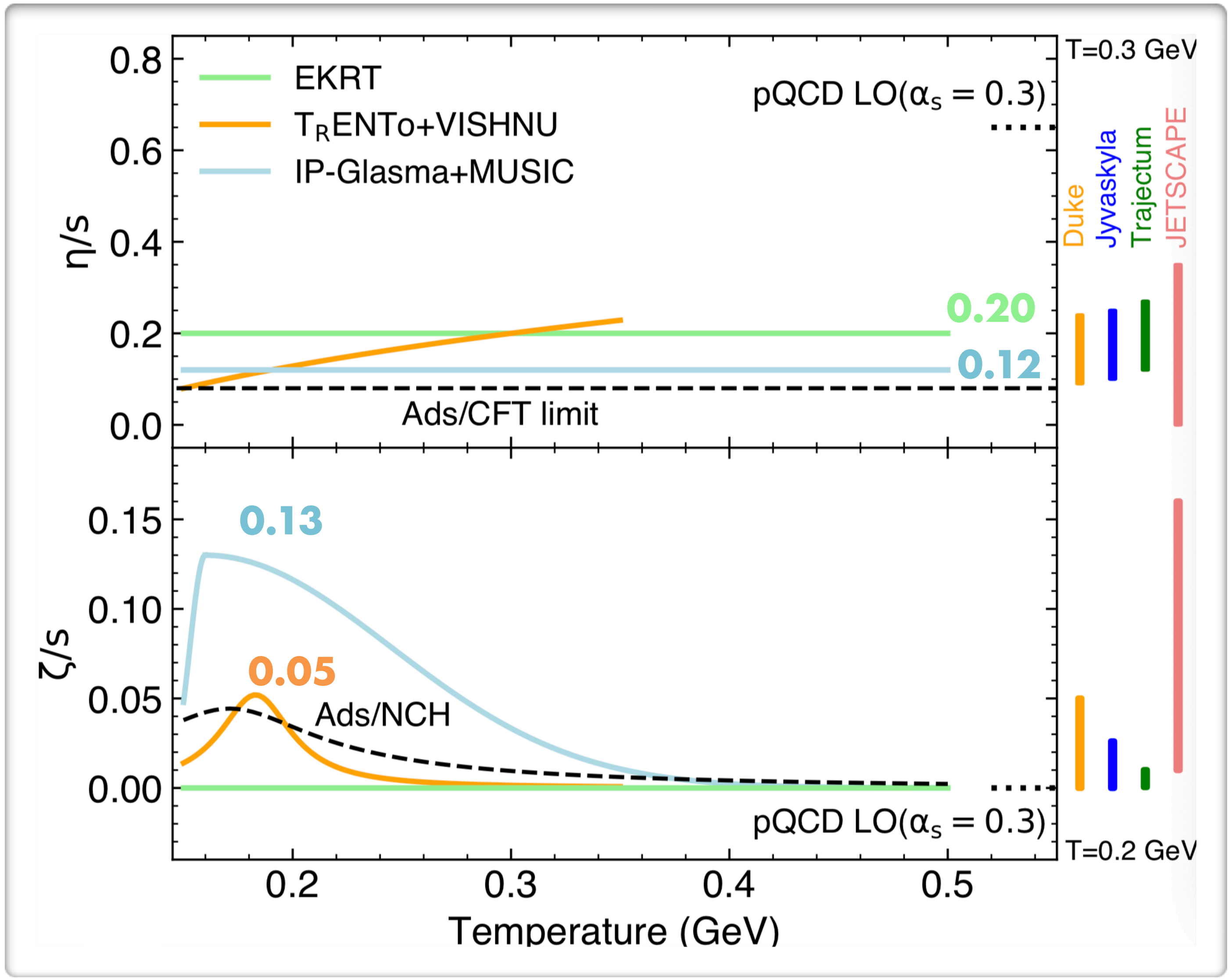

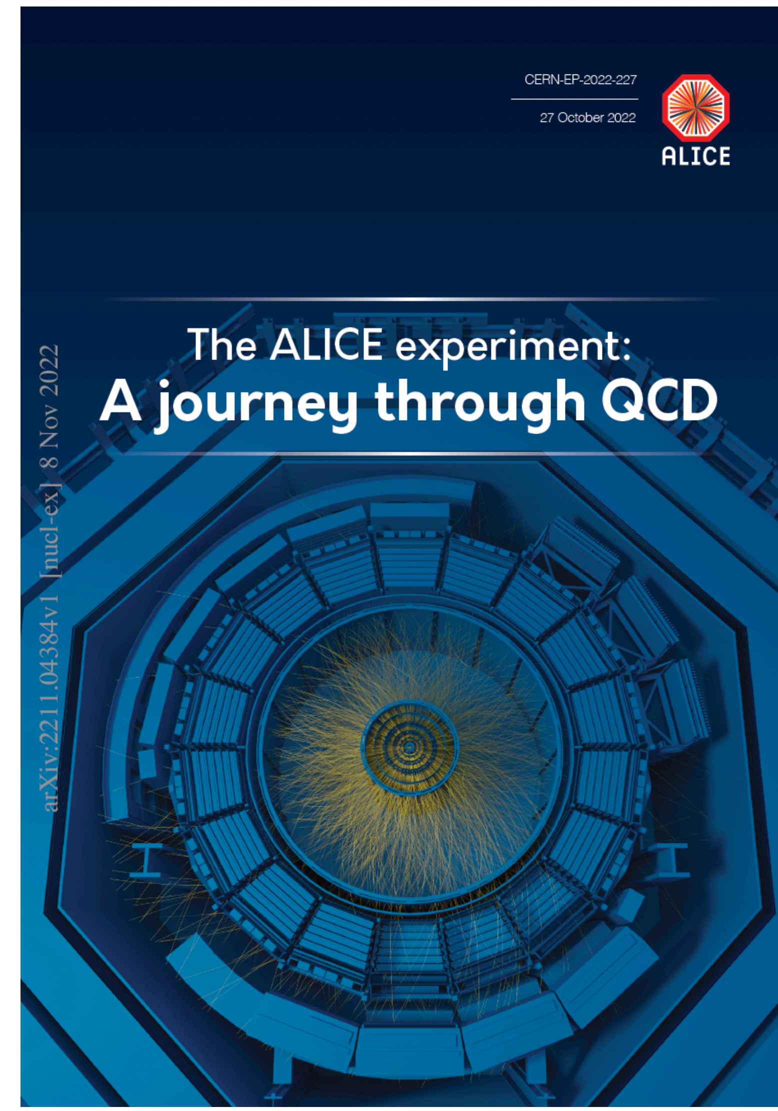

Huge uncertainties of the extracted ***QGP properties,*** due to poorly known ***initial conditions***

IC: What is our current understanding?

IC: What is our current understanding?

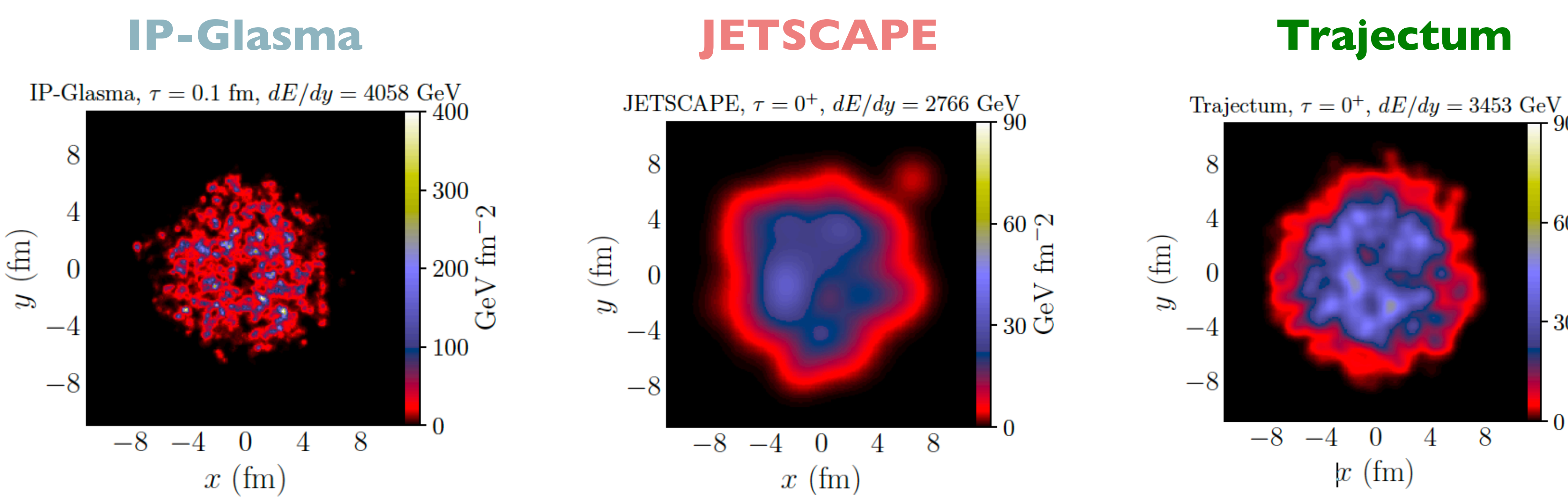

IC: What is our current understanding?

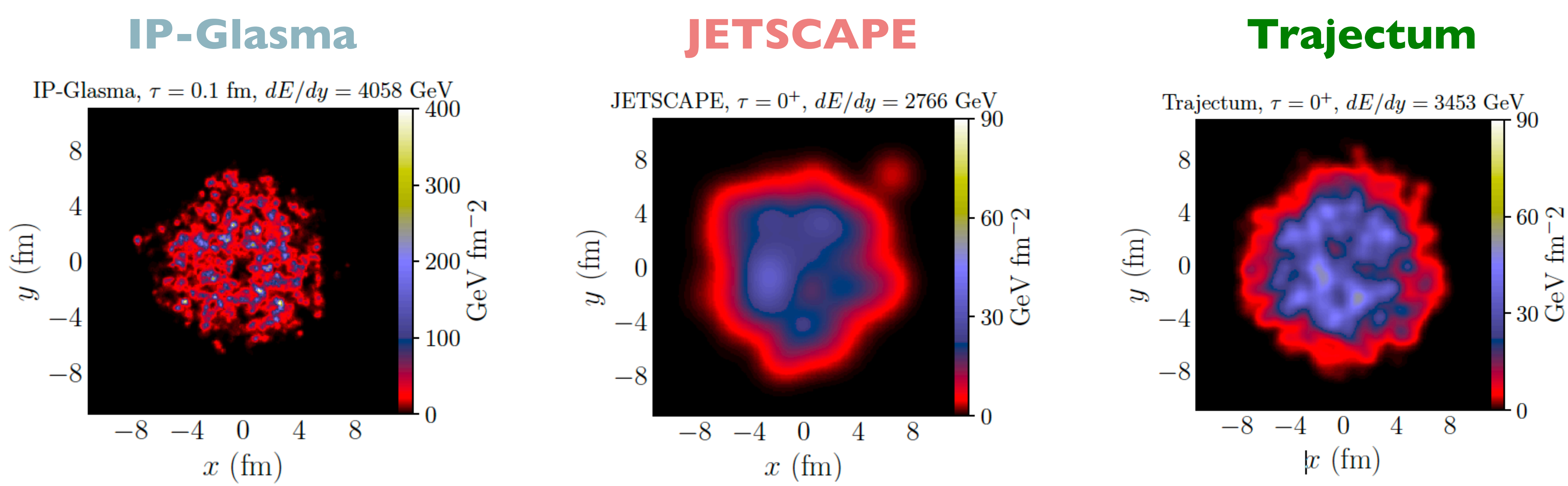

IC: What is our current understanding?

IP-Glasma

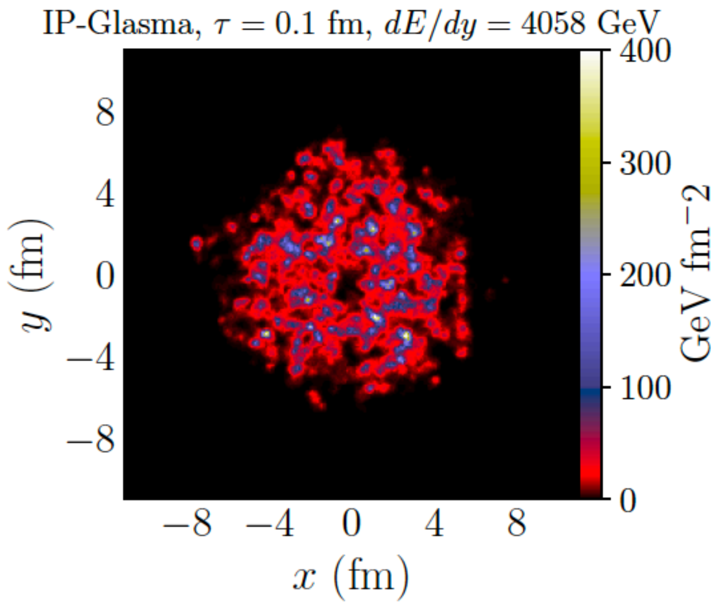

JETSCAPE

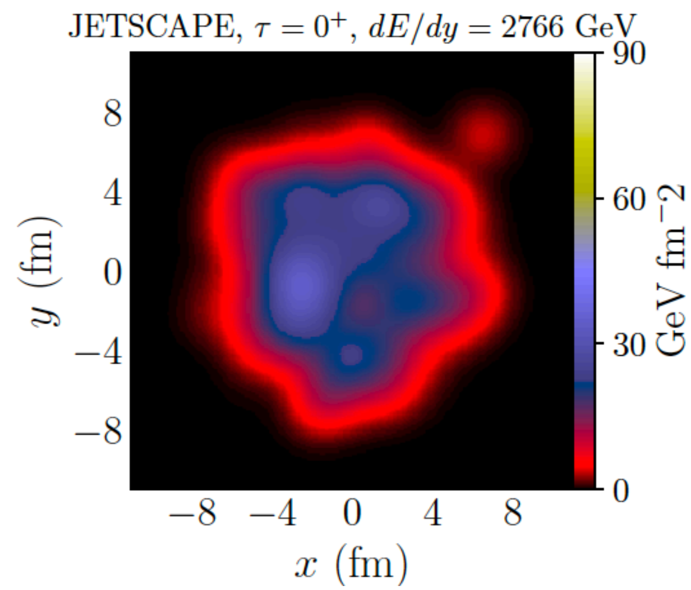

Trajectum

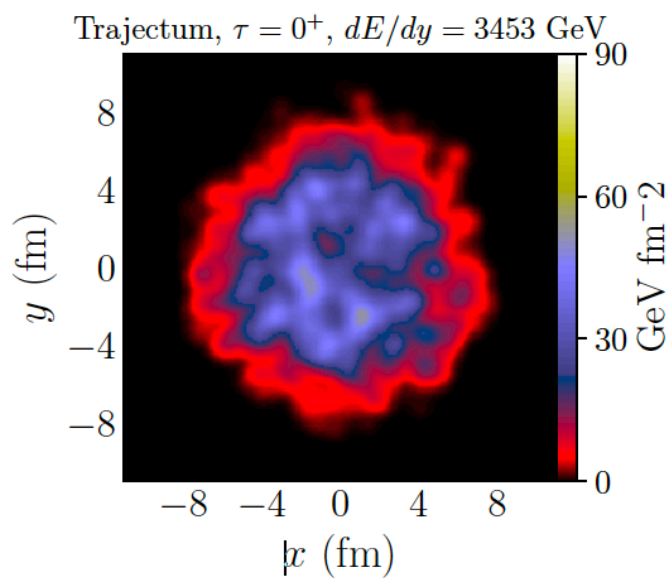

How can we access the initial conditions in EXP ?

From eccentricity to elliptic flow

❖ Spatial anisotropy in the initial state converted to momentum anisotropic particle distributions

- known as ***elliptic flow***
- reflect initial **eccentricity** and **transport properties** of QGP

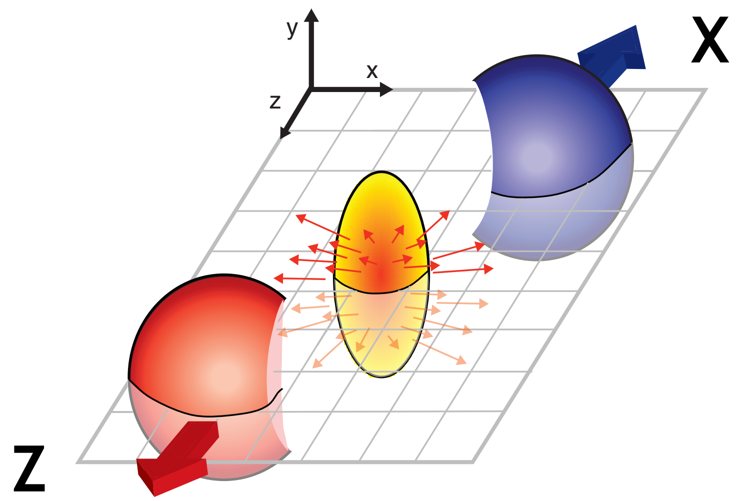

$$\varepsilon_2 = \left\langle \frac{y^2 - x^2}{y^2 + x^2} \right\rangle$$

coordinate space Eccentricity

system expansion

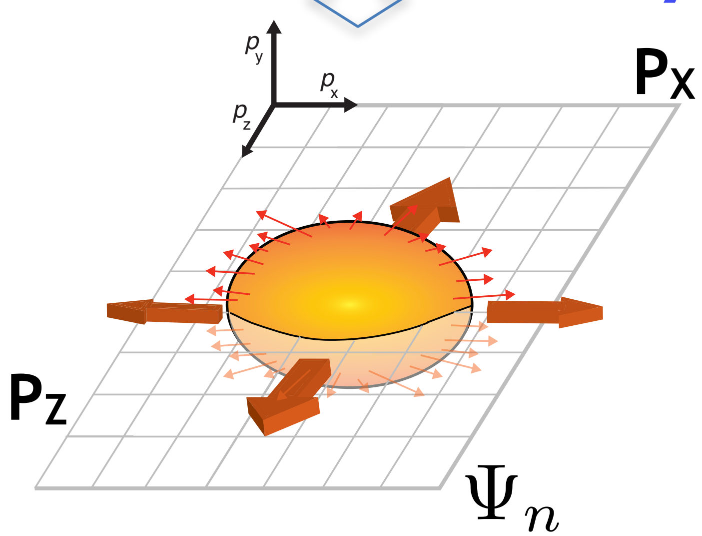

$$v_2 = \langle \cos 2 \left(\varphi - \Psi_{\mathrm{RP}} \right) \rangle$$

momentum space Elliptic Flow

From initial anisotropy to anisotropic flow

Initial state

$$\varepsilon_n = \frac{\sqrt{\langle r^n \cos(n\phi)\rangle^2 + \langle r^n \sin(n\phi)\rangle^2}}{\langle r^n \rangle}$$

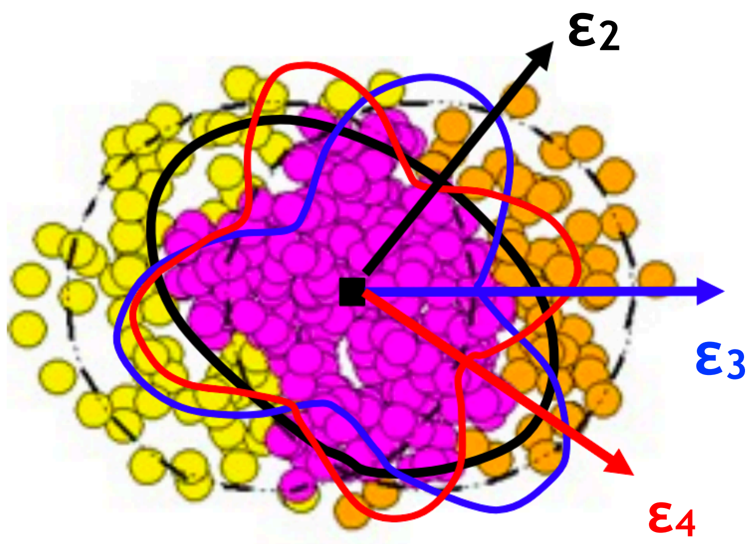

System expansion

Final state

$$\overrightarrow{V_n} = v_n \, e^{in\Psi_n}$$

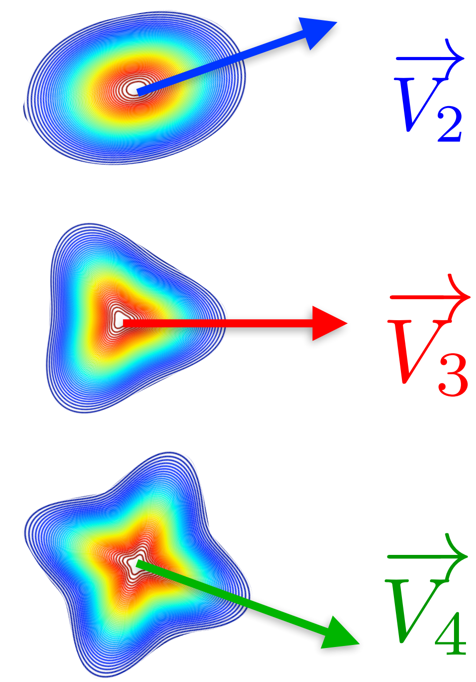

$P(\varepsilon_m, \varepsilon_n, \varepsilon_k, ..., \Phi_m, \Phi_n, \Phi_k, ...)$ → $P(v_m, v_n, v_k, ..., \Psi_m, \Psi_n, \Psi_k, ...)$

How does v_n fluctuate	How does ψ_n fluctuate	How do v_n and v_m correlate	How do ψ_n and ψ_m correlate
$P(v_n)$	$P(\Psi_n)$	$P(v_m, v_n, v_k, ...)$	$P(\Psi_m, \Psi_n, \Psi_k, ...)$

Probe QGP properties with Flow

ALICE, Physical Review Letters 116, 132302 (2016)

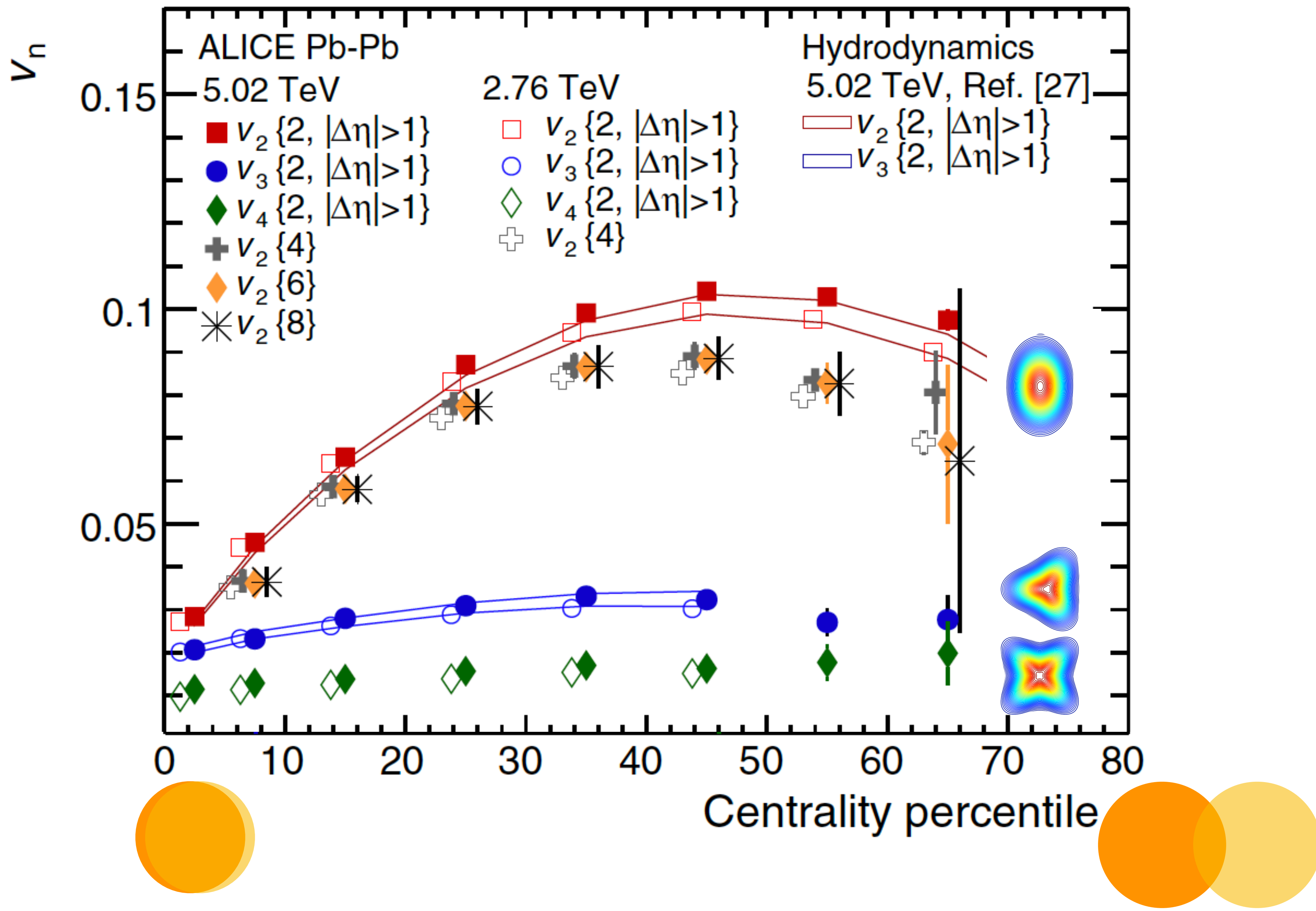

❖ Flow measurements at the top LHC energies agree with hydrodynamic predictions

- The Quark-Gluon Plasma behaves like a perfect fluid
- Constrain initial state models
  - **EKRT ✅, TRENTo ✅, IP-Glasma ✅, MC-KLN ❌, MC-Glauber ❌**

Initial geometry fluctuations

How does v_n fluctuate

$v_n\{m\}$

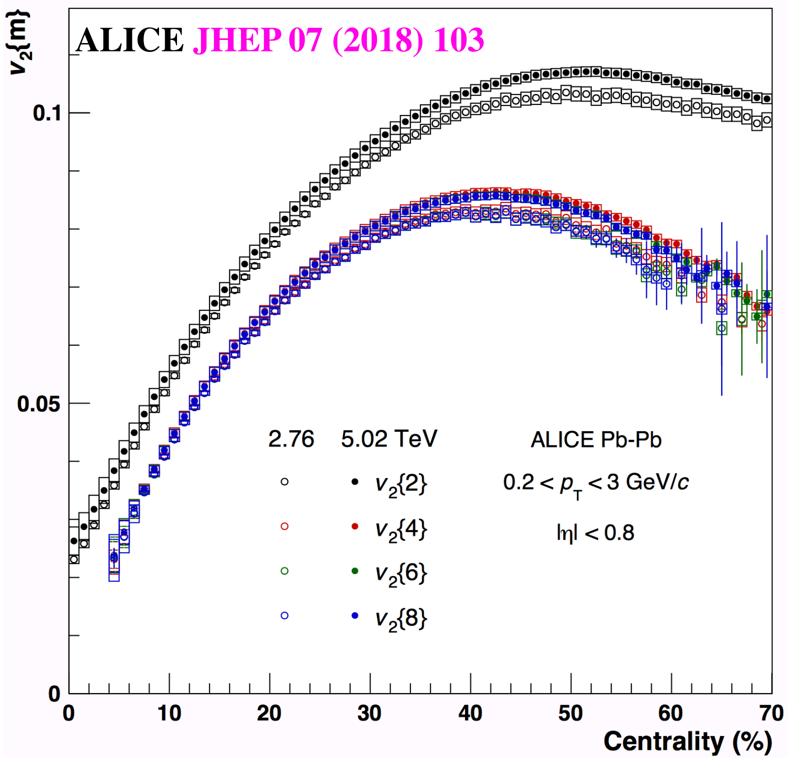

$$v_n\{2\} = \sqrt[2]{\langle v_n^2 \rangle},$$
$$v_n\{4\} = \sqrt[4]{2\langle v_n^2 \rangle^2 - \langle v_n^4 \rangle},$$
$$v_n\{6\} = \sqrt[6]{\langle v_n^6 \rangle - 9\langle v_n^2 \rangle\langle v_n^4 \rangle + 12\langle v_n^2 \rangle^3},$$
$$v_n\{8\} = \sqrt[8]{\langle v_n^8 \rangle - 16\langle v_n^2 \rangle\langle v_n^6 \rangle - 18\langle v_n^4 \rangle^2 + 144\langle v_n^2 \rangle^2\langle v_n^4 \rangle - 144\langle v_n^2 \rangle^4}.$$

Initial geometry fluctuations

How does v_n fluctuate

$v_n\{m\}$ → Moments

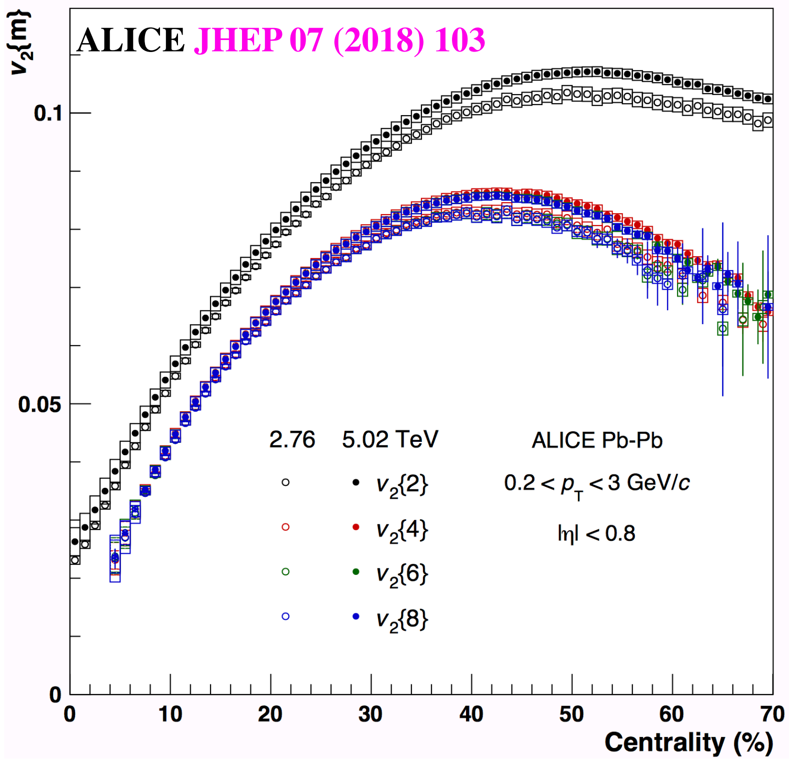

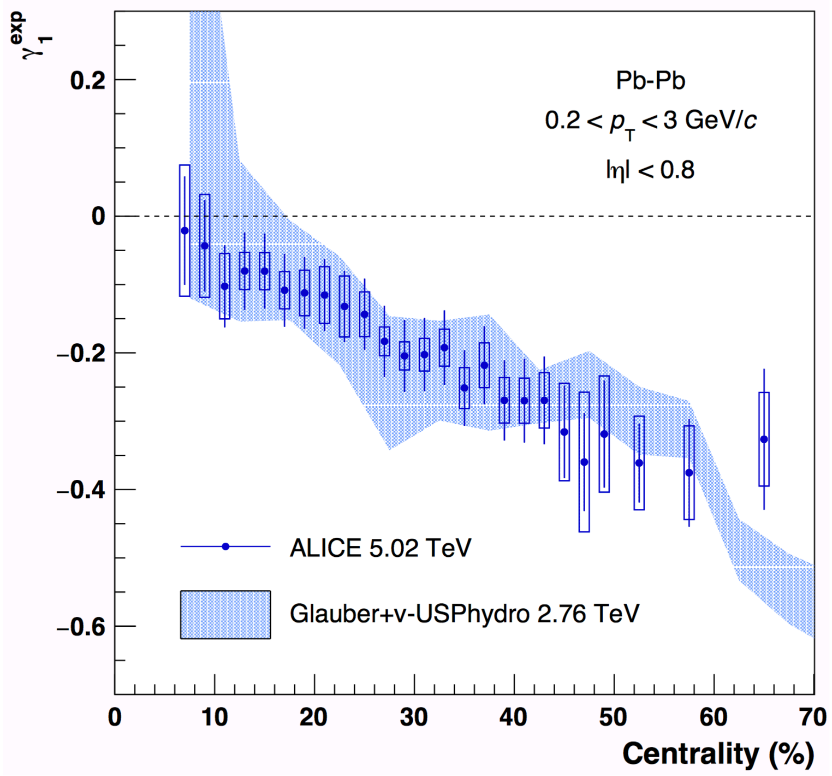

$$v_n\{2\} = \sqrt[2]{\langle v_n^2 \rangle},$$
$$v_n\{4\} = \sqrt[4]{2\langle v_n^2 \rangle^2 - \langle v_n^4 \rangle},$$
$$v_n\{6\} = \sqrt[6]{\langle v_n^6 \rangle - 9\langle v_n^2 \rangle \langle v_n^4 \rangle + 12\langle v_n^2 \rangle^3},$$
$$v_n\{8\} = \sqrt[8]{\langle v_n^8 \rangle - 16\langle v_n^2 \rangle \langle v_n^6 \rangle - 18\langle v_n^4 \rangle^2 + 144\langle v_n^2 \rangle^2 \langle v_n^4 \rangle - 144\langle v_n^2 \rangle^4}.$$

$$\gamma_1^{\rm exp} = -6\sqrt{2}\, v_2\{4\}^2 \frac{v_2\{4\} - v_2\{6\}}{(v_2\{2\}^2 - v_2\{4\}^2)^{3/2}}$$

$$\gamma_2 \simeq \gamma_2^{\rm expt} \equiv -\frac{3}{2} \frac{v_2\{4\}^4 - 12 v_2\{6\}^4 + 11 v_2\{8\}^4}{(v_2\{2\}^2 - v_2\{4\}^2)^2}$$

Initial geometry fluctuations

How does v_n fluctuate

$v_n\{m\}$ → Moments → $p(v_n)$

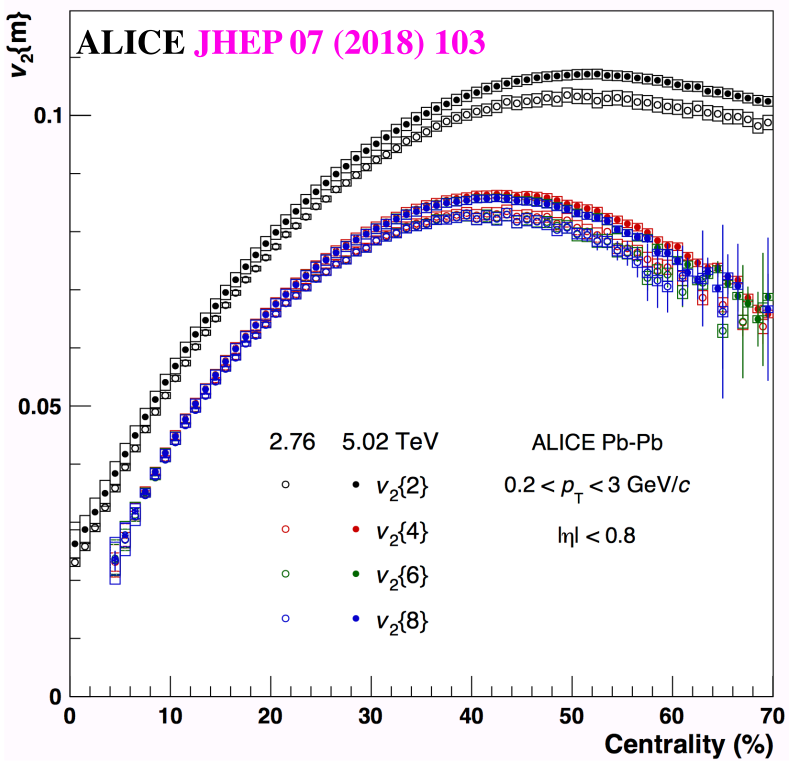

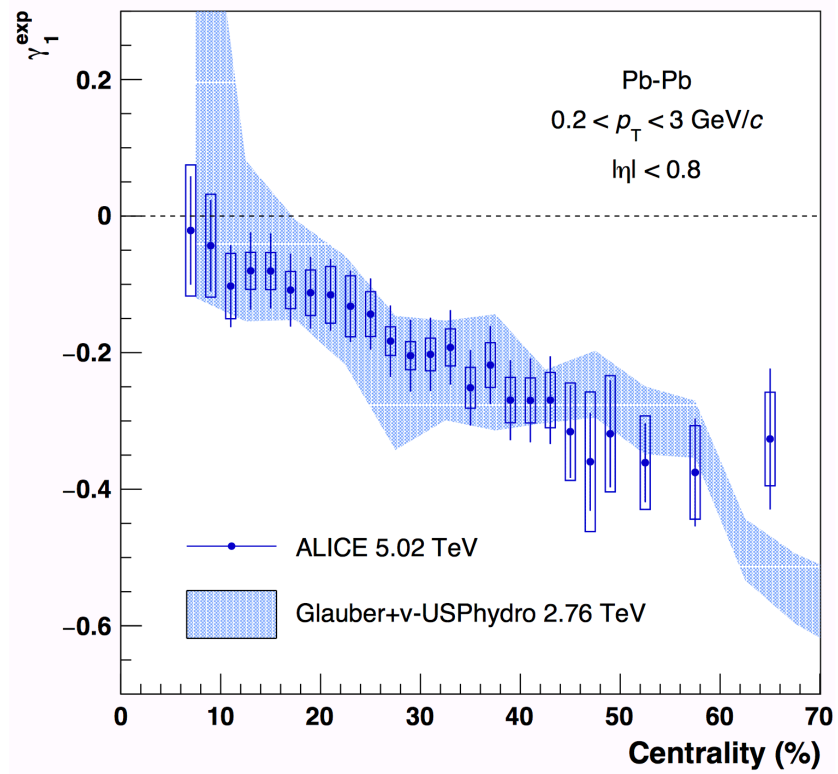

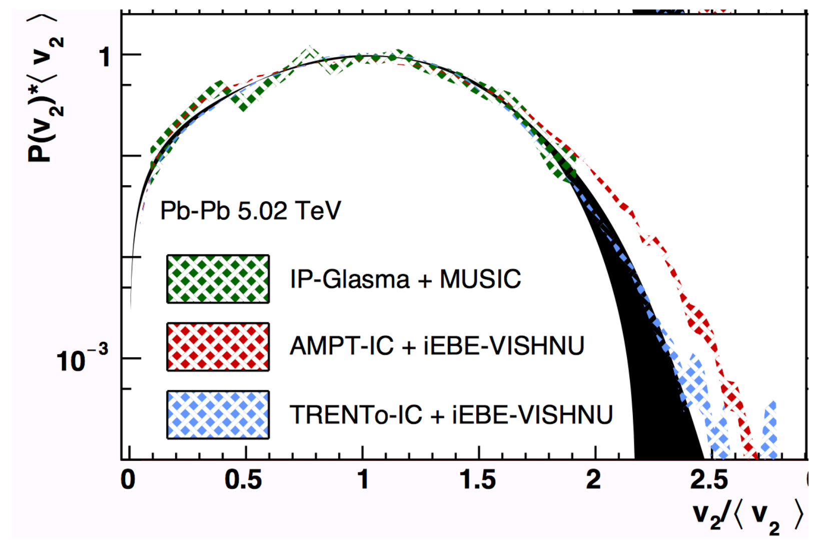

$$v_n\{2\} = \sqrt[2]{\langle v_n^2\rangle},$$
$$v_n\{4\} = \sqrt[4]{2\langle v_n^2\rangle^2 - \langle v_n^4\rangle},$$
$$v_n\{6\} = \sqrt[6]{\langle v_n^6\rangle - 9\langle v_n^2\rangle\langle v_n^4\rangle + 12\langle v_n^2\rangle^3},$$
$$v_n\{8\} = \sqrt[8]{\langle v_n^8\rangle - 16\langle v_n^2\rangle\langle v_n^6\rangle - 18\langle v_n^4\rangle^2 + 144\langle v_n^2\rangle^2\langle v_n^4\rangle - 144\langle v_n^2\rangle^4}.$$

$$\gamma_1^{\rm exp} = -6\sqrt{2}v_2\{4\}^2\frac{v_2\{4\} - v_2\{6\}}{(v_2\{2\}^2 - v_2\{4\}^2)^{3/2}}$$

$$\gamma_2 \simeq \gamma_2^{\rm expt} \equiv -\frac{3}{2}\frac{v_2\{4\}^4 - 12v_2\{6\}^4 + 11v_2\{8\}^4}{(v_2\{2\}^2 - v_2\{4\}^2)^2}$$

Initial geometry fluctuations

How does v_n fluctuate

$v_n\{m\}$ → Moments → $p(v_n)$ → $p(\varepsilon_n)$

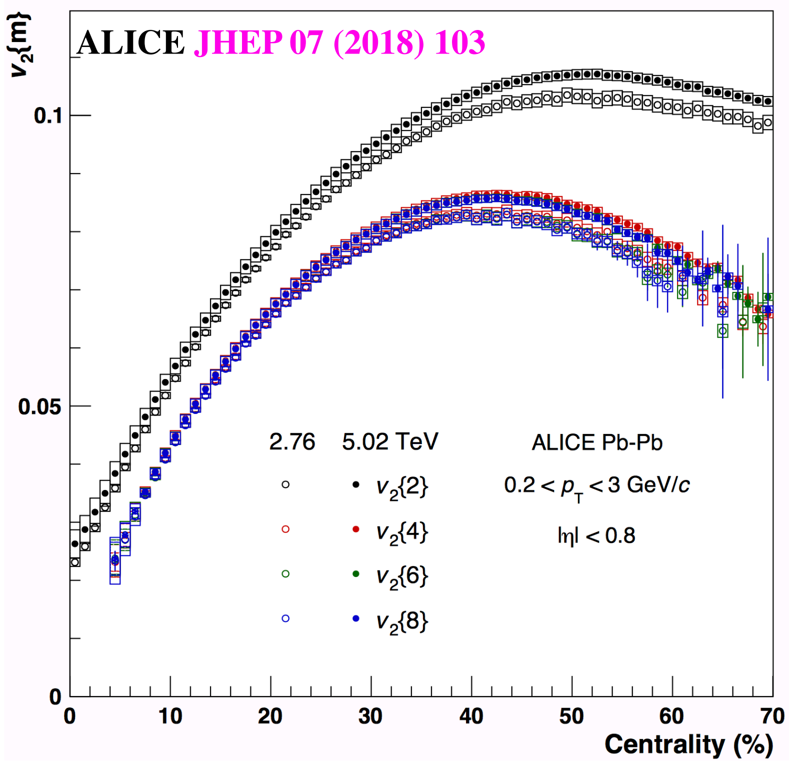

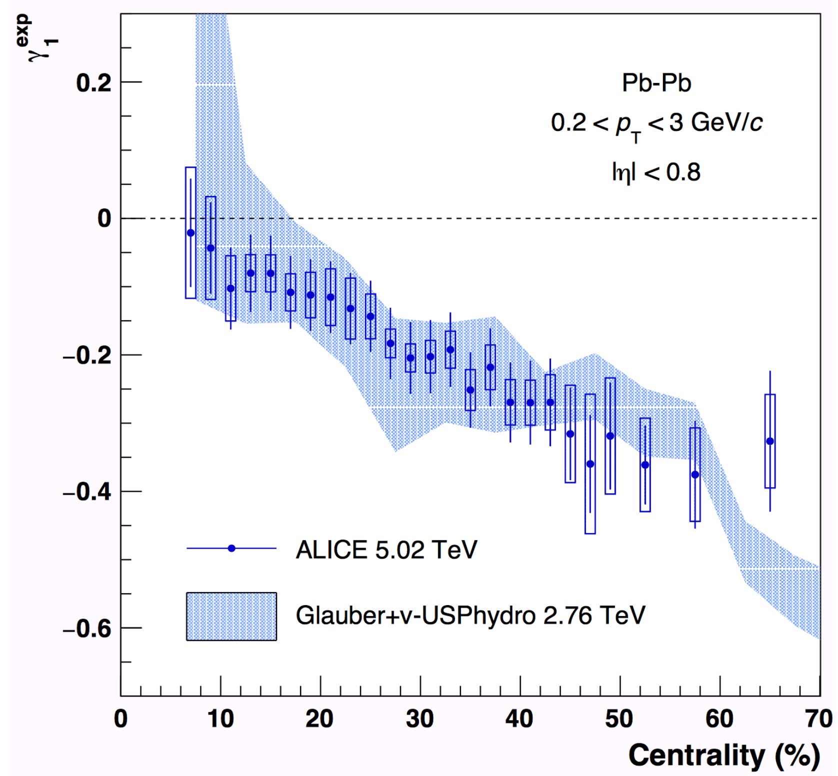

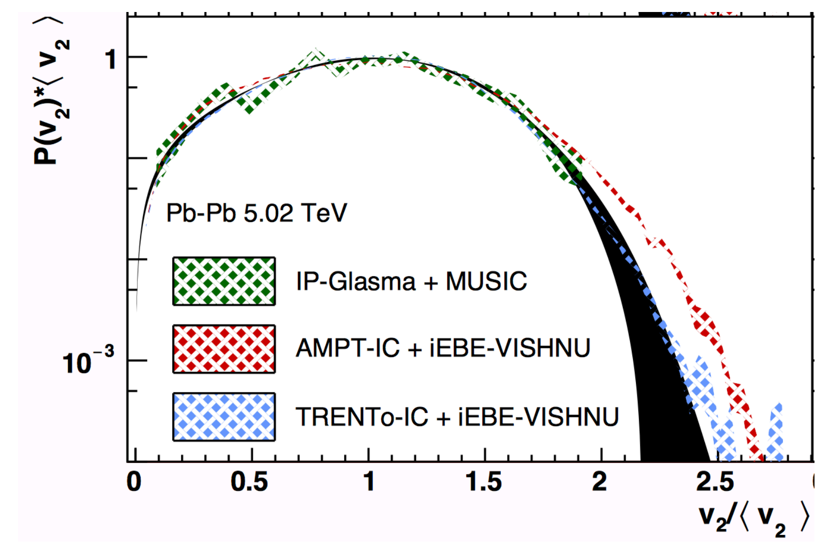

$$v_n \propto \varepsilon_n$$

$$P(v_n/\langle v_n\rangle) \approx P(\varepsilon_n/\langle\varepsilon_n\rangle)$$

$$v_n\{2\} = \sqrt[2]{\langle v_n^2\rangle},$$

$$v_n\{4\} = \sqrt[4]{2\langle v_n^2\rangle^2 - \langle v_n^4\rangle},$$

$$v_n\{6\} = \sqrt[6]{\langle v_n^6\rangle - 9\langle v_n^2\rangle\langle v_n^4\rangle + 12\langle v_n^2\rangle^3},$$

$$v_n\{8\} = \sqrt[8]{\langle v_n^8\rangle - 16\langle v_n^2\rangle\langle v_n^6\rangle - 18\langle v_n^4\rangle^2 + 144\langle v_n^2\rangle^2\langle v_n^4\rangle - 144\langle v_n^2\rangle^4}.$$

$$\gamma_1^{\rm exp} = -6\sqrt{2}\, v_2\{4\}^2 \frac{v_2\{4\} - v_2\{6\}}{(v_2\{2\}^2 - v_2\{4\}^2)^{3/2}}$$

$$\gamma_2 \simeq \gamma_2^{\rm expt} \equiv -\frac{3}{2}\frac{v_2\{4\}^4 - 12 v_2\{6\}^4 + 11 v_2\{8\}^4}{(v_2\{2\}^2 - v_2\{4\}^2)^2}$$

C. Gale etc, PRL110 (2013) 1, 012302

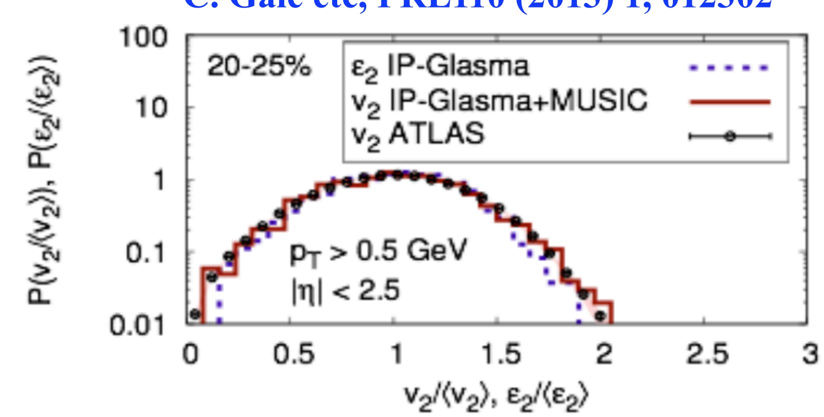

$P(v_n)$ -> $P(\varepsilon_n)$

How does v_n fluctuate

$$v_n \propto \varepsilon_n$$
$$P(v_n/\langle v_n\rangle) \approx P(\varepsilon_n/\langle \varepsilon_n\rangle)$$

Final state $P(v_2/<v_2>)$

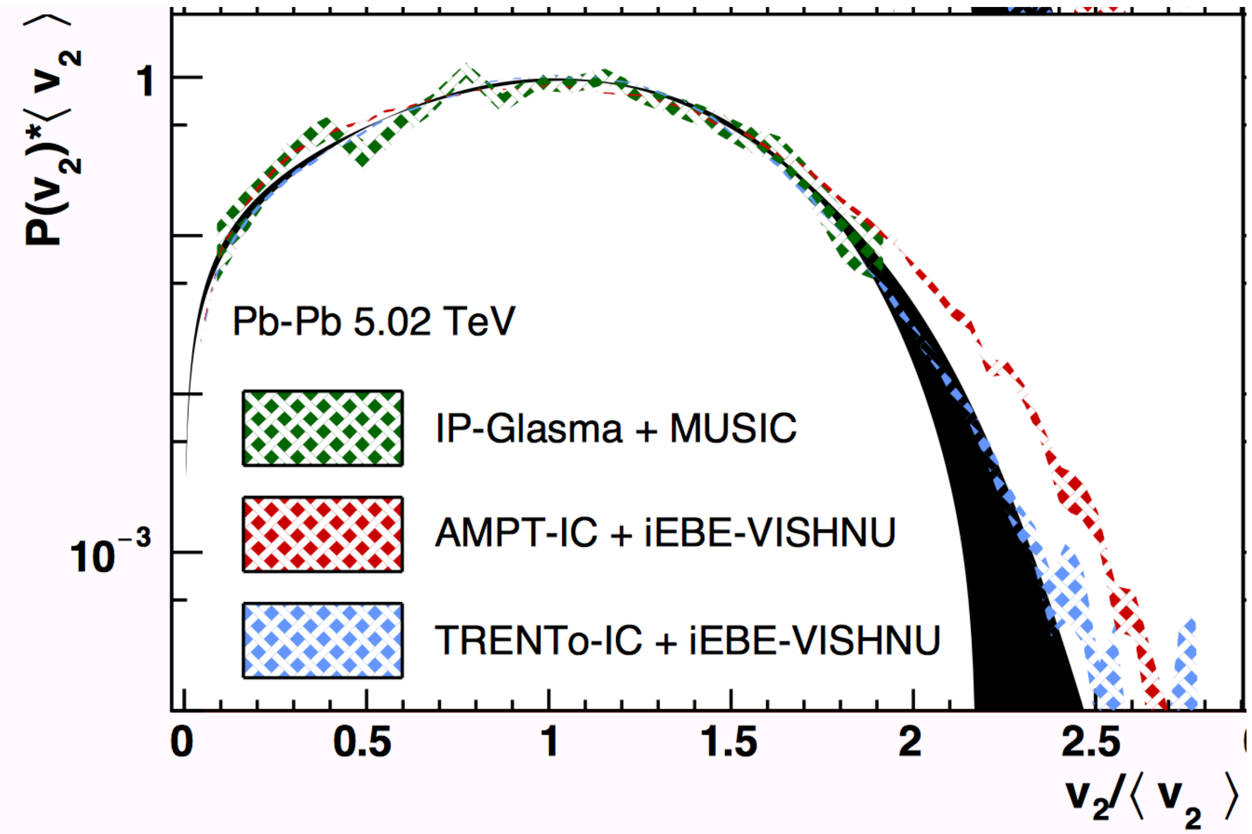

❖ Despite the precision of experimental data (ALICE, ATLAS, CMS), the differences of $P(\varepsilon_n)$ from various initial state models are minor

$P(v_n)$ -> $P(\varepsilon_n)$

How does v_n fluctuate

$$v_n \propto \varepsilon_n$$
$$P(v_n/\langle v_n\rangle) \approx P(\varepsilon_n/\langle \varepsilon_n\rangle)$$

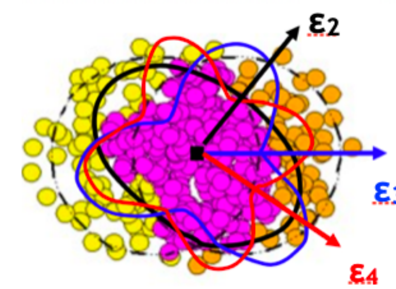

Final state $P(v_2/\langle v_2\rangle)$ → Initial state $P(\varepsilon_2/\langle \varepsilon_2\rangle)$

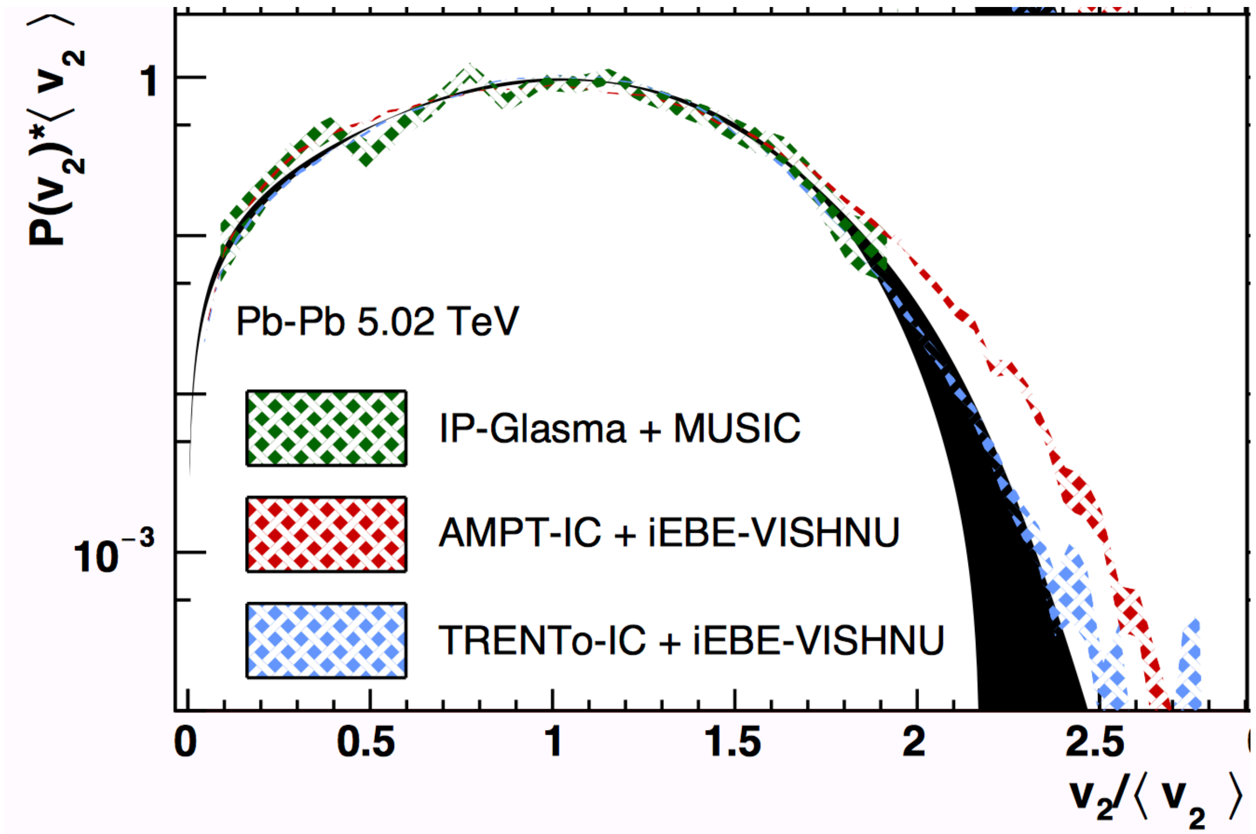

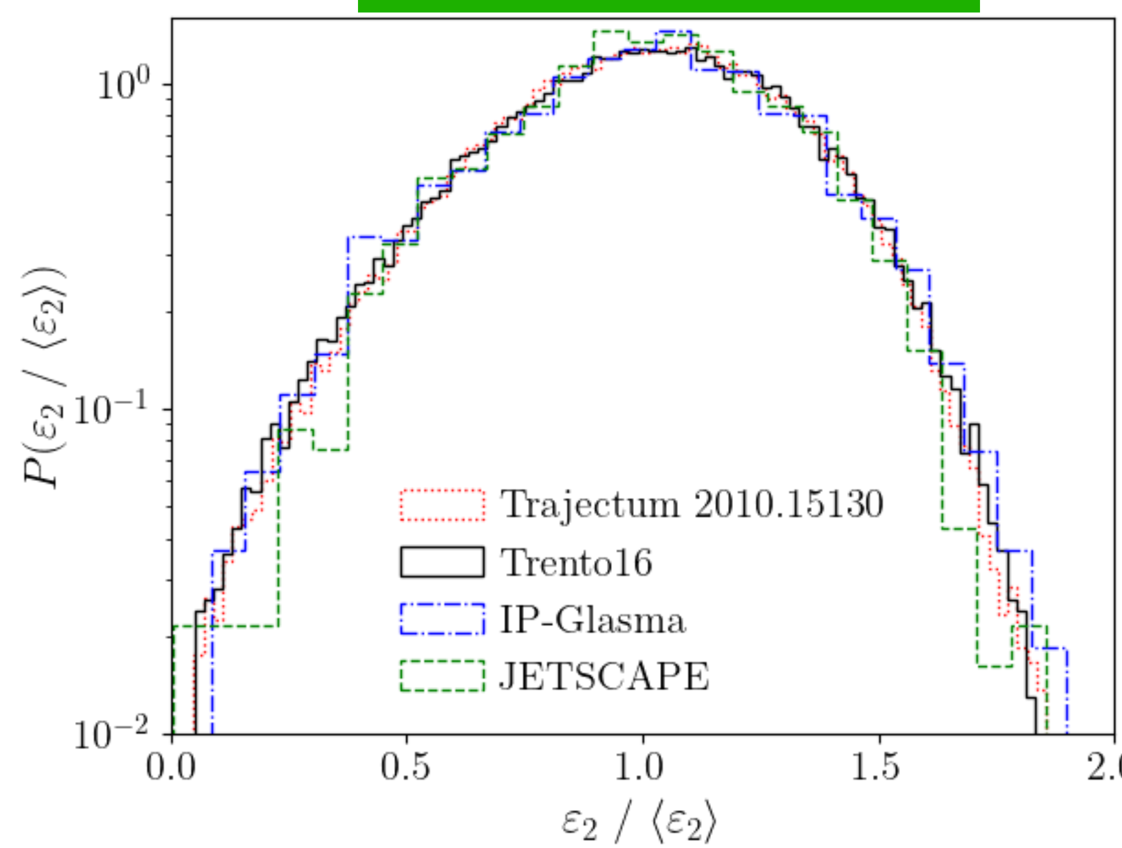

Minor difference from IC

❖ Despite the precision of experimental data (ALICE, ATLAS, CMS), the differences of $P(\varepsilon_n)$ from various initial state models are minor

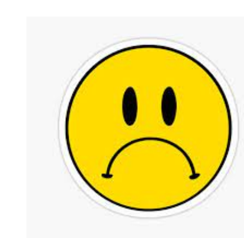

ψ_n - ψ_m correlations

How do ψ_n and ψ_m correlate

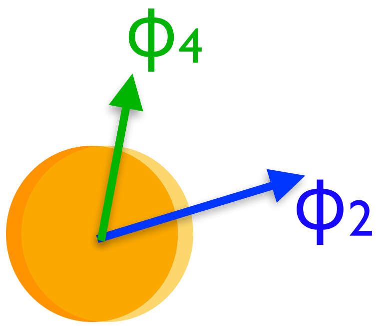

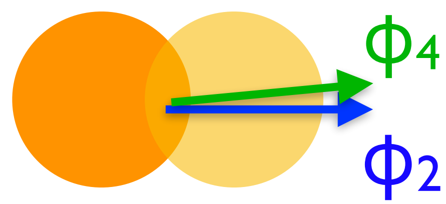

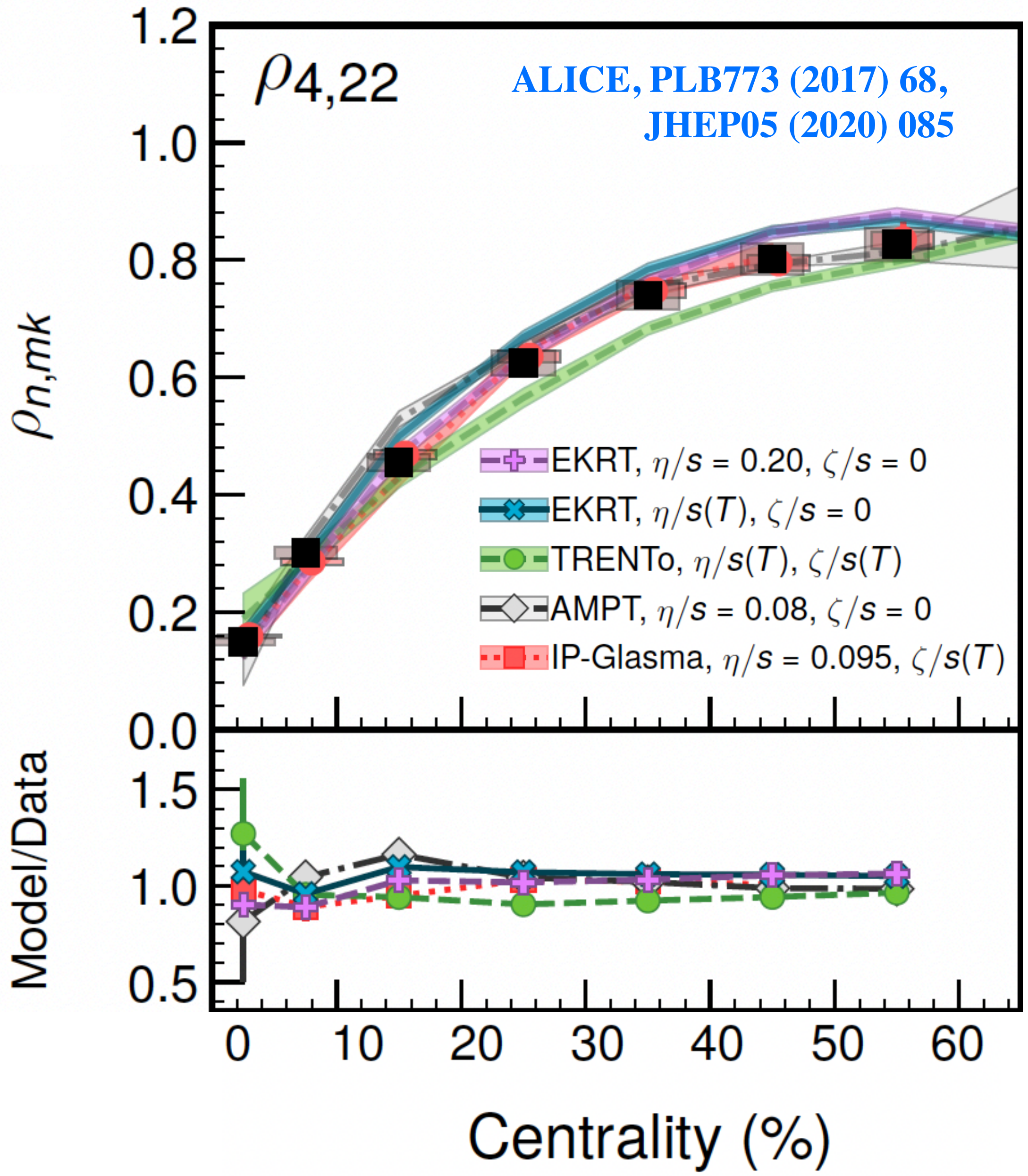

$\rho_{422} \approx \langle \cos(4\Psi_4 - 4\Psi_2) \rangle$

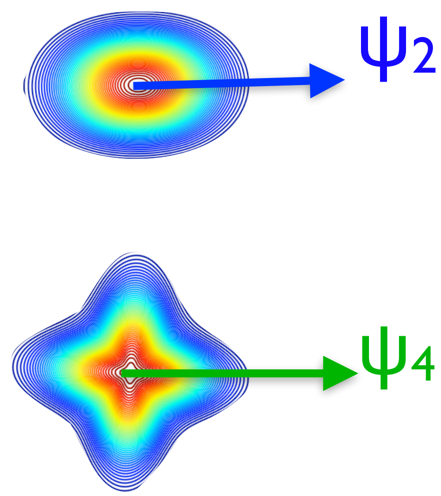

- **<u>Central collision:</u>**
  - Initial ϕ_2, ϕ_4 randomly fluctuate, weak correlations
  - <cos4(ψ_2-ψ_4)> is small
- **<u>Peripheral collisions:</u>**
  - Initial ϕ_2, ϕ_4 tend to align, strong correlations
  - <cos4(ψ_2-ψ_4)> is large

Initial conditions (size) through [p_T]

❖Shape of the fireball: Anisotropic flow

$$V_n \propto \mathcal{E}_n$$

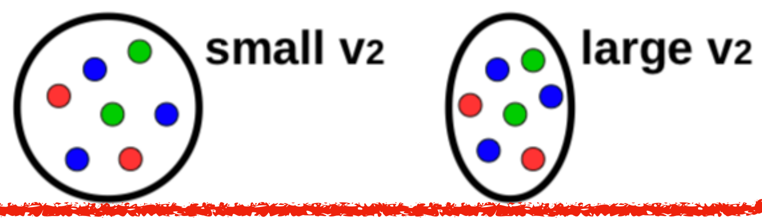

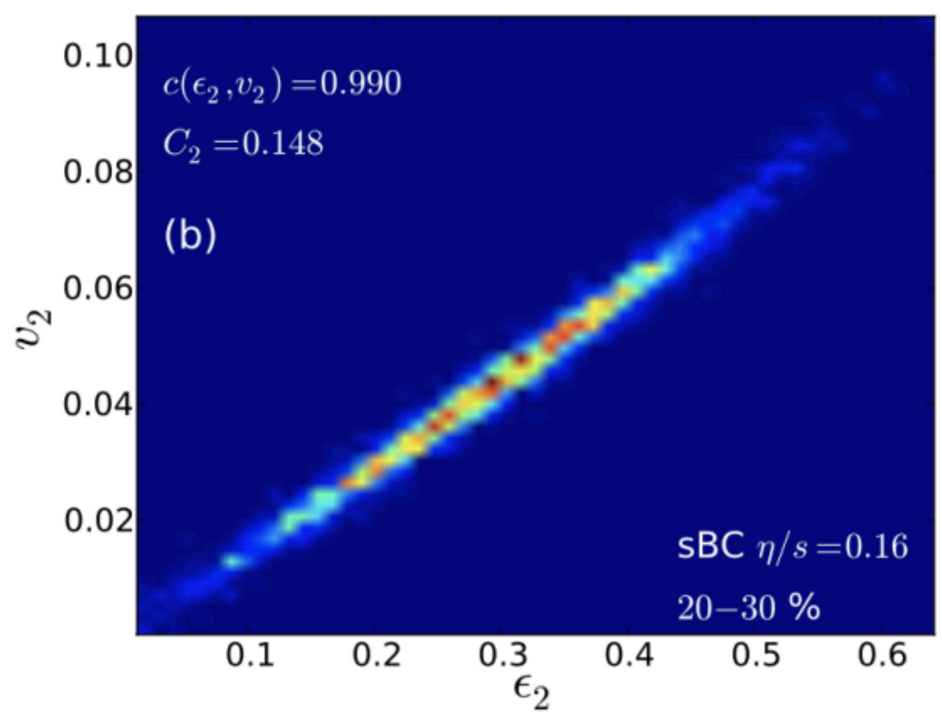

[H. Niemi et al., PRC 87 (2013) 5, 054901

Initial conditions (size) through $[p_T]$

❖Shape of the fireball: Anisotropic flow

$$V_n \propto \mathcal{E}_n$$

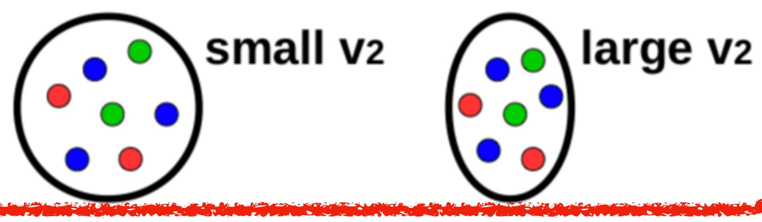

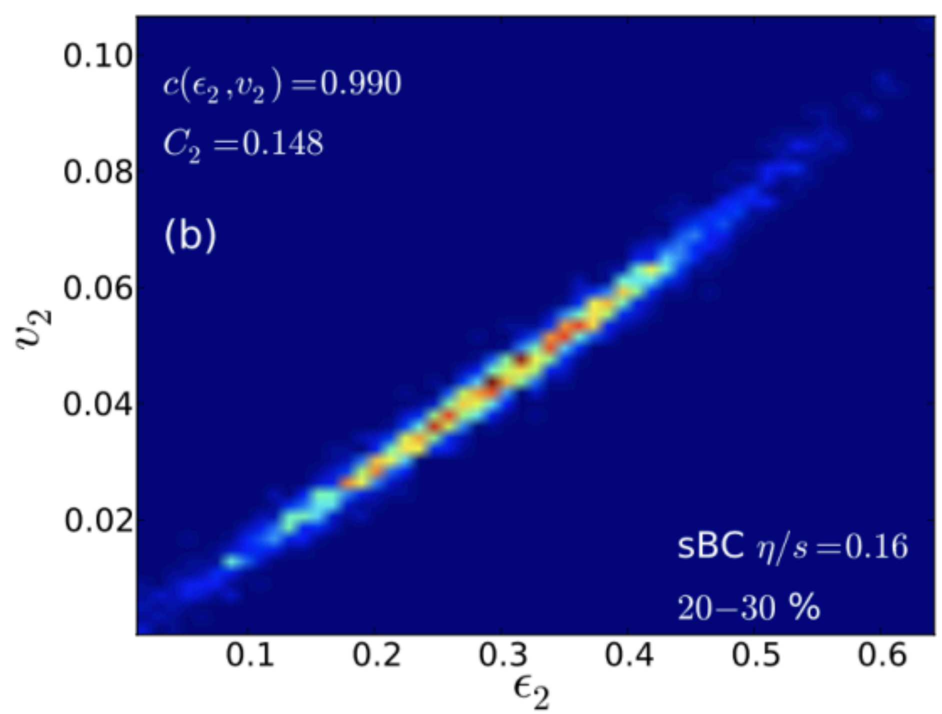

[H. Niemi et al., PRC 87 (2013) 5, 054901]

❖Size of the fireball: radial flow, $[p_T]$

$$\frac{d\langle p_t\rangle}{\langle p_t\rangle} \propto \frac{dE}{E}$$

$$\frac{d\langle p_t\rangle}{\langle p_t\rangle} \propto -\frac{dR}{R}$$

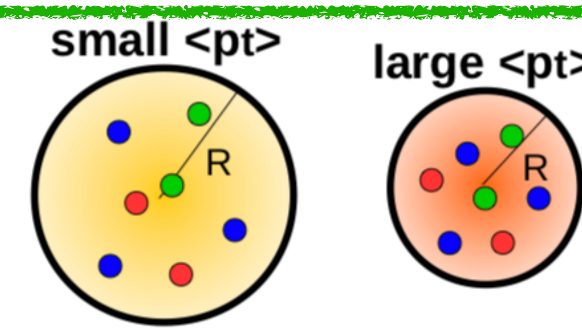

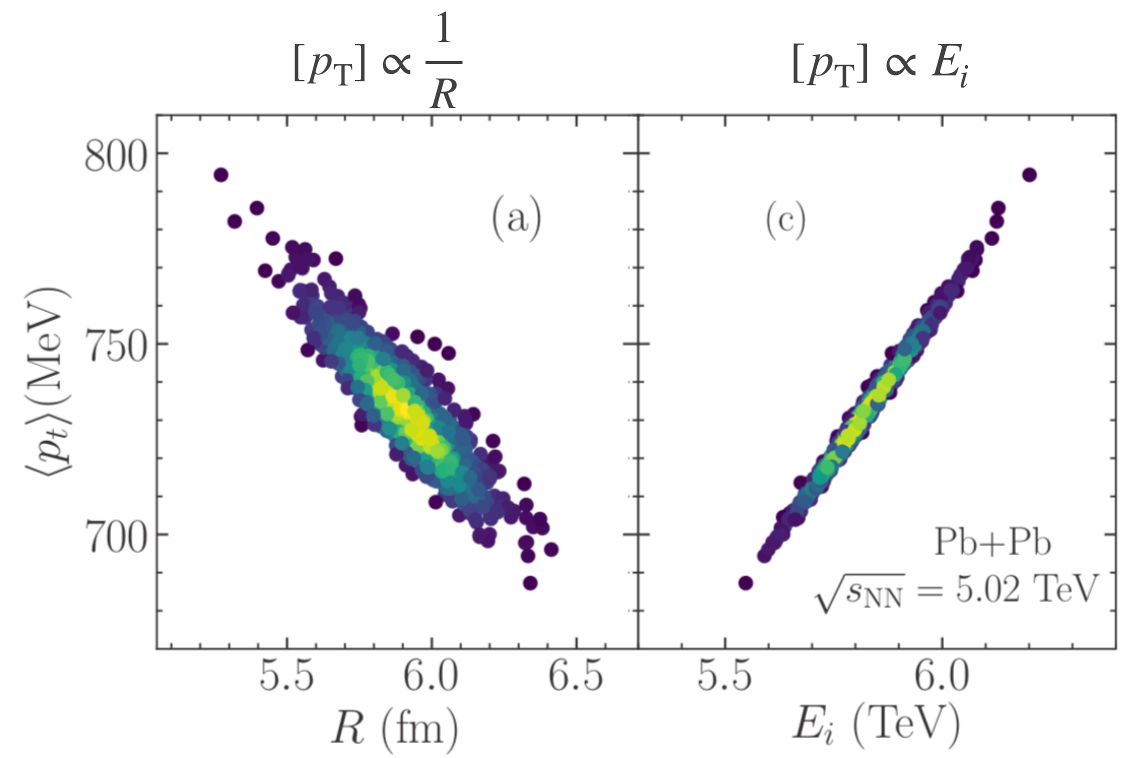

[G. Giacalone et al., PRC103 (2021) 2, 024909]

Initial conditions (size) through [p_T]

ALICE, PRC88 (2013) 044910, PRL111 (2013) 222301

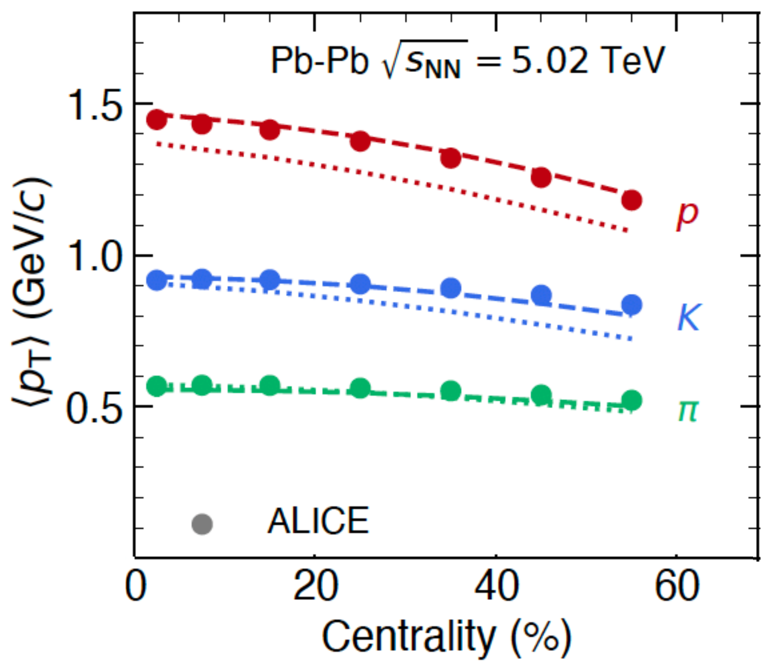

❖ Multi-particle [p_T] correlations:

$$\langle p_T \rangle = \frac{\sum_{i=1}^{N_{ch}} p_{T,i}}{N_{ch}}$$

$$\langle \Delta p_{T,i} \Delta p_{T,j} \rangle = \left\langle \frac{\sum_{i,j,\, i\neq j}^{N_{ch}} (p_{T,i} - \langle\langle p_T \rangle\rangle)(p_{T,j} - \langle\langle p_T \rangle\rangle)}{N_{ch}(N_{ch}-1)} \right\rangle_{ev}$$

$$\langle \Delta p_{T,i} \Delta p_{T,j} \Delta p_{T,k} \rangle = \left\langle \frac{\sum_{i,j,k,\, i\neq j \neq k}^{N_{ch}} (p_{T,i} - \langle\langle p_T \rangle\rangle)(p_{T,j} - \langle\langle p_T \rangle\rangle)(p_{T,k} - \langle\langle p_T \rangle\rangle)}{N_{ch}(N_{ch}-1)(N_{ch}-2)} \right\rangle_{ev}$$

❖Size of the fireball: radial flow, [p_T]

$$\frac{d\langle p_t \rangle}{\langle p_t \rangle} \propto \frac{dE}{E}$$

$$\frac{d\langle p_t \rangle}{\langle p_t \rangle} \propto -\frac{dR}{R}$$

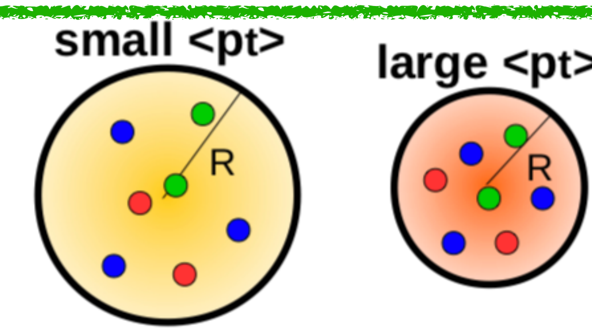

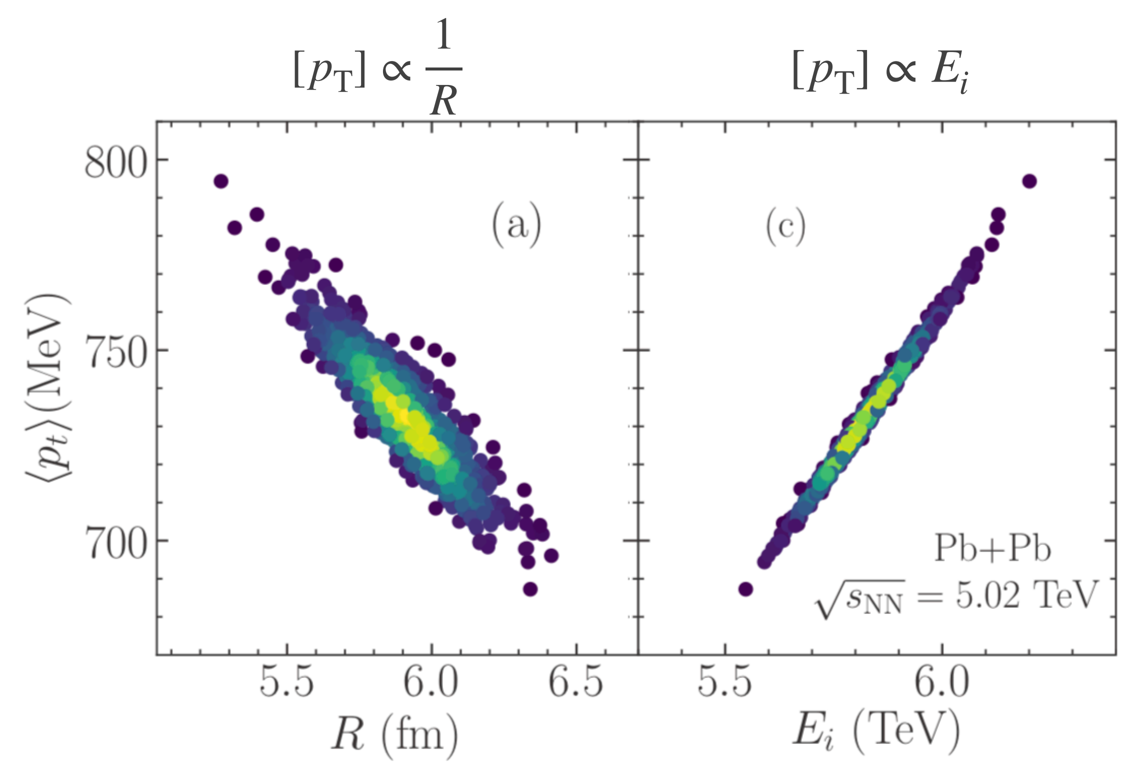

[G. Giacalone et al., PRC103 (2021) 2, 024909]

[p_T] fluctuations

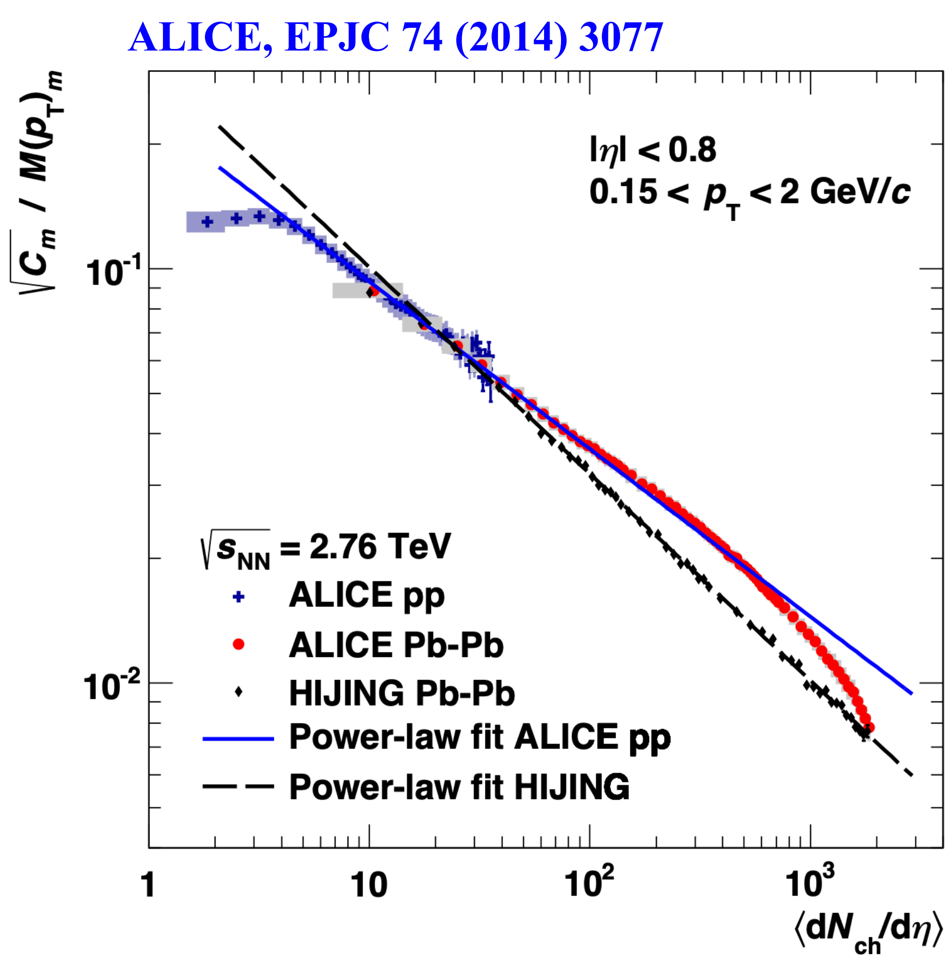

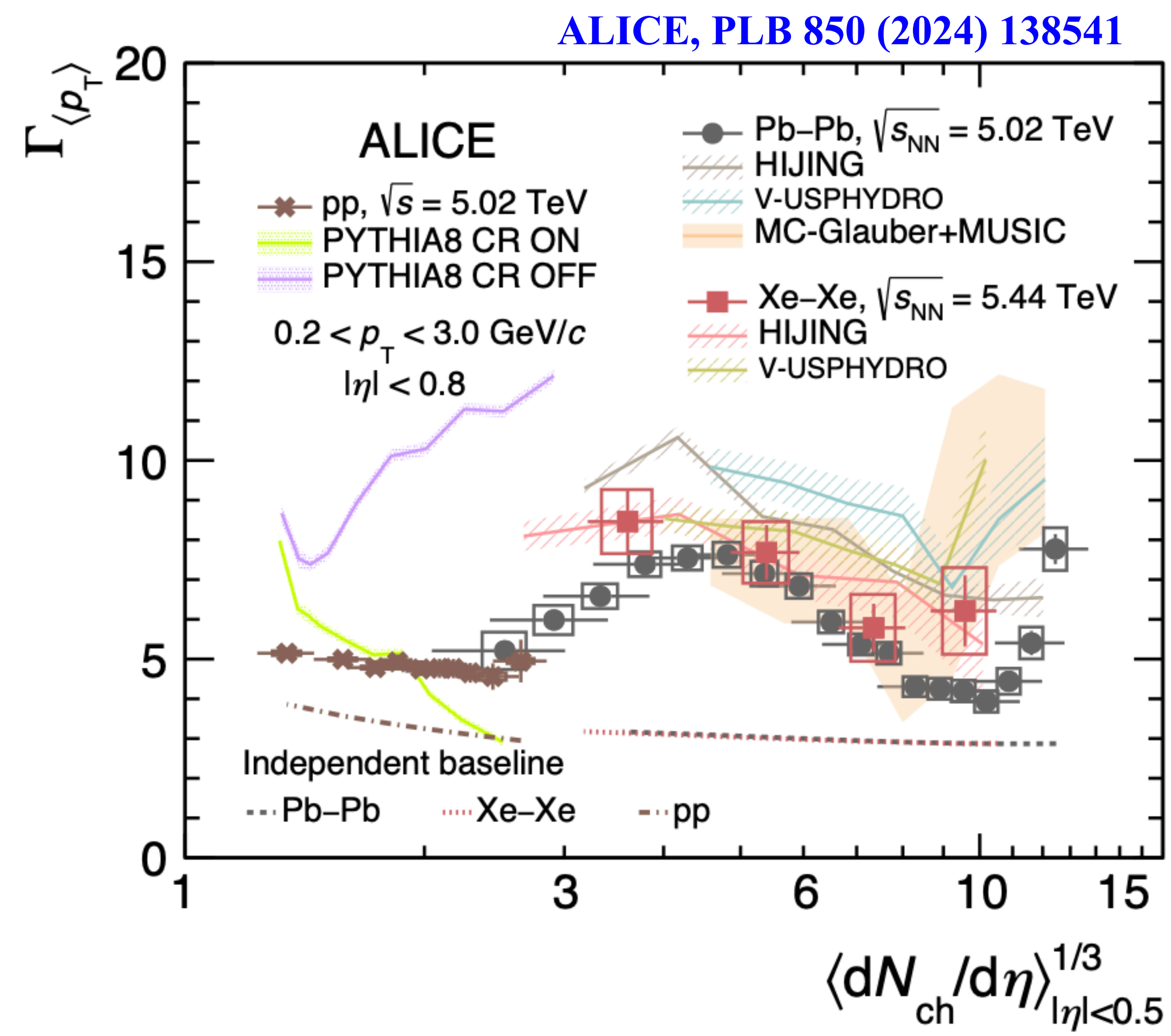

2nd-moment / 1st-moment **3rd-moment / 2nd-moment**

- [P_T] and its event-by-event fluctuations measured in heavy-ion collisions at the LHC -> probe initial ***size*** and ***size fluctuations***

Bayesian analyses: status before 2022

J.E. Bernhard etc, Nature Physics,15, 1113 (2019)

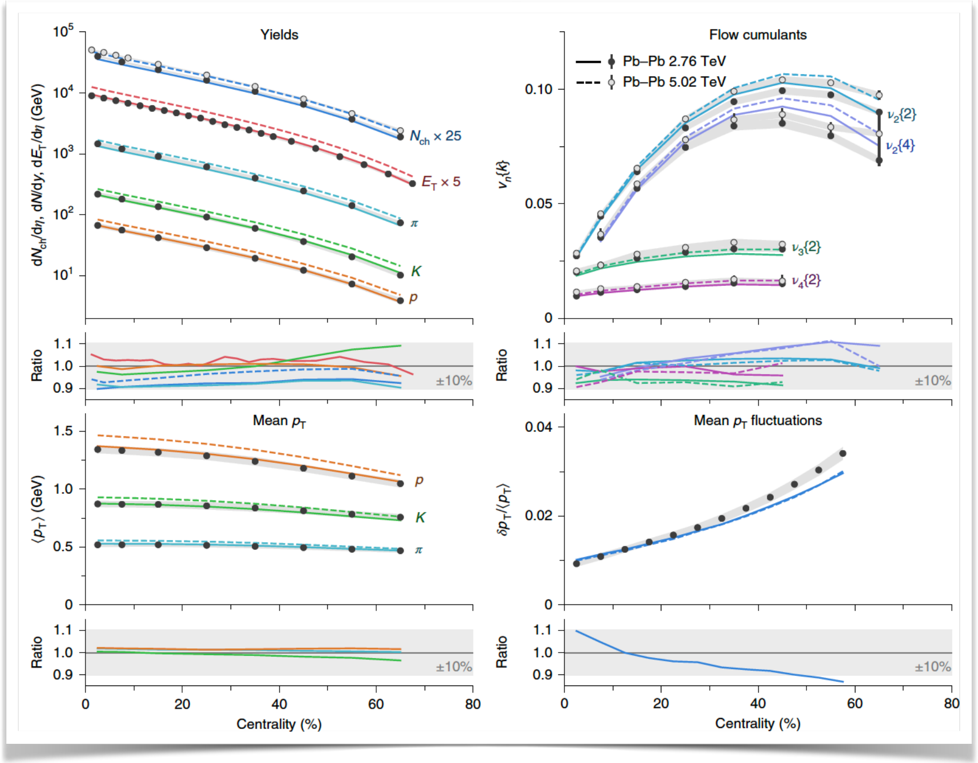

Bayesian analyses: status before 2022

J.E. Bernhard etc, Nature Physics,15, 1113 (2019)

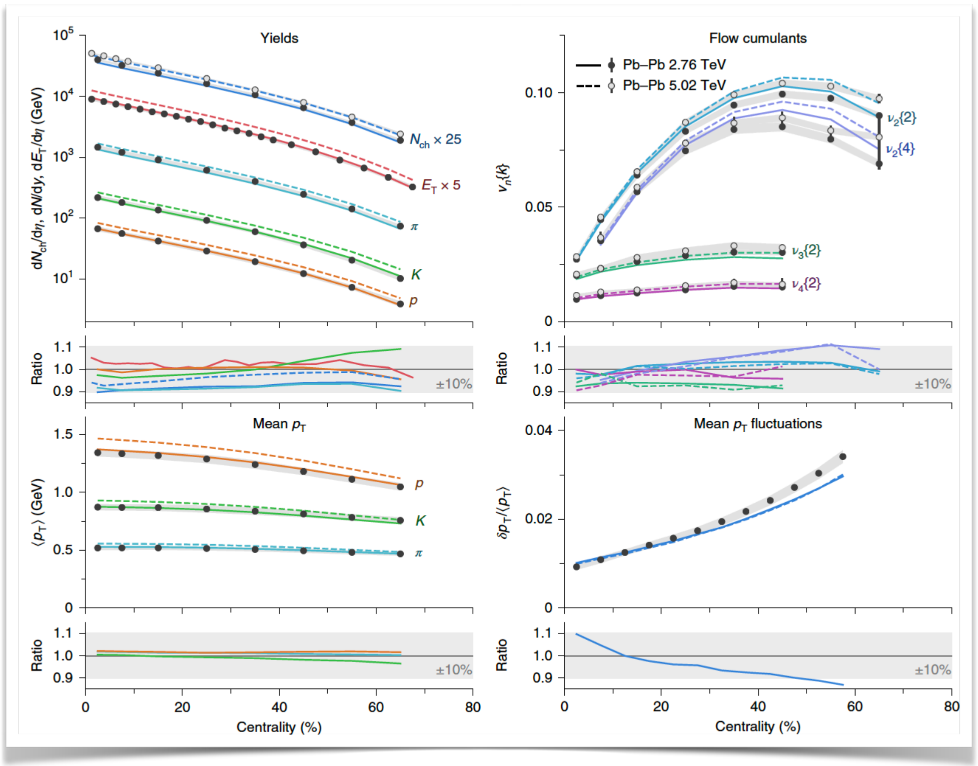

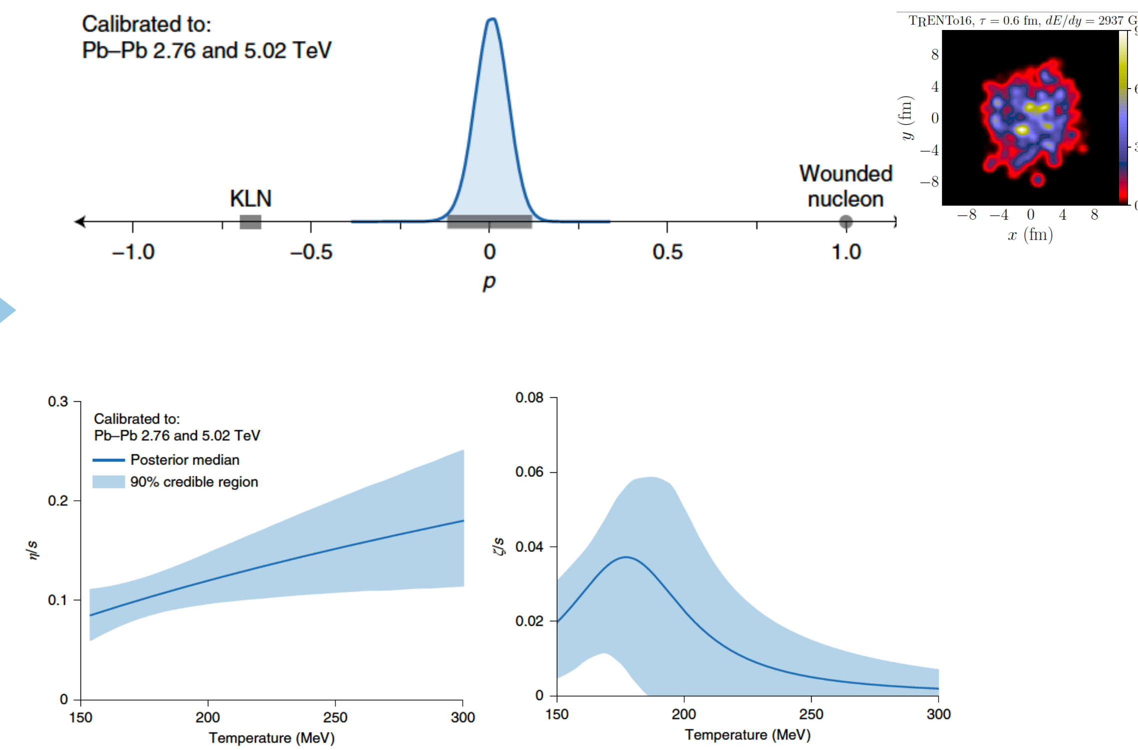

Bayesian analyses: status before 2022

J.E. Bernhard etc, Nature Physics,15, 1113 (2019)

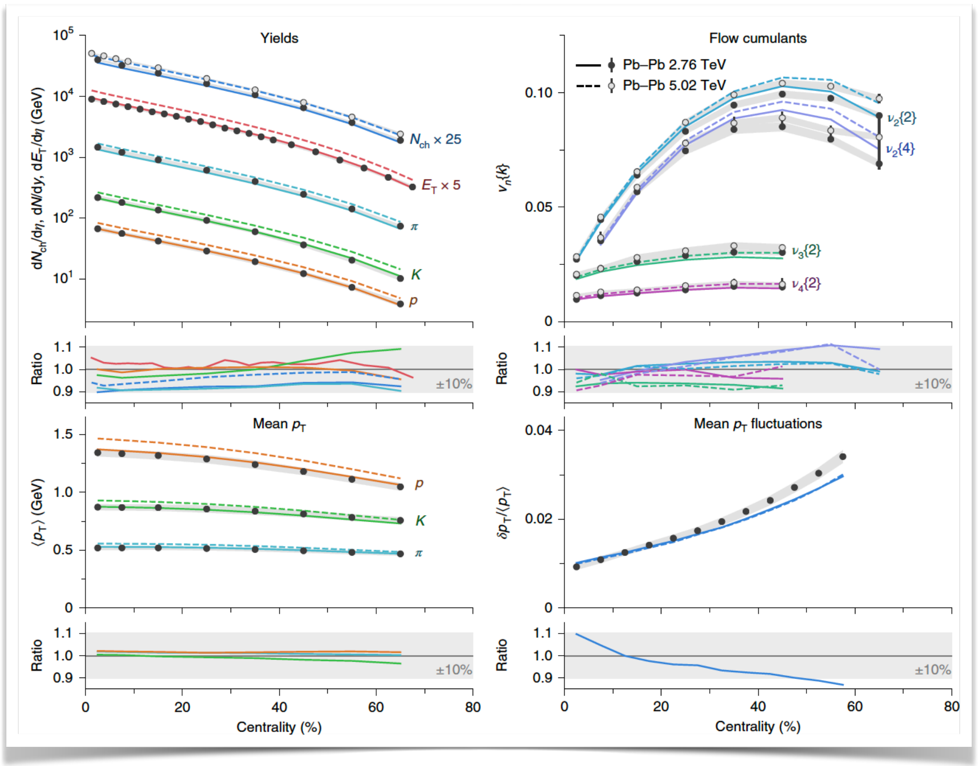

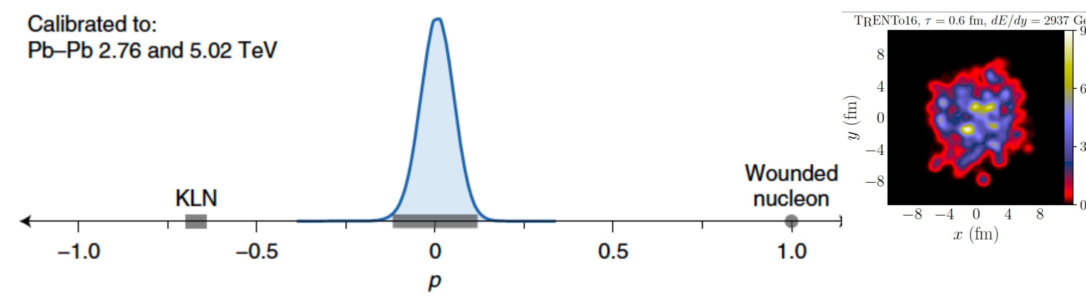

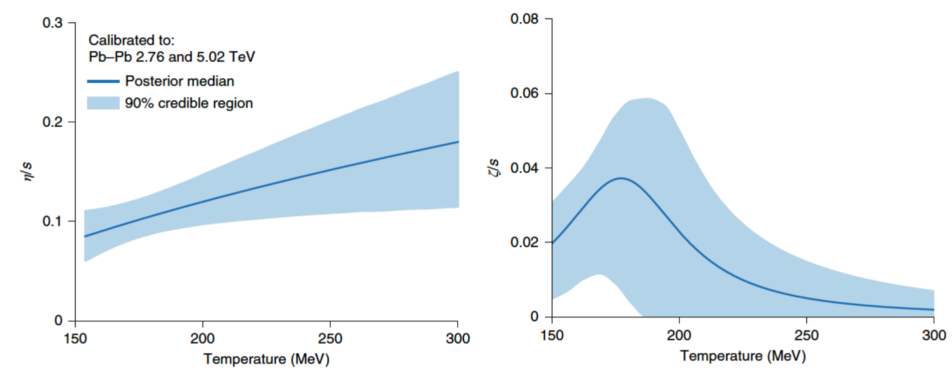

JETSCAPE, Phys. Rev. Lett. 126, 242301 (2021)

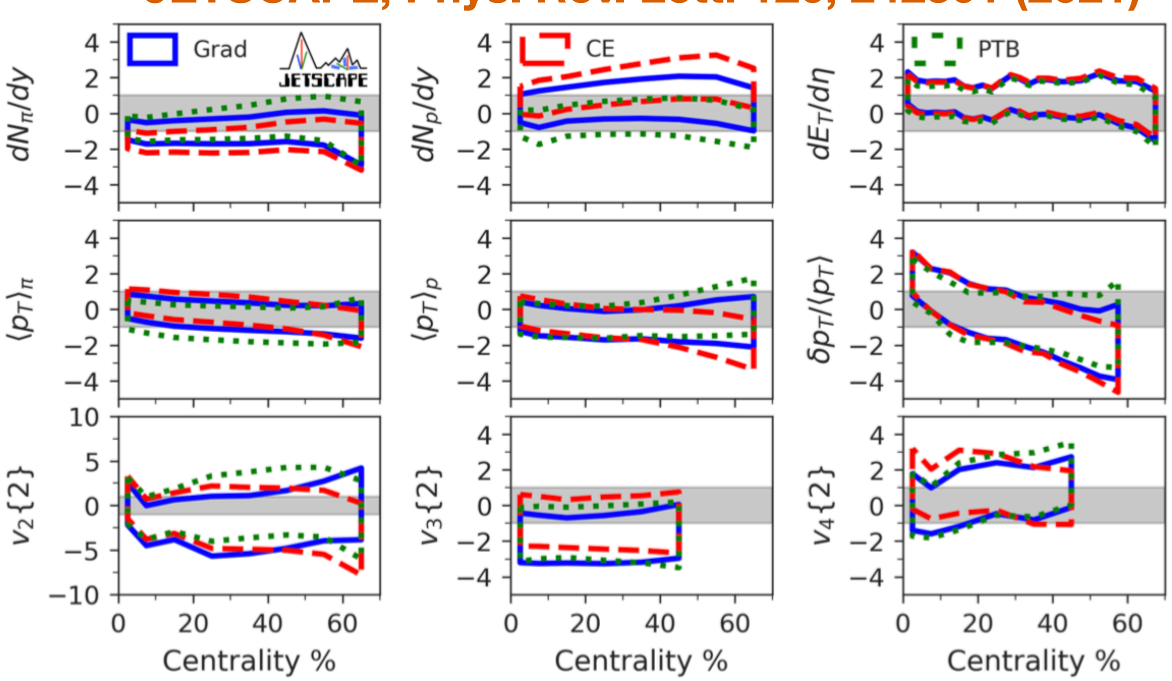

Bayesian analyses: status before 2022

J.E. Bernhard etc, Nature Physics,15, 1113 (2019)

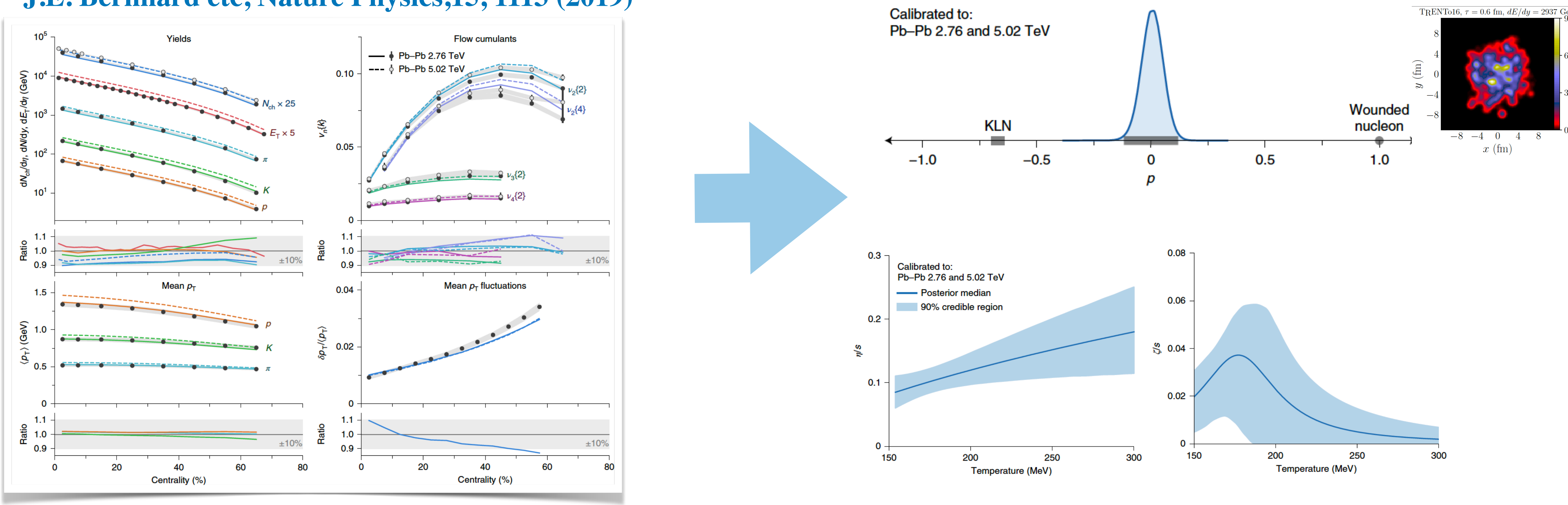

JETSCAPE, Phys. Rev. Lett. 126, 242301 (2021)

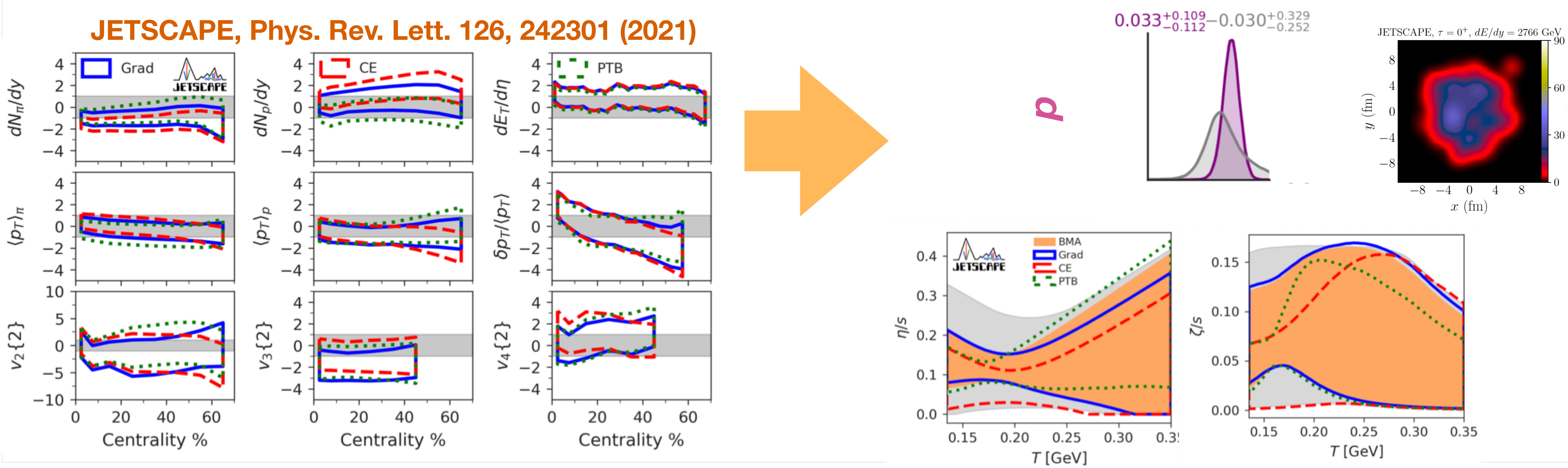

v_n-[p_T] correlations

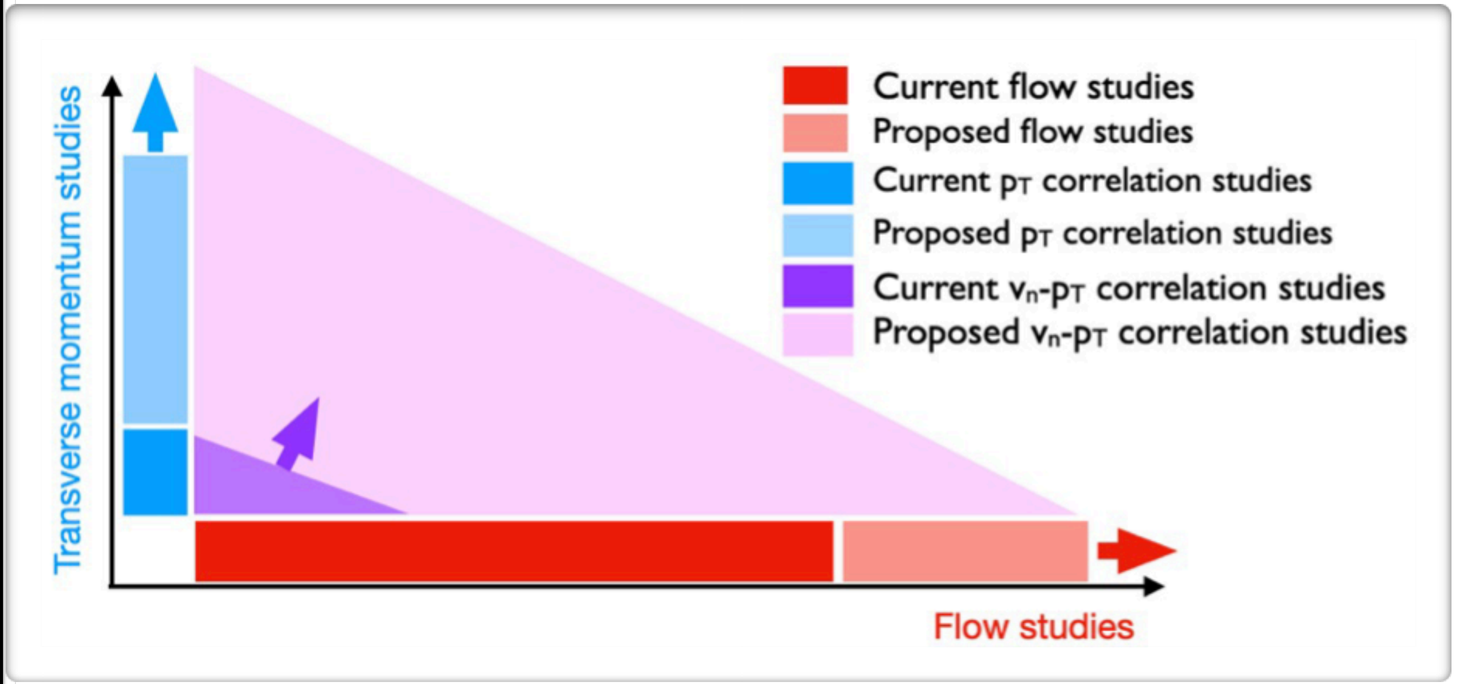

❖ **Shape** of the fireball: Anisotropic flow

❖ **Size** of the fireball: radial flow, $[p_{\mathrm{T}}]$

❖ Final state: correlation between v_n and p_{T}

$$\rho(v_n^2, [p_{\mathrm{T}}]) = \frac{cov(v_n^2, [p_{\mathrm{T}}])}{\sqrt{var(v_n^2)}\sqrt{var([p_{\mathrm{T}}])}}$$

P. Bozek etc, PRC96 (2017) 014904

❖ Considering $v_n \propto \varepsilon_n$, $[p_T] \propto E_0$

$$\rho(v_n^2, [p_{\mathrm{T}}]) = \rho(\varepsilon_n^2, [E_0])$$

final-state model calculation

Initial-state model estimation

❖ One can compare $\rho(v_n^2, [p_{\mathrm{T}}])$ measurements to $\rho(\varepsilon_n^2, [E_0])$ calculations, to constrain the initial state model

$\rho(v_n^2, [p_T])$ in Pb-Pb

ALICE, PLB 834 (2022) 137393

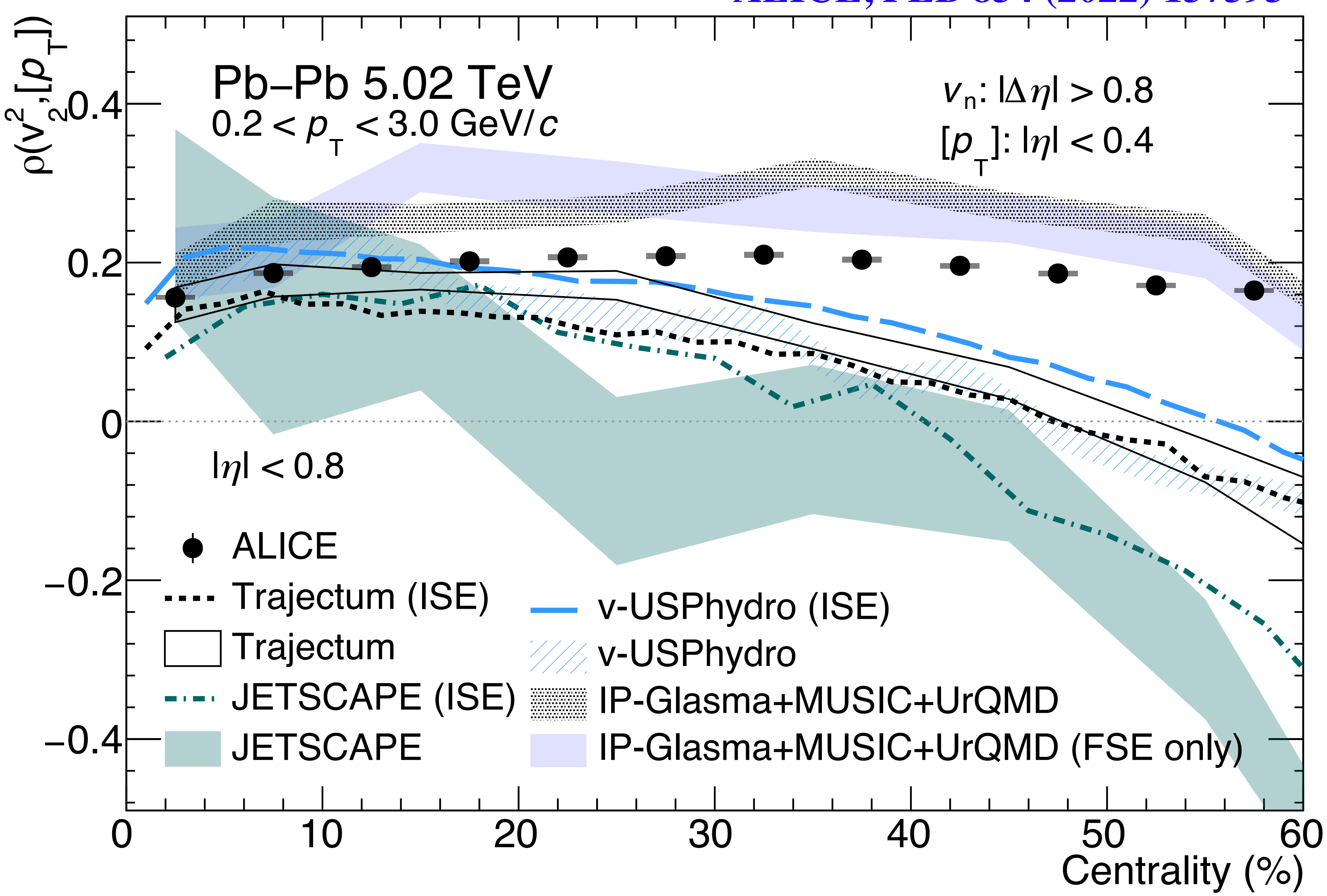

$$\rho(v_n^2, [p_T]) = \frac{cov(v_n^2, [p_T])}{\sqrt{var(v_n^2)}\sqrt{var([p_T])}}$$

v-USPhydro, PRC103 (2021) 2, 024909

IP-Glasma, PRC102, 034905 (2020)

JETSCAPE, PRL126, 242301 (2021) Privation communication

Trajectum, PRL126, 202301 (2021) Privation communication

- ❖ IP-Glasma+MUSIC+UrQMD shows a weak centrality dependence and describe the data fairly well
- ❖ State-of-the-art Bayesian results (Trajectum, JETSCAPE) with TRENTo initial conditions all show strong centrality dependence, negative values for centrality >40%

Constraining nucleon width

❖ Sensitive to the nucleon width parameter (size of nucleon)

- IP-Glasma ~ 0.4 fm; v-USPhydro ~ 0.5 fm; Trajectum~0.7 fm; JETSCAPE (TRENTo) ~ 1.1 fm
- w(IP-Glasma) < w(v-USPhydro) < w(Trajectum) < w(JETSCAPE)
- New constraints on the ***nucleon size***

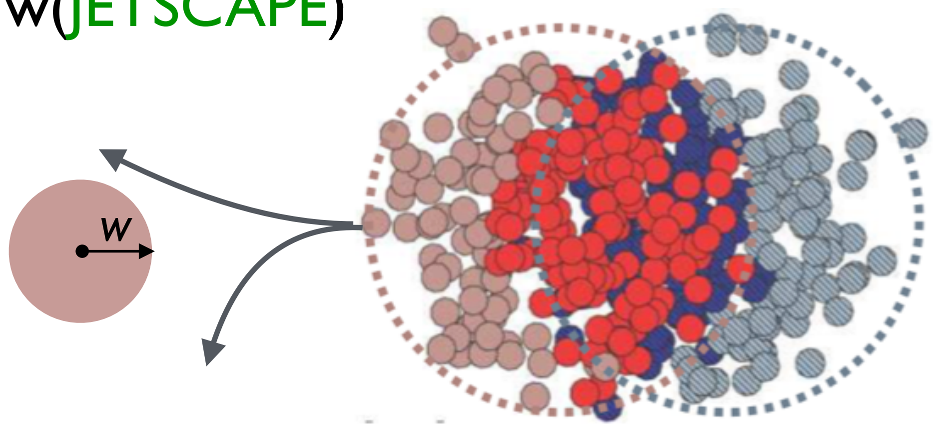

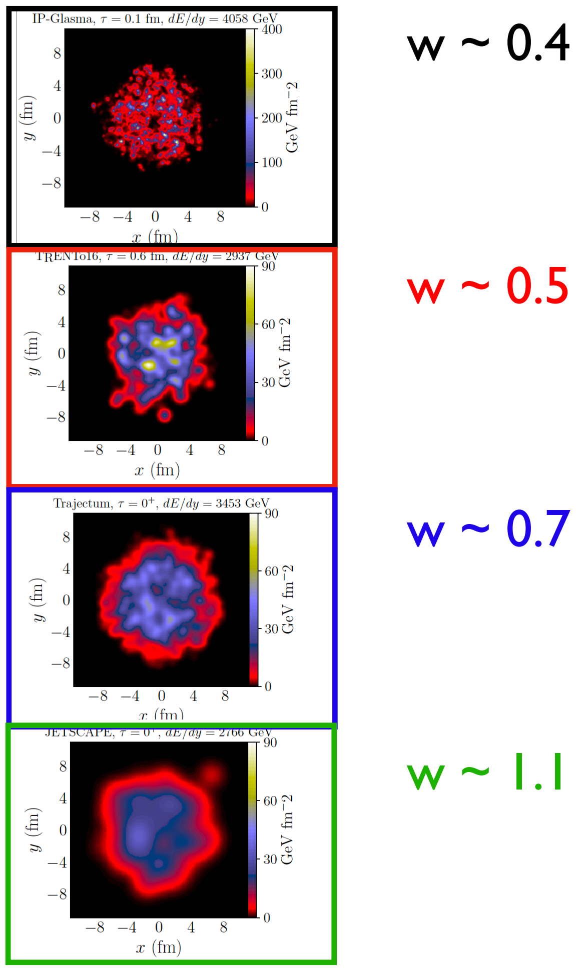

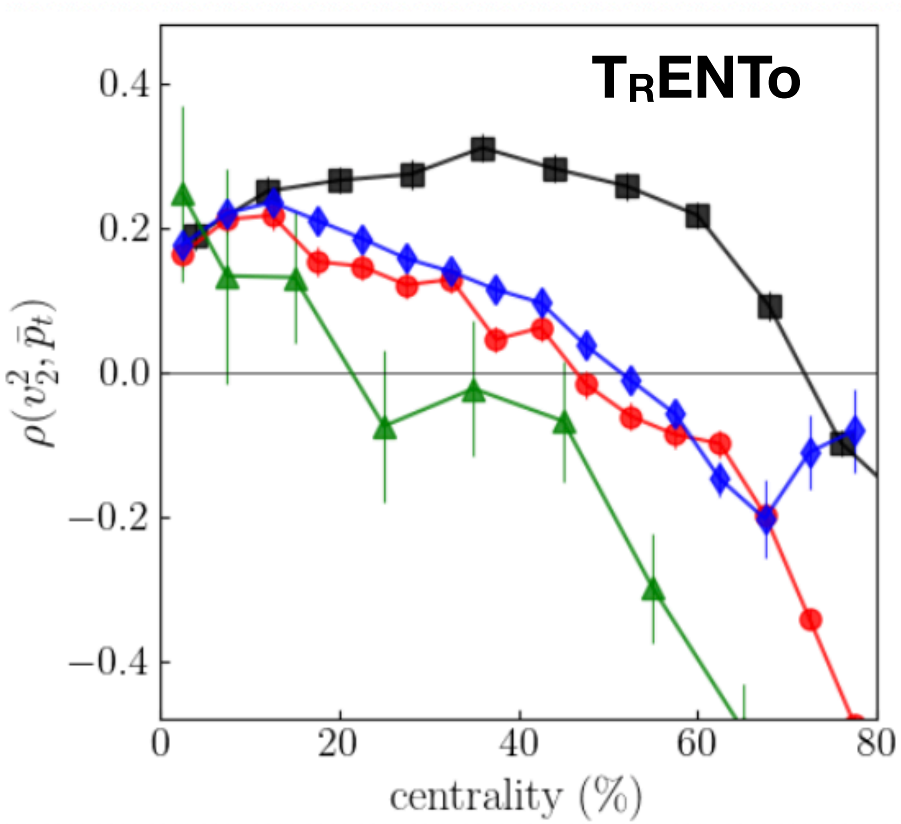

G. Giacalone etc., PRL128, 042301 (2022)

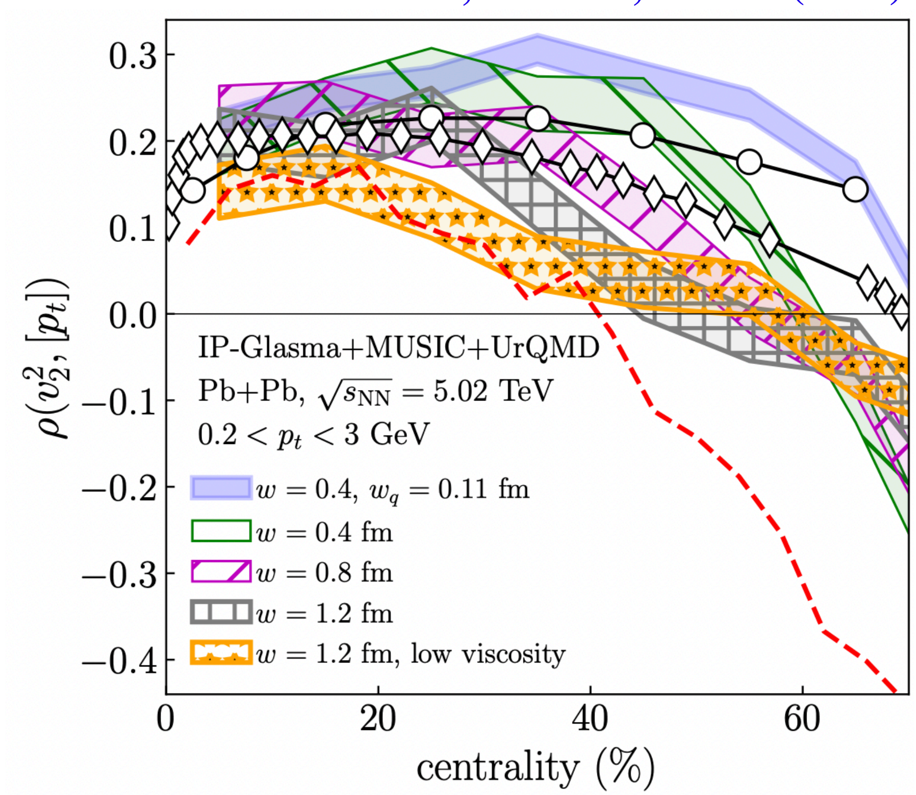

Nuclear structure at high energies

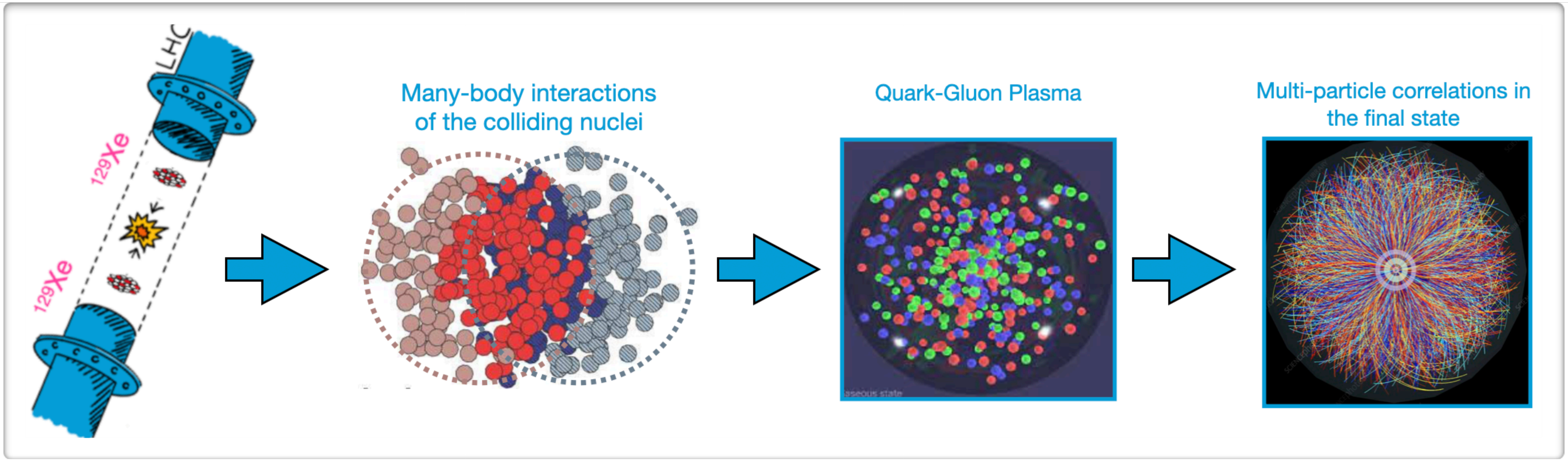

Nuclear structure at high energies

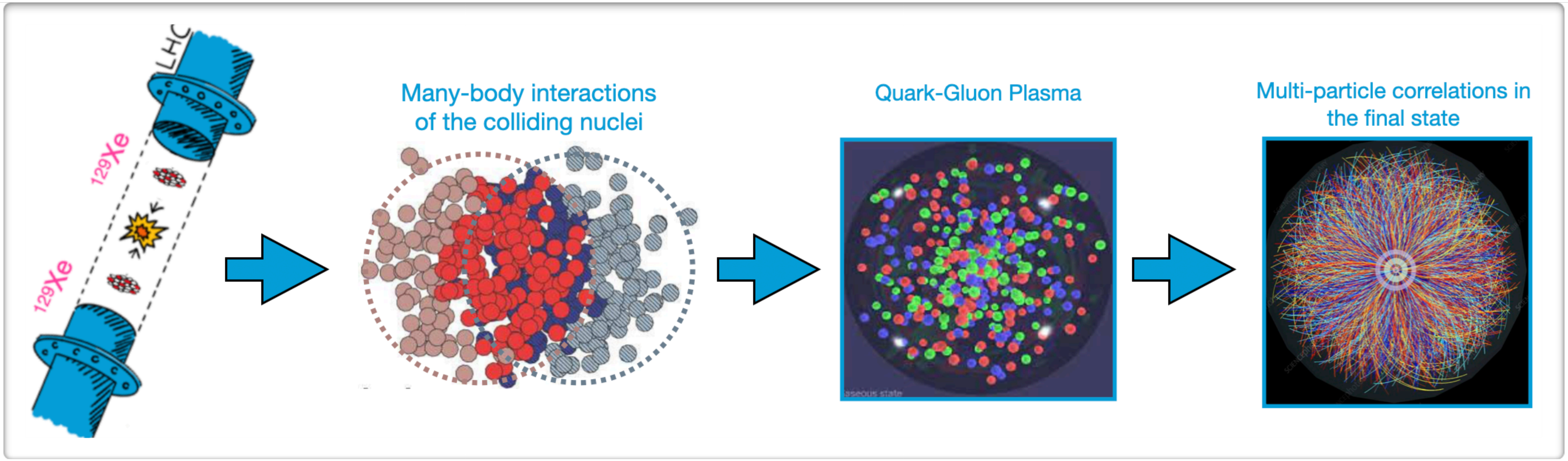

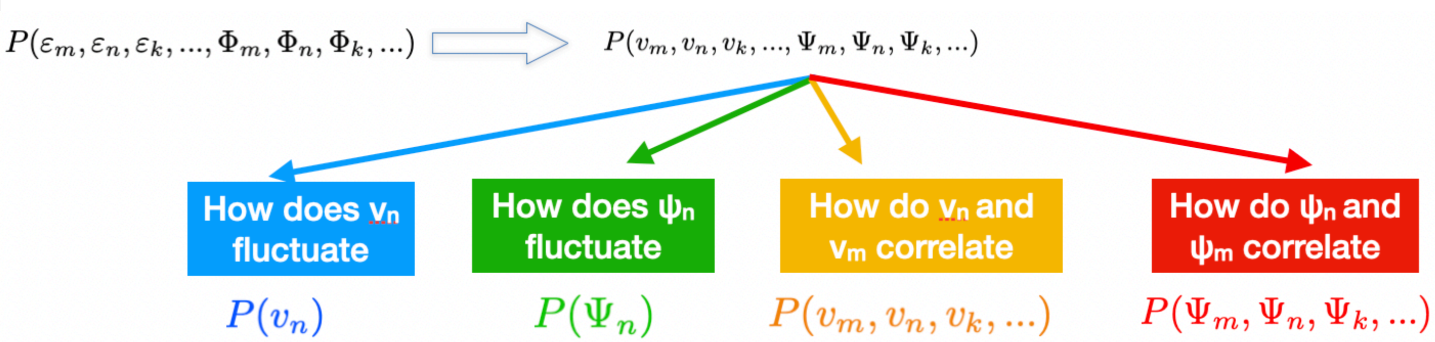

ALICE, Physics Letters B 850, 138477 (2024)
ALICE, JHEP 05 (2023) 243
ALICE, Phys. Rev. C Letters, 107 (2023) 051901
ALICE, Physics Letters B 834, 137393 (2022)
ALICE, Physics Letters B 818, 136354 (2021)
ALICE, Phys. Rev. C 104, 024903 (2021)
ALICE, Phys. Rev. C 103, 024913 (2021)
ALICE, ALICE-PUBLIC-2021-004 (2021)
ALICE, JHEP 06, 147 (2020)
ALICE, JHEP 05, 085 (2020)
ALICE, Eur. Phys. J. C 80, 846 (2020)
ALICE, Physics Letters B784 (2018) 82
ALICE, Phys. Rev. C 97, 024906 (2018)
ALICE, JHEP07 (2018) 103

Nuclear structure at high energies

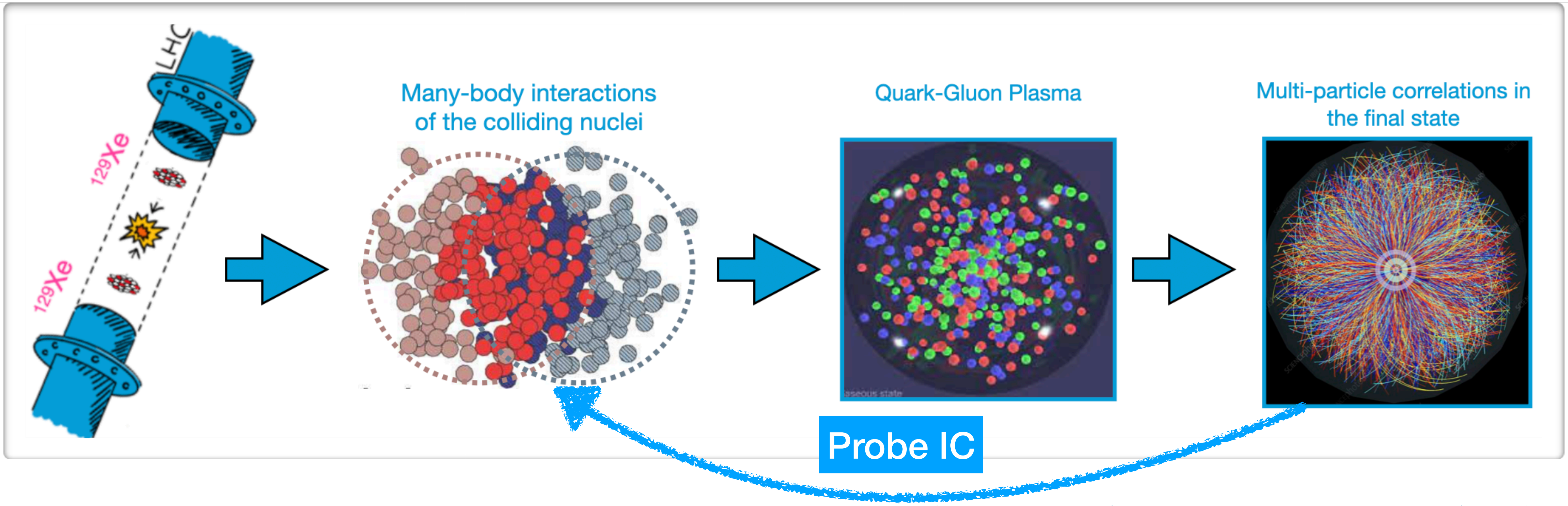

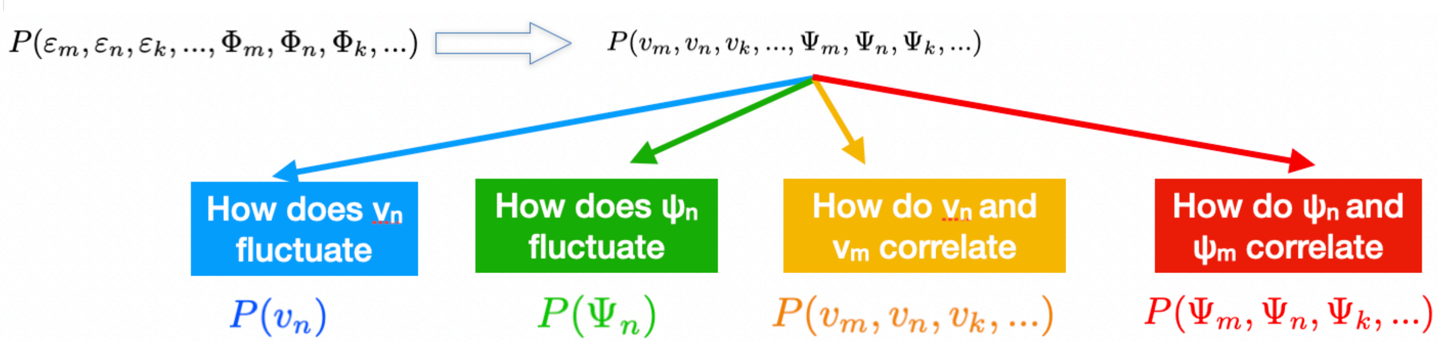

ALICE, Physics Letters B 850, 138477 (2024)
ALICE, JHEP 05 (2023) 243
ALICE, Phys. Rev. C Letters, 107 (2023) 051901
ALICE, Physics Letters B 834, 137393 (2022)
ALICE, Physics Letters B 818, 136354 (2021)
ALICE, Phys. Rev. C 104, 024903 (2021)
ALICE, Phys. Rev. C 103, 024913 (2021)
ALICE, ALICE-PUBLIC-2021-004 (2021)
ALICE, JHEP 06, 147 (2020)
ALICE, JHEP 05, 085 (2020)
ALICE, Eur. Phys. J. C 80, 846 (2020)
ALICE, Physics Letters B784 (2018) 82
ALICE, Phys. Rev. C 97, 024906 (2018)
ALICE, JHEP07 (2018) 103

Nuclear structure at high energies

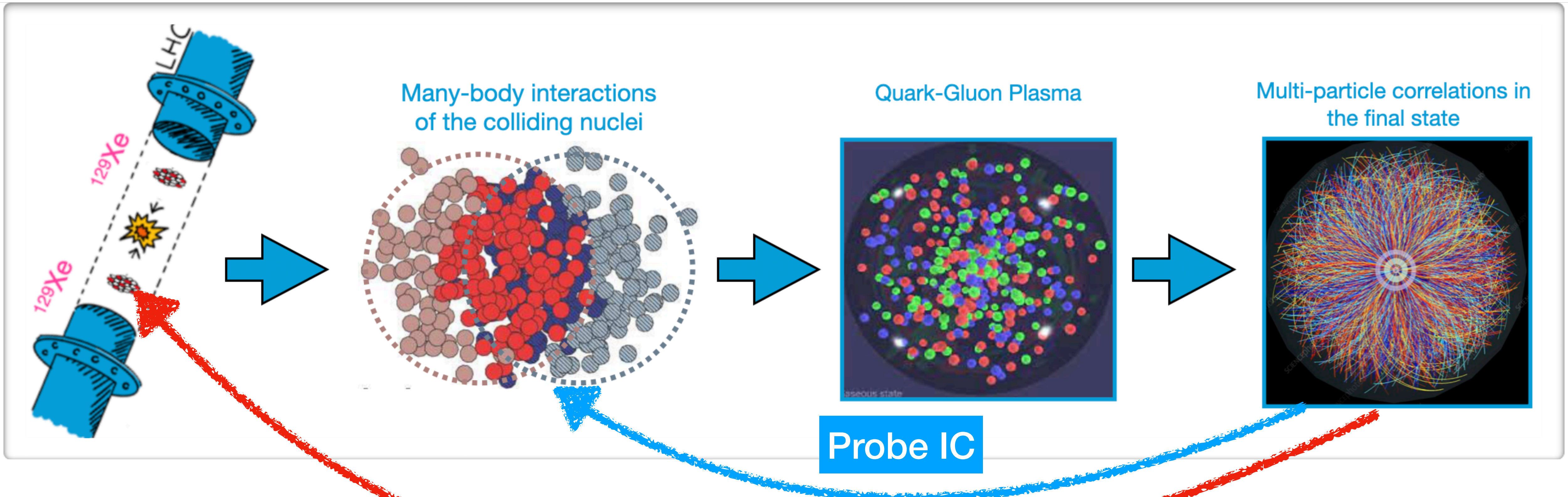

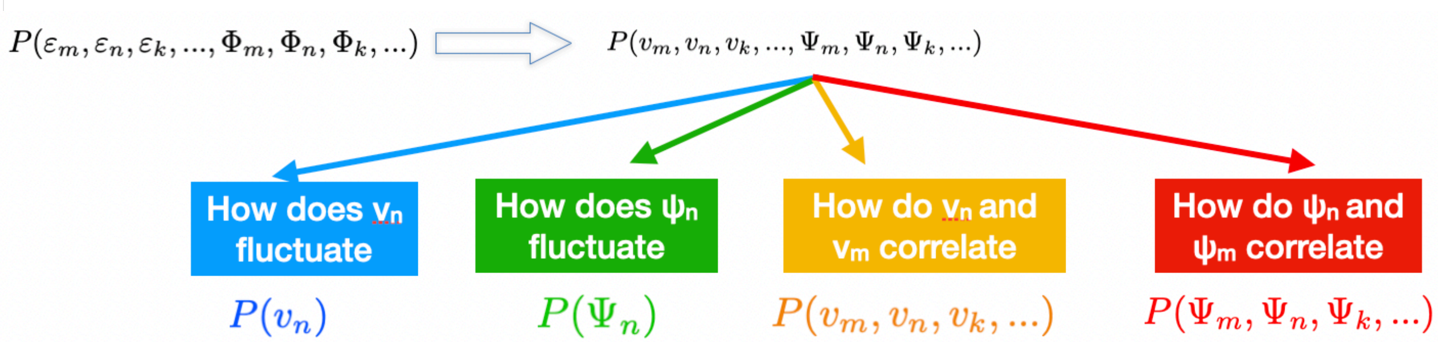

ALICE, Physics Letters B 850, 138477 (2024)
ALICE, JHEP 05 (2023) 243
ALICE, Phys. Rev. C Letters, 107 (2023) 051901
ALICE, Physics Letters B 834, 137393 (2022)
ALICE, Physics Letters B 818, 136354 (2021)
ALICE, Phys. Rev. C 104, 024903 (2021)
ALICE, Phys. Rev. C 103, 024913 (2021)
ALICE, ALICE-PUBLIC-2021-004 (2021)
ALICE, JHEP 06, 147 (2020)
ALICE, JHEP 05, 085 (2020)
ALICE, Eur. Phys. J. C 80, 846 (2020)
ALICE, Physics Letters B784 (2018) 82
ALICE, Phys. Rev. C 97, 024906 (2018)
ALICE, JHEP07 (2018) 103

Nuclear structure at low energies

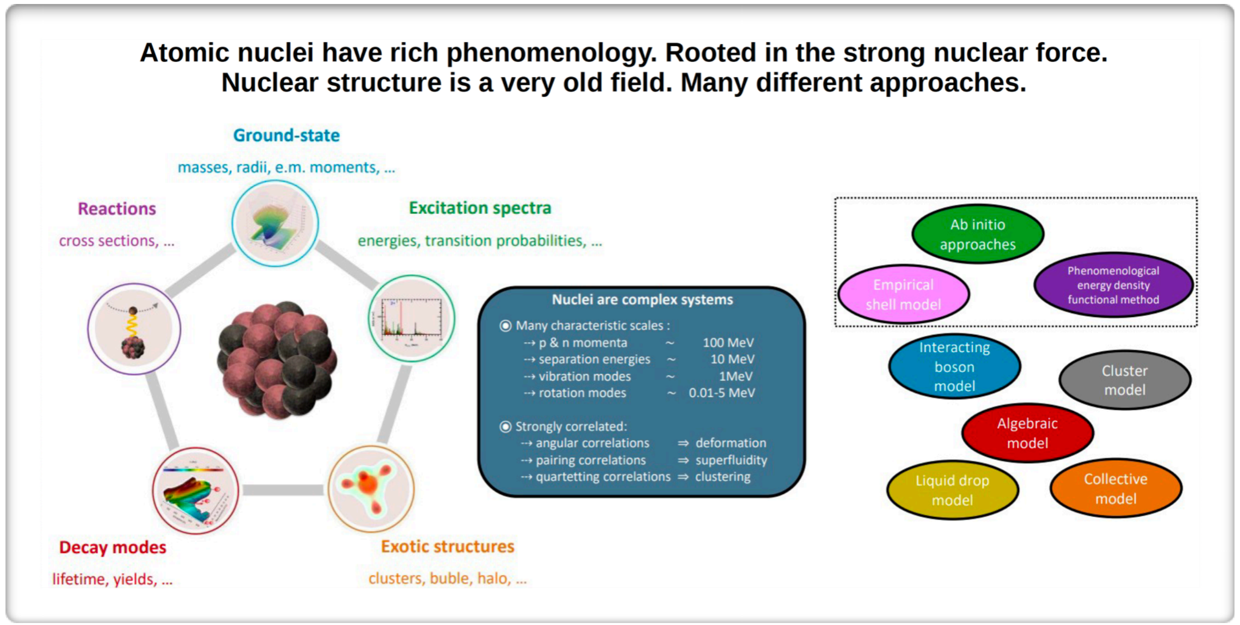

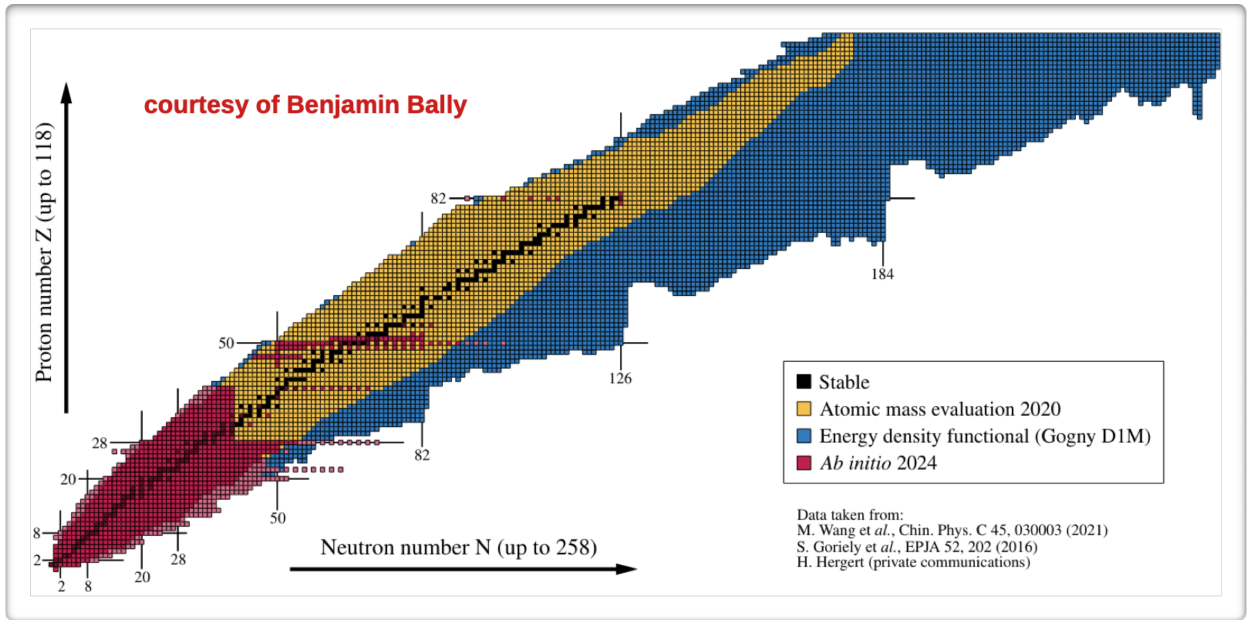

Nuclear structure at low energies

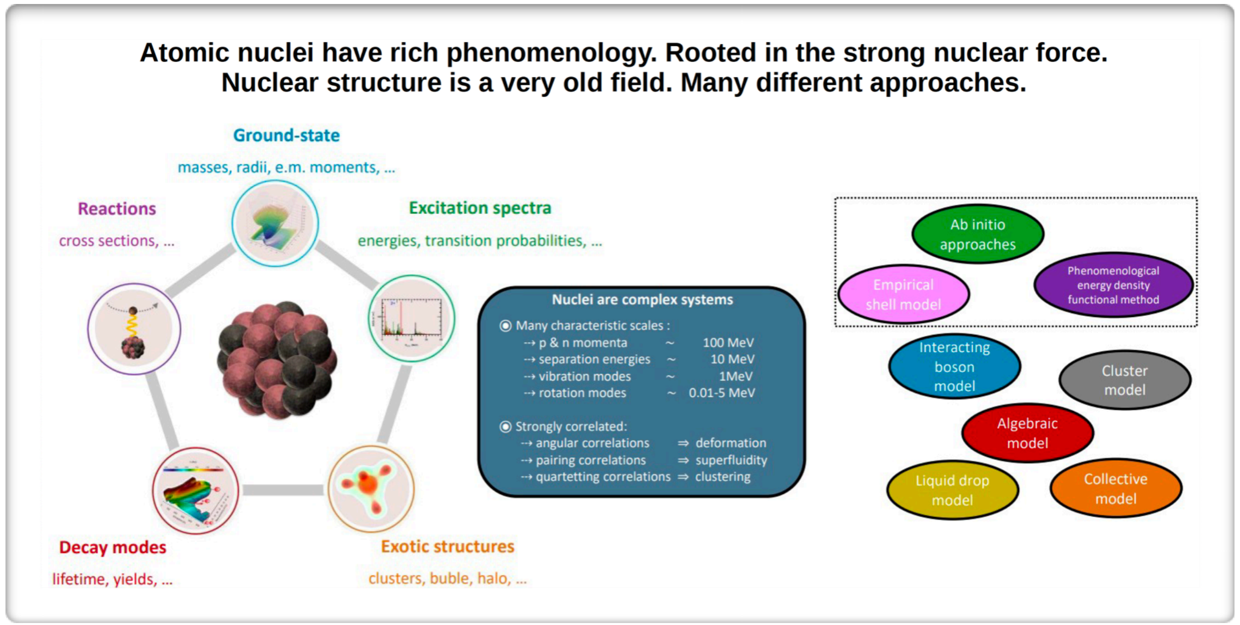

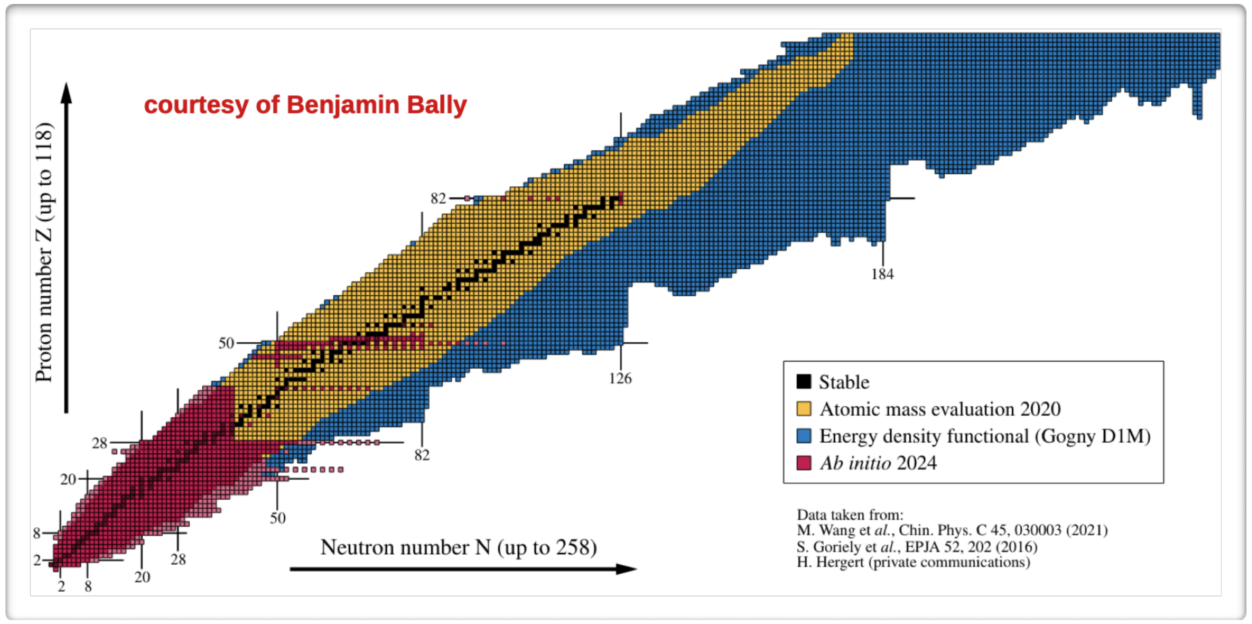

Energy density function method : accurate description of masses and radii

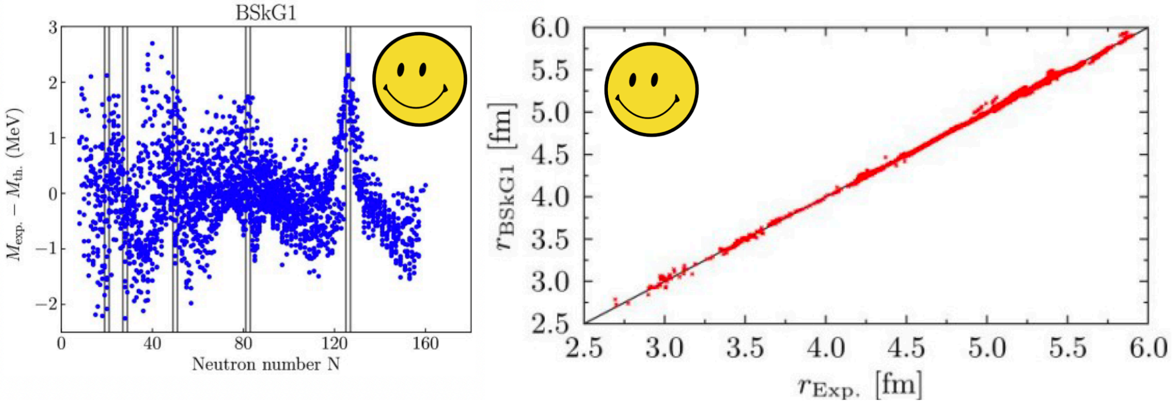

Nuclear structure at low energies

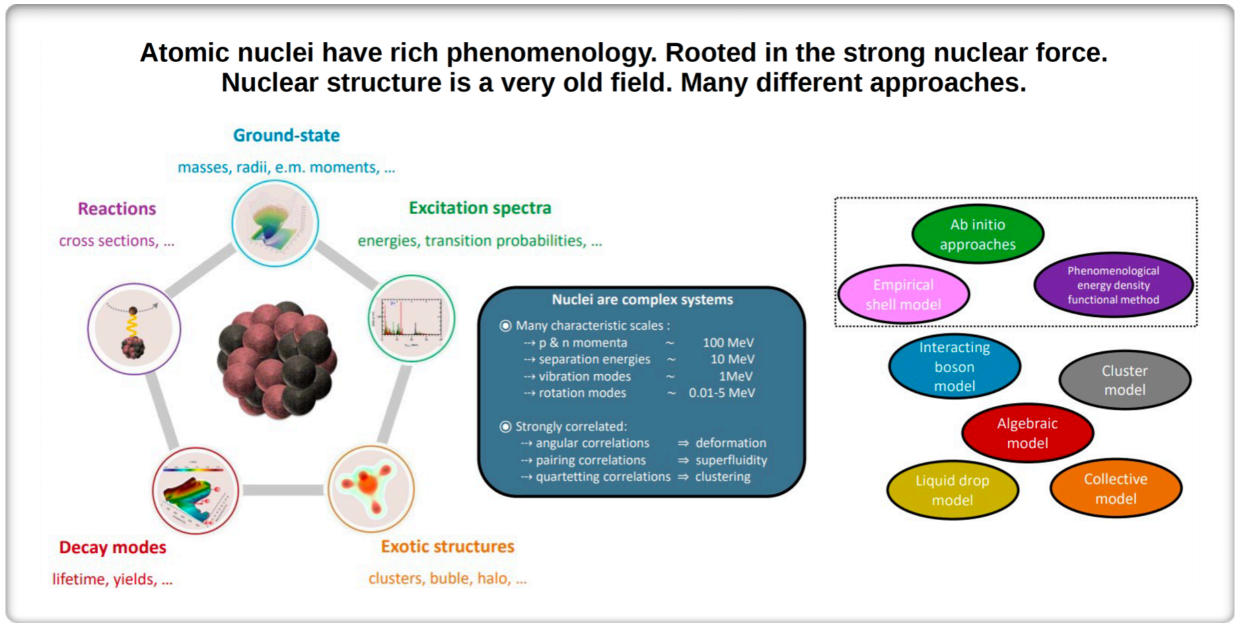

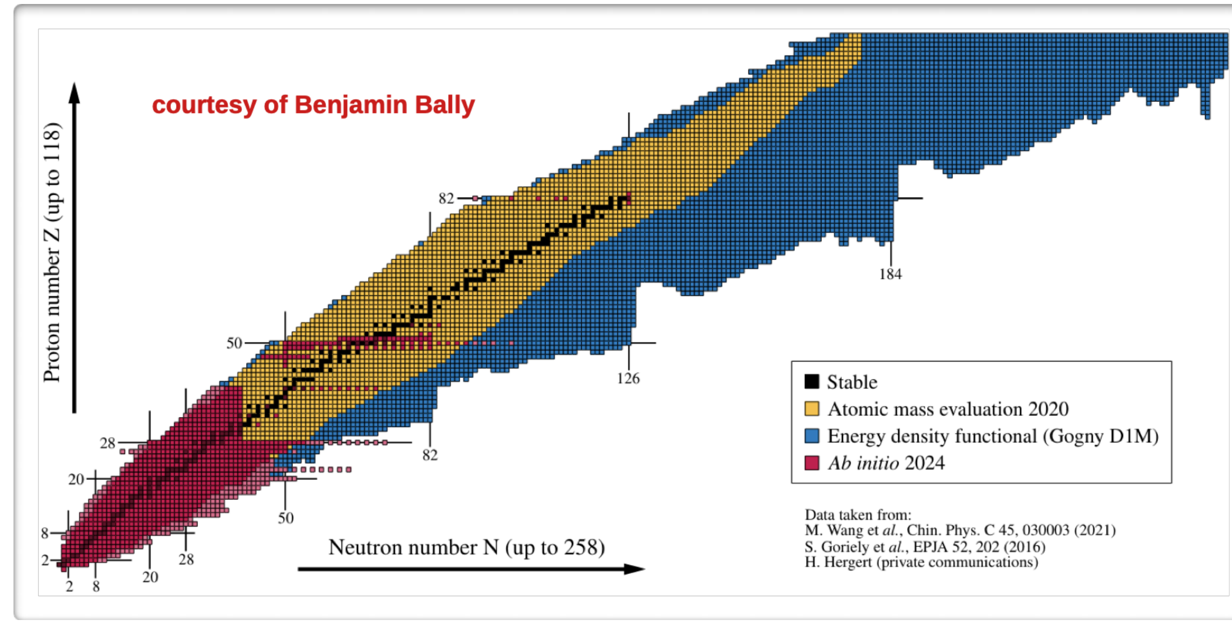

Energy density function method : accurate description of masses and radii

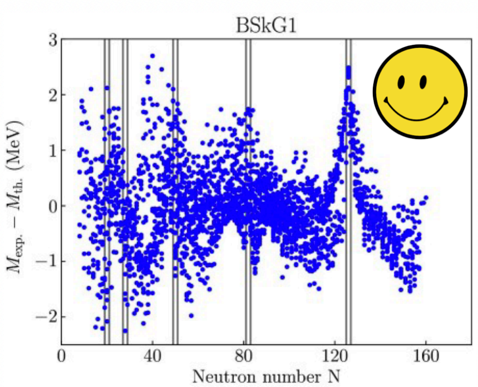

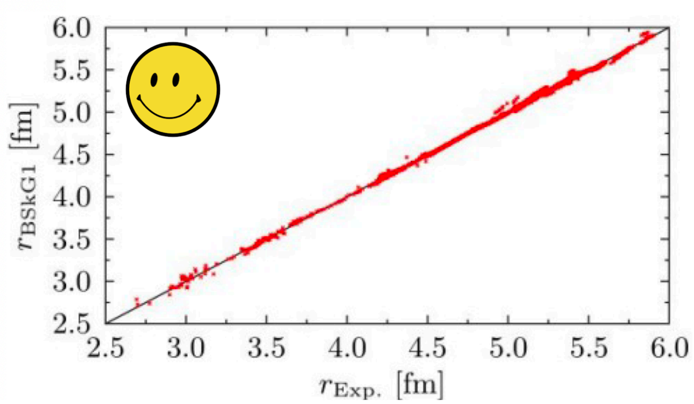

- *there are no real probes of multi-nucleon correlations*
- *huge model dependence.*

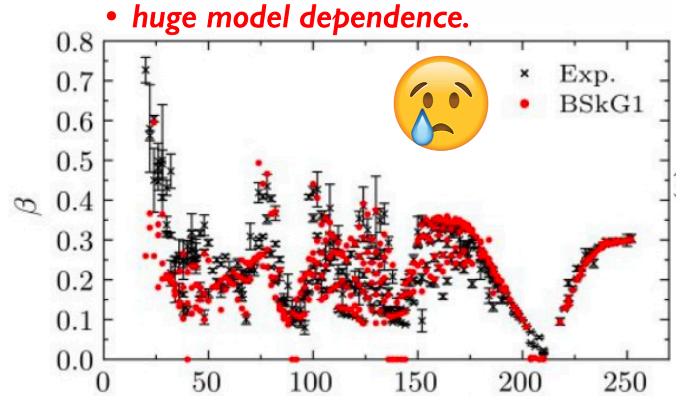

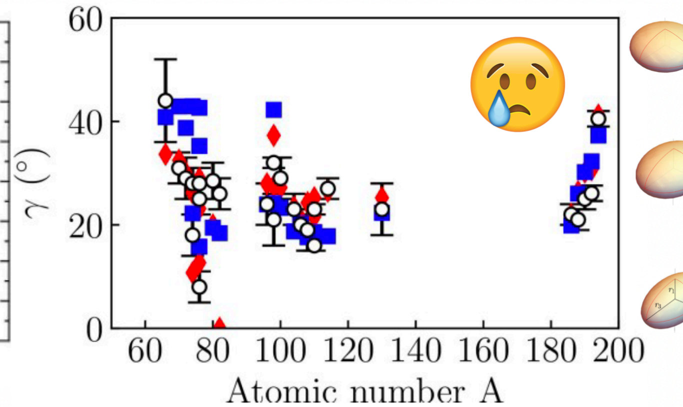

Nuclear Structure of ^{129}Xe

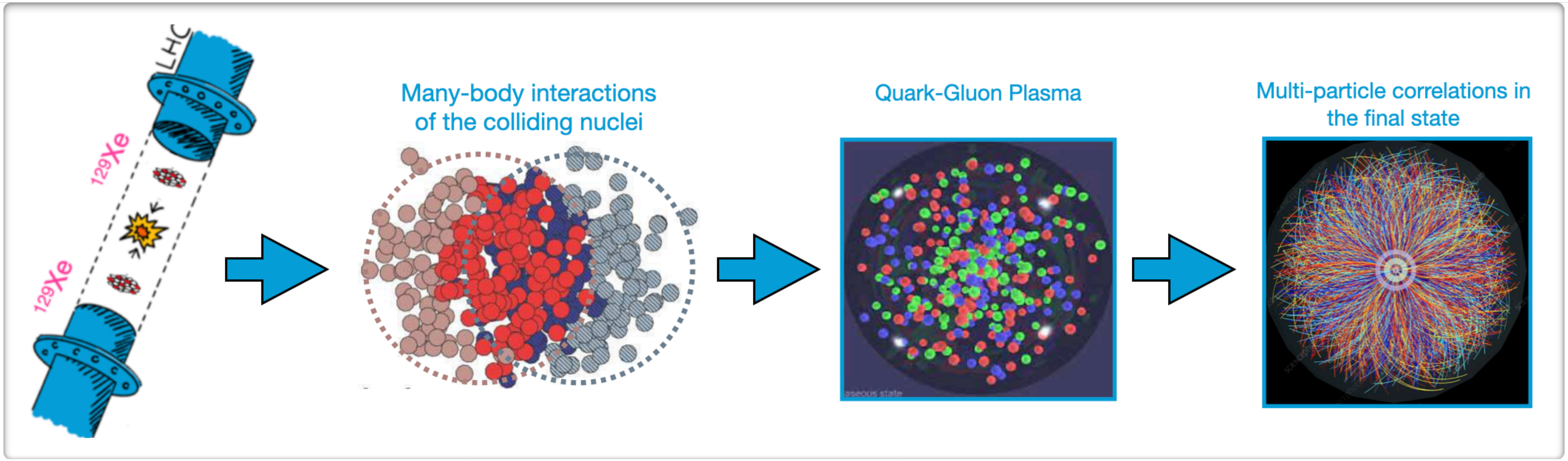

Aage Niels Bohr (NBI)

Ben Mottelson (NBI)

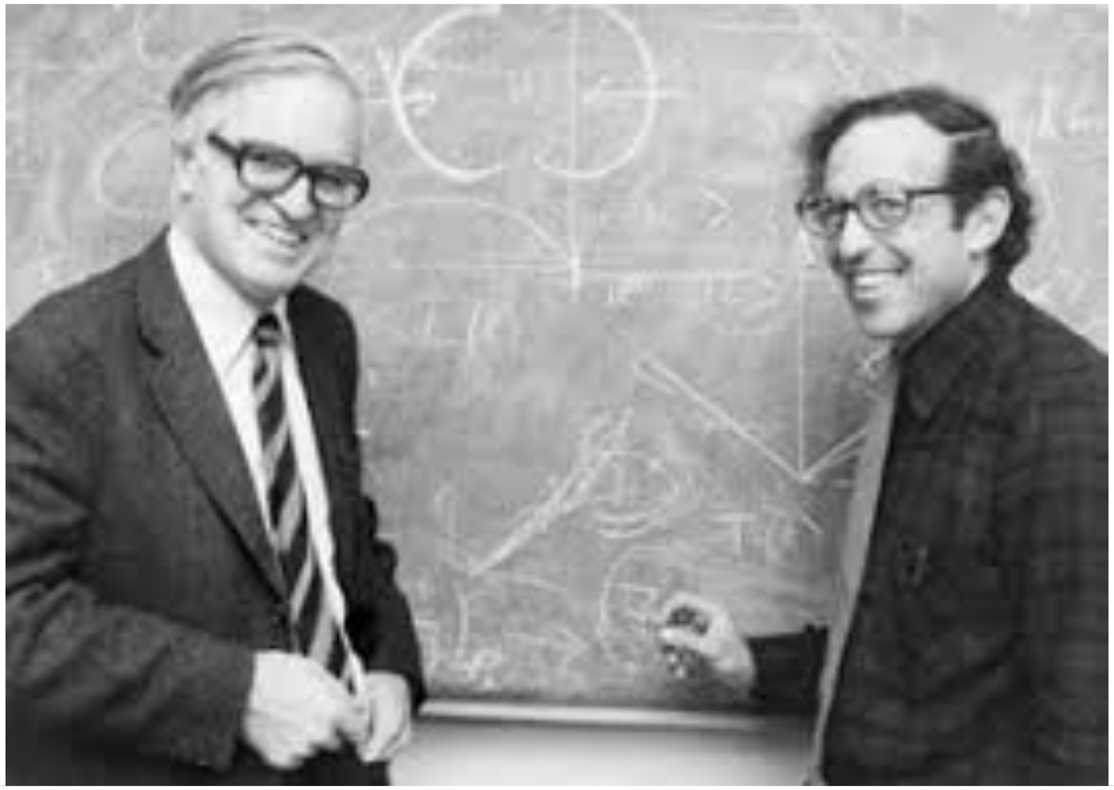

Nobelprisen i fysik
1975

Nuclear structure at high energies

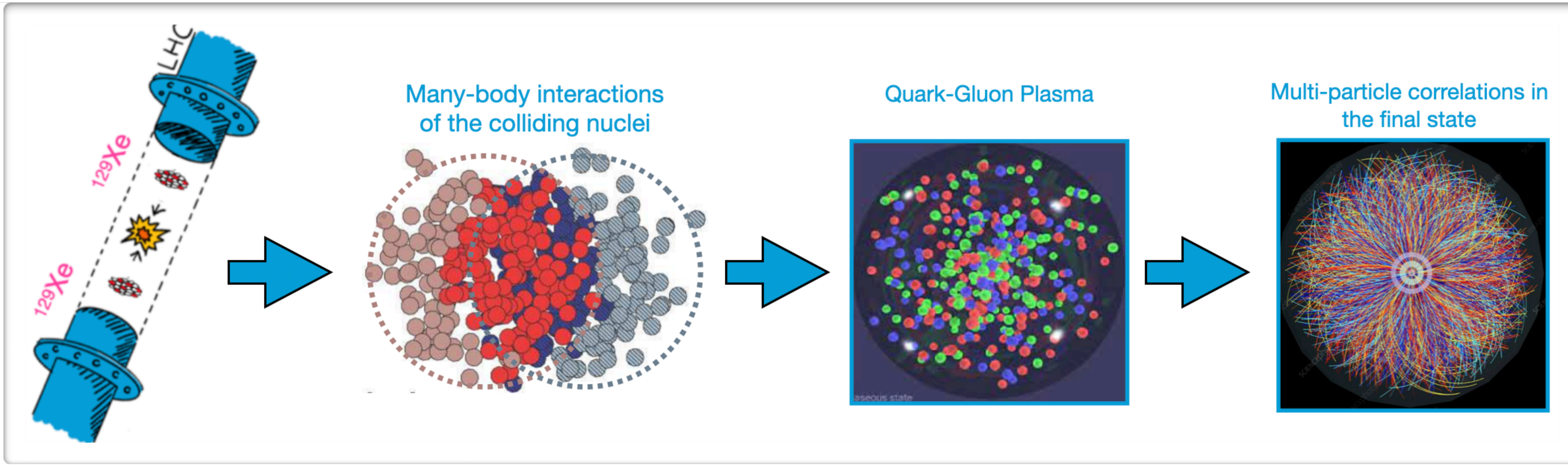

$$\rho(r,\theta,\phi) = \frac{\rho_0}{1+e^{(r-R(\theta,\phi))/a_0}} \qquad R(\theta,\phi) = R_0\left(1 + \beta_2[\cos\gamma Y_{2,0} + \sin\gamma Y_{2,2}] + \beta_3 \sum_{m=-3}^{3} \alpha_{3,m} Y_{3,m} + \beta_4 \sum_{m=-4}^{4} \alpha_{4,m} Y_{4,m}\right)$$

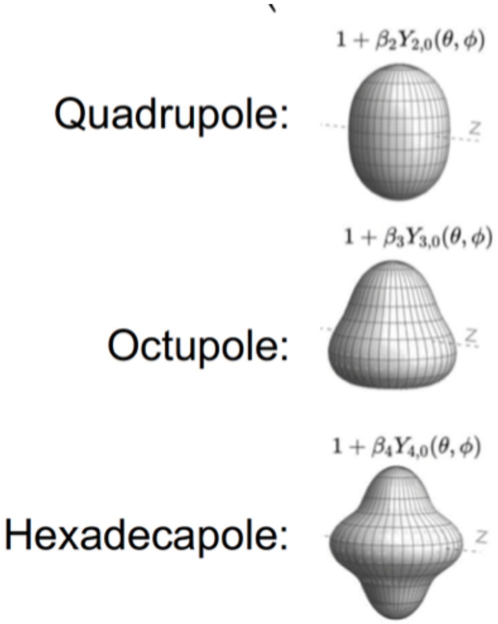

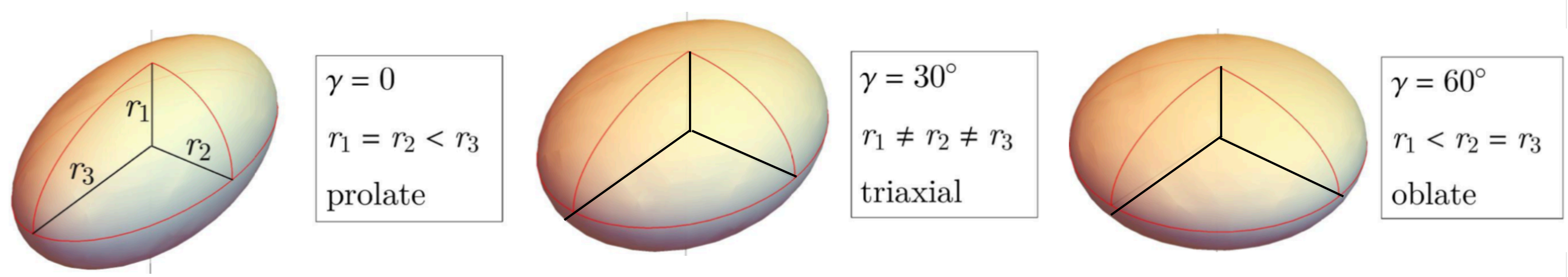

Probe nuclear structure of ^{129}Xe with v_n

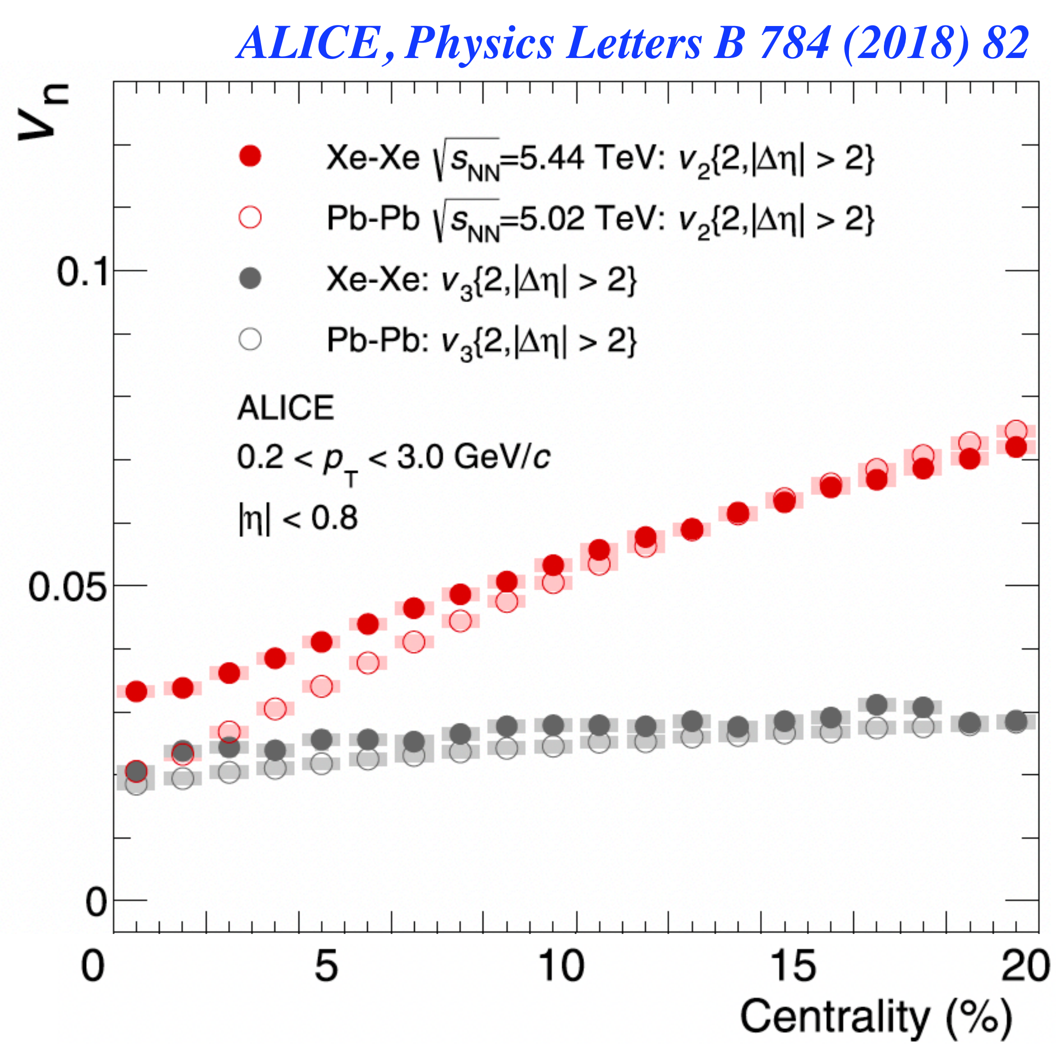

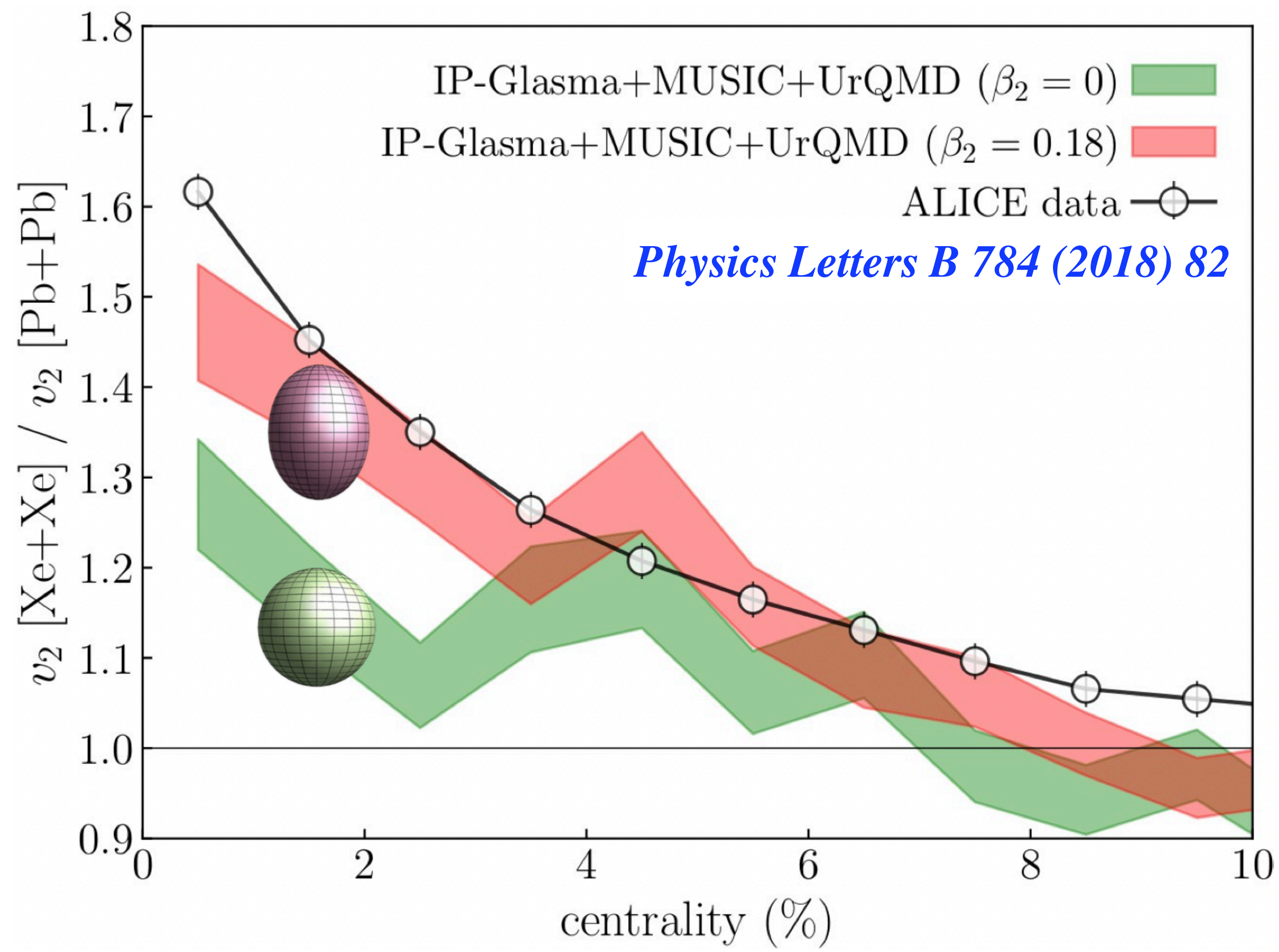

- ❖ Significant v_2 enhancements in central Xe-Xe collisions
- ❖ LHC data clearly suggests a non-zero β_2 (deformation of ^{129}Xe)

Differential flow vs p_T and η

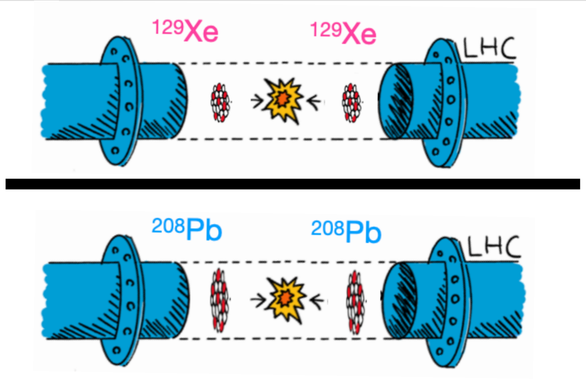

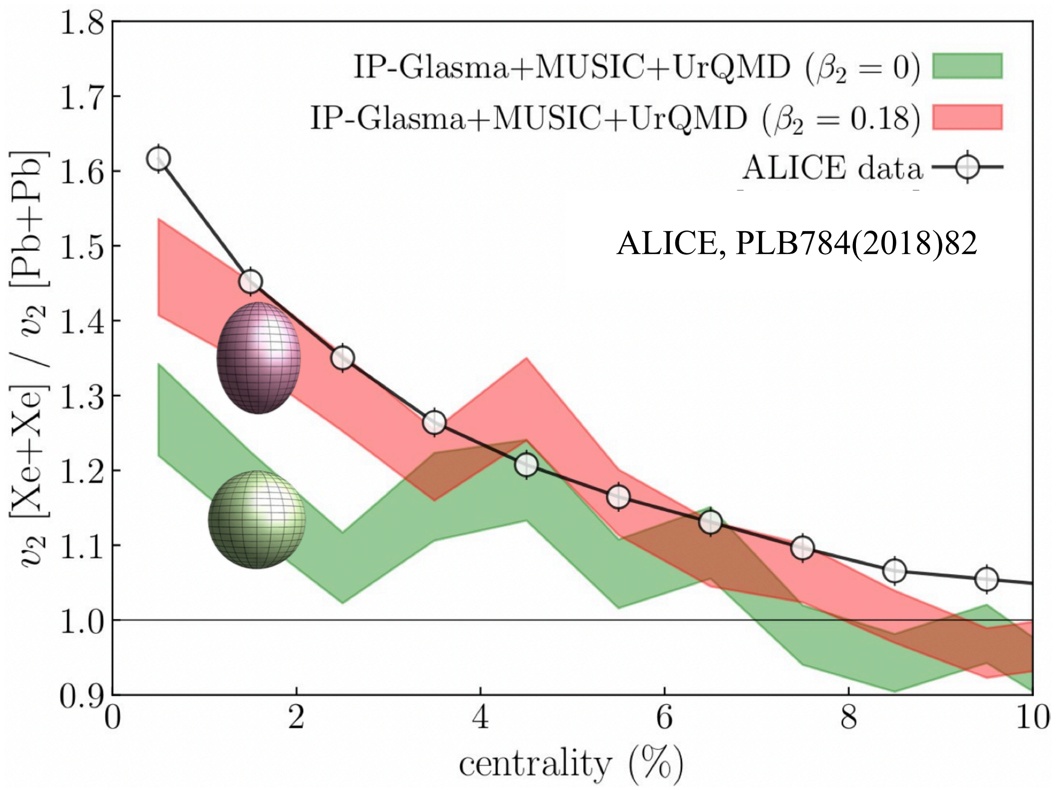

Differential flow vs p_T and η

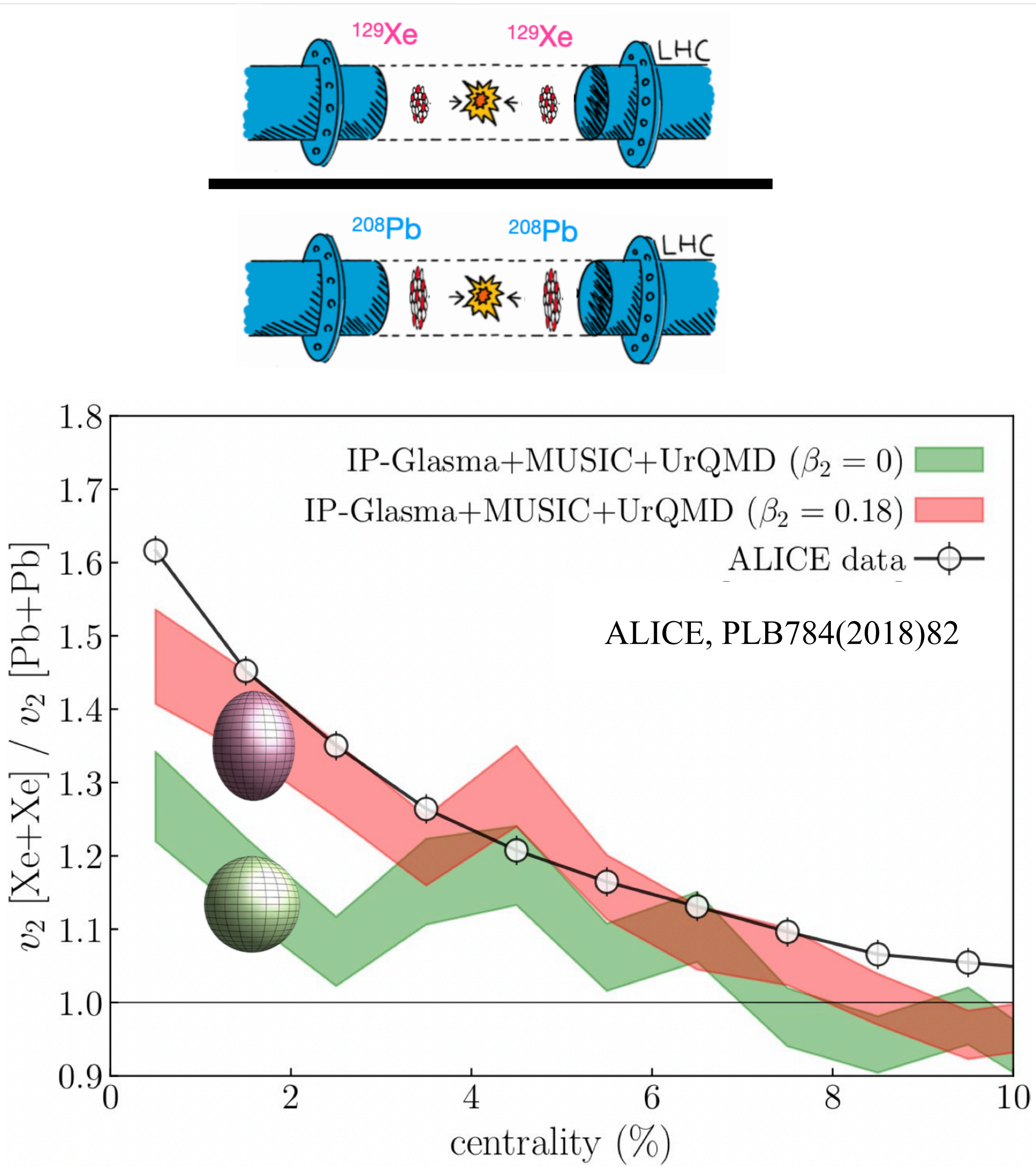

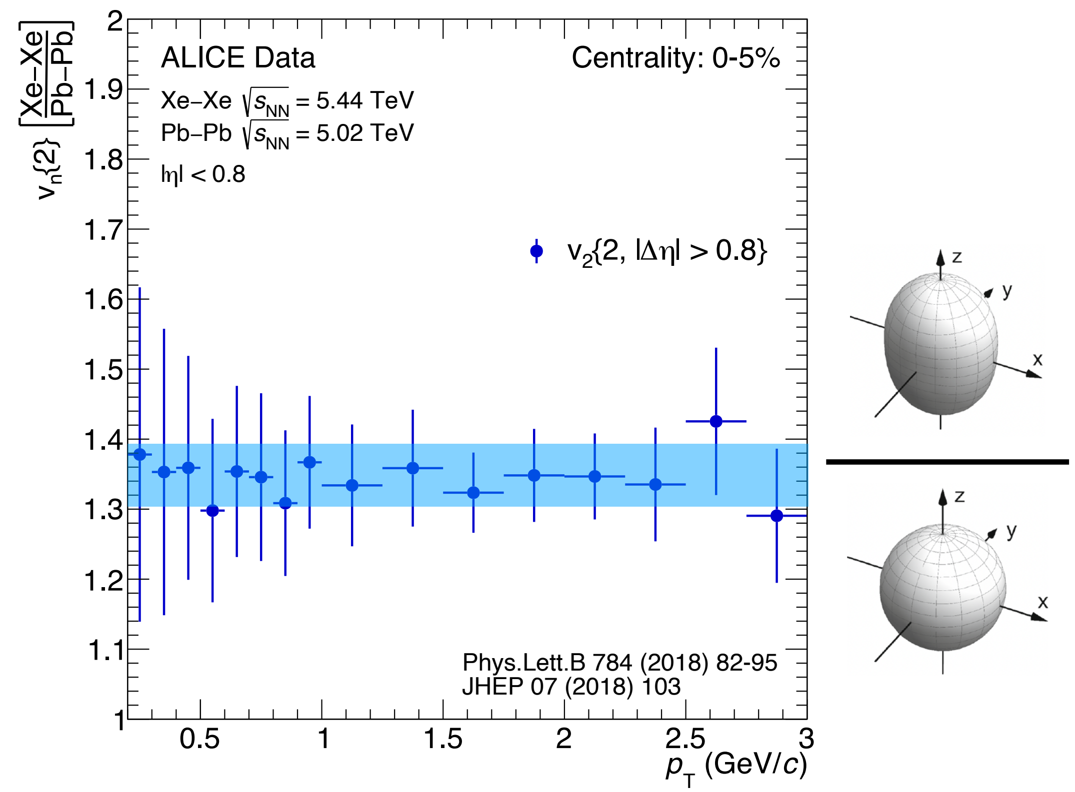

Differential flow vs p_T and η

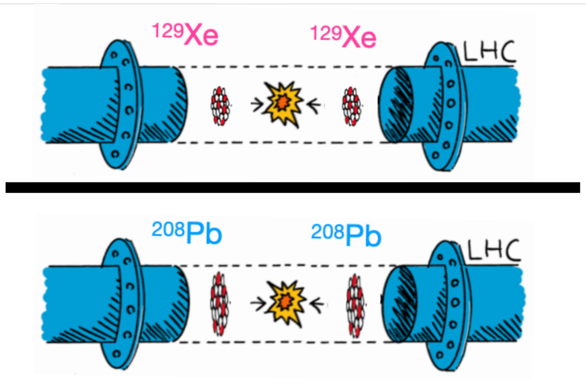

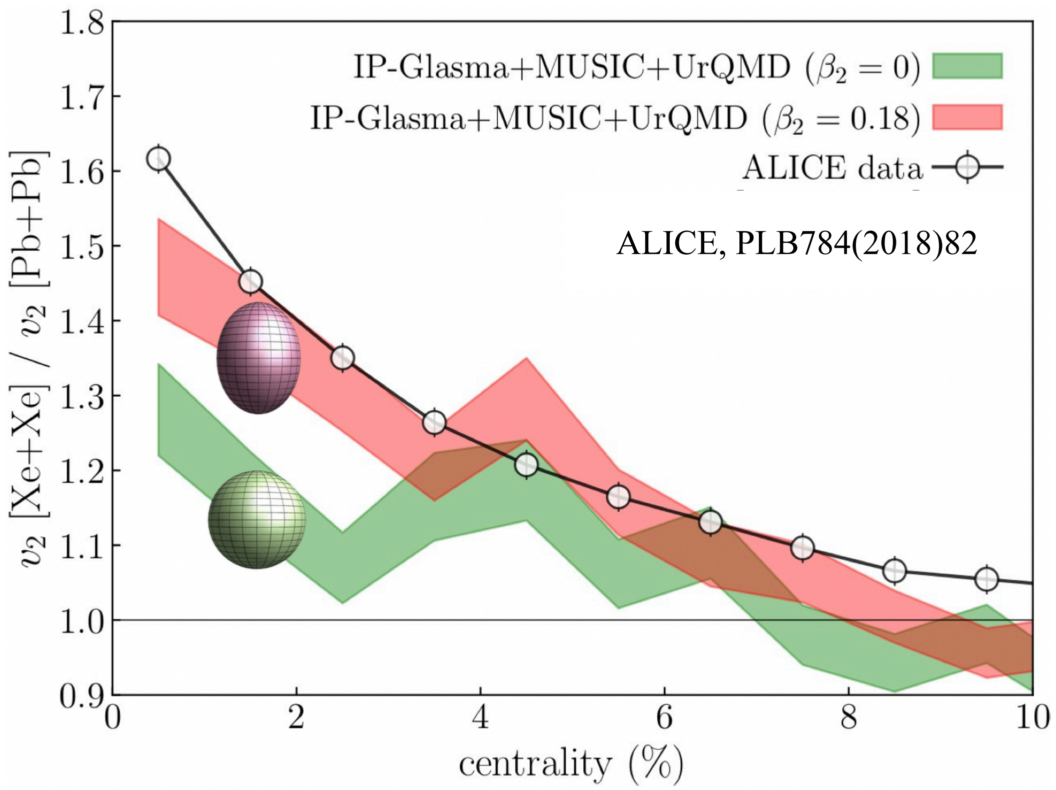

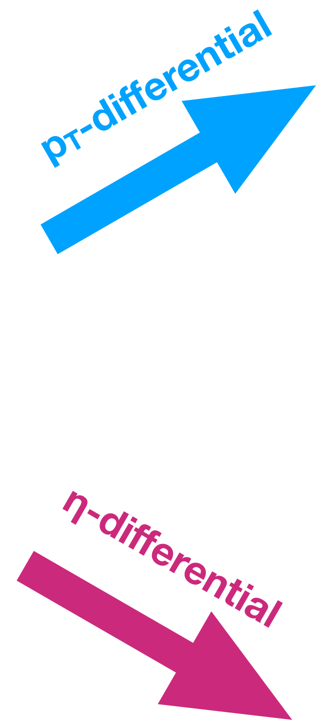

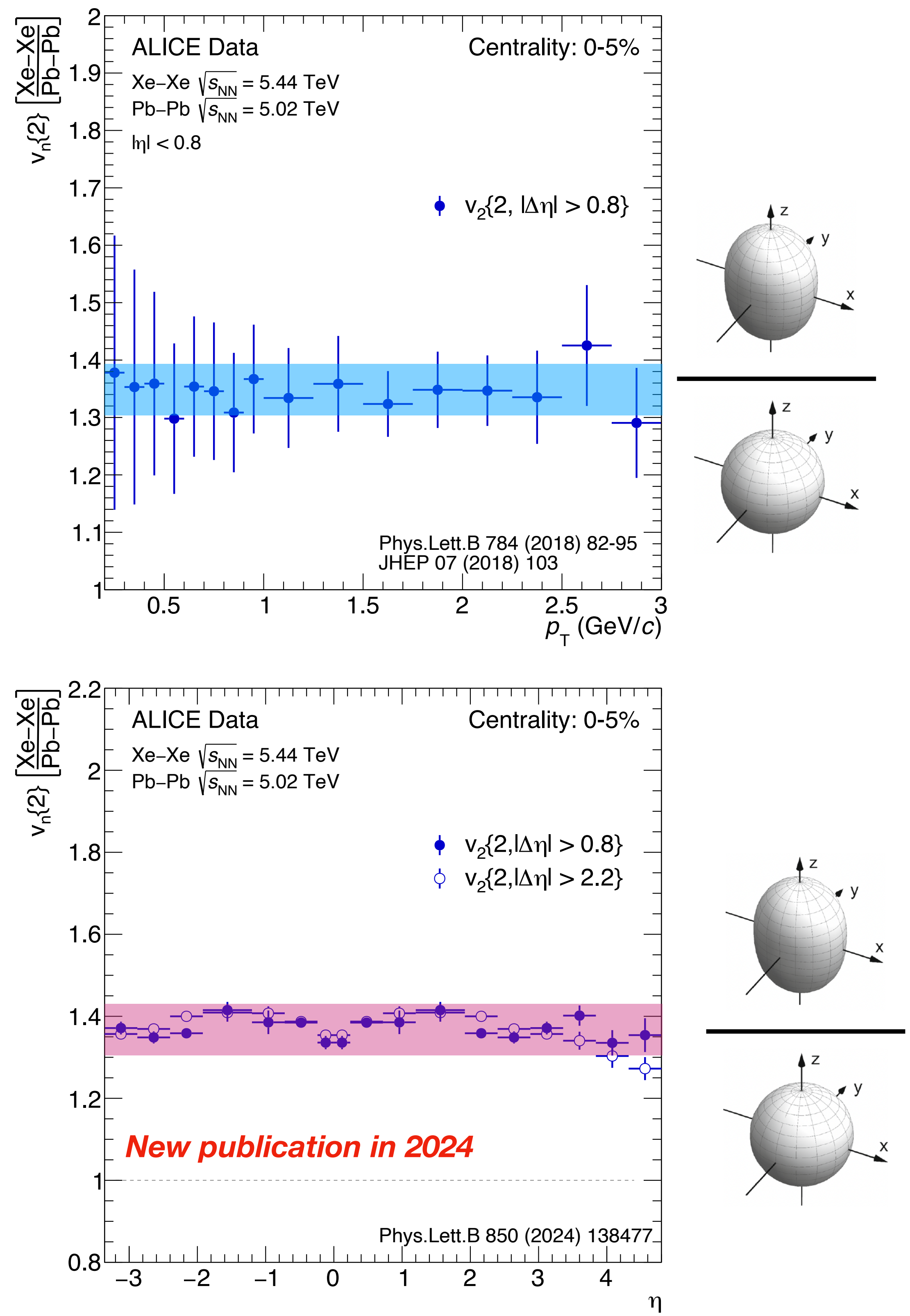

- For the first time observe the impact of NS over a very wide pseudorapidity range ($-3.5 < \eta < 5.0$)
  - New input for the low-x physics

ψn - ψm correlations

How do ψn and ψm correlate

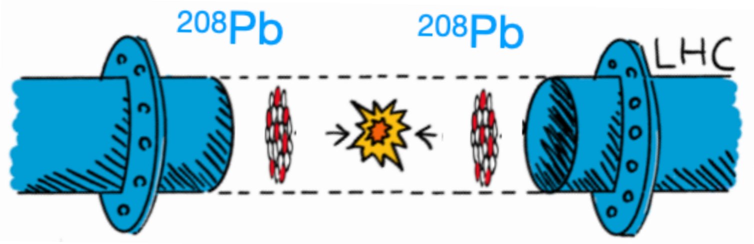

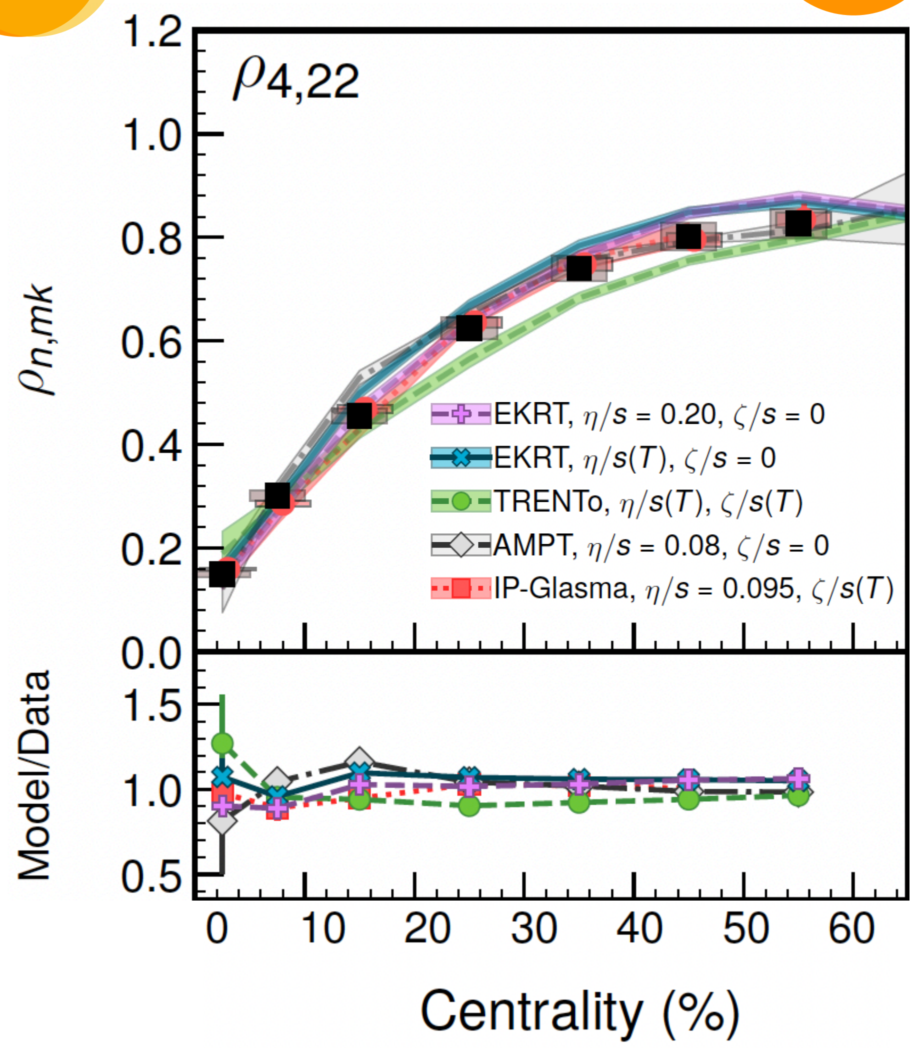

ψ_n - ψ_m correlations

How do ψ_n and ψ_m correlate

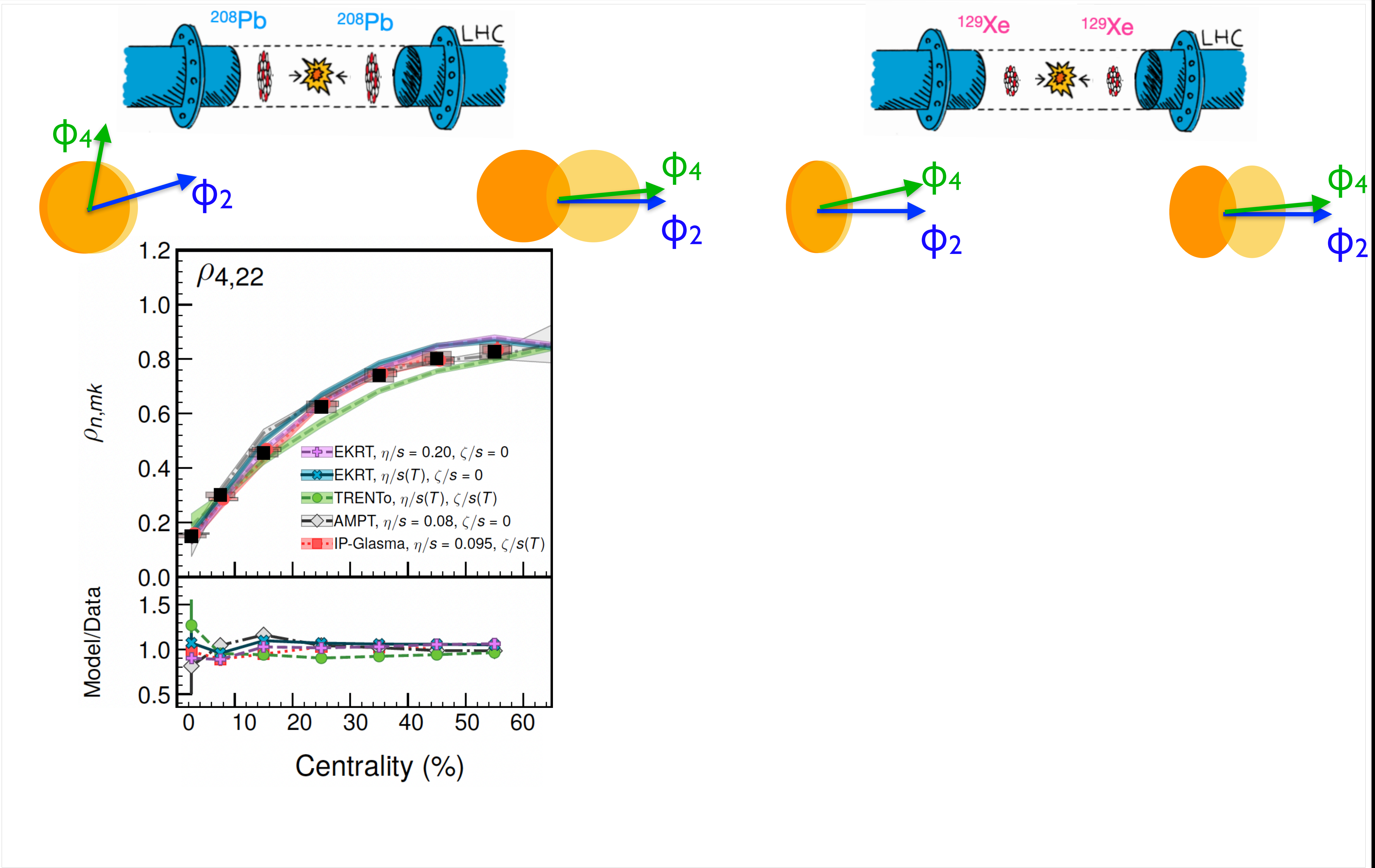

ψ_n - ψ_m correlations

How do ψ_n and ψ_m correlate

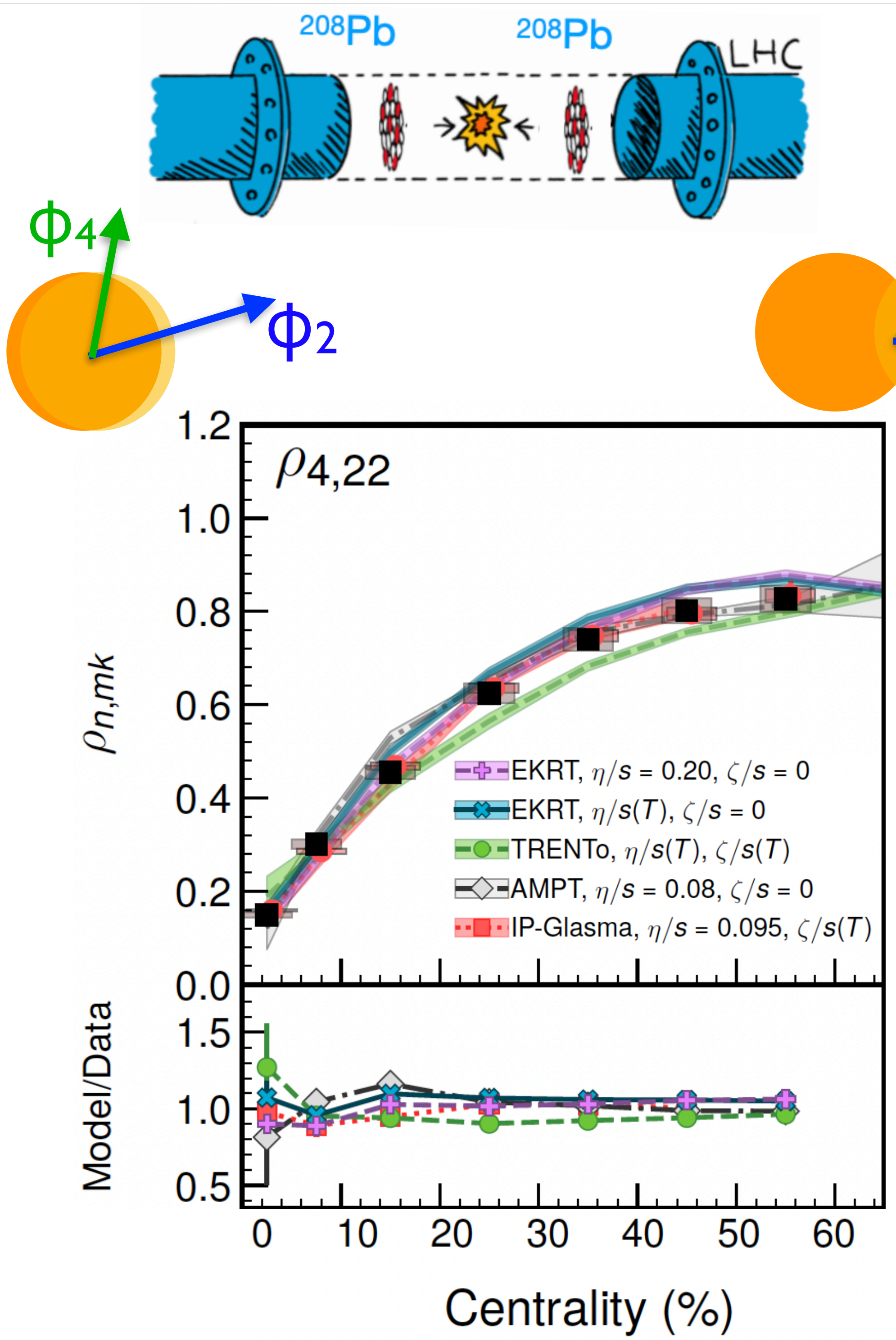

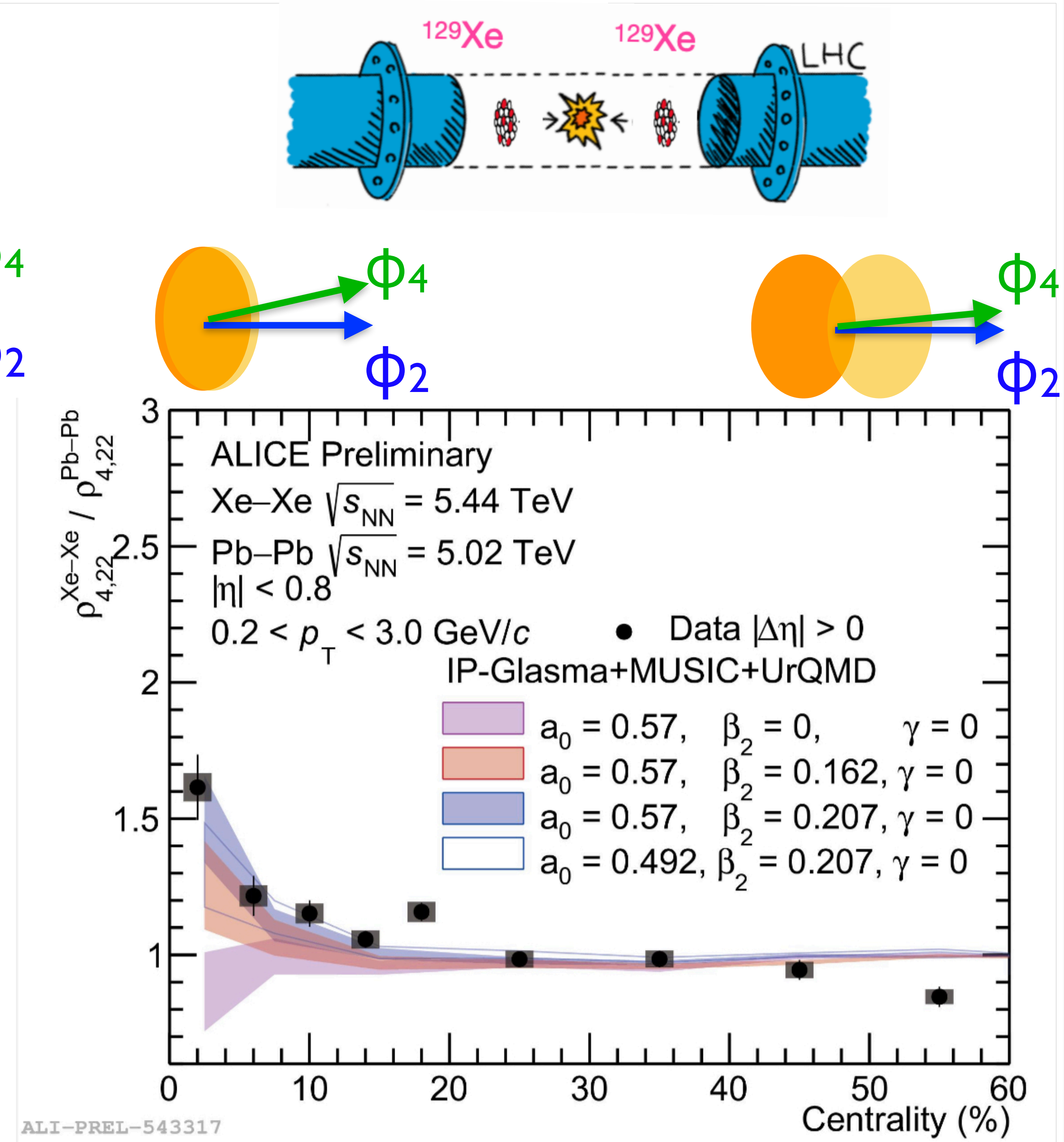

❖ A ***stronger*** correlation is observed in the Xe-Xe collisions.

Nuclear structure with Standard flow studies

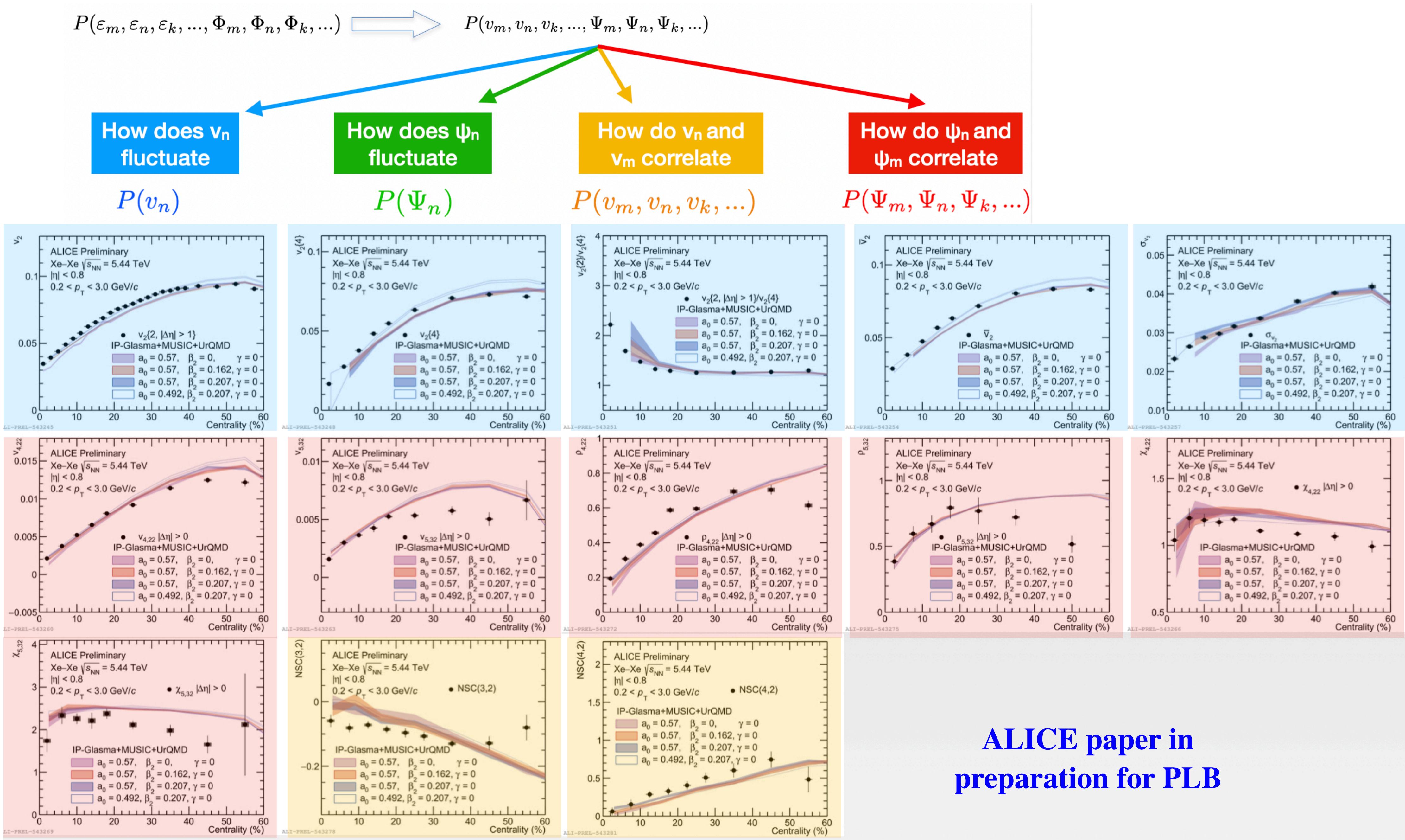

- Promising sensitivities to the nuclear deformation β_2 in central Xe-Xe collisions
- ***Insensitive*** to triaxial structure

Probe NS with two-particle [pT] correlations

Eur. Phys. J. A (2024) 60:38
https://doi.org/10.1140/epja/s10050-024-01266-x

THE EUROPEAN PHYSICAL JOURNAL A

Check for updates

Regular Article - Theoretical Physics

Generic multi-particle transverse momentum correlations as a new tool for studying nuclear structure at the energy frontier

Emil Gorm Dahlbæk Nielsen, Frederik K. Rømer, Kristjan Gulbrandsen, You Zhou[a]

Niels Bohr Institute, University of Copenhagen, 2200 Copenhagen, Denmark

Table 2 The cumulants of $d_\perp$ up to eighth order in a liquid-drop model potential averaged over random orientations. The first three entries are given in [29]

Final state Cumulant	Initial state Cumulant	Liquid-drop Model
κ_2	$\left\langle\left(\frac{\delta d_\perp}{d_\perp}\right)^2\right\rangle$	$\frac{1}{32\pi}\langle\beta_2^2\rangle$
κ_3	$\left\langle\left(\frac{\delta d_\perp}{d_\perp}\right)^3\right\rangle$	$\frac{\sqrt{5}}{896\pi^{3/2}}\langle\cos(3\gamma)\beta_2^3\rangle$
κ_4	$\left\langle\left(\frac{\delta d_\perp}{d_\perp}\right)^4\right\rangle - 3\cdot\left\langle\left(\frac{\delta d_\perp}{d_\perp}\right)^2\right\rangle^2$	$-\frac{3}{14336\pi^2}(7\langle\beta_2^2\rangle^2 - 5\langle\beta_2^4\rangle)$
κ_5	$\left\langle\left(\frac{\delta d_\perp}{d_\perp}\right)^5\right\rangle - 10\cdot\left\langle\left(\frac{\delta d_\perp}{d_\perp}\right)^3\right\rangle\cdot\left\langle\left(\frac{\delta d_\perp}{d_\perp}\right)^2\right\rangle$	$-\frac{5\sqrt{5}}{315392\pi^{5/2}}(11\langle\cos(3\gamma)\beta_2^3\rangle\langle\beta_2^2\rangle - 5\langle\beta_2^5\rangle)$
κ_6	$\left\langle\left(\frac{\delta d_\perp}{d_\perp}\right)^6\right\rangle - 15\cdot\left\langle\left(\frac{\delta d_\perp}{d_\perp}\right)^4\right\rangle\cdot\left\langle\left(\frac{\delta d_\perp}{d_\perp}\right)^2\right\rangle$	$\frac{5}{918412504\pi^3}(42042\langle\beta_2^2\rangle^3 - 5720\langle\cos(3\gamma)\beta_2^3\rangle^2$
	$+30\cdot\left\langle\left(\frac{\delta d_\perp}{d_\perp}\right)^2\right\rangle^3 - 10\cdot\left\langle\left(\frac{\delta d_\perp}{d_\perp}\right)^3\right\rangle^2$	$-45045\langle\beta_2^2\rangle\langle\beta_2^4\rangle + 8575\langle\beta_2^6\rangle + 700\langle\cos(6\gamma)\beta_2^6\rangle)$
κ_7	$\left\langle\left(\frac{\delta d_\perp}{d_\perp}\right)^7\right\rangle - 21\cdot\left\langle\left(\frac{\delta d_\perp}{d_\perp}\right)^5\right\rangle\cdot\left\langle\left(\frac{\delta d_\perp}{d_\perp}\right)^2\right\rangle$	$-\frac{15\sqrt{5}}{524812288}(2002\langle\beta_2^2\rangle^2\langle\cos(3\gamma)\beta_2^3\rangle$
	$+210\cdot\left\langle\left(\frac{\delta d_\perp}{d_\perp}\right)^3\right\rangle\cdot\left\langle\left(\frac{\delta d_\perp}{d_\perp}\right)^2\right\rangle^2$	$+715\langle\cos(3\gamma)\beta_2^3\rangle\langle\beta_2^4\rangle$
	$-35\cdot\left\langle\left(\frac{\delta d_\perp}{d_\perp}\right)^3\right\rangle\cdot\left\langle\left(\frac{\delta d_\perp}{d_\perp}\right)^4\right\rangle$	$+910\langle\cos(3\gamma)\beta_2^5\rangle\langle\beta_2^2\rangle - 175\cos(3\gamma)\beta_2^7\rangle)$
κ_8	$\left\langle\left(\frac{\delta d_\perp}{d_\perp}\right)^8\right\rangle - 28\cdot\left\langle\left(\frac{\delta d_\perp}{d_\perp}\right)^6\right\rangle\cdot\left\langle\left(\frac{\delta d_\perp}{d_\perp}\right)^2\right\rangle$	$\frac{5}{142748942336\pi^4}(2144142\langle\beta_2^2\rangle^4 - 3063060\langle\beta_2^2\rangle^2\langle\beta_2^4\rangle$
	$+420\cdot\left\langle\left(\frac{\delta d_\perp}{d_\perp}\right)^4\right\rangle\left\langle\left(\frac{\delta d_\perp}{d_\perp}\right)^2\right\rangle^2$	$-340\langle\beta_2^2\rangle\Big(2288\langle\cos(3\gamma)\beta_2^3\rangle^2 - 35\big(49\langle\beta_2^6\rangle$
	$-35\left\langle\left(\frac{\delta d_\perp}{d_\perp}\right)^4\right\rangle^2 - 630\cdot\left\langle\left(\frac{\delta d_\perp}{d_\perp}\right)^2\right\rangle^4$	$+4\langle\cos(6\gamma)\beta_2^6\rangle)\Big) + 25\Big(21879\langle\beta_2^4\rangle^2$
	$+560\cdot\left\langle\left(\frac{\delta d_\perp}{d_\perp}\right)^3\right\rangle^2\cdot\left\langle\left(\frac{\delta d_\perp}{d_\perp}\right)^2\right\rangle$	$+14144\langle\cos(3\gamma)\beta_2^3\rangle\langle\cos(3\gamma)\beta_2^5\rangle$
	$-56\cdot\left\langle\left(\frac{\delta d_\perp}{d_\perp}\right)^5\right\rangle\cdot\left\langle\left(\frac{\delta d_\perp}{d_\perp}\right)^3\right\rangle$	$-35\big(79\langle\beta_2^8\rangle + 16\langle\cos(6\gamma)\beta_2^8\rangle\big)\Big)$

Probe NS with two-particle [p_T] correlations

Eur. Phys. J. A (2024) 60:38
https://doi.org/10.1140/epja/s10050-024-01266-x
THE EUROPEAN PHYSICAL JOURNAL A
Check for updates
Regular Article - Theoretical Physics

Generic multi-particle transverse momentum correlations as a new tool for studying nuclear structure at the energy frontier

Emil Gorm Dahlbæk Nielsen, Frederik K. Rømer, Kristjan Gulbrandsen, You Zhou[a]
Niels Bohr Institute, University of Copenhagen, 2200 Copenhagen, Denmark

Table 2 The cumulants of $d_\perp$ up to eighth order in a liquid-drop model potential averaged over random orientations. The first three entries are given in [29]

Final state Cumulant	Initial state Cumulant	Liquid-drop Model
κ_2	$\left\langle\left(\frac{\delta d_\perp}{d_\perp}\right)^2\right\rangle$	$\frac{1}{32\pi}\langle\beta_2^2\rangle$
κ_3	$\left\langle\left(\frac{\delta d_\perp}{d_\perp}\right)^3\right\rangle$	$\frac{\sqrt{5}}{896\pi^{3/2}}\langle\cos(3\gamma)\beta_2^3\rangle$
κ_4	$\left\langle\left(\frac{\delta d_\perp}{d_\perp}\right)^4\right\rangle - 3\cdot\left\langle\left(\frac{\delta d_\perp}{d_\perp}\right)^2\right\rangle^2$	$-\frac{3}{14336\pi^2}(7\langle\beta_2^2\rangle^2 - 5\langle\beta_2^4\rangle)$
κ_5	$\left\langle\left(\frac{\delta d_\perp}{d_\perp}\right)^5\right\rangle - 10\cdot\left\langle\left(\frac{\delta d_\perp}{d_\perp}\right)^3\right\rangle\cdot\left\langle\left(\frac{\delta d_\perp}{d_\perp}\right)^2\right\rangle$	$-\frac{5\sqrt{5}}{315392\pi^{5/2}}(11\langle\cos(3\gamma)\beta_2^3\rangle\langle\beta_2^2\rangle - 5\langle\beta_2^5\rangle)$
κ_6	$\left\langle\left(\frac{\delta d_\perp}{d_\perp}\right)^6\right\rangle - 15\cdot\left\langle\left(\frac{\delta d_\perp}{d_\perp}\right)^4\right\rangle\cdot\left\langle\left(\frac{\delta d_\perp}{d_\perp}\right)^2\right\rangle$	$\frac{5}{918412504\pi^3}(42042\langle\beta_2^2\rangle^3 - 5720\langle\cos(3\gamma)\beta_2^3\rangle^2$
	$+30\cdot\left\langle\left(\frac{\delta d_\perp}{d_\perp}\right)^2\right\rangle^3 - 10\cdot\left\langle\left(\frac{\delta d_\perp}{d_\perp}\right)^3\right\rangle^2$	$-45045\langle\beta_2^2\rangle\langle\beta_2^4\rangle + 8575\langle\beta_2^6\rangle + 700\langle\cos(6\gamma)\beta_2^6\rangle)$
κ_7	$\left\langle\left(\frac{\delta d_\perp}{d_\perp}\right)^7\right\rangle - 21\cdot\left\langle\left(\frac{\delta d_\perp}{d_\perp}\right)^5\right\rangle\cdot\left\langle\left(\frac{\delta d_\perp}{d_\perp}\right)^2\right\rangle$	$-\frac{15\sqrt{5}}{524812288}(2002\langle\beta_2^2\rangle^2\langle\cos(3\gamma)\beta_2^3\rangle$
	$+210\cdot\left\langle\left(\frac{\delta d_\perp}{d_\perp}\right)^3\right\rangle\cdot\left\langle\left(\frac{\delta d_\perp}{d_\perp}\right)^2\right\rangle^2$	$+715\langle\cos(3\gamma)\beta_2^3\rangle\langle\beta_2^4\rangle$
	$-35\cdot\left\langle\left(\frac{\delta d_\perp}{d_\perp}\right)^3\right\rangle\cdot\left\langle\left(\frac{\delta d_\perp}{d_\perp}\right)^4\right\rangle$	$+910\langle\cos(3\gamma)\beta_2^5\rangle\langle\beta_2^2\rangle - 175\cos(3\gamma)\beta_2^7\rangle)$
κ_8	$\left\langle\left(\frac{\delta d_\perp}{d_\perp}\right)^8\right\rangle - 28\cdot\left\langle\left(\frac{\delta d_\perp}{d_\perp}\right)^6\right\rangle\cdot\left\langle\left(\frac{\delta d_\perp}{d_\perp}\right)^2\right\rangle$	$\frac{5}{142748942336\pi^4}(2144142\langle\beta_2^2\rangle^4 - 3063060\langle\beta_2^2\rangle^2\langle\beta_2^4\rangle$
	$+420\cdot\left\langle\left(\frac{\delta d_\perp}{d_\perp}\right)^4\right\rangle\left\langle\left(\frac{\delta d_\perp}{d_\perp}\right)^2\right\rangle^2$	$-340\langle\beta_2^2\rangle\Big(2288\langle\cos(3\gamma)\beta_2^3\rangle^2 - 35\big(49\langle\beta_2^6\rangle$
	$-35\left\langle\left(\frac{\delta d_\perp}{d_\perp}\right)^4\right\rangle^2 - 630\cdot\left\langle\left(\frac{\delta d_\perp}{d_\perp}\right)^2\right\rangle^4$	$+4\langle\cos(6\gamma)\beta_2^6\rangle\big)\Big) + 25\Big(21879\langle\beta_2^4\rangle^2$
	$+560\cdot\left\langle\left(\frac{\delta d_\perp}{d_\perp}\right)^3\right\rangle^2\cdot\left\langle\left(\frac{\delta d_\perp}{d_\perp}\right)^2\right\rangle$	$+14144\langle\cos(3\gamma)\beta_2^3\rangle\langle\cos(3\gamma)\beta_2^5\rangle$
	$-56\cdot\left\langle\left(\frac{\delta d_\perp}{d_\perp}\right)^5\right\rangle\cdot\left\langle\left(\frac{\delta d_\perp}{d_\perp}\right)^3\right\rangle$	$-35\big(79\langle\beta_2^8\rangle + 16\langle\cos(6\gamma)\beta_2^8\rangle\big)\Big)$

E. Nielsen etc., EPJA 60 (2024) 38

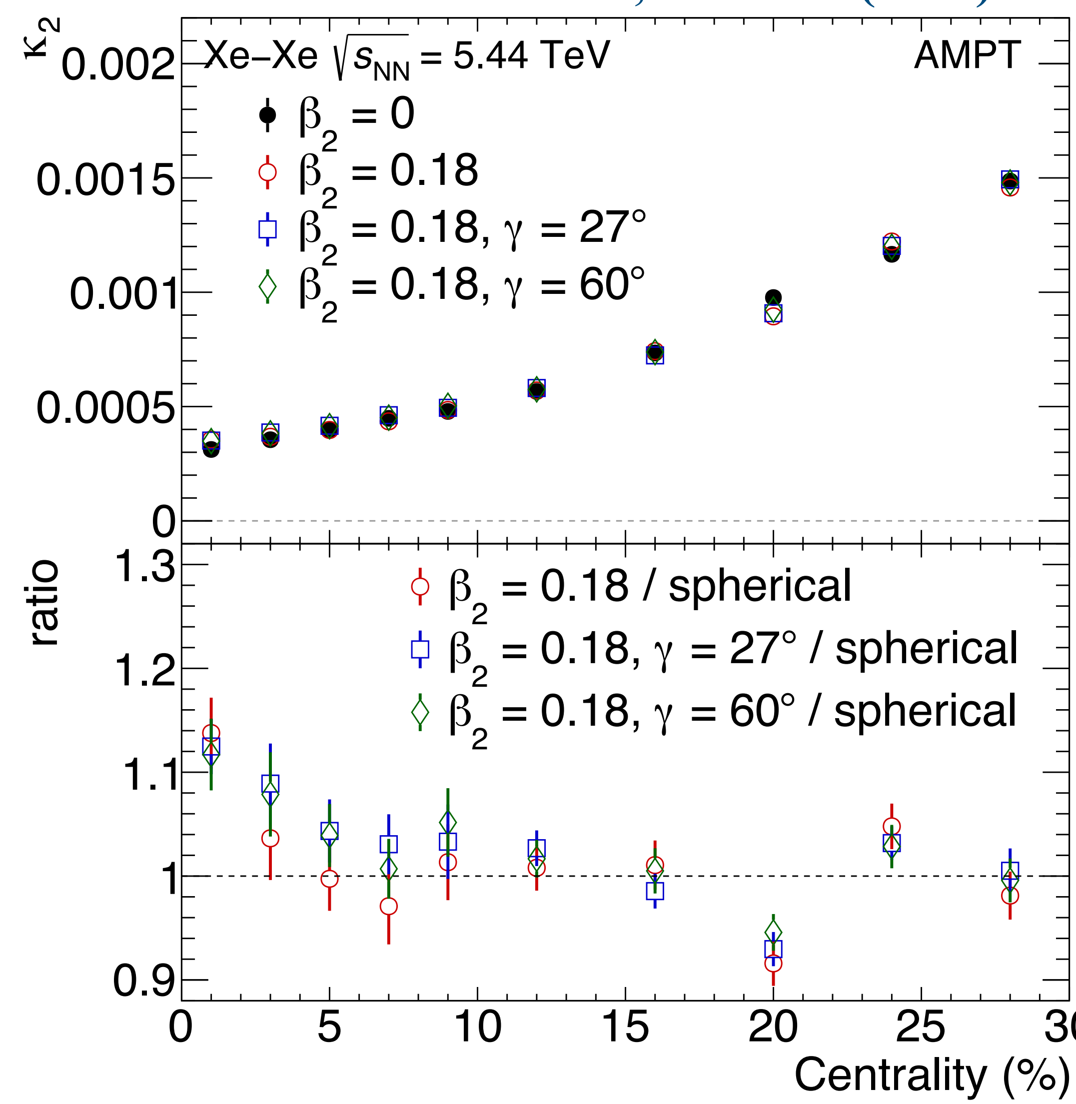

❖ These two-particle p_T correlations provide a new way to probe deformation structures of ^{129}Xe.

Probe NS with two-particle [p_T] correlations

Eur. Phys. J. A (2024) 60:38
https://doi.org/10.1140/epja/s10050-024-01266-x

THE EUROPEAN PHYSICAL JOURNAL A

Check for updates

Regular Article - Theoretical Physics

Generic multi-particle transverse momentum correlations as a new tool for studying nuclear structure at the energy frontier

Emil Gorm Dahlbæk Nielsen, Frederik K. Rømer, Kristjan Gulbrandsen, You Zhou[a]
Niels Bohr Institute, University of Copenhagen, 2200 Copenhagen, Denmark

Table 2 The cumulants of $d_\perp$ up to eighth order in a liquid-drop model potential averaged over random orientations. The first three entries are given in [29]

Final state Cumulant	Initial state Cumulant	Liquid-drop Model
κ_2	$\left\langle\left(\frac{\delta d_\perp}{d_\perp}\right)^2\right\rangle$	$\frac{1}{32\pi}\langle\beta_2^2\rangle$
κ_3	$\left\langle\left(\frac{\delta d_\perp}{d_\perp}\right)^3\right\rangle$	$\frac{\sqrt{5}}{896\pi^{3/2}}\langle\cos(3\gamma)\beta_2^3\rangle$
κ_4	$\left\langle\left(\frac{\delta d_\perp}{d_\perp}\right)^4\right\rangle - 3\cdot\left\langle\left(\frac{\delta d_\perp}{d_\perp}\right)^2\right\rangle^2$	$-\frac{3}{14336\pi^2}(7\langle\beta_2^2\rangle^2 - 5\langle\beta_2^4\rangle)$
κ_5	$\left\langle\left(\frac{\delta d_\perp}{d_\perp}\right)^5\right\rangle - 10\cdot\left\langle\left(\frac{\delta d_\perp}{d_\perp}\right)^3\right\rangle\cdot\left\langle\left(\frac{\delta d_\perp}{d_\perp}\right)^2\right\rangle$	$-\frac{5\sqrt{5}}{315392\pi^{5/2}}(11\langle\cos(3\gamma)\beta_2^3\rangle\langle\beta_2^2\rangle - 5\langle\beta_2^5\rangle)$
κ_6	$\left\langle\left(\frac{\delta d_\perp}{d_\perp}\right)^6\right\rangle - 15\cdot\left\langle\left(\frac{\delta d_\perp}{d_\perp}\right)^4\right\rangle\cdot\left\langle\left(\frac{\delta d_\perp}{d_\perp}\right)^2\right\rangle$	$\frac{5}{918412504\pi^3}(42042\langle\beta_2^2\rangle^3 - 5720\langle\cos(3\gamma)\beta_2^3\rangle^2$
	$+30\cdot\left\langle\left(\frac{\delta d_\perp}{d_\perp}\right)^2\right\rangle^3 - 10\cdot\left\langle\left(\frac{\delta d_\perp}{d_\perp}\right)^3\right\rangle^2$	$-45045\langle\beta_2^2\rangle\langle\beta_2^4\rangle + 8575\langle\beta_2^6\rangle + 700\langle\cos(6\gamma)\beta_2^6\rangle)$
κ_7	$\left\langle\left(\frac{\delta d_\perp}{d_\perp}\right)^7\right\rangle - 21\cdot\left\langle\left(\frac{\delta d_\perp}{d_\perp}\right)^5\right\rangle\cdot\left\langle\left(\frac{\delta d_\perp}{d_\perp}\right)^2\right\rangle$	$-\frac{15\sqrt{5}}{524812288}(2002\langle\beta_2^2\rangle^2\langle\cos(3\gamma)\beta_2^3\rangle$
	$+210\cdot\left\langle\left(\frac{\delta d_\perp}{d_\perp}\right)^3\right\rangle\cdot\left\langle\left(\frac{\delta d_\perp}{d_\perp}\right)^2\right\rangle^2$	$+715\langle\cos(3\gamma)\beta_2^3\rangle\langle\beta_2^4\rangle$
	$-35\cdot\left\langle\left(\frac{\delta d_\perp}{d_\perp}\right)^3\right\rangle\cdot\left\langle\left(\frac{\delta d_\perp}{d_\perp}\right)^4\right\rangle$	$+910\langle\cos(3\gamma)\beta_2^5\rangle\langle\beta_2^2\rangle - 175\cos(3\gamma)\beta_2^7\rangle)$
κ_8	$\left\langle\left(\frac{\delta d_\perp}{d_\perp}\right)^8\right\rangle - 28\cdot\left\langle\left(\frac{\delta d_\perp}{d_\perp}\right)^6\right\rangle\cdot\left\langle\left(\frac{\delta d_\perp}{d_\perp}\right)^2\right\rangle$	$\frac{5}{142748942336\pi^4}(2144142\langle\beta_2^2\rangle^4 - 3063060\langle\beta_2^2\rangle^2\langle\beta_2^4\rangle$
	$+420\cdot\left\langle\left(\frac{\delta d_\perp}{d_\perp}\right)^4\right\rangle\left\langle\left(\frac{\delta d_\perp}{d_\perp}\right)^2\right\rangle^2$	$-340\langle\beta_2^2\rangle\Big(2288\langle\cos(3\gamma)\beta_2^3\rangle^2 - 35(49\langle\beta_2^6\rangle$
	$-35\left\langle\left(\frac{\delta d_\perp}{d_\perp}\right)^4\right\rangle^2 - 630\cdot\left\langle\left(\frac{\delta d_\perp}{d_\perp}\right)^2\right\rangle^4$	$+4\langle\cos(6\gamma)\beta_2^6\rangle)\Big) + 25\Big(21879\langle\beta_2^4\rangle^2$
	$+560\cdot\left\langle\left(\frac{\delta d_\perp}{d_\perp}\right)^3\right\rangle^2\cdot\left\langle\left(\frac{\delta d_\perp}{d_\perp}\right)^2\right\rangle$	$+14144\langle\cos(3\gamma)\beta_2^3\rangle\langle\cos(3\gamma)\beta_2^5\rangle$
	$-56\cdot\left\langle\left(\frac{\delta d_\perp}{d_\perp}\right)^5\right\rangle\cdot\left\langle\left(\frac{\delta d_\perp}{d_\perp}\right)^3\right\rangle$	$-35(79\langle\beta_2^8\rangle + 16\langle\cos(6\gamma)\beta_2^8\rangle)\Big)$

E. Nielsen etc., EPJA 60 (2024) 38

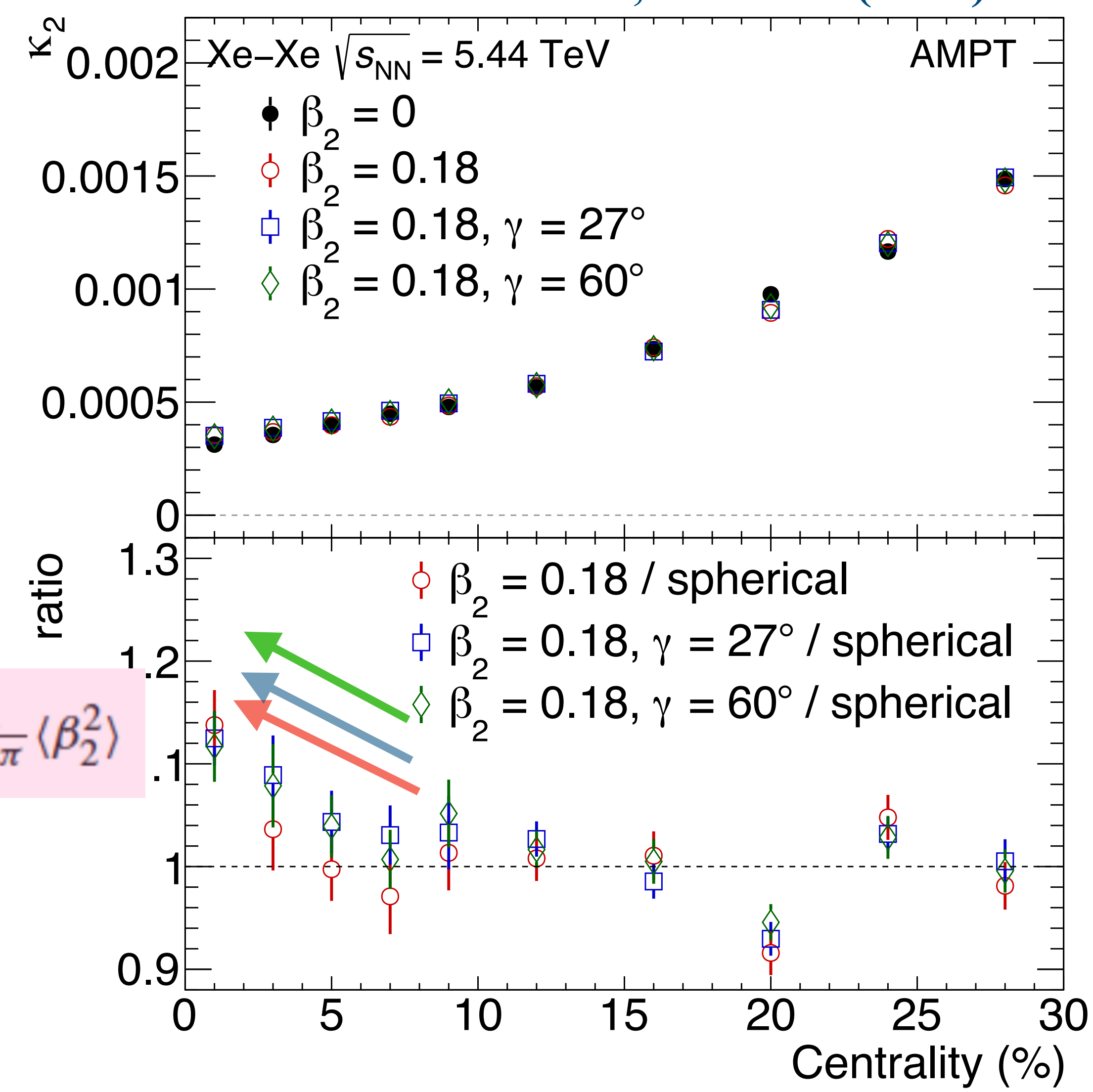

$\frac{1}{32\pi}\langle\beta_2^2\rangle$

❖ These two-particle p_T correlations provide a new way to probe deformation structures of ^{129}Xe.

Probe NS with multi-particle [p_T] correlations

Eur. Phys. J. A (2024) 60:38
https://doi.org/10.1140/epja/s10050-024-01266-x

THE EUROPEAN PHYSICAL JOURNAL A

Check for updates

Regular Article - Theoretical Physics

Generic multi-particle transverse momentum correlations as a new tool for studying nuclear structure at the energy frontier

Emil Gorm Dahlbæk Nielsen, Frederik K. Rømer, Kristjan Gulbrandsen, You Zhou[a]

Niels Bohr Institute, University of Copenhagen, 2200 Copenhagen, Denmark

Table 2 The cumulants of $d_\perp$ up to eighth order in a liquid-drop model potential averaged over random orientations. The first three entries are given in [29]

Final state Cumulant	Initial state Cumulant	Liquid-drop Model
κ_2	$\left\langle\left(\frac{\delta d_\perp}{d_\perp}\right)^2\right\rangle$	$\frac{1}{32\pi}\langle\beta_2^2\rangle$
κ_3	$\left\langle\left(\frac{\delta d_\perp}{d_\perp}\right)^3\right\rangle$	$\frac{\sqrt{5}}{896\pi^{3/2}}\langle\cos(3\gamma)\beta_2^3\rangle$
κ_4	$\left\langle\left(\frac{\delta d_\perp}{d_\perp}\right)^4\right\rangle - 3\cdot\left\langle\left(\frac{\delta d_\perp}{d_\perp}\right)^2\right\rangle^2$	$-\frac{3}{14336\pi^2}(7\langle\beta_2^2\rangle^2 - 5\langle\beta_2^4\rangle)$
κ_5	$\left\langle\left(\frac{\delta d_\perp}{d_\perp}\right)^5\right\rangle - 10\cdot\left\langle\left(\frac{\delta d_\perp}{d_\perp}\right)^3\right\rangle\cdot\left\langle\left(\frac{\delta d_\perp}{d_\perp}\right)^2\right\rangle$	$-\frac{5\sqrt{5}}{315392\pi^{5/2}}(11\langle\cos(3\gamma)\beta_2^3\rangle\langle\beta_2^2\rangle - 5\langle\beta_2^5\rangle)$
κ_6	$\left\langle\left(\frac{\delta d_\perp}{d_\perp}\right)^6\right\rangle - 15\cdot\left\langle\left(\frac{\delta d_\perp}{d_\perp}\right)^4\right\rangle\cdot\left\langle\left(\frac{\delta d_\perp}{d_\perp}\right)^2\right\rangle$	$\frac{5}{918412504\pi^3}(42042\langle\beta_2^2\rangle^3 - 5720\langle\cos(3\gamma)\beta_2^3\rangle^2$
	$+30\cdot\left\langle\left(\frac{\delta d_\perp}{d_\perp}\right)^2\right\rangle^3 - 10\cdot\left\langle\left(\frac{\delta d_\perp}{d_\perp}\right)^3\right\rangle^2$	$-45045\langle\beta_2^2\rangle\langle\beta_2^4\rangle + 8575\langle\beta_2^6\rangle + 700\langle\cos(6\gamma)\beta_2^6\rangle)$
κ_7	$\left\langle\left(\frac{\delta d_\perp}{d_\perp}\right)^7\right\rangle - 21\cdot\left\langle\left(\frac{\delta d_\perp}{d_\perp}\right)^5\right\rangle\cdot\left\langle\left(\frac{\delta d_\perp}{d_\perp}\right)^2\right\rangle$	$-\frac{15\sqrt{5}}{524812288}(2002\langle\beta_2^2\rangle^2\langle\cos(3\gamma)\beta_2^3\rangle$
	$+210\cdot\left\langle\left(\frac{\delta d_\perp}{d_\perp}\right)^3\right\rangle\cdot\left\langle\left(\frac{\delta d_\perp}{d_\perp}\right)^2\right\rangle^2$	$+715\langle\cos(3\gamma)\beta_2^3\rangle\langle\beta_2^4\rangle$
	$-35\cdot\left\langle\left(\frac{\delta d_\perp}{d_\perp}\right)^3\right\rangle\cdot\left\langle\left(\frac{\delta d_\perp}{d_\perp}\right)^4\right\rangle$	$+910\langle\cos(3\gamma)\beta_2^5\rangle\langle\beta_2^2\rangle - 175\cos(3\gamma)\beta_2^7\rangle)$
κ_8	$\left\langle\left(\frac{\delta d_\perp}{d_\perp}\right)^8\right\rangle - 28\cdot\left\langle\left(\frac{\delta d_\perp}{d_\perp}\right)^6\right\rangle\cdot\left\langle\left(\frac{\delta d_\perp}{d_\perp}\right)^2\right\rangle$	$\frac{5}{142748942336\pi^4}(2144142\langle\beta_2^2\rangle^4 - 3063060\langle\beta_2^2\rangle^2\langle\beta_2^4\rangle$
	$+420\cdot\left\langle\left(\frac{\delta d_\perp}{d_\perp}\right)^4\right\rangle\left\langle\left(\frac{\delta d_\perp}{d_\perp}\right)^2\right\rangle^2$	$-340\langle\beta_2^2\rangle\Big(2288\langle\cos(3\gamma)\beta_2^3\rangle^2 - 35\big(49\langle\beta_2^6\rangle$
	$-35\left\langle\left(\frac{\delta d_\perp}{d_\perp}\right)^4\right\rangle^2 - 630\cdot\left\langle\left(\frac{\delta d_\perp}{d_\perp}\right)^2\right\rangle^4$	$+4\langle\cos(6\gamma)\beta_2^6\rangle\big)\Big) + 25\Big(21879\langle\beta_2^4\rangle^2$
	$+560\cdot\left\langle\left(\frac{\delta d_\perp}{d_\perp}\right)^3\right\rangle^2\cdot\left\langle\left(\frac{\delta d_\perp}{d_\perp}\right)^2\right\rangle$	$+14144\langle\cos(3\gamma)\beta_2^3\rangle\langle\cos(3\gamma)\beta_2^5\rangle$
	$-56\cdot\left\langle\left(\frac{\delta d_\perp}{d_\perp}\right)^5\right\rangle\cdot\left\langle\left(\frac{\delta d_\perp}{d_\perp}\right)^3\right\rangle$	$-35\big(79\langle\beta_2^8\rangle + 16\langle\cos(6\gamma)\beta_2^8\rangle\big)\Big)$

Probe NS with multi-particle [pT] correlations

Eur. Phys. J. A (2024) 60:38
https://doi.org/10.1140/epja/s10050-024-01266-x

THE EUROPEAN PHYSICAL JOURNAL A

Check for updates

Regular Article - Theoretical Physics

Generic multi-particle transverse momentum correlations as a new tool for studying nuclear structure at the energy frontier

Emil Gorm Dahlbæk Nielsen, Frederik K. Rømer, Kristjan Gulbrandsen, You Zhou[a]

Niels Bohr Institute, University of Copenhagen, 2200 Copenhagen, Denmark

Table 2 The cumulants of $d_\perp$ up to eighth order in a liquid-drop model potential averaged over random orientations. The first three entries are given in [29]

Final state Cumulant	Initial state Cumulant	Liquid-drop Model
κ_2	$\langle (\frac{\delta d_\perp}{d_\perp})^2 \rangle$	$\frac{1}{32\pi}\langle \beta_2^2 \rangle$
κ_3	$\langle (\frac{\delta d_\perp}{d_\perp})^3 \rangle$	$\frac{\sqrt{5}}{896\pi^{3/2}}\langle \cos(3\gamma)\beta_2^3 \rangle$
κ_4	$\langle (\frac{\delta d_\perp}{d_\perp})^4 \rangle - 3 \cdot \langle (\frac{\delta d_\perp}{d_\perp})^2 \rangle^2$	$-\frac{3}{14336\pi^2}(7\langle \beta_2^2 \rangle^2 - 5\langle \beta_2^4 \rangle)$
κ_5	$\langle (\frac{\delta d_\perp}{d_\perp})^5 \rangle - 10 \cdot \langle (\frac{\delta d_\perp}{d_\perp})^3 \rangle \cdot \langle (\frac{\delta d_\perp}{d_\perp})^2 \rangle$	$-\frac{5\sqrt{5}}{315392\pi^{5/2}}(11\langle \cos(3\gamma)\beta_2^3 \rangle\langle \beta_2^2 \rangle - 5\langle \beta_2^5 \rangle)$
κ_6	$\langle (\frac{\delta d_\perp}{d_\perp})^6 \rangle - 15 \cdot \langle (\frac{\delta d_\perp}{d_\perp})^4 \rangle \cdot \langle (\frac{\delta d_\perp}{d_\perp})^2 \rangle$	$\frac{5}{918412504\pi^3}(42042\langle \beta_2^2 \rangle^3 - 5720\langle \cos(3\gamma)\beta_2^3 \rangle^2$
	$+30 \cdot \langle (\frac{\delta d_\perp}{d_\perp})^2 \rangle^3 - 10 \cdot \langle (\frac{\delta d_\perp}{d_\perp})^3 \rangle^2$	$-45045\langle \beta_2^2 \rangle\langle \beta_2^4 \rangle + 8575\langle \beta_2^6 \rangle + 700\langle \cos(6\gamma)\beta_2^6 \rangle)$
κ_7	$\langle (\frac{\delta d_\perp}{d_\perp})^7 \rangle - 21 \cdot \langle (\frac{\delta d_\perp}{d_\perp})^5 \rangle \cdot \langle (\frac{\delta d_\perp}{d_\perp})^2 \rangle$	$-\frac{15\sqrt{5}}{524812288}(2002\langle \beta_2^2 \rangle^2\langle \cos(3\gamma)\beta_2^3 \rangle$
	$+210 \cdot \langle (\frac{\delta d_\perp}{d_\perp})^3 \rangle \cdot \langle (\frac{\delta d_\perp}{d_\perp})^2 \rangle^2$	$+715\langle \cos(3\gamma)\beta_2^3 \rangle\langle \beta_2^4 \rangle$
	$-35 \cdot \langle (\frac{\delta d_\perp}{d_\perp})^3 \rangle \cdot \langle (\frac{\delta d_\perp}{d_\perp})^4 \rangle$	$+910\langle \cos(3\gamma)\beta_2^5 \rangle\langle \beta_2^2 \rangle - 175\cos(3\gamma)\beta_2^7 \rangle)$
κ_8	$\langle (\frac{\delta d_\perp}{d_\perp})^8 \rangle - 28 \cdot \langle (\frac{\delta d_\perp}{d_\perp})^6 \rangle \cdot \langle (\frac{\delta d_\perp}{d_\perp})^2 \rangle$	$\frac{5}{142748942336\pi^4}(2144142\langle \beta_2^2 \rangle^4 - 3063060\langle \beta_2^2 \rangle^2\langle \beta_2^4 \rangle$
	$+420 \cdot \langle (\frac{\delta d_\perp}{d_\perp})^4 \rangle \langle (\frac{\delta d_\perp}{d_\perp})^2 \rangle^2$	$-340\langle \beta_2^2 \rangle (2288\langle \cos(3\gamma)\beta_2^3 \rangle^2 - 35(49\langle \beta_2^6 \rangle$
	$-35 \langle (\frac{\delta d_\perp}{d_\perp})^4 \rangle^2 - 630 \cdot \langle (\frac{\delta d_\perp}{d_\perp})^2 \rangle^4$	$+4\langle \cos(6\gamma)\beta_2^6 \rangle)) + 25(21879\langle \beta_2^4 \rangle^2$
	$+560 \cdot \langle (\frac{\delta d_\perp}{d_\perp})^3 \rangle^2 \cdot \langle (\frac{\delta d_\perp}{d_\perp})^2 \rangle$	$+14144\langle \cos(3\gamma)\beta_2^3 \rangle\langle \cos(3\gamma)\beta_2^5 \rangle$
	$-56 \cdot \langle (\frac{\delta d_\perp}{d_\perp})^5 \rangle \cdot \langle (\frac{\delta d_\perp}{d_\perp})^3 \rangle$	$-35(79\langle \beta_2^8 \rangle + 16\langle \cos(6\gamma)\beta_2^8 \rangle))$

E. Nielsen etc., EPJA 60 (2024) 38

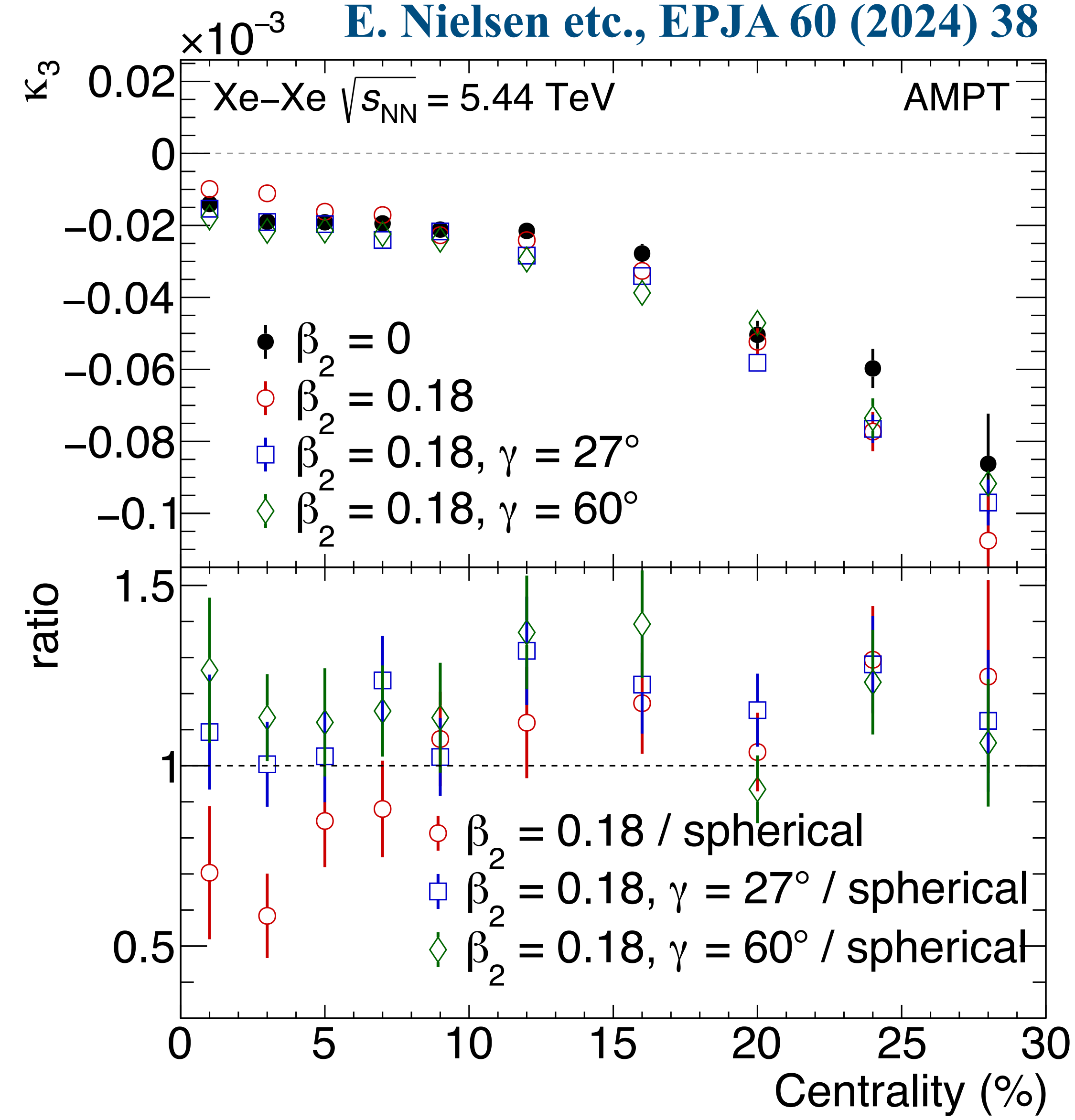

Probe NS with multi-particle [pT] correlations

Eur. Phys. J. A (2024) 60:38
https://doi.org/10.1140/epja/s10050-024-01266-x

THE EUROPEAN PHYSICAL JOURNAL A

Check for updates

Regular Article - Theoretical Physics

Generic multi-particle transverse momentum correlations as a new tool for studying nuclear structure at the energy frontier

Emil Gorm Dahlbæk Nielsen, Frederik K. Rømer, Kristjan Gulbrandsen, You Zhou[a]
Niels Bohr Institute, University of Copenhagen, 2200 Copenhagen, Denmark

Table 2 The cumulants of $d_\perp$ up to eighth order in a liquid-drop model potential averaged over random orientations. The first three entries are given in [29]

Final state Cumulant	Initial state Cumulant	Liquid-drop Model
κ_2	$\left\langle\left(\frac{\delta d_\perp}{d_\perp}\right)^2\right\rangle$	$\frac{1}{32\pi}\langle\beta_2^2\rangle$
κ_3	$\left\langle\left(\frac{\delta d_\perp}{d_\perp}\right)^3\right\rangle$	$\frac{\sqrt{5}}{896\pi^{3/2}}\langle\cos(3\gamma)\beta_2^3\rangle$
κ_4	$\left\langle\left(\frac{\delta d_\perp}{d_\perp}\right)^4\right\rangle - 3\cdot\left\langle\left(\frac{\delta d_\perp}{d_\perp}\right)^2\right\rangle^2$	$-\frac{3}{14336\pi^2}(7\langle\beta_2^2\rangle^2 - 5\langle\beta_2^4\rangle)$
κ_5	$\left\langle\left(\frac{\delta d_\perp}{d_\perp}\right)^5\right\rangle - 10\cdot\left\langle\left(\frac{\delta d_\perp}{d_\perp}\right)^3\right\rangle\cdot\left\langle\left(\frac{\delta d_\perp}{d_\perp}\right)^2\right\rangle$	$-\frac{5\sqrt{5}}{315392\pi^{5/2}}(11\langle\cos(3\gamma)\beta_2^3\rangle\langle\beta_2^2\rangle - 5\langle\beta_2^5\rangle)$
κ_6	$\left\langle\left(\frac{\delta d_\perp}{d_\perp}\right)^6\right\rangle - 15\cdot\left\langle\left(\frac{\delta d_\perp}{d_\perp}\right)^4\right\rangle\cdot\left\langle\left(\frac{\delta d_\perp}{d_\perp}\right)^2\right\rangle$	$\frac{5}{918412504\pi^3}(42042\langle\beta_2^2\rangle^3 - 5720\langle\cos(3\gamma)\beta_2^3\rangle^2$
	$+30\cdot\left\langle\left(\frac{\delta d_\perp}{d_\perp}\right)^2\right\rangle^3 - 10\cdot\left\langle\left(\frac{\delta d_\perp}{d_\perp}\right)^3\right\rangle^2$	$-45045\langle\beta_2^2\rangle\langle\beta_2^4\rangle + 8575\langle\beta_2^6\rangle + 700\langle\cos(6\gamma)\beta_2^6\rangle)$
κ_7	$\left\langle\left(\frac{\delta d_\perp}{d_\perp}\right)^7\right\rangle - 21\cdot\left\langle\left(\frac{\delta d_\perp}{d_\perp}\right)^5\right\rangle\cdot\left\langle\left(\frac{\delta d_\perp}{d_\perp}\right)^2\right\rangle$	$-\frac{15\sqrt{5}}{524812288}(2002\langle\beta_2^2\rangle^2\langle\cos(3\gamma)\beta_2^3\rangle$
	$+210\cdot\left\langle\left(\frac{\delta d_\perp}{d_\perp}\right)^3\right\rangle\cdot\left\langle\left(\frac{\delta d_\perp}{d_\perp}\right)^2\right\rangle^2$	$+715\langle\cos(3\gamma)\beta_2^3\rangle\langle\beta_2^4\rangle$
	$-35\cdot\left\langle\left(\frac{\delta d_\perp}{d_\perp}\right)^3\right\rangle\cdot\left\langle\left(\frac{\delta d_\perp}{d_\perp}\right)^4\right\rangle$	$+910\langle\cos(3\gamma)\beta_2^5\rangle\langle\beta_2^2\rangle - 175\cos(3\gamma)\beta_2^7\rangle)$
κ_8	$\left\langle\left(\frac{\delta d_\perp}{d_\perp}\right)^8\right\rangle - 28\cdot\left\langle\left(\frac{\delta d_\perp}{d_\perp}\right)^6\right\rangle\cdot\left\langle\left(\frac{\delta d_\perp}{d_\perp}\right)^2\right\rangle$	$\frac{5}{142748942336\pi^4}(2144142\langle\beta_2^2\rangle^4 - 3063060\langle\beta_2^2\rangle^2\langle\beta_2^4\rangle$
	$+420\cdot\left\langle\left(\frac{\delta d_\perp}{d_\perp}\right)^4\right\rangle\left\langle\left(\frac{\delta d_\perp}{d_\perp}\right)^2\right\rangle^2$	$-340\langle\beta_2^2\rangle\Big(2288\langle\cos(3\gamma)\beta_2^3\rangle^2 - 35\big(49\langle\beta_2^6\rangle$
	$-35\left\langle\left(\frac{\delta d_\perp}{d_\perp}\right)^4\right\rangle^2 - 630\cdot\left\langle\left(\frac{\delta d_\perp}{d_\perp}\right)^2\right\rangle^4$	$+4\langle\cos(6\gamma)\beta_2^6\rangle\big)\Big) + 25\Big(21879\langle\beta_2^4\rangle^2$
	$+560\cdot\left\langle\left(\frac{\delta d_\perp}{d_\perp}\right)^3\right\rangle^2\cdot\left\langle\left(\frac{\delta d_\perp}{d_\perp}\right)^2\right\rangle$	$+14144\langle\cos(3\gamma)\beta_2^3\rangle\langle\cos(3\gamma)\beta_2^5\rangle$
	$-56\cdot\left\langle\left(\frac{\delta d_\perp}{d_\perp}\right)^5\right\rangle\cdot\left\langle\left(\frac{\delta d_\perp}{d_\perp}\right)^3\right\rangle$	$-35\big(79\langle\beta_2^8\rangle + 16\langle\cos(6\gamma)\beta_2^8\rangle\big)\Big)$

E. Nielsen etc., EPJA 60 (2024) 38

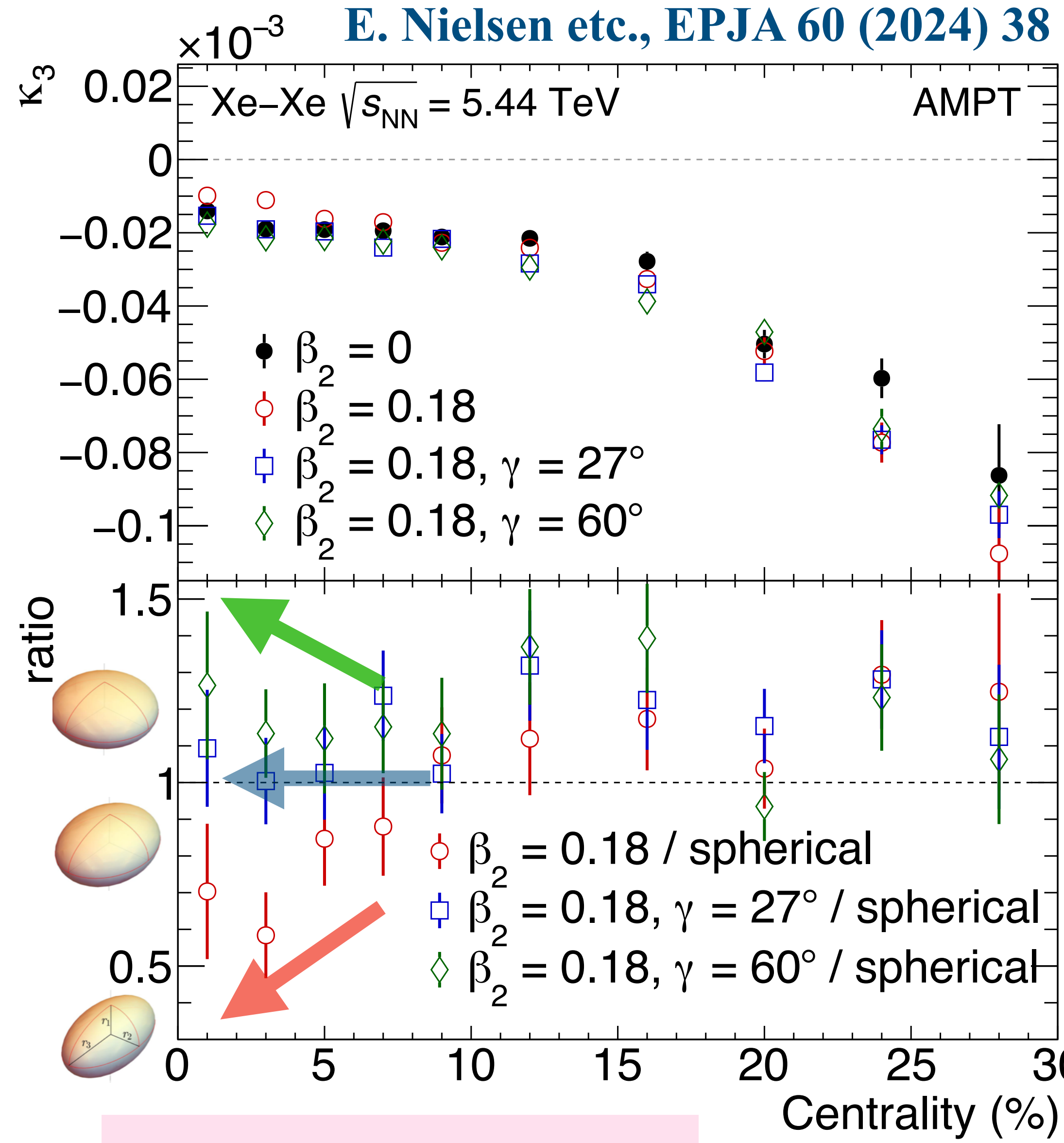

$$\frac{\sqrt{5}}{896\pi^{3/2}}\langle\cos(3\gamma)\beta_2^3\rangle$$

- Multi-particle [pT] correlation reflects the initial size fluctuations, also bring new information on the ***triaxial*** structure.

Probe triaxial structure of ^{129}Xe

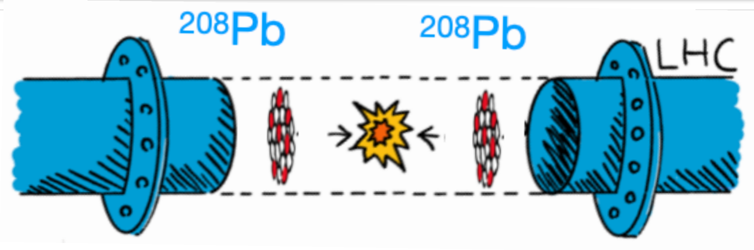

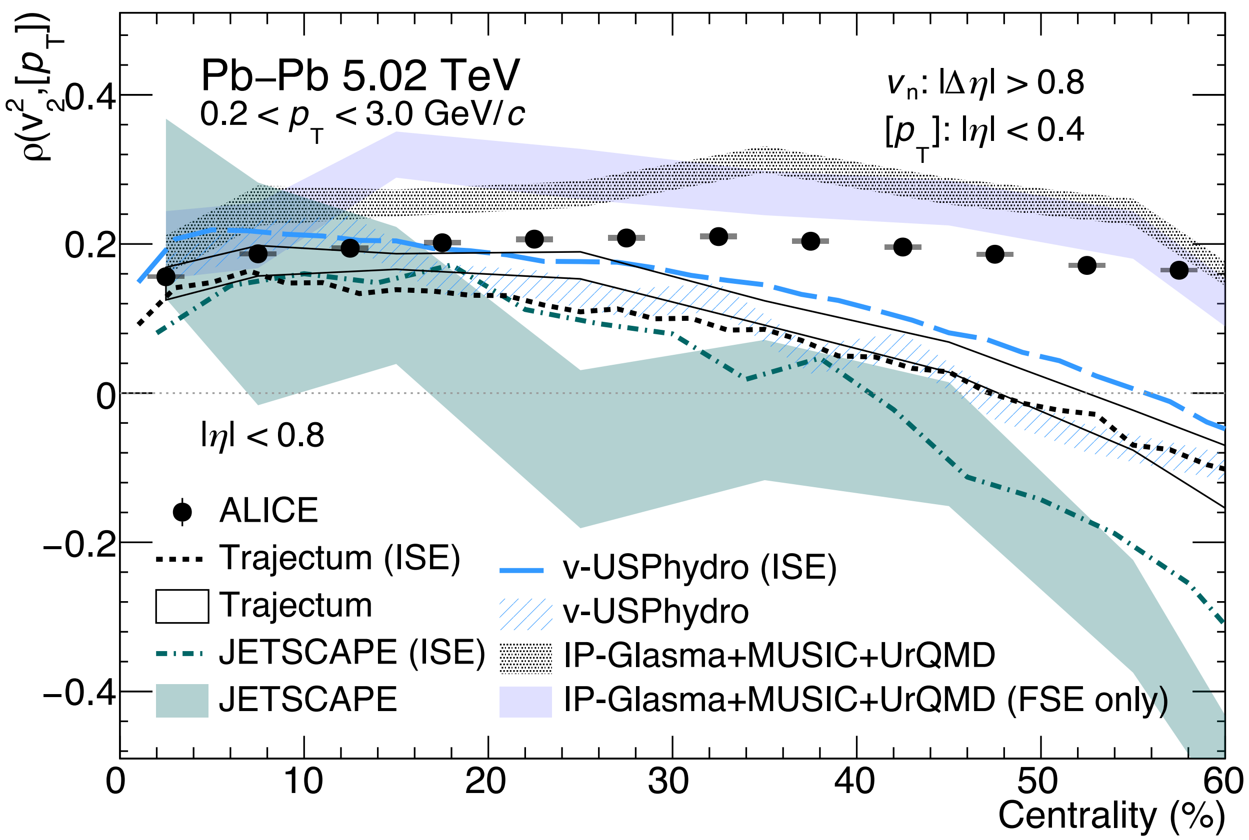

Probe triaxial structure of ^{129}Xe

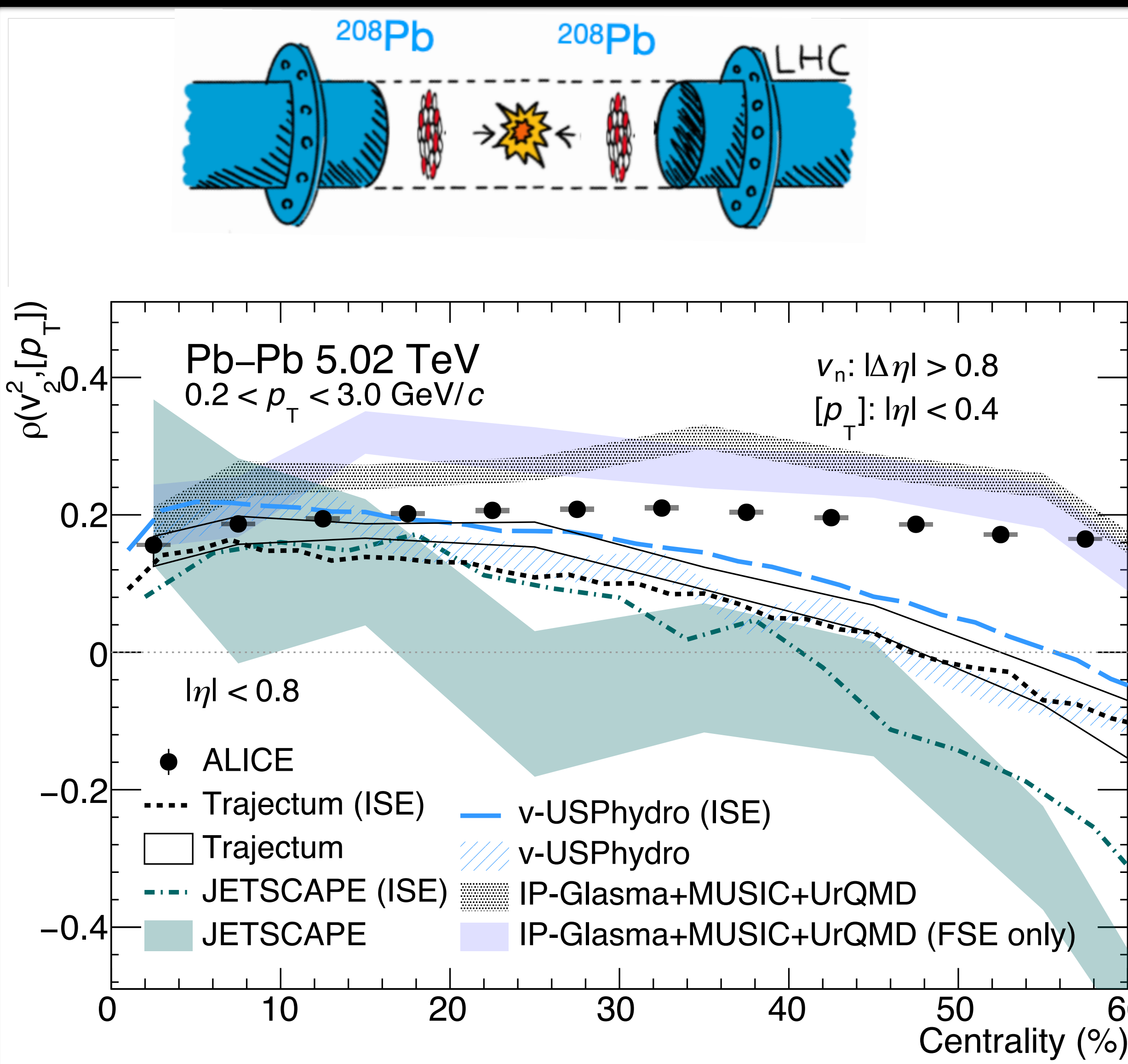

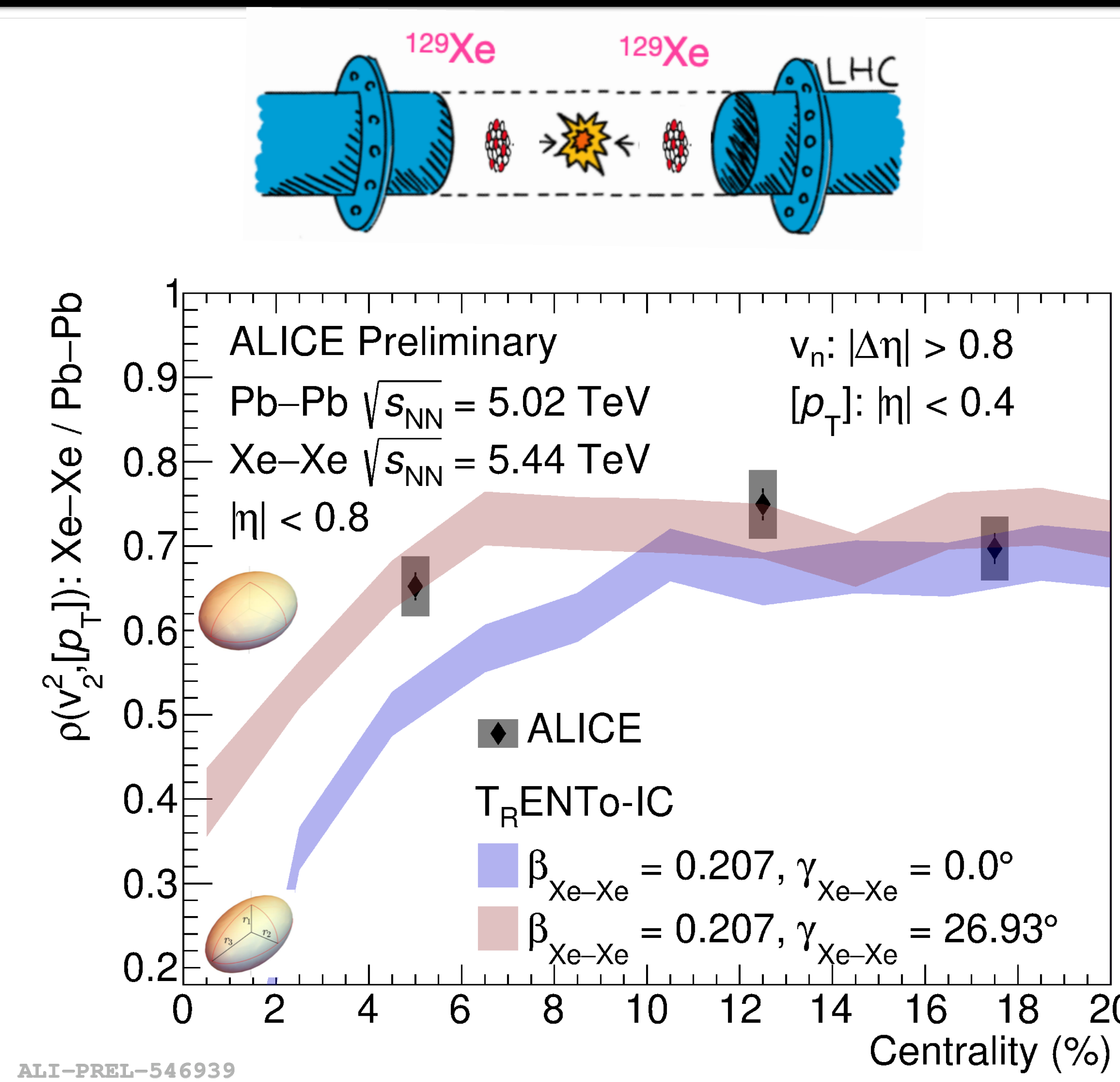

Probe triaxial structure of ^{129}Xe

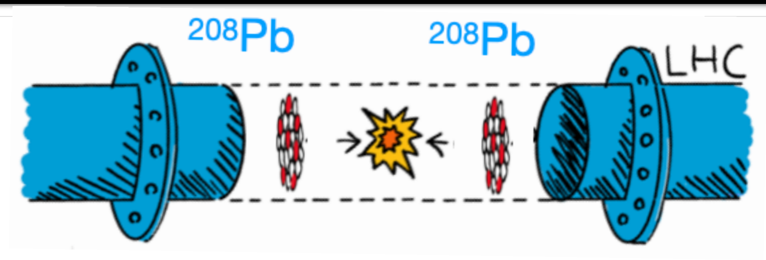

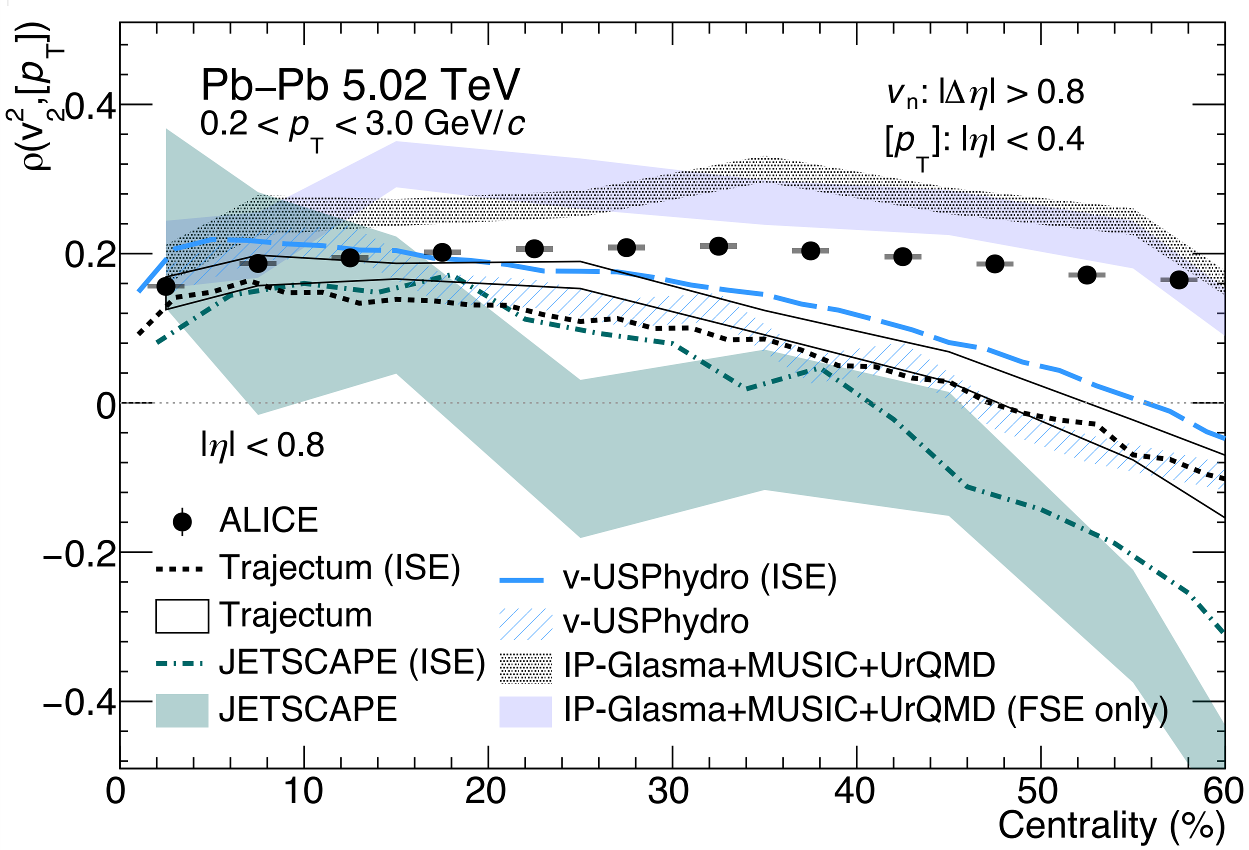

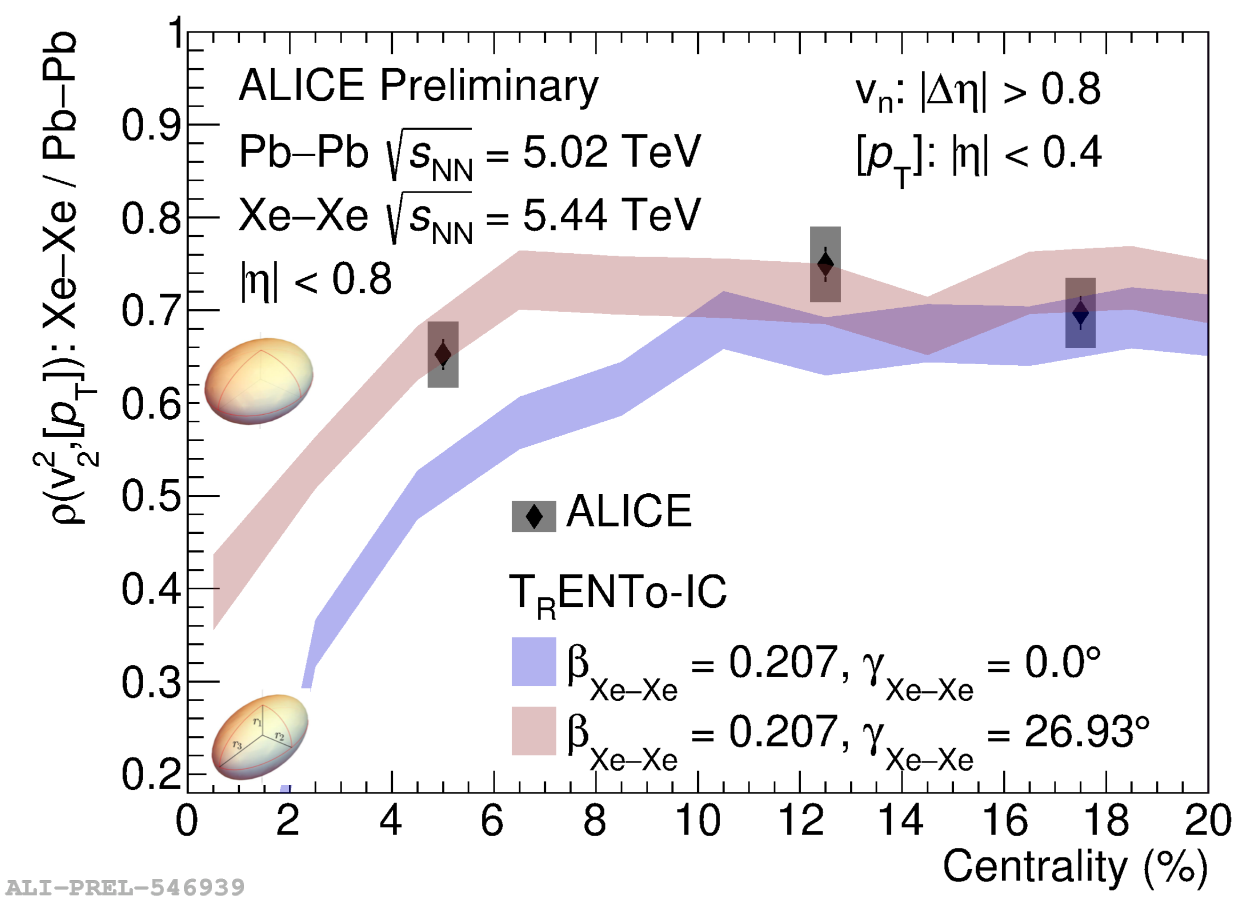

- Better agreement between LHC data and calculations with γ = 26.93°
  - First study of triaxial structure of ^{129}Xe at high energy collisions at the LHC
  - Similar results confirmed by ATLAS
  - ***Evidence of triaxial structure of ^{129}Xe?*** **B. Bally etc, PRL128 (2022) 8, 082301**

Probe γ-soft structure of ^{129}Xe

arXiv:2403.07441, submitted to *PRL*

Nuclear Theory

[Submitted on 12 Mar 2024]

Exploring the Nuclear Shape Phase Transition in Ultra-Relativistic ^{129}Xe+^{129}Xe Collisions at the LHC

Shujun Zhao, Hao-jie Xu, You Zhou, Yu-Xin Liu, Huichao Song

The shape phase transition for certain isotope or isotone chains, associated with the quantum phase transition of finite nuclei, is an intriguing phenomenon in nuclear physics. A notable case is the Xe isotope chain, where the structure transits from a γ-soft rotor to a spherical vibrator, with the second-order shape phase transition occurring in the vicinity of $^{128-130}$Xe. In this letter, we focus on investigating the γ-soft deformation of ^{129}Xe associated with the second-order shape phase transition by constructing novel correlators for ultra-relativistic ^{129}Xe+^{129}Xe collisions. In particular, our iEBE-VISHNU model calculations show that the $v_2^2-[p_T]$ correlation ρ_2 and the mean transverse momentum fluctuation Γ_{p_T}, which were previously interpreted as the evidence for the rigid triaxial deformation of ^{129}Xe, can also be well explained by the γ-soft deformation of ^{129}Xe. We also propose two novel correlators $\rho_{4,2}$ and $\rho_{2,4}$, which carry non-trivial higher-order correlations and show unique capabilities to distinguish between the γ-soft and the rigid triaxial deformation of ^{129}Xe in ^{129}Xe+^{129}Xe collisions at the LHC. The present study also provides a novel way to explore the second-order shape phase transition of finite nuclei with ultra-relativistic heavy ion collisions.

3-particle [p_T] correlatior

$$\Gamma_{p_T} = \frac{\langle \delta p_{T,i}\delta p_{T,j}\delta p_{T,k}\rangle\langle[p}{\langle \delta p_{T,i}\delta p_{T,j}\rangle^2}$$

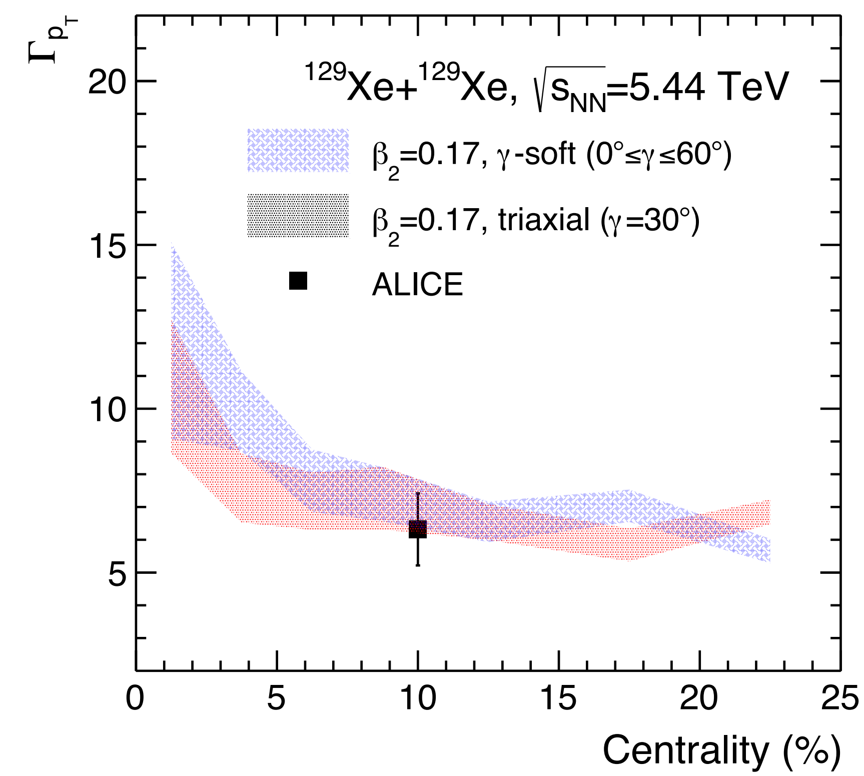

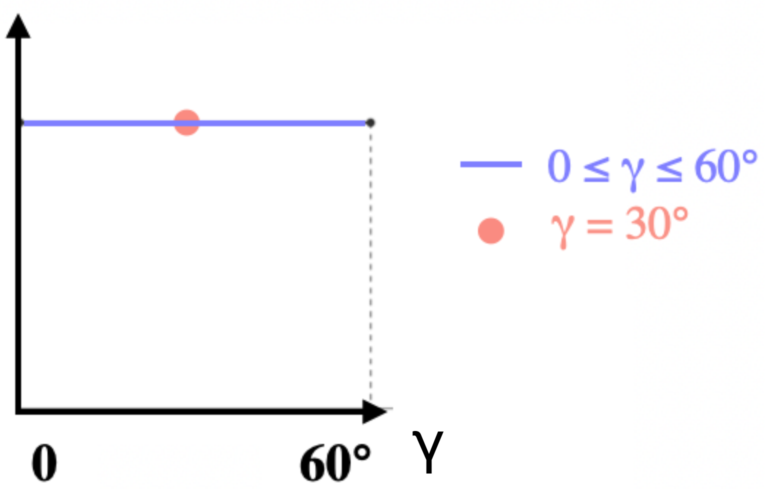

3-particle v_n^2 — [p_T] correlation

$$\rho_2 \equiv \frac{\mathrm{cov}(v_2\{2\}^2, [p_T])}{\sqrt{\mathrm{var}(v_2\{2\}^2)}\sqrt{\mathrm{var}([p_T])}}$$

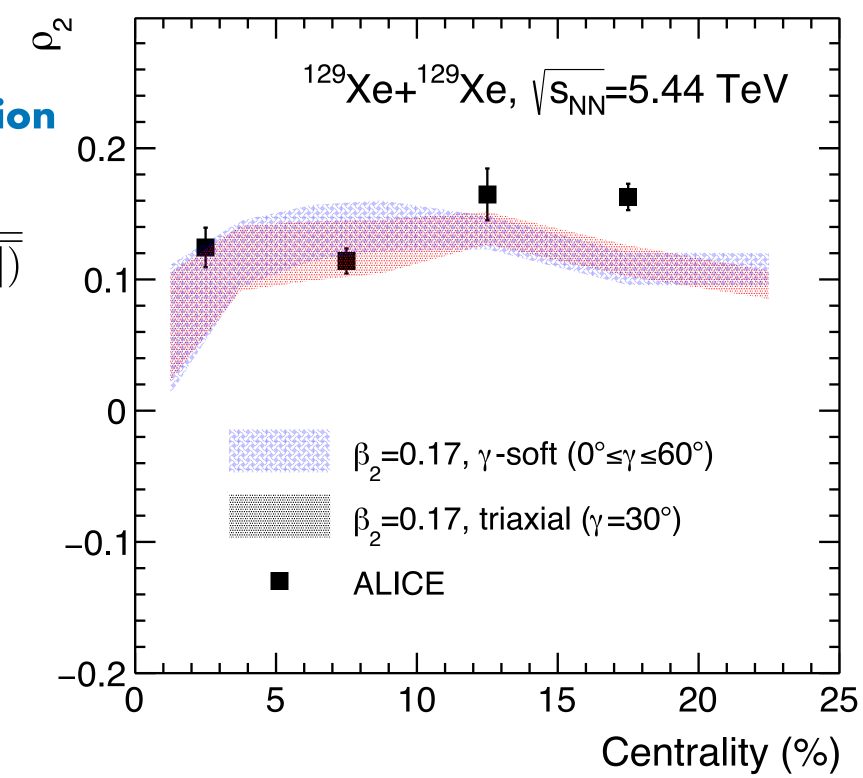

❖As soon as the <cos (3γ)> is the same, the ρ_2 and Γ_{pt} are identical

- One can ***NOT*** distinguish triaxial (fixed γ = 30°) and γ-soft (fluctuating γ) structures with existing 3-particle correlations

Simple logic

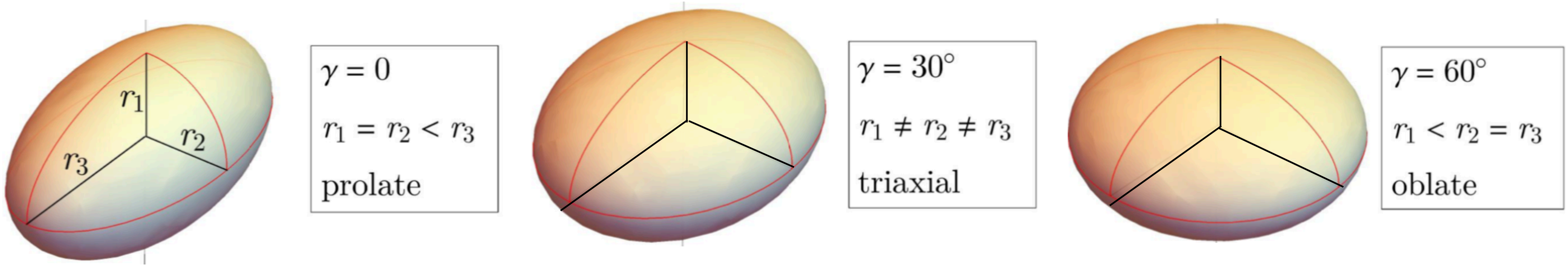

Simple logic

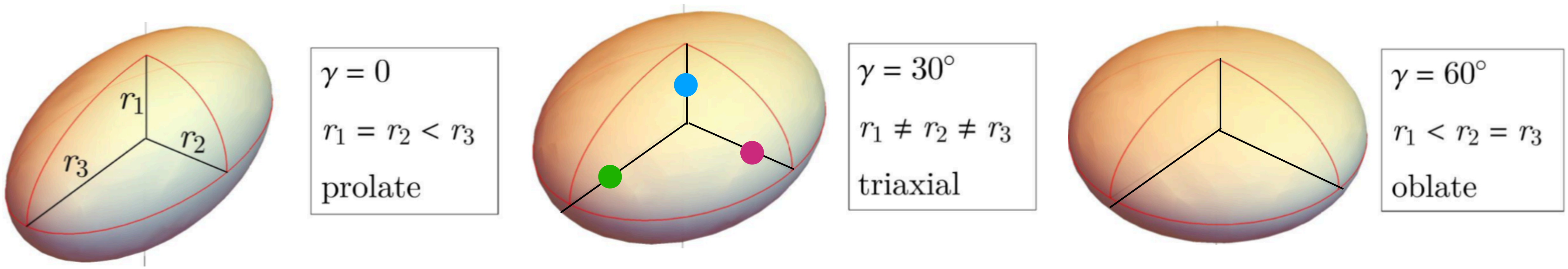

❖ To probe the relation of r_1, r_2 and r_3, we need 3-particle correlations

Simple logic

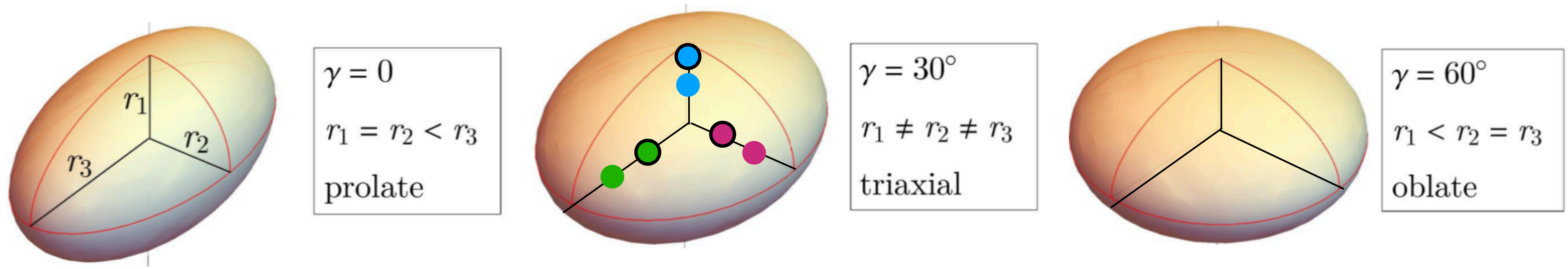

- ❖ To probe the relation of r_1, r_2 and r_3, we need 3-particle correlations
- ❖ To probe the γ fluctuations, we need 6-particle correlations

New probe for the γ-soft structure

New proposals:

$$\rho_{4,2} \equiv \left(\frac{\langle \varepsilon_2^4 \delta d_\perp^2 \rangle}{\langle \varepsilon_2^4 \rangle \langle d_\perp \rangle^2}\right)_c \equiv \frac{1}{\langle \varepsilon_2^4 \rangle \langle d_\perp \rangle^2}\left[\langle \varepsilon_2^4 \delta d_\perp^2 \rangle + 4\langle \varepsilon_2^2 \rangle^2 \langle \delta d_\perp^2 \rangle - \langle \varepsilon_2^4 \rangle \langle \delta d_\perp^2 \rangle - 4\langle \varepsilon_2^2 \rangle \langle \varepsilon_2^2 \delta d_\perp^2 \rangle - 4\langle \varepsilon_2^2 \delta d_\perp \rangle^2\right]$$

$$\rho_{2,4} \equiv \left(\frac{\langle \varepsilon_2^2 \delta d_\perp^4 \rangle}{\langle \varepsilon_2^2 \rangle \langle d_\perp \rangle^4}\right)_c \equiv \frac{1}{\langle \varepsilon_2^2 \rangle \langle d_\perp \rangle^4}\left[\langle \varepsilon_2^2 \delta d_\perp^4 \rangle - 6\langle \varepsilon_2^2 \delta d_\perp^2 \rangle \langle \delta d_\perp^2 \rangle - 4\langle \varepsilon_2^2 \delta d_\perp \rangle \langle \delta d_\perp^3 \rangle - \langle \varepsilon_2^2 \rangle \langle \delta d_\perp^4 \rangle + 6\langle \varepsilon_2^2 \rangle \left(\langle \delta d_\perp^2 \rangle\right)\right]$$

Expectations:

$$\langle \varepsilon_2^4 \rangle \rho_{4,2} = A\beta_2^6(53 + 16\langle \cos(6\gamma) \rangle) + f_{4,2}(\beta_2^6, \langle \cos(3\gamma) \rangle)$$

$$\langle \varepsilon_2^2 \rangle \rho_{2,4} = \frac{A}{16}\beta_2^6(43 - 14\langle \cos(6\gamma) \rangle) + f_{2,4}(\beta_2^6, \langle \cos(3\gamma) \rangle)$$

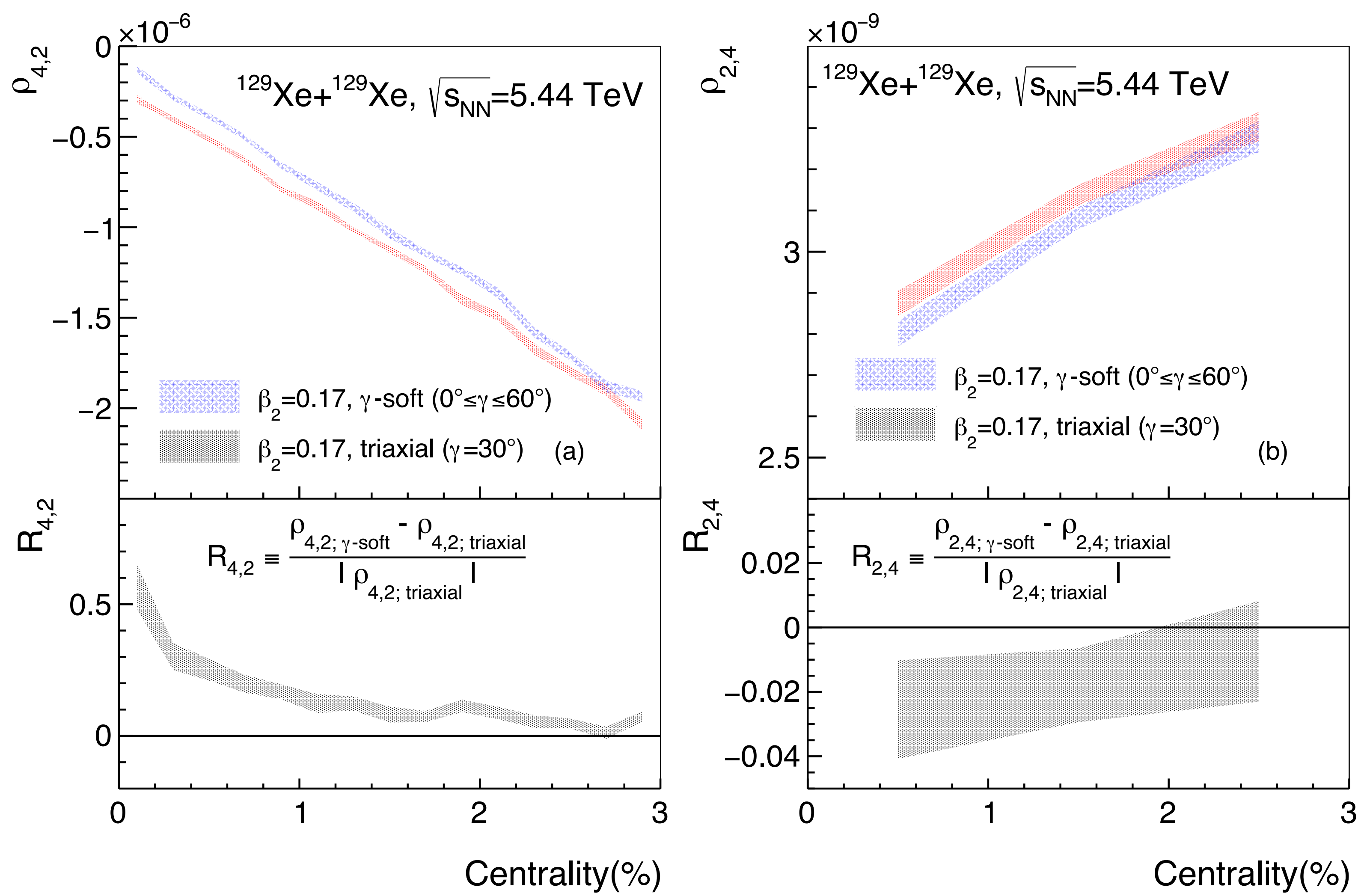

- The six-particle correlations allow to differentiate triaxial (fixed γ = 30°) and γ-soft (fluctuating γ) structures.
- Difference in $\rho_{4,2}$ can reach 50% in the ultra-central collisions.
- ***Opening a new pathway to probe nuclear shape phase transition at the ultra-relativistic energies.***

Massive Pb-Pb data

Run 2

2017 (pilot)

8 hours **data taken**

Massive Pb-Pb data

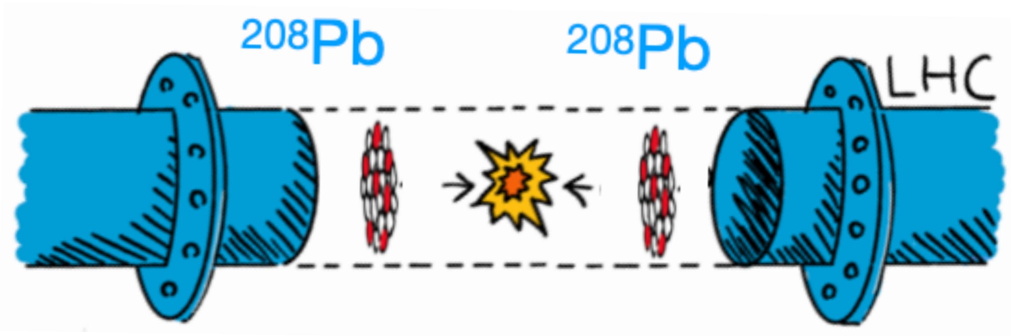

Run 2 **2017 (pilot)**

8 hours **data taken**

Run 1 **2010, 2011**

Run 2 **2015, 2018**

Run 3 **2022 (pilot), 2023, 2024**

4-6 weeks **each period**

Neutron skin study at High Energy

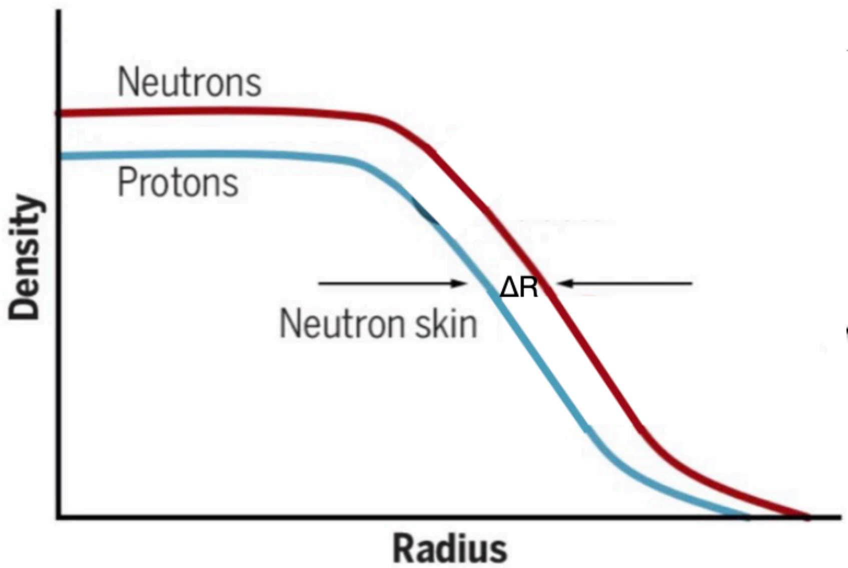

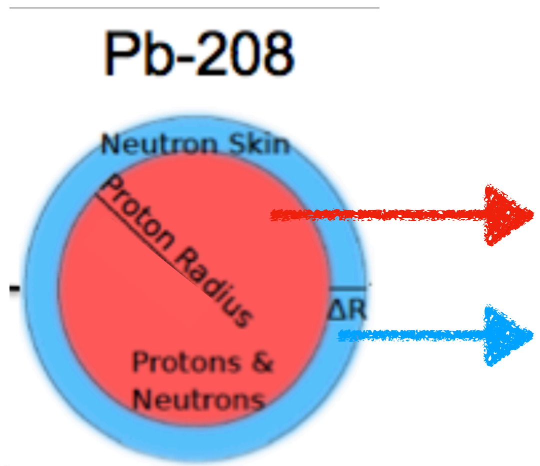

$$\rho(r,\Theta,\Phi) \propto \frac{1}{1+\exp\left(\left[r - R(\Theta,\Phi)\right]/a\right)}$$

$$\rho_p(r,\Theta,\Phi) \propto \frac{1}{1+\exp\left(\left[r_p - R_p(\Theta,\Phi)\right]/a_p\right)}$$

$$\rho_n(r,\Theta,\Phi) \propto \frac{1}{1+\exp\left(\left[r_n - R_n(\Theta,\Phi)\right]/a_n\right)}$$

a_p = 0.448 fm,
R_p = 6.680 fm,
r_p = 5.436 fm,
R_n = 6.690 fm

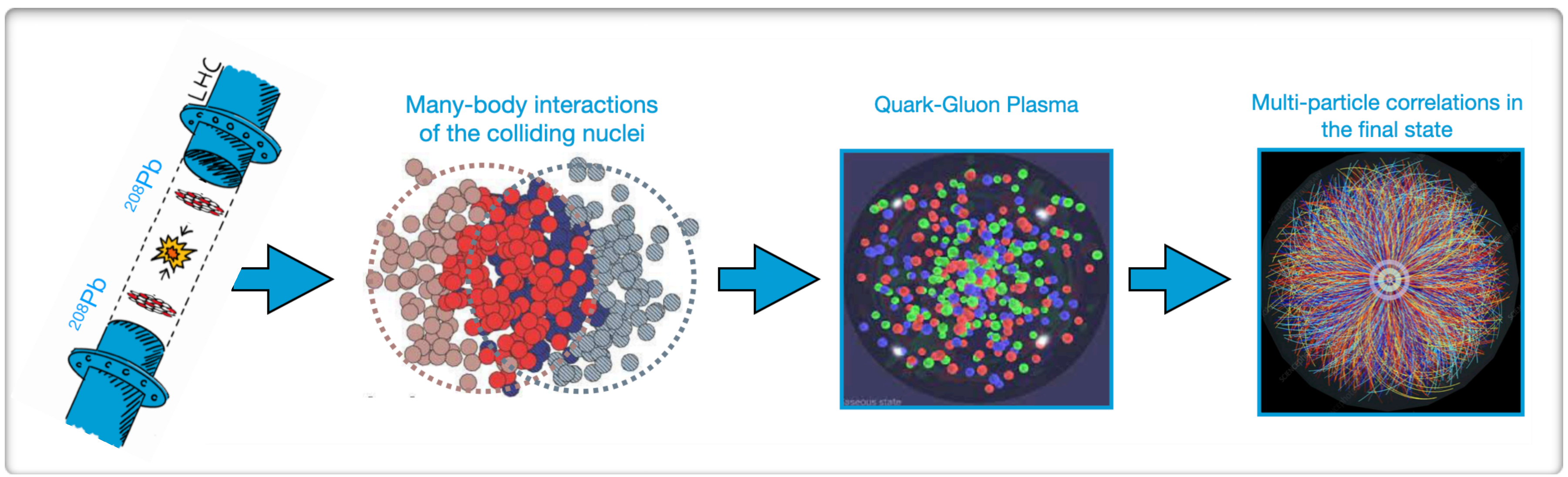

Large neutron skin → Large Initial size → Smaller $[p_T]$ & stronger $[p_T]$ fluctuations

Large Initial size → Weaker flow fluctuations

Extracting neutron skin of ^{208}Pb

CERN

Thick-skinned: Using heavy-ion collisions at the LHC, scientists determine the thickness of neutron “skin” in lead-208 nuclei

This is the first measurement of the neutron skin of lead-208 using exchanges predominantly involving gluons and it can provide insight into the structure of nuclei and neutron stars

15 NOVEMBER, 2023 | By Naomi Dinmore

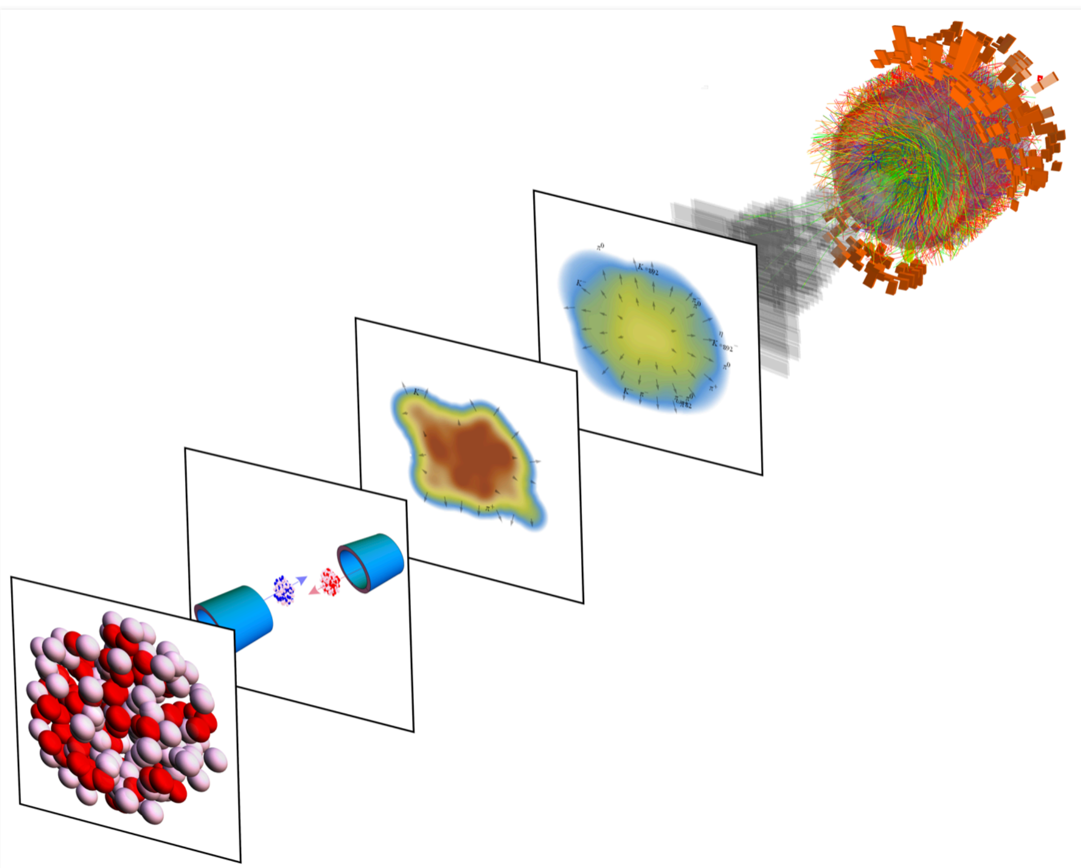

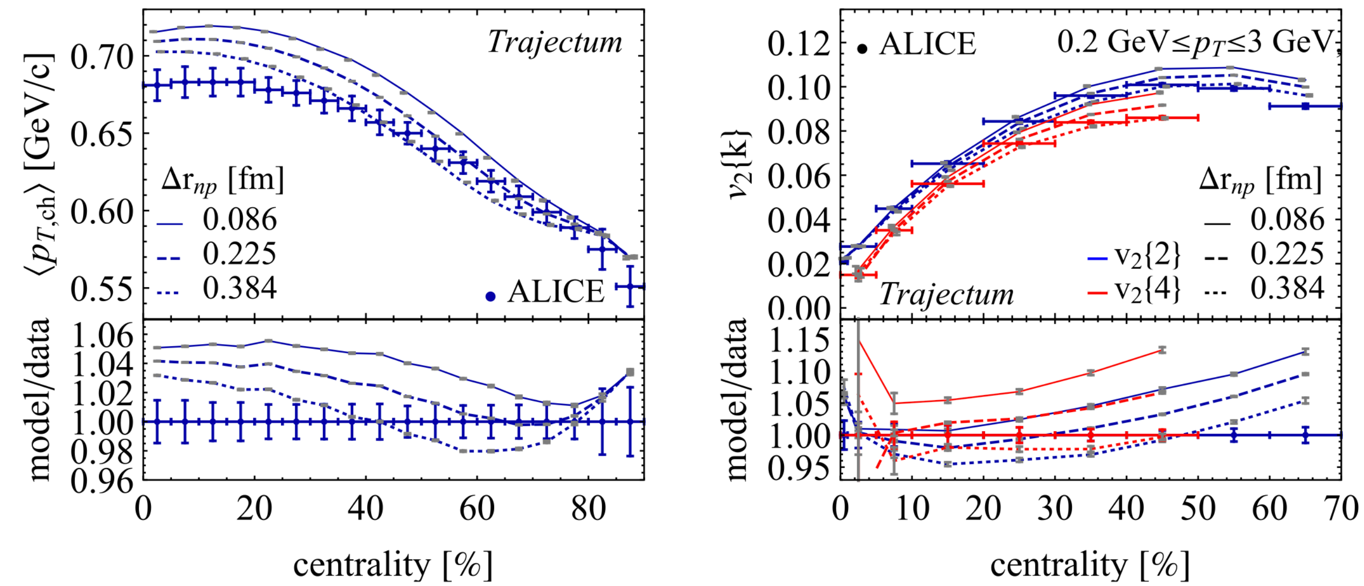

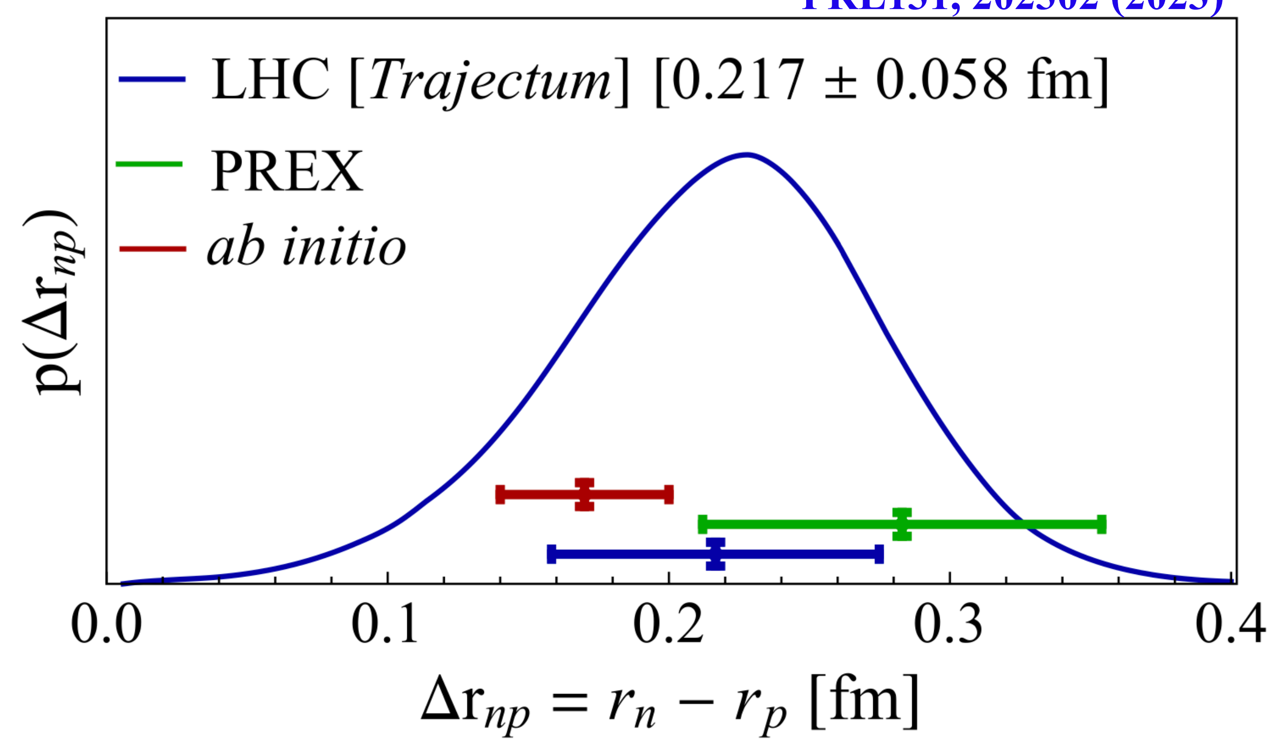

Connecting to astrophysics

neutron skin → Symmetry energy EoS of Nuclear Matter → Critical size & mass of neutron stars

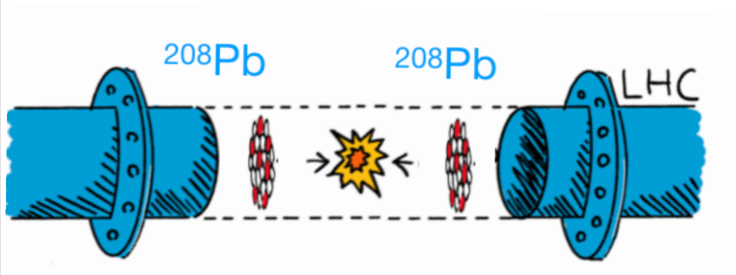

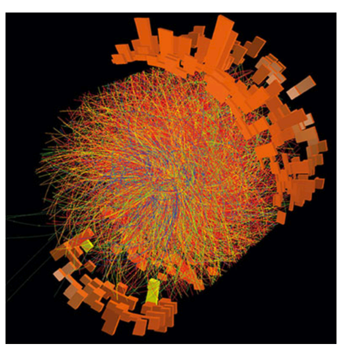

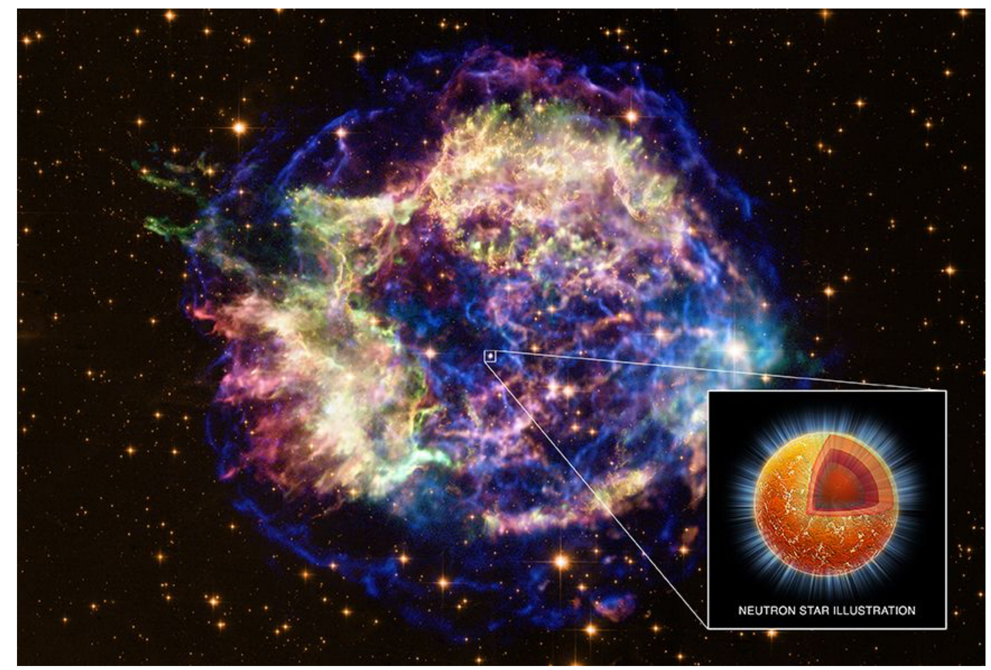

Heavy-ion collisions

Neutron stars

And more

❖ More than just flow and [p_T]

PHYSICAL REVIEW C
covering nuclear physics

Highlights Recent Accepted Collections Authors Referees Search Press About Editorial Tean

Open Access

Effect of initial nuclear deformation on dielectron photoproduction in hadronic heavy-ion collisions

Jiaxuan Luo, Xinbai Li, Zebo Tang, Xin Wu, and Wangmei Zha
Phys. Rev. C **108**, 054906 – Published 27 November 2023

arXiv > hep-ph > arXiv:2405.16491

Search..
Help

High Energy Physics – Phenomenology

[Submitted on 26 May 2024]

Nuclear deformation effects in photoproduction of ρ mesons in ultraperipheral isobaric collisions

Shuo Lin, Jin-Yu Hu, Hao-Jie Xu, Shi Pu, Qun Wang

O-O collisions at the LHC in 2025

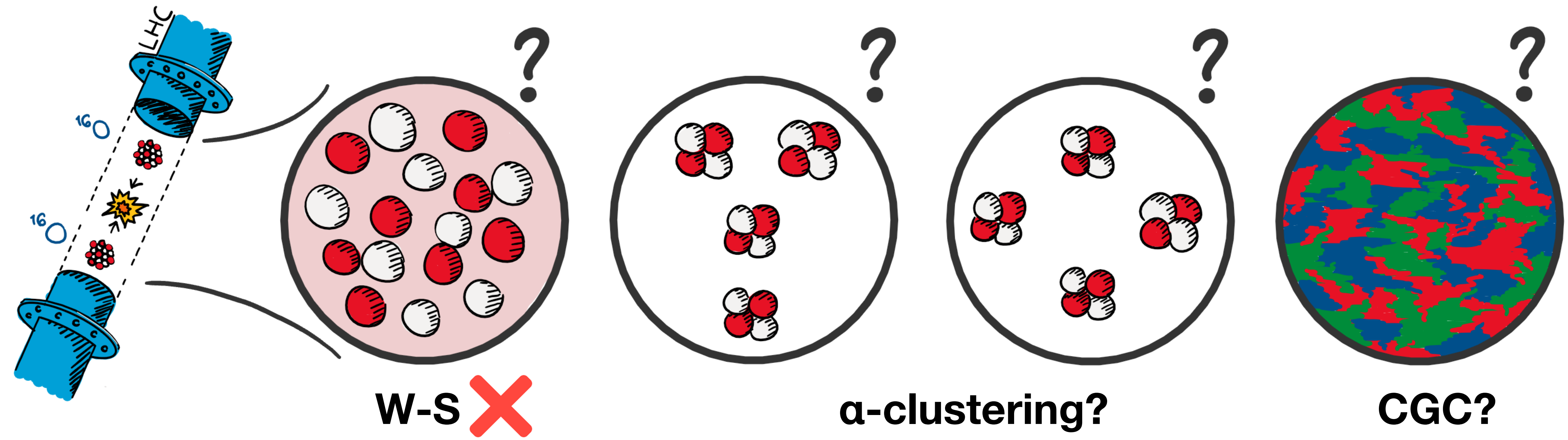

arXiv: 2402.05995

The unexpected uses of a bowling pin: exploiting ^{20}Ne isotopes for precision characterizations of collectivity in small systems

Giuliano Giacalone,[1,*] Benjamin Bally,[2] Govert Nijs,[3] Shihang Shen,[4]
Thomas Duguet,[5,6] Jean-Paul Ebran,[7,8] Serdar Elhatisari,[9,10] Mikael Frosini,[11] Timo A. Lähde,[12,13]
Dean Lee,[14] Bing-Nan Lu,[15] Yuan-Zhuo Ma,[14] Ulf-G. Meißner,[10,16,17] Jacquelyn Noronha-Hostler,[18]
Christopher Plumberg,[19] Tomás R. Rodríguez,[20] Robert Roth,[21,22] Wilke van der Schee,[3,23,24] and Vittorio Somà[5]

arXiv: 2404.08385

***Ab-initio* nucleon-nucleon correlations and their impact on high energy ^{16}O+^{16}O collisions**

Chunjian Zhang,[1,2,3,*] Jinhui Chen,[1,2,†] Giuliano Giacalone,[4,‡] Shengli Huang,[3,§] Jiangyong Jia,[3,5,¶] and Yu-Gang Ma[1,2,**]
[1]*Key Laboratory of Nuclear Physics and Ion-beam Application (MOE), and Institute of Modern Physics, Fudan University, Shanghai 200433, China*
[2]*Shanghai Research Center for Theoretical Nuclear Physics, NSFC and Fudan University, Shanghai 200438, China*
[3]*Department of Chemistry, Stony Brook University, Stony Brook, NY 11794, USA*
[4]*Institut für Theoretische Physik, Universität Heidelberg, Philosophenweg 16, 69120 Heidelberg, Germany*
[5]*Physics Department, Brookhaven National Laboratory, Upton, NY 11976, USA*

Investigating nucleon-nucleon correlations inherent to the strong nuclear force is one of the core goals in nuclear physics research. We showcase the unique opportunities offered by collisions of ^{16}O nuclei at high-energy facilities to reveal detailed many-body properties of the nuclear ground state. We interface existing knowledge about the geometry of ^{16}O coming from *ab-initio* calculations of nuclear structure with transport simulations of high-energy ^{16}O+^{16}O collisions. Bulk observables in these processes, such as the elliptic flow or the fluctuations of the mean transverse momentum, are found to depend significantly on the input nuclear model and to be sensitive to realistic clustering and short-range repulsive correlations, effectively opening a new avenue to probe these features experimentally. This finding demonstrates collisions of oxygen nuclei as a tool to elucidate initial conditions of small collision systems while fostering connections with effective field theories of nuclei rooted in quantum chromodynamics (QCD).

arXiv:2404.09780

Nuclear cluster structure effect in ^{16}O+^{16}O collisions at the top RHIC energy

Xin-Li Zhao,[1,2,3] Guo-Liang Ma,[2,3,*] You Zhou,[4,†] Zi-Wei Lin,[5] and Chao Zhang[6]
[1]*College of Science, University of Shanghai for Science and Technology, Shanghai 200093, China*
[2]*Key Laboratory of Nuclear Physics and Ion-beam Application (MOE), Institute of Modern Physics, Fudan University, Shanghai 200433, China*
[3]*Shanghai Research Center for Theoretical Nuclear Physics, NSFC and Fudan University, Shanghai 200438, China*
[4]*Niels Bohr Institute, Jagtvej 155A, 2200 Copenhagen, Denmark*
[5]*Department of Physics, East Carolina University, Greenville, NC 27858, USA*
[6]*School of Science, Wuhan University of Technology, Wuhan, 430070, China*

The impact of nuclear structure has garnered considerable attention in the high-energy nuclear physics community in recent years. This work focuses on studying the potential nuclear cluster structure in ^{16}O nuclei using anisotropic flow observables in O+O collisions at 200 GeV. Employing an improved AMPT model with various cluster structure configurations, we find that an extended effective parton formation time is necessary to align with the recent STAR experimental data. In addition, we reveal that the presented flow observables serve as sensitive probes for differentiating configurations of α-clustering of ^{16}O nuclei. The systematic AMPT calculations presented in this paper, along with comprehensive comparisons to forthcoming experimental measurements at RHIC and the LHC, pave the way for a novel approach to investigate the α-clustering structure of ^{16}O nuclei using O + O collisions at the ultra-relativistic energies.

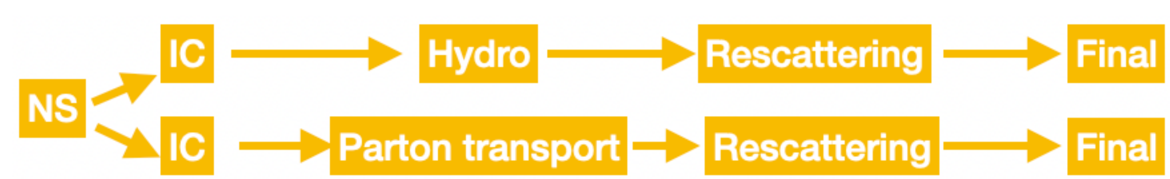

Future possibilities

CERN (11.2024)

TH Institute Light Ions at the LHC

- ☆ organised by CERN-TH, YZ (NBI), Qipeng Hu (USTC) etc.
- ☆ a dedicated workshop to discuss the new colliding light ions

❖ Neutron skin ^{40}Ca and ^{48}Ca

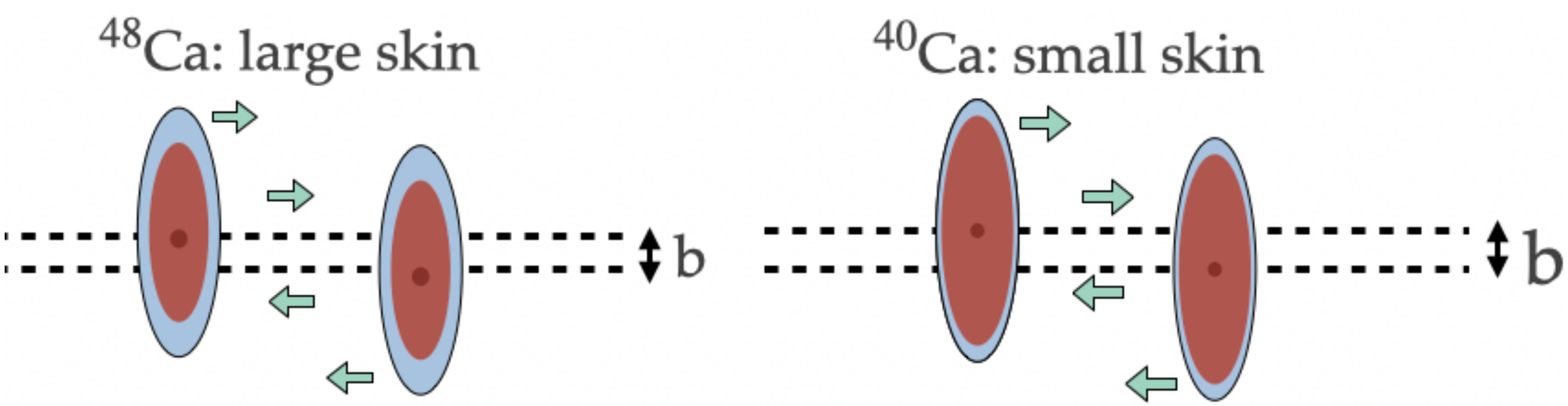

Future possibilities

CERN (11.2024)

TH Institute Light Ions at the LHC

- ☆ organised by CERN-TH, YZ (NBI), Qipeng Hu (USTC) etc.
- ☆ a dedicated workshop to discuss the new colliding light ions

❖ Neutron skin ^{40}Ca and ^{48}Ca

❖ Further understanding on the α-clustering structure with ^{20}Ne

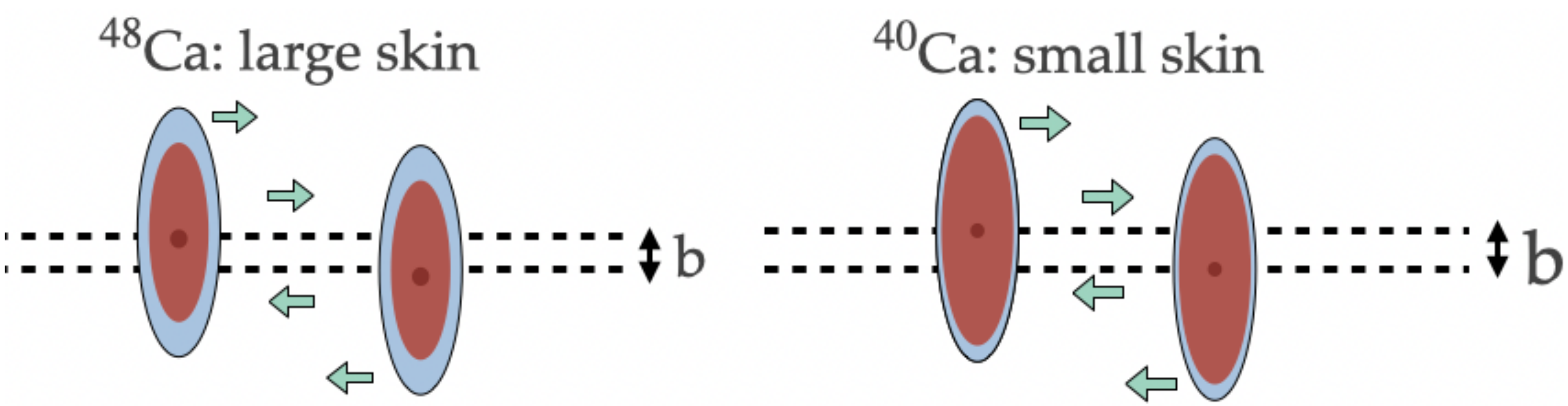

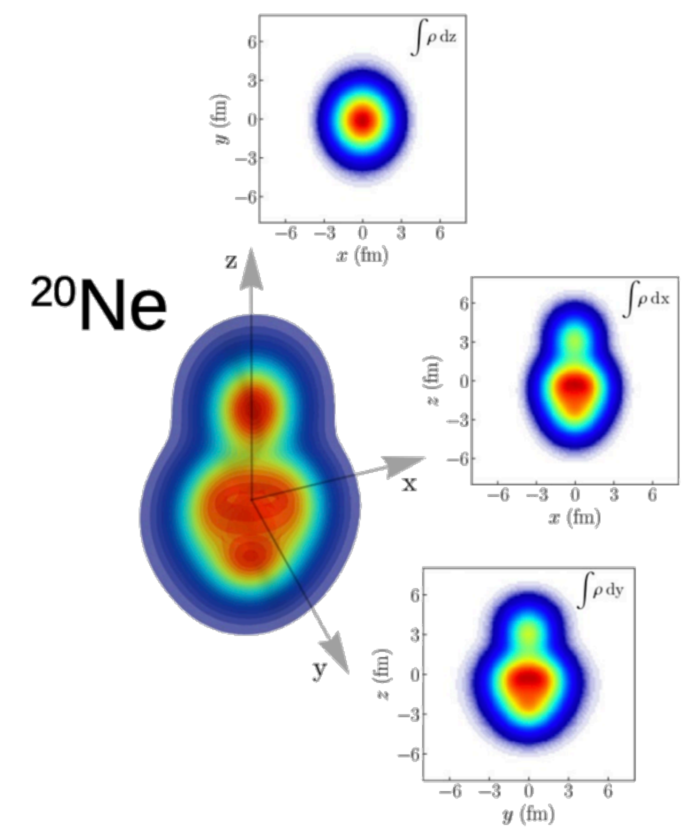

Future possibilities

CERN (11.2024)

TH Institute Light Ions at the LHC

- ☆ organised by CERN-TH, YZ (NBI), Qipeng Hu (USTC) etc.
- ☆ a dedicated workshop to discuss the new colliding light ions

❖ Neutron skin ^{40}Ca and ^{48}Ca

❖ Further understanding on the α-clustering structure with ^{20}Ne

❖ New isobar runs ^{40}Ca vs ^{40}Ar (well within the capability of nuclear EFT calculations)

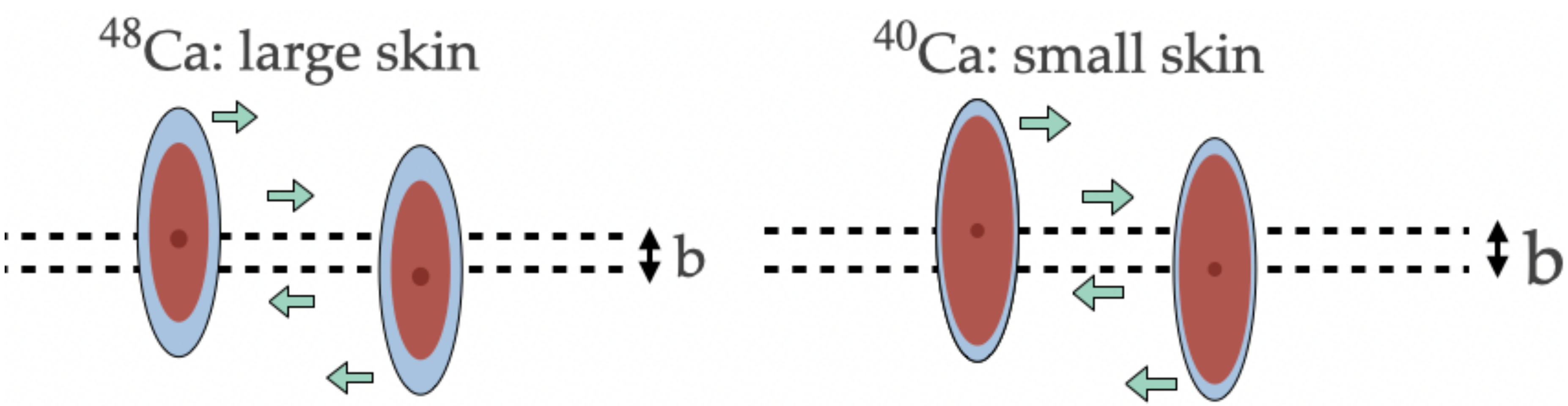

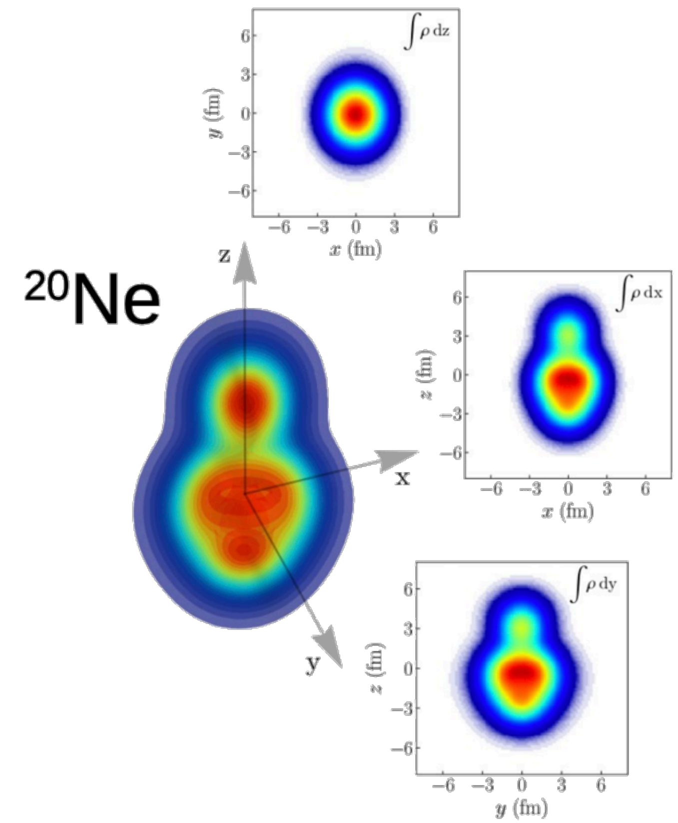

Possible open questions

Are the existing NS study at high energies model independent?

TH

IC → Hydrodynamics → Rescattering → Final

IC → Parton transport → Rescattering → Final

Possible open questions

Are the existing NS study at high energies model independent?

Q: Will the same NS input gives the same Initial Conditions?

- Will TRENTo gives the same $\varepsilon_2\{4\}/\varepsilon_2\{2\}$ as IP-Glasma or AMPT?

Possible open questions

Are the existing NS study at high energies model independent?

Q: Will the same NS input gives the same Initial Conditions?

- Will TRENTo gives the same $\varepsilon_2\{4\}/\varepsilon_2\{2\}$ as IP-Glasma or AMPT?

Q: Any difference by using hydrodynamics and parton transport (AMPT)?

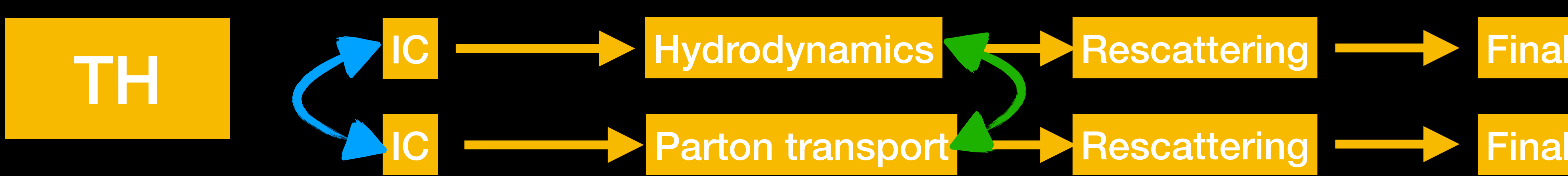

Possible open questions

Are the existing NS study at high energies model <u>independent</u>?

Q: Will the same NS input gives the same Initial Conditions?

- Will TRENTo gives the same $\varepsilon_2\{4\}/\varepsilon_2\{2\}$ as IP-Glasma or AMPT?

Q: Any difference by using hydrodynamics and parton transport (AMPT)?

Q: Will the choices of hadronic rescattering models (SMASH, UrQMD, ART) matter for the NS study?

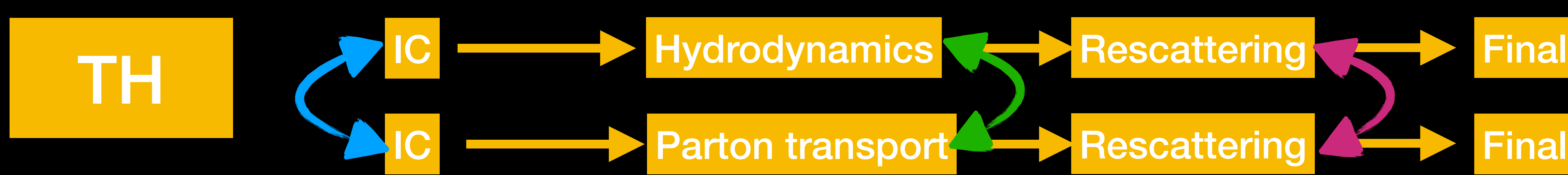

~~Conclusion~~ Remarks

- **The nuclear structure studies at the high energies (i.e., RHIC & LHC) can not replace the efforts of NS at low energies, OBVIOUSLY.**

- **They complement each other**
  - *NS@LE covers much wider range in the nuclide chart*
  - *NS@HE enables novel opportunity to resolve some challenging questions (many-body, shape etc) with a few selected nuclei*

- **The interactions between two communities are crucial**
  - *Can we have a unified description of nuclear structure through the entire energy scale from MeV to TeV*

Thanks !

erc

INDEPENDENT
RESEARCH FUND
DENMARK

- ★ **2 Postdoc (1 Flow, 1 FoCal)**
  - **starting Early 2025**
  - **600,000 RMB/year**
- ★ **1 PhD (Flow)**
  - **Open call in spring 2025**
  - **450,000 RMB/year**
- ★ **Contact You Zhou: *You.Zhou AT cern.ch***

Bakcup

Recent Activities @ High Energies

BNL (01.2022)

link

GSI (05.2022)

EMMI Rapid Reaction Task Force: "Nuclear physics confronts relativistic collisions of isobars" (part 1/2)

30 May 2022 to 3 June 2022
Heidelberg University

link

GSI (10.2022)

EMMI Rapid Reaction Task Force: "Nuclear physics confronts relativistic collisions of isobars" (part 2/2)

12-14 October 2022
Heidelberg University

link

CEA, Saclay (09.2022)

Deciphering nuclear phenomenology across energy scales

Back to the ESNT page

20-23 September 2022

PROGRAM ESNTprogram19Sept2022DefVf.pdf

link

INT (02.2023)

INT PROGRAM INT-23-1A

Intersection of nuclear structure and high-energy nuclear collisions

link

NBI (06.2023)

link

Activities in 2024 and beyond

PKU (04.2024)
Beijing

(Program + workshop for two communities)

RHIC (0.2 TeV):
- U-U vs Au-Au
- Zr-Zr vs Ru-Ru
- O-O

LHC (~ 5 TeV):
- Xe-Xe vs Pb-Pb
- O-O

Exploring nuclear physics across energy scales 2024: intersection between nuclear structure and high energy nuclear collisions

15–26 Apr 2024
Asia/Shanghai timezone

Enter your search term

- Overview
- Participant List
- Committees
- Meeting and Hotel Information
- About Beijing
- Visa to China
- Transportation

Contact
huichaosong@pku.edu.cn

Introduction： Recently, it has been realized that relativistic heavy ion collisions could provide new approaches to study some fundamental properties of atomic nuclei. It is therefore timely to gather scientists from both the low-energy and high-energy nuclear physics communities to discuss the recent progress and future perspective in this research direction. The two-week program+workshop on "Exploring Nuclear Physics across Energy Scales" emphasizes the intersection between nuclear structure and high-energy nuclear collisions, with a focus on the following questions: How does the low-energy structure of nuclei manifest in high-energy collisions? How do the observations made at colliders complement our knowledge of nuclear structure? During the program days (April 15-18, April 23-26) the two invited speakers each day are expected to give a one-hour seminar with sufficient time for discussions. The embedded workshop (20-22 April) will be 3 days with 25-30 invited talks and 3 short discussion sections.

The scientific program includes the following topics, which emphasises the intersections between nuclear structure and high-energy collisions.

- Manifestation of nuclear deformations across energy scales
- Neutron skin determinations and applications
- Many-body correlations and clustering in light nuclei
- Bayesian analysis for high-energy collisions and nuclear structure
- Role of nuclear structure in low- and intermediate-energy collisions
- Connection to Ultra-peripheral Collisions (UPCs) and the future Electron-Ion Collider (EIC)
- Opportunities with colliding new species at future high-energy experiments

(Normalized) Symmetric Cumulant

How do v_n and v_m correlate

Symmetric cumulants:

$$SC(m,n) = \langle v_m^2\, v_n^2 \rangle - \langle v_m^2 \rangle \langle v_n^2 \rangle$$

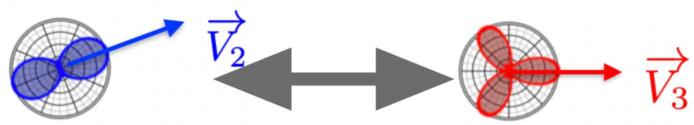

ALICE, PRL117, 182301 (2016)

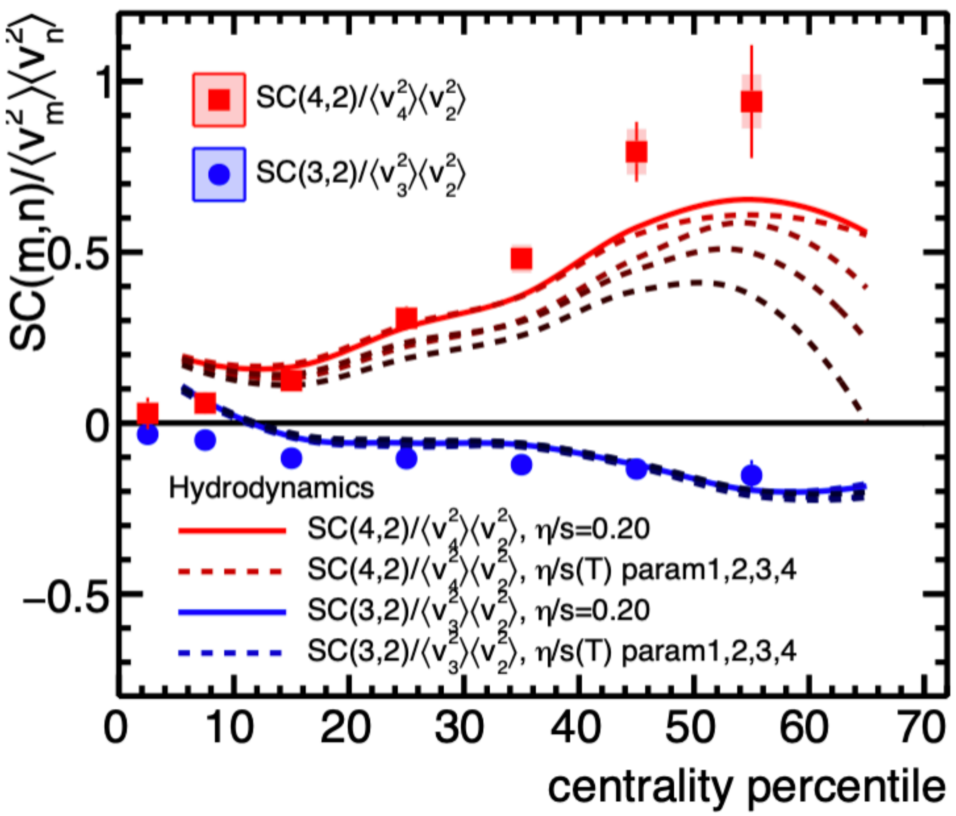

PHYSICAL REVIEW C **89**, 064904 (2014)

Generic framework for anisotropic flow analyses with multiparticle azimuthal correlations

Ante Bilandzic,[1] Christian Holm Christensen,[1] Kristjan Gulbrandsen,[1] Alexander Hansen,[1] and You Zhou[2,3]

[1]*Niels Bohr Institute, Blegdamsvej 17, 2100 Copenhagen, Denmark*

[2]*Nikhef, Science Park 105, 1098 XG Amsterdam, The Netherlands*

[3]*Utrecht University, P.O. Box 80000, 3508 TA Utrecht, The Netherlands*

Xiangrong Zhu, YZ, Haojie Xu, and Huichao Song, PRC95, 044902 (2017)

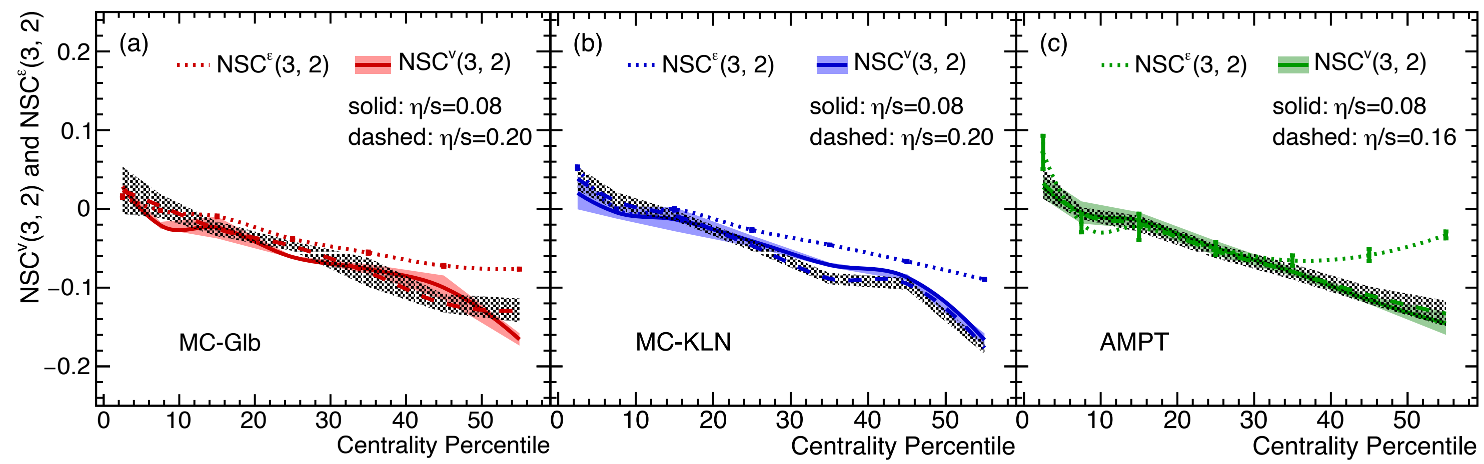

$$v_2 \propto \varepsilon_2 \qquad v_3 \propto \varepsilon_3$$

$$\frac{\langle v_2^2\, v_3^2 \rangle - \langle v_2^2 \rangle \langle v_3^2 \rangle}{\langle v_2^2 \rangle \langle v_3^2 \rangle} = \frac{\langle \varepsilon_2^2\, \varepsilon_3^2 \rangle - \langle \varepsilon_2^2 \rangle \langle \varepsilon_3^2 \rangle}{\langle \varepsilon_2^2 \rangle \langle \varepsilon_3^2 \rangle}$$

Or: $NSC^v(3,2) = NSC^\varepsilon(3,2)$

- The very first direct measurement of correlations between v_n and v_m
  - NSC(3,2) is insensitive to η/s
  - NSC(3,2) measurements provide a direct access into the initial conditions (despite details of systems evolution)
  - Can we use NSC to explore the nuclear structure?

Probe IC with NSC(3,2)

How do v_n and v_m correlate

$NSC^v(3,2) = NSC^\varepsilon(3,2)$

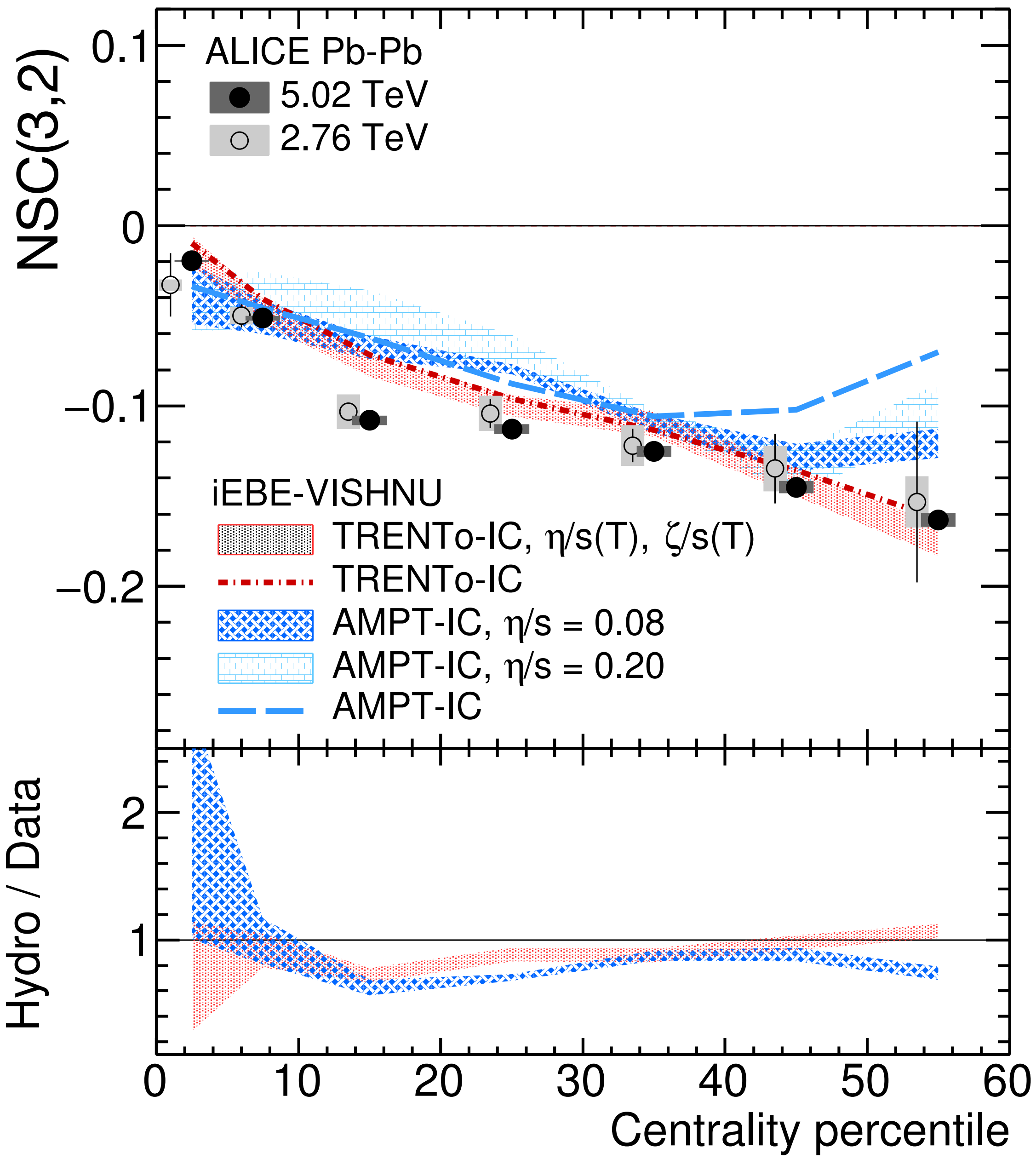

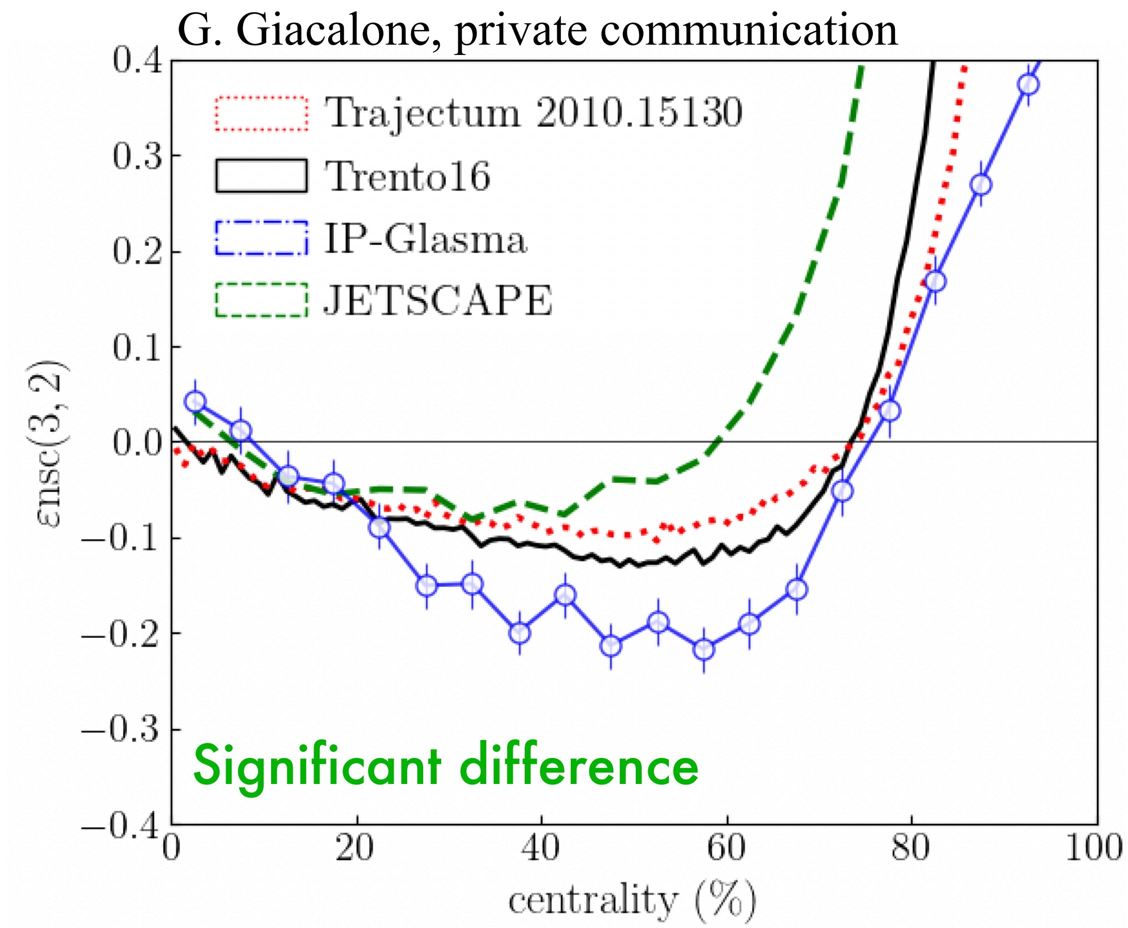

- Precision NSC(3,2) data provides tight constraints on the initial state models
- what is the general correlation between any order of v_n^k and v_m^p and the correlations among multiple flow coefficients

ALICE, PLB818 (2021) 136354

iEBE-VISHNU, M. Li, YZ etc, PRC104, 024903 (2021)

A reminder

J. Jia, JPG41 (2014) 124003

	pdfs	cumulants
Flow-amplitudes	$p(v_n)$	$v_n\{2k\},\ k = 1,2,...$
	$p(v_n, v_m)$	$\langle v_n^2 v_m^2\rangle - \langle v_n^2\rangle\langle v_m^2\rangle,\ n \neq m$ ...
	$p(v_n, v_m, v_l)$	$\langle v_n^2 v_m^2 v_l^2\rangle + 2\langle v_n^2\rangle\langle v_m^2\rangle\langle v_l^2\rangle - \langle v_n^2 v_m^2\rangle\langle v_l^2\rangle - \langle v_m^2 v_l^2\rangle\langle v_n^2\rangle - \langle v_l^2 v_n^2\rangle\langle v_m^2\rangle$ $n \neq m \neq l$ ...
	...	Obtained recursively as above
EP-correlation	$p(\Phi_n, \Phi_m, ...)$	$\langle v_n^{\lvert c_n\rvert} v_m^{\lvert c_m\rvert} ... \cos(c_n n\Phi_n + c_m m\Phi_m + ...)\rangle$ $\sum_k kc_k = 0$
Mixed-correlation	$p(v_l, \Phi_n, \Phi_m, ...)$	$\langle v_l^2 v_n^{\lvert c_n\rvert} v_m^{\lvert c_m\rvert} ... \cos(c_n n\Phi_n + c_m m\Phi_m + ...)\rangle - \langle v_l^2\rangle\langle v_n^{\lvert c_n\rvert} v_m^{\lvert c_m\rvert} ... \cos(c_n n\Phi_n + c_m m\Phi_m + ...)\rangle$ $\sum_k kc_k = 0,\ n \neq m \neq l ...$

PHYSICAL REVIEW C **103**, 024913 (2021)

Generic algorithm for multiparticle cumulants of azimuthal correlations in high energy nucleus collisions

Zuzana Moravcova, Kristjan Gulbrandsen,* and You Zhou†
Niels Bohr Institute, Blegdamsvej 17, 2100 Copenhagen, Denmark

m-particle cumulant

```
complex Cumulant(int* harmonic, int n, bool remove_zeros=true, int negsplit=-1,
    int mult = 1, int skip = 0)
  {
   bool remove_term = false;
   if (remove_zeros)
   {
    int har_sum = 0;
    for (int i = 0; i<mult; ++i) har_sum += harmonic[n-1+i];
    if (har_sum != 0) remove_term = true;
   }
   complex c = 0;
   if (!remove_term)
   {
    c = Corr(harmonic+(n-1), mult);
    if (n == 1) return c;
    c *= negsplit*Cumulant(harmonic, n-1, remove_zeros, negsplit-1);
   }

   int h_hold = harmonic[n-2];
   for (int counter = 0; counter <= n-2-skip; ++counter)
   {
    harmonic[n-2] = harmonic[counter];
    harmonic[counter] = h_hold;
    c += Cumulant(harmonic, n-1, remove_zeros, negsplit, mult+1, n-2-counter);
    harmonic[counter] = harmonic[n-2];
   }
   harmonic[n-2] = h_hold;
   return c;
  }
```

m-particle correlation

```
complex Correlator(int* harmonic, int n, int mult = 1, int skip = 0)
 {
  int har_sum = 0;
  for (int i = 0; i<mult; ++i) har_sum += harmonic[n-1+i];
  complex c(Q(har_sum, mult));
  if (n == 1) return c;
  c *= Correlator(harmonic, n-1);
  if (n == 1+skip) return c;

  complex c2 = 0;
  int h_hold = harmonic[n-2];
  for (int counter = 0; counter <= n-2-skip; ++counter)
  {
   harmonic[n-2] = harmonic[counter];
   harmonic[counter] = h_hold;
   c2 += Correlator(harmonic, n-1, mult+1, n-2-counter);
   harmonic[counter] = harmonic[n-2];
  }
  harmonic[n-2] = h_hold;
  return c-mult*c2;
 }
```

- One algorithm for any particle cumulant
  - Multi-particle mixed harmonic cumulants
  - correlation between v_m^k, v_n^l and v_p^q
  - correlation between v_m^k and v_n^l
  - No need of any package !

Mixed harmonic cumulants

How do v_n and v_m correlate

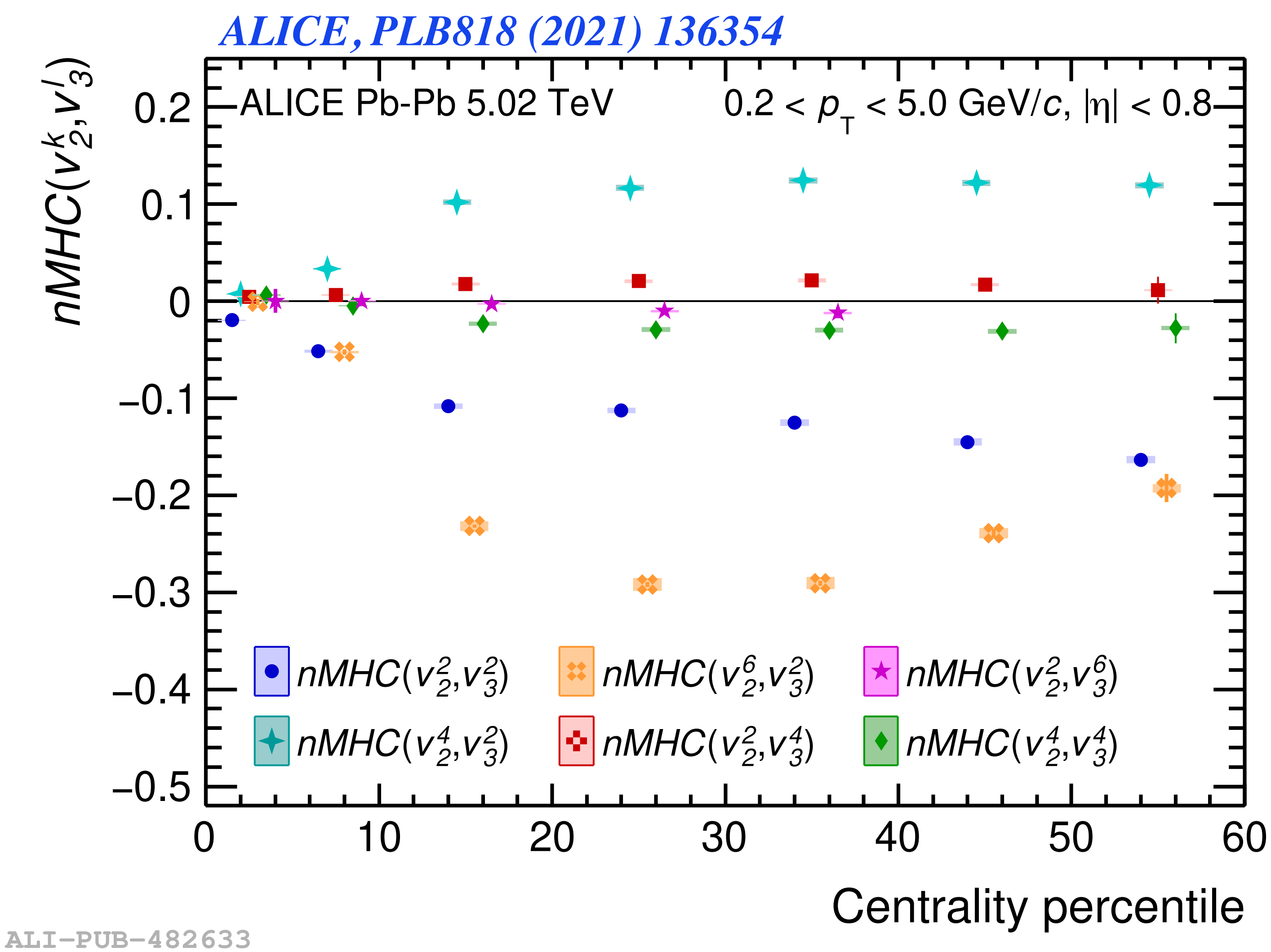

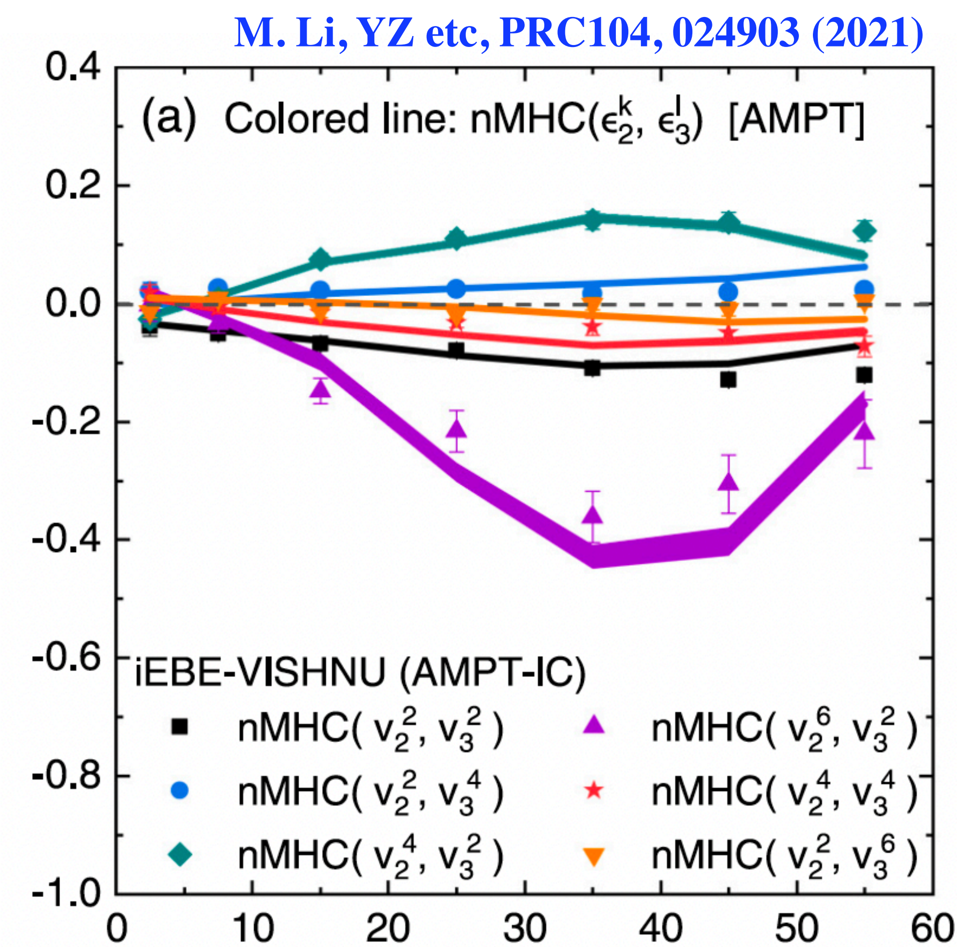

- First measurement of correlations between higher order moments of v_2 and v_3
  - Final state results quantitatively reproduced by the initial state correlations
  - Experimental data provides direct constraints on the correlations of higher order moments of eccentricity coefficients from initial state models

TRENTo IC

- Fully parametrised initial conditions

$$P_{\text{wounded}} = 1 - \exp\left(-\sigma_{gg}\int d\boldsymbol{x}\rho_A(\boldsymbol{x})\rho_B(\boldsymbol{x})\right), \qquad \rho_{A/B} \propto \exp\left(\frac{-|\boldsymbol{x}-\boldsymbol{x}_{A/B}|^2}{2w^2}\right)$$

- Deposit energy into each nucleus' thickness function

$$T_{A/B} = \sum_{i\in\text{wounded } A/B} \gamma \exp(-|\boldsymbol{x}-\boldsymbol{x}_i|^2/2w^2)$$

- Modify to include quark constituents $\rho_A = \frac{1}{n_c}\sum_{i=1^{n_c}} \rho_c(\boldsymbol{x}-\boldsymbol{x}_i)$

- Generalised mean of thickness functions

$$\left.\frac{dS}{d^2x_\perp d\eta}\right|_{\eta=0} \propto \left(\frac{(T_A+T_B)^p}{2}\right)^{1/p} \Rightarrow \left.\frac{dS}{d\eta}\right|_{\eta=0} \propto \begin{cases} max(T_A, T_B) & p \to +\infty \\ (T_A+T_B)/2 & p = +1 \text{ (arithmetic)} \\ \sqrt{T_A T_B} & p = 0 \text{ (geometric)} \\ 2T_A T_B/(T_A+T_B & p = -1 \text{ (harmonic)} \\ min(T_A, T_B) & p \to -\infty \end{cases}$$

Pictures at low energy and high energy

Low energy

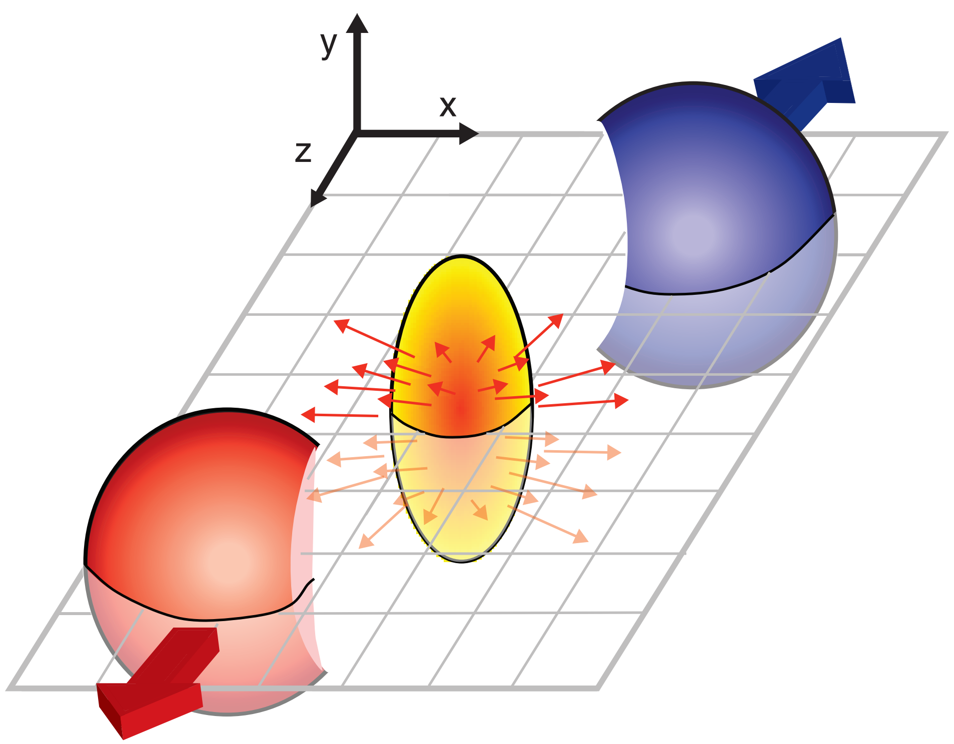

High energy

$$\rho(r,\theta,\phi) = \frac{\rho_0}{1 + e^{(r-R(\theta,\phi))/a_0}}$$

$$R(\theta,\phi) = R_0\left(1 + \beta_2[\cos\gamma Y_{2,0} + \sin\gamma Y_{2,2}] + \beta_3 \sum_{m=-3}^{3} \alpha_{3,m} Y_{3,m} + \beta_4 \sum_{m=-4}^{4} \alpha_{4,m} Y_{4,m}\right)$$

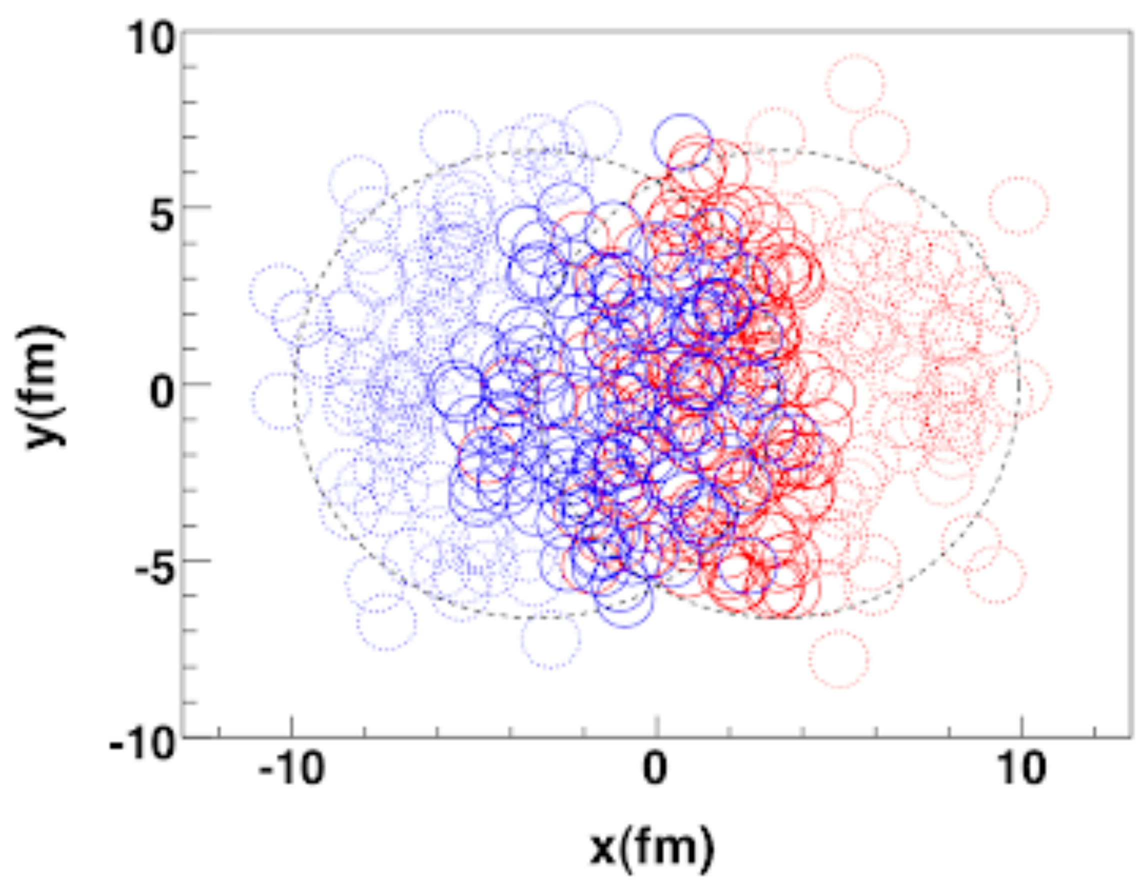

❖ Even with the fixed parameters (nuclear structure), the nucleon distributions are not fixed (not identical but vary from one event to the other)

Initial geometry correlations

PHYSICAL REVIEW C **89**, 064904 (2014) **309 citations**

Generic framework for anisotropic flow analyses with multiparticle azimuthal correlations

Ante Bilandzic,[1] Christian Holm Christensen,[1] Kristjan Gulbrandsen,[1] Alexander Hansen,[1] and You Zhou[2,3]
[1]*Niels Bohr Institute, Blegdamsvej 17, 2100 Copenhagen, Denmark*
[2]*Nikhef, Science Park 105, 1098 XG Amsterdam, The Netherlands*
[3]*Utrecht University, P.O. Box 80000, 3508 TA Utrecht, The Netherlands*

Symmetric cumulants:

$$SC(m,n) = \langle v_m^2\, v_n^2 \rangle - \langle v_m^2 \rangle \langle v_n^2 \rangle$$

$$v_2 \propto \varepsilon_2$$
$$v_3 \propto \varepsilon_3$$

$$\frac{\langle v_2^2\, v_3^2 \rangle - \langle v_2^2 \rangle \langle v_3^2 \rangle}{\langle v_2^2 \rangle \langle v_3^2 \rangle} = \frac{\langle \varepsilon_2^2\, \varepsilon_3^2 \rangle - \langle \varepsilon_2^2 \rangle \langle \varepsilon_3^2 \rangle}{\langle \varepsilon_2^2 \rangle \langle \varepsilon_3^2 \rangle}$$

Or: $NSC^v(3,2) = NSC^\varepsilon(3,2)$

ALICE, PRL117, 182301 (2016)

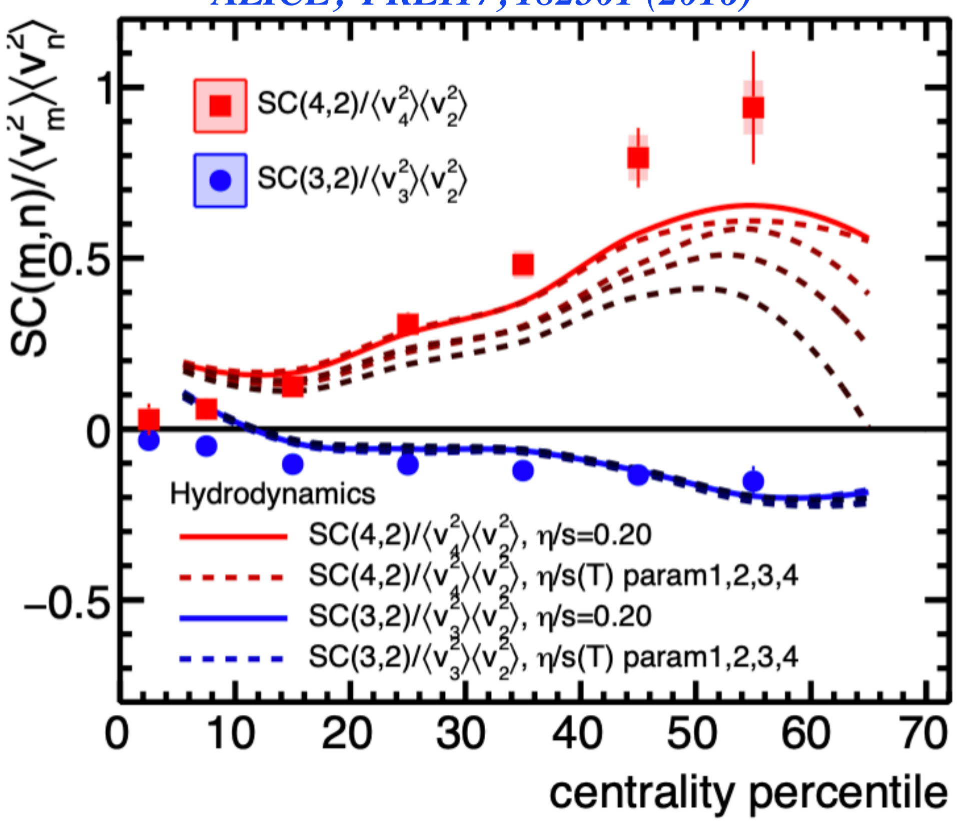

X. Zhu etc, PRC95, 044902 (2017)

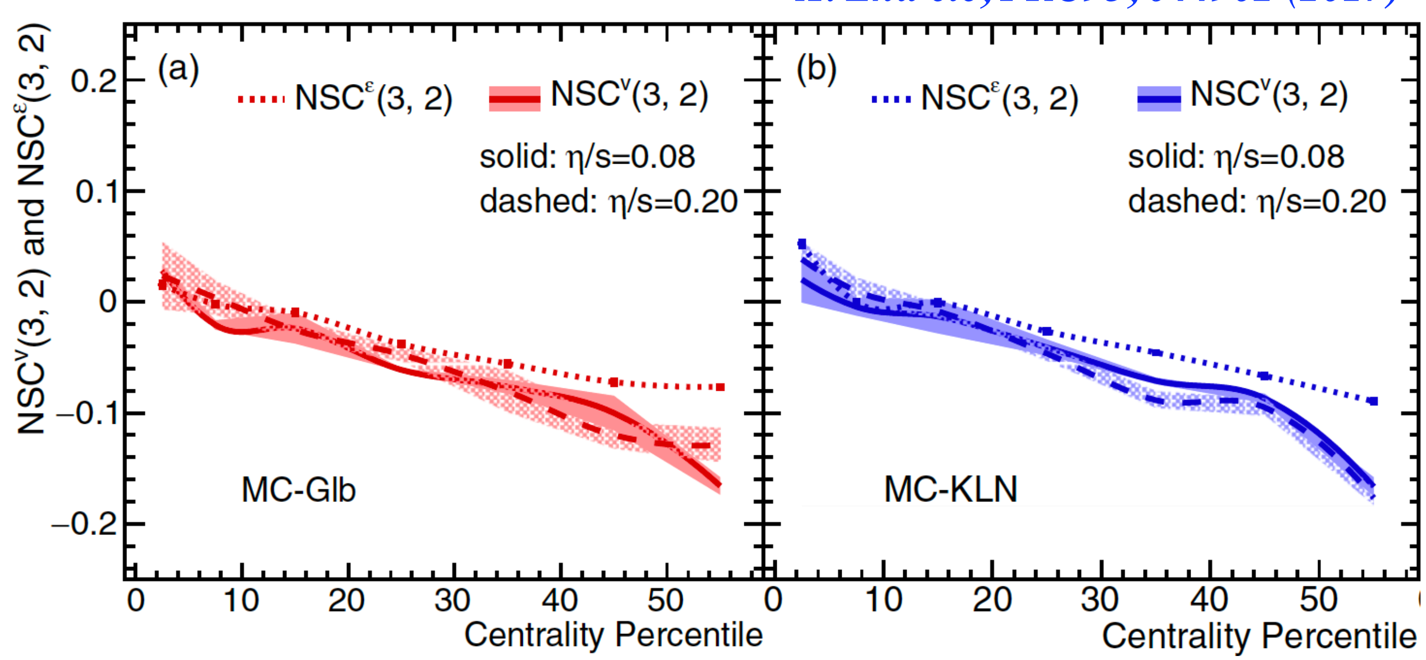

ALICE, PLB818 (2021) 136354
M. Li, YZ etc, PRC104, 024903 (2021)

Probe Nuclear structure with NSC(3,2)

Normalised Symmetric cumulants:

$$v_2 \propto \varepsilon_2$$
$$v_3 \propto \varepsilon_3$$

$$\frac{\langle v_2^2\, v_3^2\rangle - \langle v_2^2\rangle \langle v_3^2\rangle}{\langle v_2^2\rangle \langle v_3^2\rangle} = \frac{\langle \varepsilon_2^2\, \varepsilon_3^2\rangle - \langle \varepsilon_2^2\rangle \langle \varepsilon_3^2\rangle}{\langle \varepsilon_2^2\rangle \langle \varepsilon_3^2\rangle}$$

Or: $NSC^{v}(3,2) = NSC^{\varepsilon}(3,2)$

Z. Lu, M.Zhao, J. Jia, YZ, Eur. Phys. J. A (2023) 59, 279

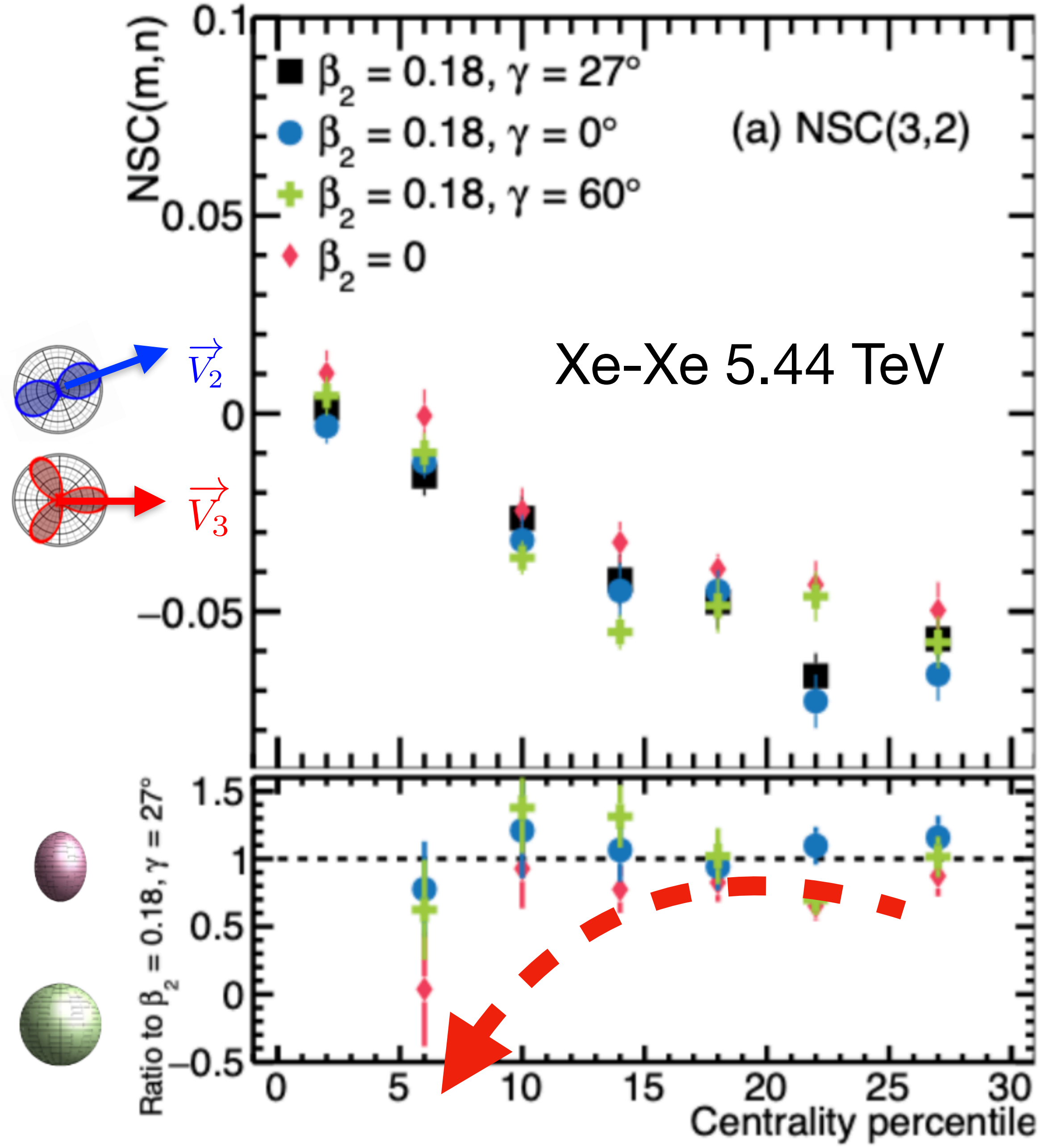

❖ Different results due to nuclear deformation observed in NSC(3,2)

❖ New measurements should allow the constrain the β₂ but not γ

Skewness of mean transverse momentum fluctuations in heavy-ion collisions

Giuliano Giacalone[1,2] Fernando G. Gardim,[3] Jacquelyn Noronha-Hostler,[4] and Jean-Yves Ollitrault[1]
[1] *Université Paris Saclay, CNRS, CEA, Institut de physique théorique, 91191 Gif-sur-Yvette, France*
[2] *Institut für Theoretische Physik, Universität Heidelberg, Philosophenweg 16, 69120 Heidelberg, Germany*
[3] *Instituto de Ciência e Tecnologia, Universidade Federal de Alfenas, 37715-400 Poços de Caldas, Minas Gerais, Brazil*
[4] *Department of Physics, University of Illinois at Urbana-Champaign, Urbana, Illinois 61801, USA*

$$\Gamma_{p_t} \equiv \frac{\langle \Delta p_i \Delta p_j \Delta p_k \rangle \langle\langle p_t \rangle\rangle}{\langle \Delta p_i \Delta p_j \rangle^2}$$

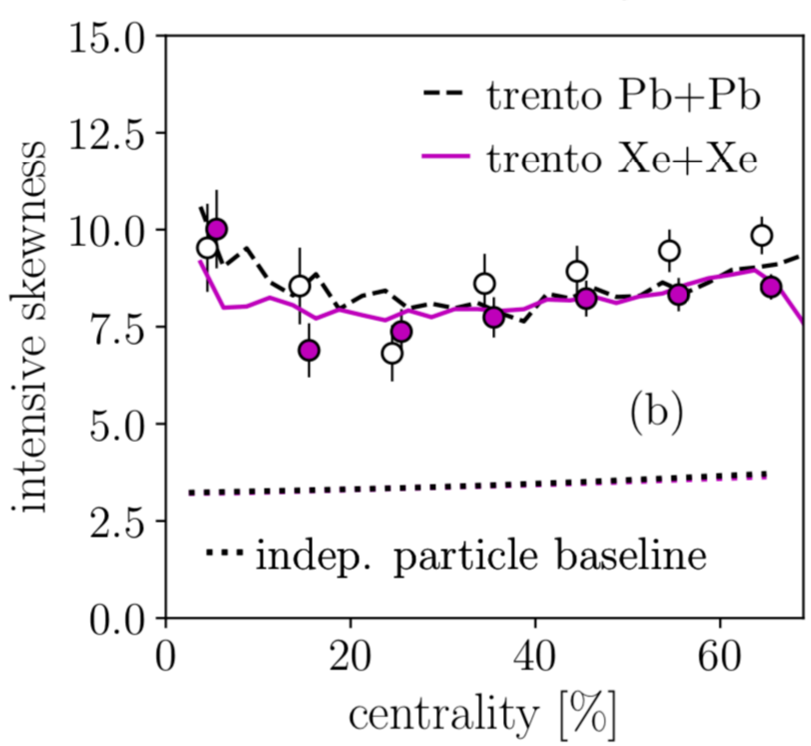

Higher-order transverse momentum fluctuations in heavy-ion collisions

Somadutta Bhatta,[1] Chunjian Zhang,[1] and Jiangyong Jia[1,2,*]
[1] *Department of Chemistry, Stony Brook University, Stony Brook, New York 11794, USA*
[2] *Physics Department, Brookhaven National Laboratory, Upton, New York 11976, USA*

$$k_2 = \frac{\langle c_2 \rangle}{\langle\langle p_T \rangle\rangle^2}, \quad k_3 = \frac{\langle c_3 \rangle}{\langle\langle p_T \rangle\rangle^3},$$

$$k_4 = \frac{\langle c_4 \rangle - 3\langle c_2 \rangle^2}{\langle\langle p_T \rangle\rangle^4}, \quad k_{2,2\text{sub}} = \frac{\langle c_{2,2\text{sub}} \rangle}{\langle\langle p_T \rangle\rangle_a \langle\langle p_T \rangle\rangle_c},$$

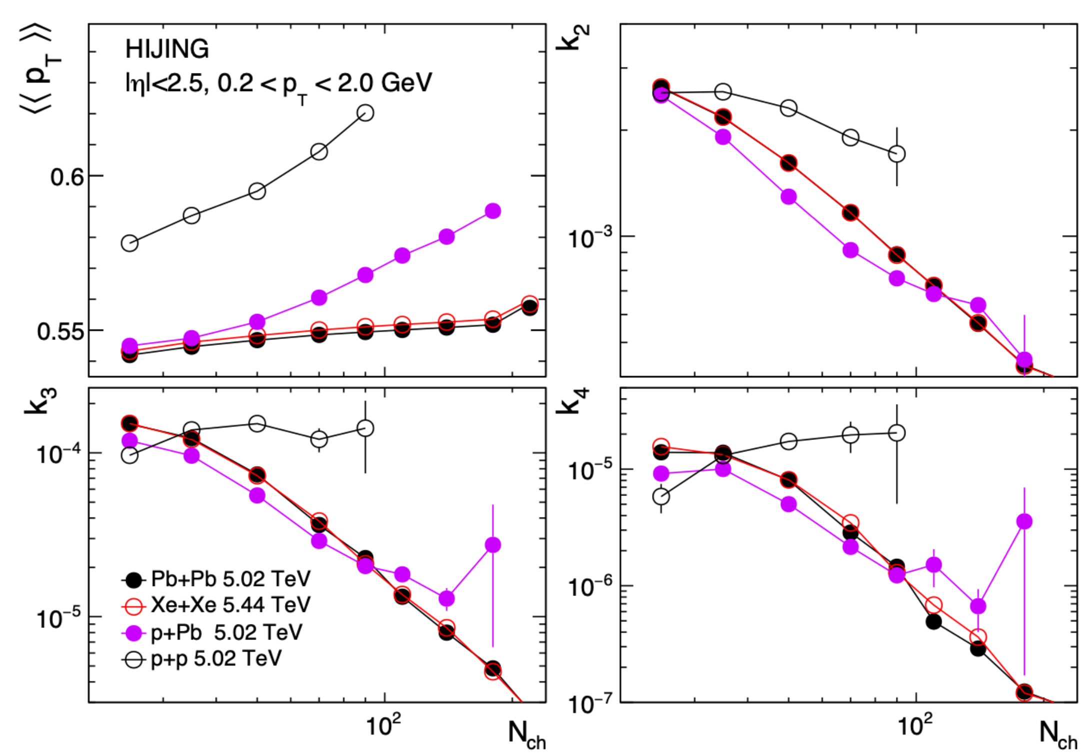

$$d_\perp = \sqrt{N_{\text{part}}/\langle r_\perp^2\rangle}$$

$$\frac{\delta d_\perp}{d_\perp} = \sqrt{\frac{5}{16\pi}}\beta_2\Big(\cos(\gamma)D^2_{0,0}(\Omega) + \frac{\sin(\gamma)}{\sqrt{2}}[D^2_{0,2}(\Omega) + D^2_{0,-2}(\Omega)]\Big)$$

Final state cumulant	Initial state cumulant	Liquid-drop model
κ_2	$\left\langle\left(\frac{\delta d_\perp}{d_\perp}\right)^2\right\rangle$	$\frac{1}{32\pi}\langle\beta_2^2\rangle$
κ_3	$\left\langle\left(\frac{\delta d_\perp}{d_\perp}\right)^3\right\rangle$	$\frac{\sqrt{5}}{896\pi^{3/2}}\langle\cos(3\gamma)\beta_2^3\rangle$
κ_4	$\left\langle\left(\frac{\delta d_\perp}{d_\perp}\right)^4\right\rangle - 3\cdot\left\langle\left(\frac{\delta d_\perp}{d_\perp}\right)^2\right\rangle^2$	$-\frac{3}{14336\pi^2}(7\langle\beta_2^2\rangle - 5\langle\beta_2^4\rangle)$
κ_5	$\left\langle\left(\frac{\delta d_\perp}{d_\perp}\right)^5\right\rangle - 10\cdot\left\langle\left(\frac{\delta d_\perp}{d_\perp}\right)^3\right\rangle\cdot\left\langle\left(\frac{\delta d_\perp}{d_\perp}\right)^2\right\rangle$	$-\frac{5\sqrt{5}}{315392\pi^{5/2}}(11\langle\cos(3\gamma)\beta_2^3\rangle\langle\beta_2^2\rangle - 5\langle\beta_2^5\rangle)$
κ_6	$\left\langle\left(\frac{\delta d_\perp}{d_\perp}\right)^6\right\rangle - 15\cdot\left\langle\left(\frac{\delta d_\perp}{d_\perp}\right)^4\right\rangle\cdot\left\langle\left(\frac{\delta d_\perp}{d_\perp}\right)^2\right\rangle$ $+30\cdot\left\langle\left(\frac{\delta d_\perp}{d_\perp}\right)^2\right\rangle^3 - 10\cdot\left\langle\left(\frac{\delta d_\perp}{d_\perp}\right)^3\right\rangle^2$	$\frac{5}{918412504\pi^3}(42042\langle\beta_2^2\rangle^3 - 5720\langle\cos(3\gamma)\beta_2^3\rangle^2$ $-45045\langle\beta_2^2\rangle\langle\beta_2^4\rangle + 8575\langle\beta_2^6\rangle + 700\langle\cos(6\gamma)\beta_2^6\rangle)$
κ_7	$\left\langle\left(\frac{\delta d_\perp}{d_\perp}\right)^7\right\rangle - 21\cdot\left\langle\left(\frac{\delta d_\perp}{d_\perp}\right)^5\right\rangle\cdot\left\langle\left(\frac{\delta d_\perp}{d_\perp}\right)^2\right\rangle$ $+210\cdot\left\langle\left(\frac{\delta d_\perp}{d_\perp}\right)^3\right\rangle\cdot\left\langle\left(\frac{\delta d_\perp}{d_\perp}\right)^2\right\rangle^2$ $-35\cdot\left\langle\left(\frac{\delta d_\perp}{d_\perp}\right)^3\right\rangle\cdot\left\langle\left(\frac{\delta d_\perp}{d_\perp}\right)^4\right\rangle$	$-\frac{15\sqrt{5}}{524812288}(2002\langle\beta_2^2\rangle^2\langle\cos(3\gamma)\beta_2^3\rangle$ $+715\langle\cos(3\gamma)\beta_2^3\rangle\langle\beta_2^4\rangle$ $+910\langle\cos(3\gamma)\beta_2^5\rangle\langle\beta_2^2\rangle - 175\cos(3\gamma)\beta_2^7\rangle)$
κ_8	$\left\langle\left(\frac{\delta d_\perp}{d_\perp}\right)^8\right\rangle - 28\cdot\left\langle\left(\frac{\delta d_\perp}{d_\perp}\right)^6\right\rangle\cdot\left\langle\left(\frac{\delta d_\perp}{d_\perp}\right)^2\right\rangle$ $+420\cdot\left\langle\left(\frac{\delta d_\perp}{d_\perp}\right)^4\right\rangle\left\langle\left(\frac{\delta d_\perp}{d_\perp}\right)^2\right\rangle^2$ $-35\left\langle\left(\frac{\delta d_\perp}{d_\perp}\right)^4\right\rangle^2 - 630\cdot\left\langle\left(\frac{\delta d_\perp}{d_\perp}\right)^2\right\rangle^4$ $+560\cdot\left\langle\left(\frac{\delta d_\perp}{d_\perp}\right)^3\right\rangle^2\cdot\left\langle\left(\frac{\delta d_\perp}{d_\perp}\right)^2\right\rangle$ $-56\cdot\left\langle\left(\frac{\delta d_\perp}{d_\perp}\right)^5\right\rangle\cdot\left\langle\left(\frac{\delta d_\perp}{d_\perp}\right)^3\right\rangle$	$\frac{5}{142748942336\pi^4}(2144142\langle\beta_2^2\rangle^4 - 3063060\langle\beta_2^2\rangle^2\langle\beta_2^4\rangle$ $-340\langle\beta_2^2\rangle\Big(2288\langle\cos(3\gamma)\beta_2^3\rangle^2 - 35(49\langle\beta_2^6\rangle$ $+4\langle\cos(6\gamma)\beta_2^6\rangle)\Big) + 25\Big(21879\langle\beta_2^4\rangle^2$ $+14144\langle\cos(3\gamma)\beta_2^3\rangle\langle\cos(3\gamma)\beta_2^5\rangle$ $-35(79\langle\beta_2^8\rangle + 16\langle\cos(6\gamma)\beta_2^8\rangle))\Big)$

Multi-particle p_T correlations

PHYSICAL REVIEW C **103**, 024910 (2021)

Skewness of mean transverse momentum fluctuations in heavy-ion collisions

Giuliano Giacalone,[1,2] Fernando G. Gardim,[3] Jacquelyn Noronha-Hostler,[4] and Jean-Yves Ollitrault[1]
[1]*Université Paris Saclay, CNRS, CEA, Institut de physique théorique, 91191 Gif-sur-Yvette, France*
[2]*Institut für Theoretische Physik, Universität Heidelberg, Philosophenweg 16, 69120 Heidelberg, Germany*
[3]*Instituto de Ciência e Tecnologia, Universidade Federal de Alfenas, 37715-400 Poços de Caldas, Minas Gerais, Brazil*
[4]*Department of Physics, University of Illinois at Urbana-Champaign, Urbana, Illinois 61801, USA*

PHYSICAL REVIEW C **105**, 024904 (2022)

Higher-order transverse momentum fluctuations in heavy-ion collisions

Somadutta Bhatta,[1] Chunjian Zhang,[1] and Jiangyong Jia[1,2,*]
[1]*Department of Chemistry, Stony Brook University, Stony Brook, New York 11794, USA*
[2]*Physics Department, Brookhaven National Laboratory, Upton, New York 11976, USA*

$$\Gamma_{p_t} \equiv \frac{\langle \Delta p_i \Delta p_j \Delta p_k \rangle \langle\langle p_t \rangle\rangle}{\langle \Delta p_i \Delta p_j \rangle^2}$$

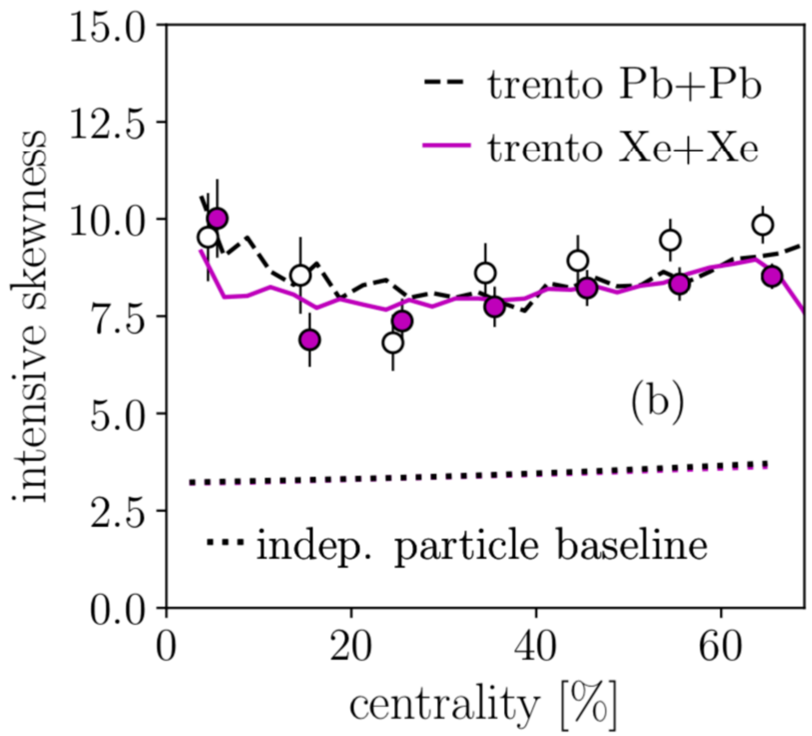

$$k_2 = \frac{\langle c_2 \rangle}{\langle\langle p_T \rangle\rangle^2}, \quad k_3 = \frac{\langle c_3 \rangle}{\langle\langle p_T \rangle\rangle^3},$$

$$k_4 = \frac{\langle c_4 \rangle - 3\langle c_2 \rangle^2}{\langle\langle p_T \rangle\rangle^4}, \quad k_{2,2\mathrm{sub}} = \frac{\langle c_{2,2\mathrm{sub}} \rangle}{\langle\langle p_T \rangle\rangle_a \langle\langle p_T \rangle\rangle_c},$$

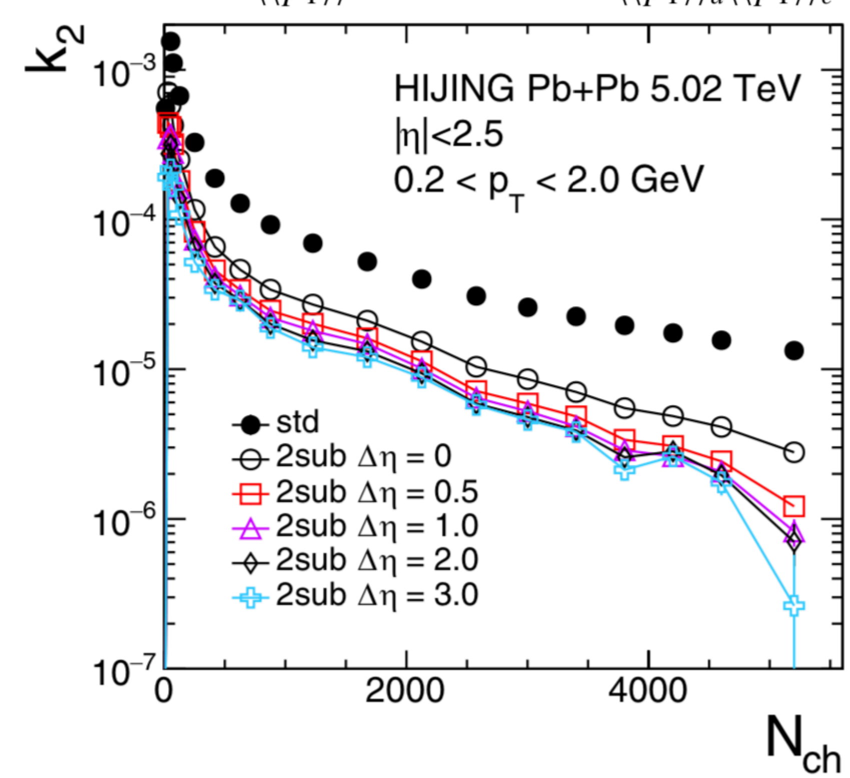

- $[P_T]$ and its event-by-event fluctuations measured in heavy-ion collisions at the LHC -> probe initial ***size*** and ***size fluctuations***

Enhanced Ψ_n correlations in models

- $\rho_{4,22}$ probes correlations between Ψ_2 and Ψ_4 ~ $\langle \cos 4(\Psi_2 - \Psi_4) \rangle$

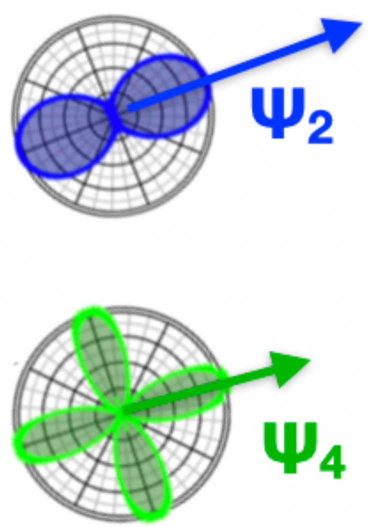

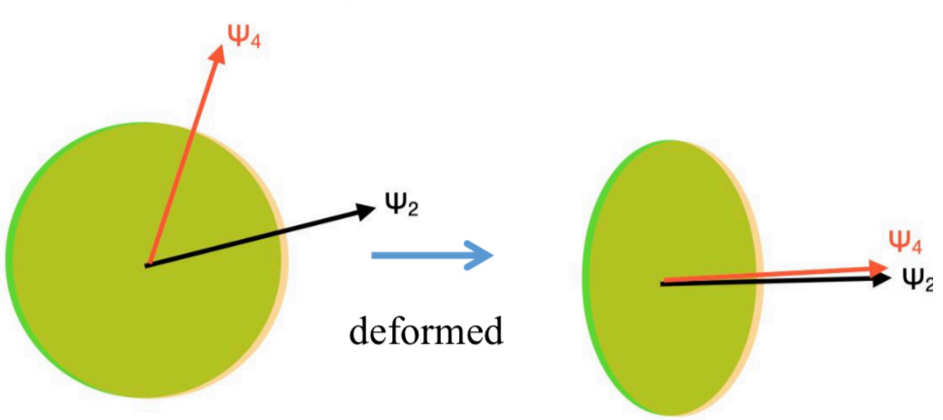

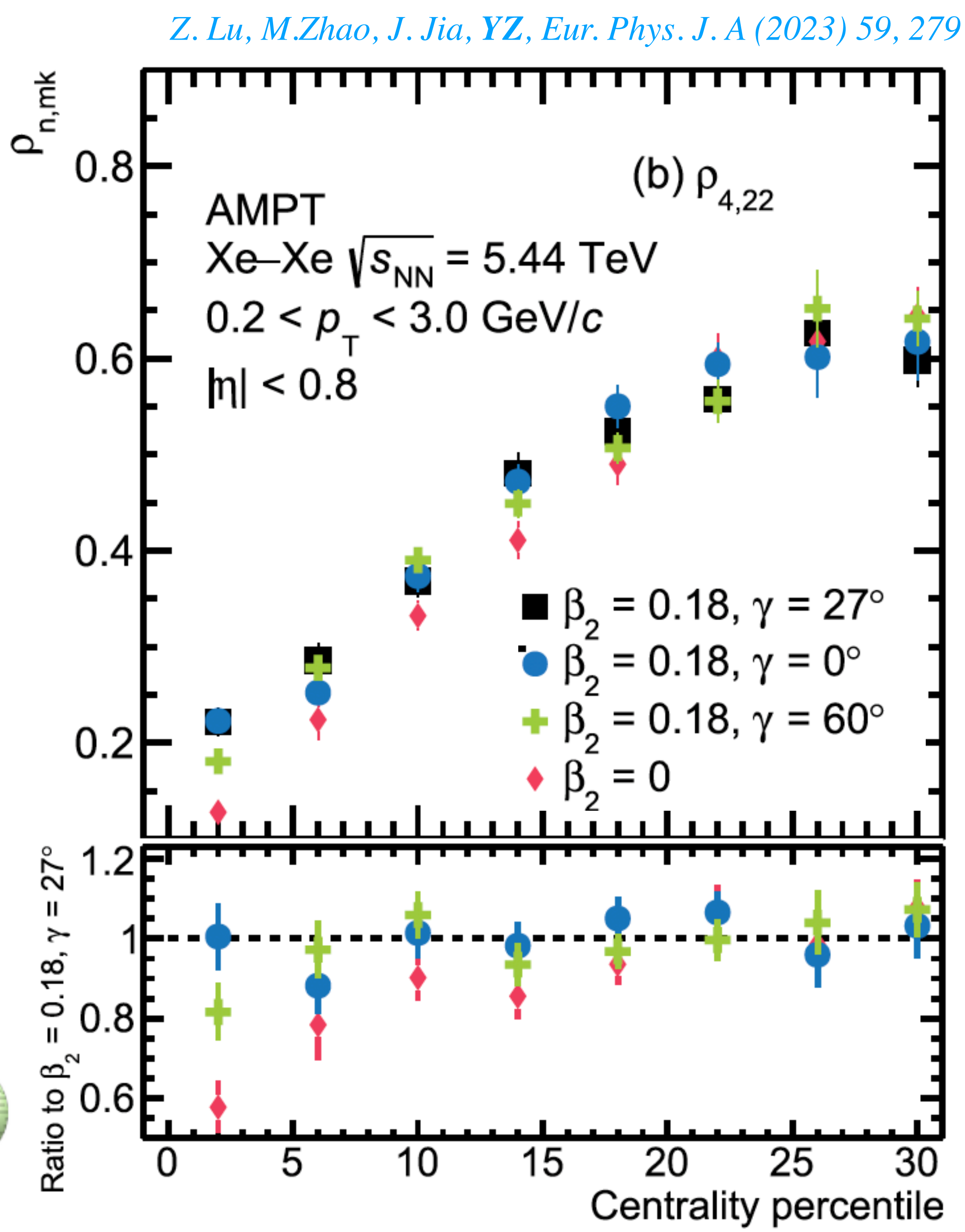

- A stronger correlation is well explained by the transport model using deformed ^{129}Xe nuclei using transport model

[p_T] - v_n correlations

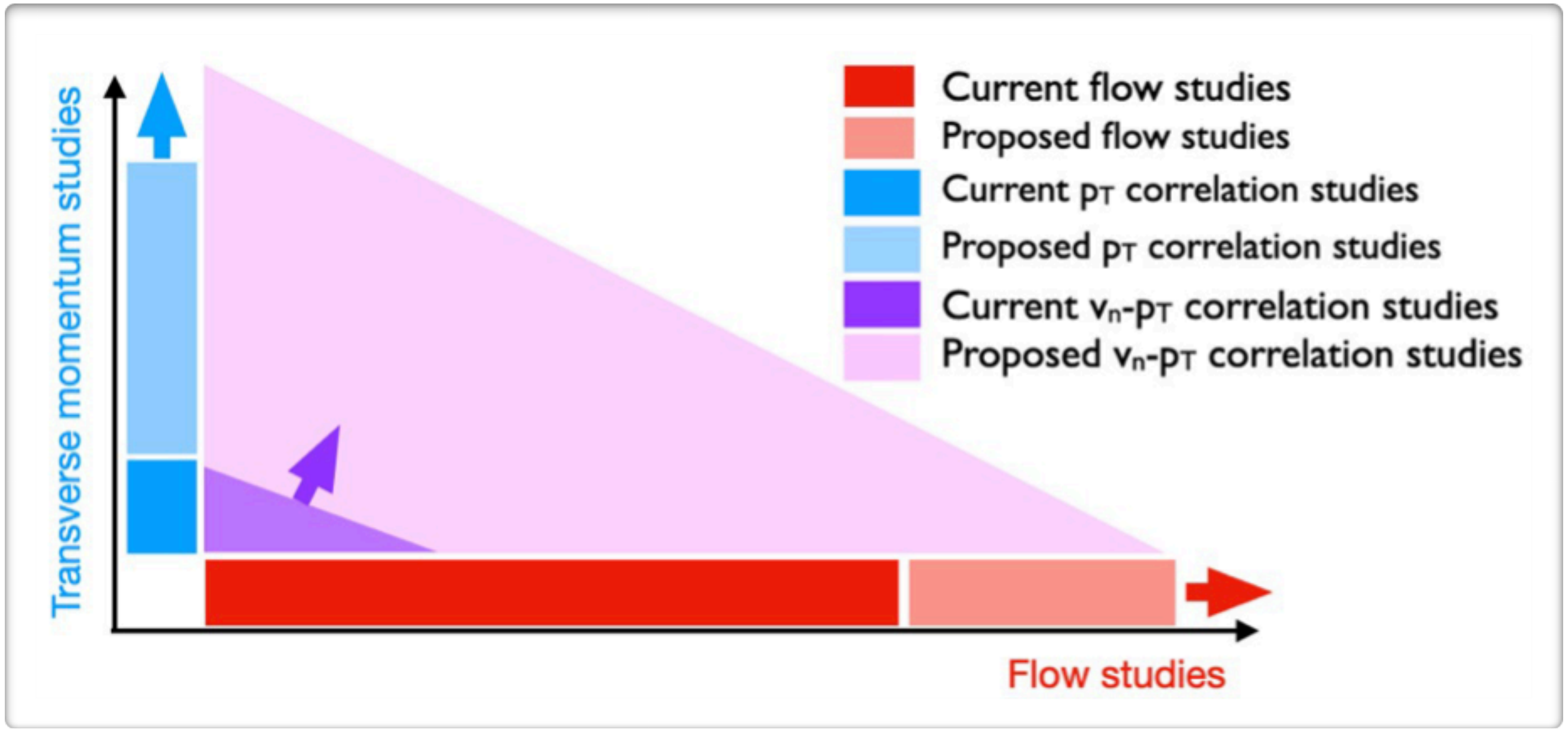

❖**Shape** of the fireball: Anisotropic flow

❖**Size** of the fireball: radial flow [p_T]

❖Final state: correlation between v_n and p_T

$$\rho(v_n^2, [p_T]) = \frac{cov(v_n^2, [p_T])}{\sqrt{var(v_n^2)}\sqrt{var([p_T])}}$$

P. Bozek etc, PRC96 (2017) 014904

❖ Assuming $v_n \propto \varepsilon_n$, [p_T] $\propto E_0$

$$\rho(v_n^2, [p_T]) = \rho(\varepsilon_n^2, [E_0])$$

final-state model calculation

Initial-state model estimation

❖ One can compare $\rho(v_n^2, [p_T])$ measurements to $\rho(\varepsilon_n^2, [E_0])$ calculations, to constrain the initial state model

O-O collisions at RHIC and the LHC

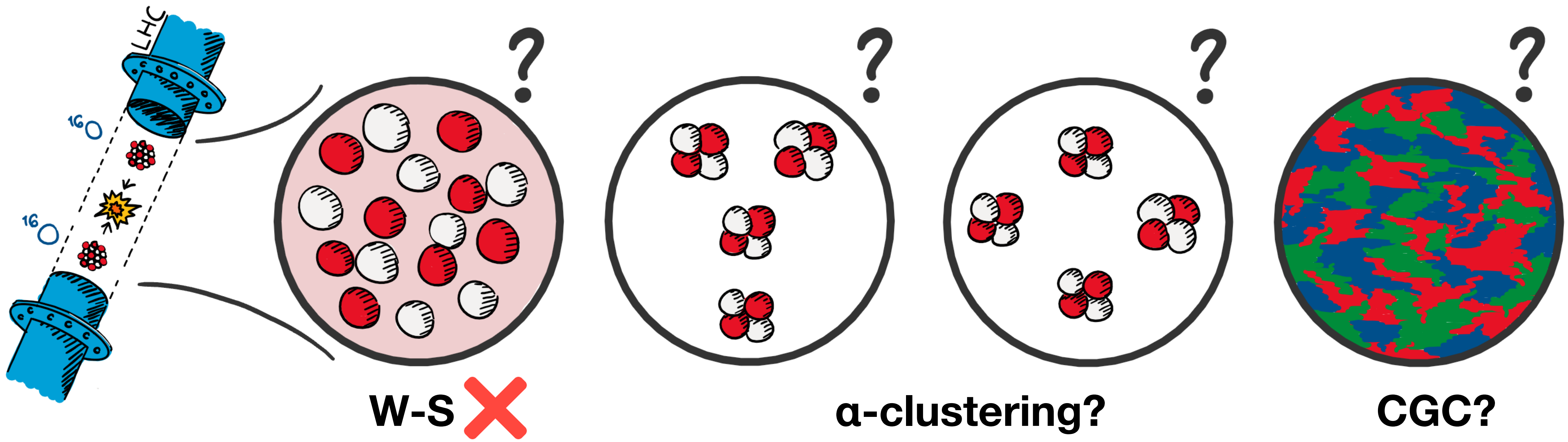

ALICE-PUBLIC-2021-004

EUROPEAN ORGANIZATION FOR NUCLEAR RESEARCH

ALICE

ALICE-PUBLIC-2021-004

ALICE physics projections for a short oxygen-beam run at the LHC

ALICE Collaboration[*]

Abstract

This document collects performance projections for a selection of measurements that can be carried out with a short O–O run during the LHC Run 3. The baseline centre-of-mass energy per nucleon–nucleon collision is $\sqrt{s_{NN}} = 6.37$ TeV and measurement uncertainties are given for the integrated luminosity $L_{int} = 1$ nb^{-1}. Some projections for p–O collisions are also included. These studies were presented at the CERN workshop on Opportunities of O–O and p–O collisions at the LHC [1,2].